Characterisation of STRO-1 expression on human mesenchymal stem cells and identification of putative cancer stem cells in osteosarcoma: prevention by micronutrients.

Shameem B.B. Fawdar

School of Life Sciences

CHARACTERISATION OF STRO-1 EXPRESSION ON HUMAN MESENCHYMAL STEM CELLS AND IDENTIFICATION OF PUTATIVE CANCER STEM CELLS IN OSTEOSARCOMA

Shameem B.B. Fawdar

A THESIS SUBMITTED IN PARTIAL FULFILMENT OF THE REQUIREMENTS OF THE UNIVERSITY OF WESTMINSTER FOR THE DEGREE OF DOCTOR OF PHILOSOPHY

APRIL 2010

Abstract

It is becoming increasingly more common to use culture expanded human mesenchymal stem cells (hMSCs) in regenerative medicine due to their low incidence *in vivo*. However, their successful application is hampered by a lack of selective markers to positively identify the expanded multipotent cells. This study aimed to characterise STRO-1 antigen as a potential biomarker of multipotency on cultured bone marrow derived hMSCs. In an attempt to identify the nature of this antigen, two techniques were implemented: peptide phage display technology and a microarray based approach.

Changes in the expression of STRO-1 were investigated during culture expansion of hMSCs. STRO-1 expression positively correlated with cellular morphology and multilineage potential, whereby senescent cells down-regulated STRO-1 antigen and exhibited decreased adipogenic and osteogenic potential. Furthermore, STRO-1 was found to be heterogeneously expressed on hMSC populations and enrichment followed by lineage specific induction of the STRO-1^{BRIGHT} fraction resulted in enhanced adipogenic and osteogenic differentiation potential. The expression of STRO-1 antigen was further characterised as a marker of differentiation, whereby differentiating cells were found to down-regulate STRO-1. A cellular hierarchy in hMSC population was therefore proposed based on STRO-1 status, with the highest STRO-1 expressive cells representing the multipotent subset. In an attempt to identify the epitope that STRO-1 IgM antibody recognised, peptide phage display technology was used as solid and liquid phase panning systems but the approach yielded no promising peptide candidate. Subsequently, comparative gene expression microarray analysis of osteosarcoma cell lines (143B, CAL72, G-292, HOS, MG-63, Saos-2 and U-2-OS) was implemented and a list of eight potential candidate genes encoding STRO-1 antigen was selected.

This work ultimately led to the identification of putative cancer stem cells (CSCs) in seven osteosarcoma cell lines initially based on STRO-1 expression. With MG-63 strongly expressing STRO-1, the maintenance of MSC-like properties by STRO-1 expressing cell lines was investigated. A heterogeneous pattern of osteogenic differentiation was observed between and within the cell lines. Closer inspection revealed a cellular hierarchy comprising of holoclones and paraclones, with the holoclones representing the putative CSCs in osteosarcoma. Overall, this thesis addressed the fields of regenerative medicine as well as oncology by proposing STRO-1 antigen as a marker of multipotency on hMSCs and osteosarcoma holoclonal cells as the putative cancer stem cell targets for anti-cancer drug development.

Acknowledgements

The years I spent in Westminster have been wonderful and culminated in the completion of a PhD, facilitated by the Cavendish Campus Research Scholarship award. Although this work represents a very personal achievement, it would not have been possible without the support of a number of people who directly or indirectly contributed to it and acknowledging them here is the least I could do.

First and foremost, I would like to express my sincere gratitude towards my Director of Studies, Dr Mark O. Clements. He has been an inspiration to most, if not all PhD students in the School of Life Sciences and his guidance is always greatly valued. It has been a privilege working under his primary supervision and I would like to thank him for his relentless support throughout the whole of this PhD. I would also like to thank my second supervisor Dr Angray S. Kang for his valuable support throughout this project, Dr Mark Kerrigan (University of Westminster) and Dr Francesc Miralles (St George's, University of London) for their kind assistance with confocal microscopy and immunofluorescence work respectively, and also Dr Stephen Henderson (The Cancer Institute, University College London) who performed the bioinformatics analysis, indicated herein. I immensely appreciate the help of the School of Life Sciences' technical staff, both former and current.

My laboratory experience has been unique and full of lovely and lively memories thanks to my two dear friends Bernard Anani and Victor Ujor. I would also like to thank my friends for always being there for me on this exceptional journey and also for all the fun and good times, namely Hannah Everitt, Madhuri Shamanna, Omeco White, Dr Anatoliy Markiv, Dr Tania Murphy, Dr Flavia Sorrentino and Dr Headley Williams, to name a few.

I would like to extend my gratitude to the Domun family and Varsally family for their constant encouragement and for always providing me with a homely environment. Last but not least, I would like to dedicate this achievement to my family back home, especially my parents, for their continuous support and encouragement but above all, for always believing in me.

Section **Page**

Figure Page

Figure **Page**

Figure **Page**

Table **Page**

The abbreviations used in this thesis are as follows:

Abbreviation	Full name
♀	Female
♂	Male
2/3D	Two or Three Dimensional
ABC	ATP-Binding Cassette
ABTS	2,2'-Azino-bis(3-Ethylbenzthiazoline-6-sulfonic acid)
ADAMTS2	ADAM metallopeptidase with thrombospondin type 1 motif, 2
ADIP	Adipogenic
ALDH	Aldehyde Dehydrogenase
Alk	Activin receptor-like kinase
ALP	Alkaline Phosphatase
AR	Alizarin Red
ARHGEF4 (Asef)	Rho guanine nucleotide exchange factor 4
ASC	Adult Stem Cell
Asef (ARHGEF4)	APC-stimulated guanine nucleotide exchange factor
BCP	1-bromo-3-chloro propane
bFGF	basic Fibroblastic Growth Factor
BMP	Bone Morphogenetic Proteins
BMPR1B	Bone Morphogenic Protein Receptor type-1B
BMSC	Bone Marrow Stromal Cell
bp	base pair
BSA	Bovine Serum Albumin
BSP	Bone Sialoprotein
C10orf116	Chromosome 10 open reading frame 116
C19orf66	Chromosome 19 open reading frame 66
Cbfa	Core binding factor alpha-1
CCL5	Chemokine (C-C motif) ligand 5
CD	Cluster of Differentiation
(c)DNA	(complementary) Deoxyribonucleic Acid
CFLAR	CASP8 and FADD-Like Apoptosis Regulator
CFSE	Carboxy Fluorescein Succinimidyl Ester
CFU-F	Colony Forming Unit Fibroblast
CNT	Control
Col1A1	Alpha 1 Collagen Type 1
CPD	Carboxypeptidase D
CSC	Cancer Stem Cell
CT	C Terminal
CXCR4	Chemokine (CXC motif) Receptor 4
D0	Day 0

DAB	Diaminobenzidine
DAPI	4'-6-diamino-2-phenylindole
DDX3Y	DEAD Box protein 3
DEPC	Diethylpyrocarbonate
DKK1	Dickkopfs 1
dNTP	Deoxyribonucleotide Triphosphate
DPBS	Dulbecco's Phosphase Buffered Saline
Dsh	Dishevelled
DSHB	Developmental Studies Hybridoma Bank
EDTA	Ethylenediaminetetraacetic acid
EIF1AY	Eukaryotic translation initiation factor 1A, Y-linked
ELISA	Enzyme-Linked Iimmunosorbent Assay
EMT	Epithelial-Mesenchymal Transition
EPC	Endothelial Progenitor Cell
EWS	Ewing's Sarcoma
F13A1	Coagulation factor XIII, A1 polypeptide
FACS	Fluorescent Activated Cell Sorting
FCS	Foetal Calf Serum
FITC	Fluorescein Isothiocyanate
Fzd1	Frizzled 1
GVHD	Graft-Versus-Host Disease
h	hour
HCl	Hydrochloric Acid
hMSC	human Mesenchymal Stem Cell
Holo	Holoclone
Hoxa2	Homeo box A2
HRP	Horse Raddish Peroxidase
HSC	Haematopoietic Stem Cell
IBMX	3-isobutyl-1-methylxanthine
ICAM	Inter-Cellular Adhesion Molecule
Ig	Immunoglobulin
IG	Intergenic region
IND	Induced
INT	Intermediate
ISCT	International Society for Cellular Therapy
kb	kilobase
KDM5D	Lysine (K)-specific Demethylase 5D
KHz	KiloHertz
LB	Luria-Bertani
LEF	Lymphoid Enhancer-binding Factor
LIF-R	Leukemia Inhibitory Factor Receptor
LMF1	Lipase Maturation Factor 1

LNGFR	Low-affinity Nerve Growth Factor Receptor
Lpr	Lipoprotein receptor-related protein
MACS	Magnetic Assisted Cell Sorting
MAPC	Multipotent Adult Progenitor Cell
MAPK	Mitogen-Activated Protein Kinase
MASCS	Mesenchymal Adult Stem Cells
MET	Mesenchyma-Epithelial Transition
MgCl2	Magnesium Chloride
MHC	Major Histocompatibility Complex
MIAMI	Marrow-Isolated Adult Multipotent Inducible cell
min	minute
mL	milli-Litre
mM	milli-Molar
mMSC	mature Mesenchymal Stem Cell
MNNG	*N*-methyl-*N*'-nitro-*N*-nitrosoguanidine
MSC	Mesenchymal Stem Cell
MSX2	Muscle Segment Homeobox Homolog
NEB	New England Biolabs
Nfatc1	Nuclear factor activated T cell 1
nM	nano Molar
NTRK3	Neurotrophic Tyrosine Kinase Receptor type 3
O.D	Optical Density
OCN	Osteocalcin
OP	Osteopontin
OPRL1	Opiod Receptor-Like 1
ORO	Oil Red O
OS	Osteosarcoma
OSE2	Osteoblast-specific *cis*-acting element 2
OST or OSTEO	Osteogenic
Osx	Osteorix
p	passage number
P2RY6	Purinoreceptor 6
Para	Paraclone
PBS	Phosphate Buffered Saline
PCR	Polymerase Chain Reaction
PE	Phycoerythrin
pfu	plaque forming unit
PGA	Poly Glycolic Acid
PI	Propidium Iodide
PLA	Poly Lactic Acid
p-NPP	p-nitrophenyl phosphate
PPSC	Pluripotent Stem Cell

PTH-R	Parathyroid Hormone Receptor
Rb	Retinoblastoma
RER	Rough Endoplasmic Reticulum
RNA	Ribonucleic Acid
RPE	R-Phycoerythrin
rpm	revolution per minute
RPMI	Roswell Park Memorial Institute
RPS4Y1	Ribosomal Protein S4, Y-linked 1
RS	Recycling Stem cell
RT-PCR	Reverse Transcriptase Polymerase Chain Reaction
Runx2	Runt-related 2
Satb2	Special AT-rich sequence-binding protein 2
SC	Stem Cell
SDF-1	Stromal Derived Growth Factor
SDS	Sodium Dodecyl Sulphate
sec	second
Shn3	Schnurri 3
SP	Side Population
ssDNA	single stranded De-oxy Ribo Nucleic Acid
SSEA-1/4	Stage-Specific Embryonic Antigen 1 or 4
Stat1	Signal transducer and activator of transcription 1
TBST	Tris-Buffered Saline Tween-20
TCF	T-cell-specific transcription Factor
TD	Terminally Differentiated
TGFβ	Transforming Growth Factor β
TNFSF11	Tumour Necrosis Factor (ligand) Superfamily member 11
USP9Y	Ubiquitin specific peptidase 9, Y-linked
UV	Ultra-violet
VCAM-1	Vascular Cell Adhesion Molecule-1
VEGFR2	Vascular Endothelial Growth Factor Receptor 2
VSEL	Very Small Embryonic-like Stem Cell
vWF	Von Willebrand Factor
w/v	weight by volume
ZFY	Zinc Finger Y-chromosomal protein
α-MEM	Alpha-Minimal Essential Medium
μm	Micrometre

Chapter 1
General Introduction

1.1 Introduction to stem cells

Stem cells have been described as cells having extensive self-renewal capacity and the ability to generate a number of differentiated progeny of multiple types (Lajtha, 1979, Hall and Watt, 1989, Joseph and Morrison, 2005). Additional characteristics associated with stem cells include quiescence *in vivo*, the ability to undergo asymmetric cell division and the ability to regenerate tissue following injury (Morrison *et al.*, 1997). However, these characteristics vary with stem cell populations and within a single stem cell population with time (Potten and Loeffler, 1990).

The isolation of stem cells from embryos as well as adult tissues demonstrates that these cells are present throughout the development of an organism and therefore, stem cells have been categorised based on their developmental potential. Totipotency refers to cells which are able to form all extra-embryonic and embryonic tissues and is a characteristic of the fertilised egg (Sell, 2004). Pluripotency defines cells which are able to give rise to the three embryonic germ layers which are the: endoderm (cells forming the gastrointestinal tract and internal organs such as the liver), mesoderm (blood, blood vessels and connective tissue such as bone) and ectoderm (skin and nervous system). Pluripotent cells can be derived from the inner cell mass of the blastocyst four to five days post-fertilisation and are termed embryonic stem cells (Thomson *et al.*, 1998). Work on these cells was pioneered by Martin and Evans who successfully isolated and expanded embryonic stem cells from mice *in vitro* (Martin and Evans, 1975, Martin, 1981). Stem cell populations which give rise to several cell lineages, generally within one germ layer are termed multipotent or oligopotent; adult stem cells are classically described in this way, although controversial cases of trans-differentiation of adult stem cells have been documented (Raff, 2003). Multipotent cells are able to give rise to unipotent progenitors of multiple cell types, which ultimately form the mature functional tissues of the organism (Sell, 2004).

Stem cell populations are commonly identified by virtue of their surface marker expression and specific functional characteristics (Alison *et al.*, 2006a). The key properties of stem cells are demonstrated *in vivo* by the regeneration of a specific tissue

type from a single cell after transplantation into an animal model, from which further stem cells can be derived displaying the same properties, although most work demonstrating stem cell properties are based on *in vitro* work (Weissman and Shizuru, 2008). *In vitro*, stem cells are assessed by the ability of clonal populations to form differentiated cells of multiple types (Joseph and Morrison, 2005, Watt *et al.*, 2006).

The prospect of expanding and manipulating stem cells *in vitro* present them as promising candidates in the field of regenerative medicine. Stem cells can be cultured extensively and differentiated to the required cell type to be implemented in cell-based therapies. More importantly, the ability to study stem cells in a laboratory setting provides a means of understanding the mechanisms regulating ontogeny, thereby increasing our knowledge of cellular development and differentiation.

1.1.1 Adult stem cells (ASCs)

The development of a multi-cellular organism is driven by a series of events pre-programmed in the genome from the time of fertilisation. These events encompass cell proliferation, lineage commitment, lineage progression, lineage expression, cellular inhibition and regulated cell death (Young and Black, 2004). The sequential progression of cells through these events culminates in the formation of differentiated cells, tissues and organs that constitute an individual. Although most cells undergo these crucial stages during growth, a subset of cells exit the developmental continuum at specific time points and become quiescent cells. The quiescent cells have been identified as adult stem cells (ASCs) and have been derived from almost every organ of the body, including the brain (Morrison *et al.*, 1999, Uchida *et al.*, 2000). ASCs reside in specific locations within the tissue or organ and are responsible for continual cellular turn-over and tissue repair following trauma or disease.

ASCs is the general term used for cells which are isolated from a post-natal individual and which have the potential to self-renew and give rise to differentiated cells with specific functions. ASCs are multipotent and, as such, are able to give rise to differentiated cells of the germ layer or organ in which they reside. However, there

have been reports of ASC trans-differentiation, whereby ASCs isolated from one organ could be re-programmed to form tissues of another organ (Forbes *et al.*, 2002, Poulsom *et al.*, 2002). This issue of ASC plasticity has been challenged over the past decade and there is limited evidence suggesting the presence of lineage-uncommitted pluripotent stem cells (PPSCs) (Romero-Ramos *et al.*, 2002, Young and Black, 2004). PPSCs are thought to be pluripotent (endo-, meso- and ectodermal precursors), therefore having a wider differentiation spectrum than ASCs which are committed to a specific germ layer. Young and colleagues (Young *et al.*, 2001) suggested the presence of contaminating PPSCs in the organ-specific ASCs population isolated in the studies claiming trans-differentiation. Following exposure to inductive factors different to those present in the organ from which they were derived, PPSCs are able to respond and differentiate into specialised cells of a totally different organ; for instance bone marrow derived stem cells forming neurons (Brazelton *et al.*, 2000) or hepatocytes (Petersen *et al.*, 1999). While it is not clear whether presumed trans-differentiation is actually the work of PPSCs, cell fusion has also been proposed as an explanation for the observed plasticity in ASCs (Forbes *et al.*, 2002, Poulsom *et al.*, 2002). There are reports confirming the presence of fused bone marrow cells among the differentiated cells in the newly formed organ, albeit at low frequency. Bone marrow cells from GFP transgenic mice were shown to fuse to embryonic stem cells, thereby adopting the phenotypic and pluripotent characteristics of the latter (Terada *et al.*, 2002, Ying *et al.*, 2002).

1.1.2 Bone marrow derived adult stem cells

The bone marrow is an organ composed of two main systems: the haematopoietic tissue proper and the associated supporting stroma, which are maintained by two distinct sets of stem cells, namely the haematopoietic stem cells (HSCs) and the mesenchymal stem cells (MSCs) respectively (Bonnet, 2003). Both sets of stem cells co-exist and function as two distinct populations in the same organ.

HSCs form specialised cells of the haematopoietic lineage and therefore are responsible for the production and maintenance of all the mature blood cell types. From the early post-natal period and onwards, haematopoiesis (formation of new blood cells) occurs in

the bone marrow with the progenitor cells entering the circulation where they are able to home to specific locations and undergo maturation. In the bone marrow, MSCs are responsible for the formation of bone (osteocytes), cartilage (chondrocytes), fat (adipocytes) and haematopoiesis-supporting stroma. It is generally accepted that MSCs line the endosteal and trabecular surfaces of the bone structure, along side other cells of mesenchymal origin (Aubin and Liu, 1996).

After development of the bone and the bone marrow, a dynamic relationship is established between the compartments of the two stem cell populations. The marrow cavities in all bones of newborn mammals are made up of the haematopoietic tissue and the haematopoiesis supportive stroma (haematopoietic micro-environment), a composite referred to as red bone marrow. During growth, the haematopoietic micro-environment, mainly in bones of the extremities, is gradually replaced by lipid-containing mesenchymal cells forming a fatty tissue referred to as yellow or fatty bone marrow. Therefore with age, the haematopoietic micro-environment in tubular bones is converted to fatty tissue and thus loses its ability to support haematopoiesis. However, cancellous bones are able to support haematopoiesis permanently despite the accumulation of some fat-containing cells. Cancellous bone, by virtue of its spongy structure, has a larger internal bone surface area than tubular bone and therefore harbours more MSCs which are able to form the haematopoiesis-supporting stroma, thus sustaining haematopoiesis (Gurevitch *et al.*, 2009).

Haematopoiesis is dependent on MSCs as these cells are the precursors of the supportive stroma required for the maintenance of the haematopoietic tissue. The formation of haematopoiesis-supportive stroma acts as an intermediate step between the MSC precursor and adipocyte formation. Gurevitch and co-workers (2007) describe an *in vivo* transition of stromal cells (arising from MSCs) to adipose tissue, thus gradually forming yellow marrow. Therefore with age, the continual formation of haematopoiesis-supportive stroma tends to deplete the MSC pool, while increasing the ratio of yellow to red bone marrow (Gurevitch *et al.*, 2007).

1.2 Mesenchymal Stem Cells (MSCs)

MSCs are multipotent stem cells which were first described in the bone marrow of guinea pigs by Friedenstein and colleagues (Friedenstein *et al.*, 1970). The cells were referred to as 'osteogenic stem cells' and described as clonal and fibroblastic stromal cells able to form adherent colonies in culture and possessing robust osteogenic potential (Friedenstein *et al.*, 1987). The terminology used to describe these cells have been debated over the years, namely colony forming unit fibroblasts (CFU-F) (Friedenstein *et al.*, 1970), mesenchymal stromal cells (MSC) (Lazarus *et al.*, 1995), bone marrow stromal cells (BMSC) (Gronthos *et al.*, 2003) and mesenchymal adult stem cells (MASCS) (Belema-Bedada *et al.*, 2008).

In 1991, the term 'mesenchymal stem cells' (MSCs) was coined by Caplan based on their self-renewal ability and capacity to commit to a distinctive phenotypic pathway to regenerate mesenchymal tissues (Caplan, 1991). Therefore consistent with this terminology, mesenchymal stem cells will be adopted to refer to the adherent population of bone marrow derived cells in this thesis. The multilineage differentiation potential into bone, cartilage, fat and marrow-supportive stroma was further characterised by Pittenger and co-workers (2009). This group undertook a large scale MSC investigation (bone marrow MSC isolated from 350 patients) to show that a subset of clonally expanded adherent cells retained multilineage potential. This further supported the true nature of MSC as possessing stem cell properties. Interestingly, some clones were only able to commit to one or two lineages suggesting that the adherent cell population may comprise of a set of lineage committed progenitors or the loss of multilineage properties upon *in vitro* expansion (Pittenger *et al.*, 1999). Since the discovery of MSCs in the bone marrow, cells with MSC-like characteristics have been identified in a number of adult and foetal tissues (Figure 1.1). The bone marrow derived non-haemaopoietic stem cells have been ascribed different names and further categorised (Section 1.2.4). Moreover, trans-differentiation of MSCs to non-mesodermal lineages such as ectodermal skin (Sasaki *et al.*, 2008) and neurons (Woodbury *et al.*, 2000, Kopen *et al.*, 1999) and endodermal myocytes (Ferrari *et al.*, 1998) and hepatocytes (Sato *et al.*, 2005) has been reported. However the validity of these plasticity studies is still being

questioned, mainly due to the variety of MSC isolation techniques employed and inappropriate differentiation assays used whereby differentiated cells are not characterised by functional assays (Phinney and Prockop, 2007). Despite these reports of MSCs' ability to differentiate to cells of the three germ layers, the consensus within the field is that the cells are 'multipotent' rather than 'pluripotent'.

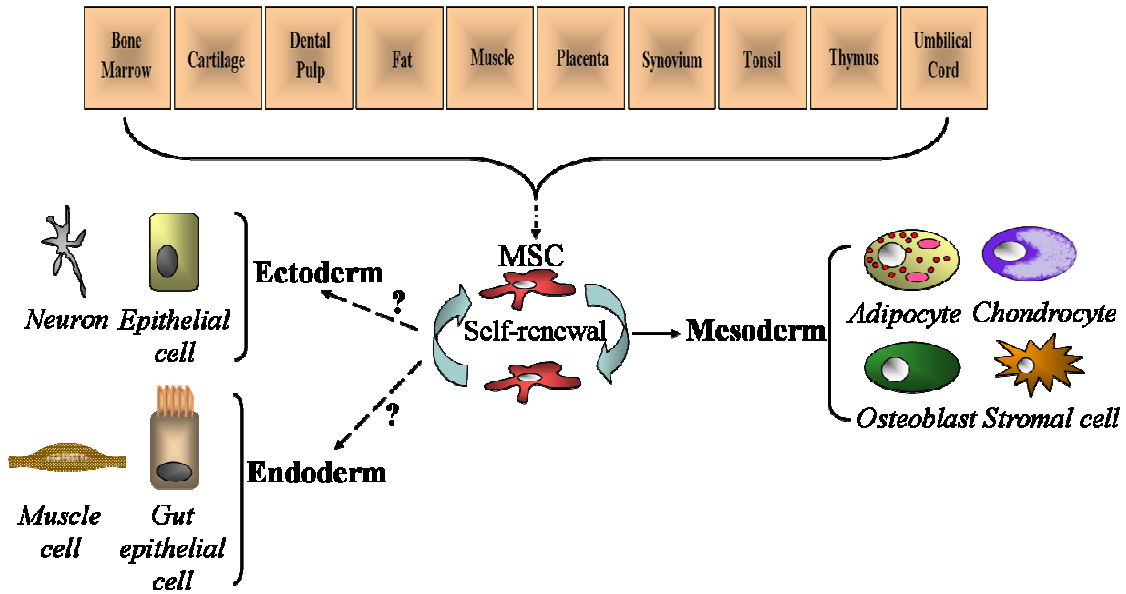

Figure 1.1: Sources of mesenchymal stem cells (MSCs) and their multi-lineage potential. Clonal population of MSCs has been shown to give rise to cells of the mesodermal lineage, whereas their potential to differentiate to the ectodermal and endodermal lineages is still under debate (denoted by ?).

1.2.1 Surface marker characterisation of hMSCs

Despite the significant progress in understanding MSC biology, to date there is ongoing controversy over the cell surface antigen that uniquely identifies MSCs *in vitro* and *in vivo* (Jones and McGonagle, 2008). In an attempt to assign a uniform mode of identification of MSCs, the International Society for Cellular Therapy (ISCT) has established three minimal criteria based on the current state of knowledge (Horwitz *et al.*, 2005, Dominici *et al.*, 2006). MSCs isolated from the bone marrow and other tissues of mesenchymal origin must demonstrate *in vitro* (i) plastic adherence in standard culture conditions, (ii) specific surface antigenic profile, and (iii) multipotent differentiation potential along the osteogenic, chondrogenic and adipogenic lineages as

confirmed by histological staining and other methods. Plastic adherence and multipotency to the required lineages are the undisputed criteria that all workers in the field abide by. The limitation lies in the varied antigenic profile employed by different groups to positively identify the hMSC populations even though it is from a common source, for instance the bone marrow (Table 1.1).

The consensus of the ISCT, which is not based on the source of the isolated MSCs and subject to future modification, dictates that flow cytometry measurements must show at least 95 % of the MSC population to express CD73 (ecto-5'-nucleotidase), CD90 (Thy-1) and CD105 (endoglin), and no more than 2 % of the cell population may express CD34 (haematopoietic progenitor and endothelial cell marker), CD45 (pan-leukocyte marker), CD11b or CD14 (monocyte and macrophage markers), CD19 or CD79α (B cell markers), and HLA-DR (marker of stimulated hMSCs). Further to the list of markers produced by the ISCT, other surface antigens defining hMSC populations have been described, although the issue remains whether the markers characterised are able to identify freshly isolated as well as cultured hMSCs. Jones and co-workers (Jones *et al.*, 2004) characterised CD271 (also referred to as low-affinity nerve growth factor receptor, LNGFR) as a positive marker to identify MSCs *in vivo*. Their purification protocol consisted of the exclusion of fibroblasts using D7-FIB, and the subsequent sorting of the cells to yield hMSCs, of which more than 95 % expressed CD271. However, the cells positive for CD271 also expressed HLA-DR (Jones *et al.*, 2006b), which according to the ISCT criteria may indicate that the isolated population of cells was activated (Dominici *et al.*, 2006). More recently, CD146 (MCAM//MUC18) has been identified as a putative marker for the detection of MSCs. CD146 is expressed on sub-endothelial cells (also referred to as pericytes) which share the properties of hMSCs in terms of their ability to support the haematopoetic micro-environment and differentiate towards the adipogenic, osteogenic and chondrogenic lineages (Doherty *et al.*, 1998, Farrington-Rock *et al.*, 2004). In this aspect, hMSCs and pericytes are thought to share the same identity (Section 1.2.3) (Crisan *et al.*, 2008). This hypothesis is further supported by the observation that both cell populations share a common set of markers, among which is STRO-1 (Shi and Gronthos, 2003).

Marker/marker combination	Application	Reference
CD49a	Isolation	(Deschaseaux and Charbord, 2000)
CD105 (SH2)	Isolation and Characterisation	(Majumdar *et al.*, 2000)
CD45/GlyA	Isolation	(Reyes *et al.*, 2001)
CD271 (LNGFR), D45/GlyA	Isolation and Characterisation	(Quirici *et al.*, 2002)
D7-FIB/CD45/CD271/GlyA	Isolation and Characterisation	(Jones *et al.*, 2002)
STRO-1/CD106 (VCAM-1)	Isolation and Characterisation	(Gronthos *et al.*, 2003)
STRO-1/CD146	Isolation and Characterisation	(Shi and Gronthos, 2003)
STRO-1/ CD63 (HOP-26), CD49, CD166	Isolation	(Stewart *et al.*, 2003)
CD49, CD45	Isolation and Characterisation	(Deschaseaux *et al.*, 2003)
CD105, D7-FIB	Isolation and Characterisation	(Campioni *et al.*, 2003)
CD45/GlyA, lineage negative cocktail (CD3, CD14, CD19, CD38, CD66)	Isolation	(Tondreau *et al.*, 2004)
CD73 (SH3), CD105, CD90, CD49, CD45	Isolation	(Boiret *et al.*, 2005)

Table 1.1: A review of recently used antibodies to identify bone marrow derived MSCs (Adapted from Jones *et al.* 2006b).

1.2.2 STRO-1 as a marker of hMSCs

STRO-1 is an IgM monoclonal antibody discovered by Simmons and Torok-Storb (1991) binding to a minor subset, between (0.001 % and 0.01 %) of bone marrow mononuclear cells. In an attempt to raise antibodies against progenitor and precursor cells from the CD34 positive bone marrow cells, STRO-1 was identified as an antibody selecting for the adherent portion of cells from the bone marrow. Mice were immunised intra-splenically with a population of human CD34 positive bone marrow cells and boosted four times at 3-week intervals. Hybridomas were produced by fusion of the splenocytes with myeloma cells and cultured for supernatant collections which were then screened for antibodies negatively reacting to a panel of B- and T-cells. STRO-1 was then identified as an antibody that reacted with less than 10 % of the bone marrow mononuclear cells which also included nucleated erythroid progenitors (Glycophorin A positive cells). Using FACS, the STRO-1^{+}/glycophorin A^{-} cell population was found to form an adherent layer in culture possessing an enhanced ability to support haematopoiesis and exhibiting differentiation potential.

Analysis of STRO-1 expression on fresh bone marrow cells showed that the number of positive cells increased over the first two weeks in culture, corresponding to the period of adherent layer establishment, followed by a progressive decline. This modulation in STRO-1 expression was argued to be either an *in vitro* epiphenomenon unrelated to the normal regulation of STRO-1 expression taking place *in vivo*, or the developmentally programmed antigen down-regulation caused by *in vitro* maturation of stromal precursors into more differentiated stromal cell types. Since the nature of the STRO-1 antigen is as yet unknown (apart from being trypsin-resistant), its role in the regulation of MSC's behaviour remains unclear. One interesting feature which Simmons and Torok-Storb (Simmons and Torok-Storb, 1991) observed was the higher expression of STRO-1 on pre-adipocytes compared to mature adipocytes, indicating that the STRO-1 antigen may be a differentiation antigen present on the cell's surface before maturation. However this aspect of STRO-1 function and its modulation under different conditions have not been fully investigated, hence became one of the primary purpose of this thesis.

Among the panel of markers used to isolate hMSCs, STRO-1 was the only one to exhibit a heterogeneous expression characterised by the fluorescence intensity of FACS measurement defined by low expression (STRO-1^{DULL}), intermediate expression (STRO-1^{INT}) and high expression (STRO-1^{BRIGHT}) (Gronthos *et al.*, 2003). Following sorting, the STRO-1^{DULL} sub-population failed to form the MSC-characteristic adherent fibroblastic colonies indicating that the multipotent MSCs reside in the STRO-1^{BRIGHT} and STRO-1^{INT} sub-populations. By using CD106 (also known as, vascular cell adhesion molecule-1, VCAM-1) as an accessory marker, the freshly isolated STRO-1^{+}/$CD106^{+}$ population exhibited phenotypic characteristics previously attributed to stem cells in other renewing tissues; lack of Ki-67 antigen indicating quiescence *in vivo*, telomerase activity in the parent population and their progeny and the undifferentiated state as demonstrated by the absence of gene products attributed to mature stromal elements such as adipocytes, osteocytes and chondrocytes. More importantly, highly proliferative clones derived from single STRO-1^{BRIGHT}/$CD106^{+}$ exhibited the tri-lineage potential of hMSCs further demonstrating that the multipotent progenitors reside in the STRO-1^{BRIGHT} fraction of the population (Gronthos *et al.*, 2003). As such, the adherent population of bone marrow mononuclear cells represent a mixed population of multi-, bi- and uni-potential progenitors at different stages of differentiation (Owen and Friedenstein, 1988, Pittenger *et al.*, 1999) and the heterogeneous expression of STRO-1 may be an indicator of the stage of differentiation a cell is at; the multipotent cells being the most expressive of STRO-1, although this has yet to be proven.

1.2.3 The perivascular niche of hMSCs

The stem cell niche has been described as a dynamic micro-environment including extracellular matrix that mediates local and systemic cues to ultimately influence stem cell fate (Chen, 2010). The concept of stem cell niche was first described in the context of haematopoiesis by Schofield (Schofield, 1978). The niche encompasses stem cells as well as the support cells with the secretory mediators which interact to dictate stem cell behaviour. As such, conditions created within the micro-environment by the support cells maintain the cells in a quiescent state or trigger proliferation (symmetric and asymmetric division) and differentiation in response to inductive factors.

The anatomical location and phenotypic characteristics of hMSCs *in vivo* have not been well defined so far because of the lack of definitive marker to identify the cells *in situ*. Several studies have shown that cells with hMSC characteristics are present in a variety of adult tissues (Figure 1.1). This observation led to the concept of hMSCs residing in a perivascular niche in close association with blood vessels (Shi and Gronthos, 2003, Crisan *et al.*, 2008). A number of recent reports suggest that hMSCs are directly comparable to pericytes by virtue of their phenotypic and differentiation similarities and there is mounting evidence indicating that the two cell types may be one and the same (Crisan *et al.*, 2008). Pericytes (also known as Rouget or mural cells; mesangial cells in the kidney; Ito cells in the liver) are located adjacent to endothelial cells of capillaries and microvessels, and are associated with the smooth muscle cells of macrovessels (Andreeva *et al.*, 1998, Tintut *et al.*, 2003). Similar to pericytes, hMSCs have also been isolated from small and large blood vessels and both cell types share a number of common markers such as STRO-1, α-smooth muscle actin, CD44, CD73, CD90, CD105 and CD146 (Shi and Gronthos, 2003, Sacchetti *et al.*, 2007, Crisan *et al.*, 2008). Their similarity is further demonstrated by the ability of pericytes to undergo multi-lineage differentiation potential, a crucial characteristic of hMSCs (Doherty *et al.*, 1998, Tintut *et al.*, 2003, Farrington-Rock *et al.*, 2004). Having hMSCs in a perivascular niche throughout the body may be beneficial as this could enhance their migratory capability and may allow them to home into local and distant tissues in response to systemic influences following trauma or disease.

1.2.4 Heterogeneity of non-haematopoietic bone marrow derived stem cells

It is a well established concept that the bone marrow is the reservoir of a heterogeneous mix of stem cells capable of regenerating various tissues and organs, categorised as the haematopoietic and non-haematopoietic lineage. Following Fridenstein's (Friedenstein *et al.*, 1987) initial discovery of the plastic adherent MSC population in the bone-marrow, the non-haematopoietic stem cells have been further characterised and sub-populations identified. The presence of these various populations of stem cells in the bone marrow is believed to be the result of 'developmental migration' of stem cells during ontogenesis, whereby the cells are responsive to chemo-attractants such as stromal derived growth factor (SDF-1), and home into the bone marrow which provides a permissive environment (Nagasawa, 2000). Based on the different experimental strategies used to isolate the non-haematopoietic stem cells (Table 1.1), it is very likely that the same cell population may have been assigned different names given the common expression of certain markers (Table 1.2). More-so, the observed phenomenon of trans-differentiation (Figure 1.1) may be due to the isolation of a heterogeneous population of MSCs with a subset of cells having a more primitive status.

Endothelial progenitor cells (EPCs)

Bone marrow from post-natal humans and animals have been shown to contain EPCs which contribute to vascularisation at injury sites (Asahara *et al.*, 1997, Asahara *et al.*, 1999). The EPCs residing in the marrow may be released in response to specific growth factors and are able to home to distant locations where they contribute to the reconstruction of the vascular network (Kawamoto *et al.*, 2001, Shintani *et al.*, 2001). More recently, the recruitment of EPCs in pathologic neovascularisation in diabetic retinopathy has been documented (Liu *et al.*, 2010). Furthermore, EPCs are reported to participate in angiogenesis supporting tumour growth and development in a number of cancers including lung and breast (Nowak *et al.*, 2010, Le Bourhis *et al.*, 2010).

Multipotent adult progenitor cells (MAPCs)

MAPCs isolated from bone marrow mononuclear cells have been associated with MSCs in terms of their fibroblastic morphology, although these cells were reported to be pluripotent and having greater proliferation ability than MSCs, possibly due to the fact that they are grown in different culture conditions to MSCs. These cells were first identified by Verfaillie's team in 2002 which was then subject to controversy (Jiang *et al.*, 2002). The reported ability of MAPCs to give rise to the non-mesodermal lineages has now been confirmed by a Chinese group which employed a modified protocol to that used by Verfaillie's group to isolate MAPCs from rat bone marrow (Ji *et al.*, 2008). More recently, Verfaillie's group have published a stepwise method to isolate MAPCs from rodent bone marrow, a protocol which promises to be reproducible by more independent laboratories (Subramanian *et al.*, 2010).

Marrow-isolated adult multilineage inducible (MIAMI) cells

This cell population was isolated from the bone marrow of people aged three to seventy-two years old. The cells were cultured at low density in low oxygen tension conditions and on fibronectin to mimic an *in vivo* environment (D'Ippolito *et al.*, 2004). MIAMI cells exhibited a high proliferative potential with no sign of senescence and retained multilineage differentiation potential assessed by the expression of several markers of the three germ layers. However, the contribution of MIAMI cells to blastocyst development thus confirming their pluripotency has not been tested to date and the *in vitro* isolation of this same population awaits confirmation by other laboratories.

Very small embryonic-like stem cells (VSELs)

VSELs were first identified in murine bone marrow and then in other organs such as foetal liver, spleen and thymus (Kucia *et al.*, 2006). The same group later identified VSELs in human cord blood and presented evidence of its presence in bone marrow of young patients (Kucia *et al.*, 2007). VSELs have been reported to have similar features as embryonic stem cells, namely expression of Oct-4 and Nanog among others and their relatively small size containing a large nucleus and minimal peripheral cytoplasm. Ratajczak and colleagues (Ratajczak *et al.*, 2007) postulate that VSELs are pluripotent

stem cells derived from the inner cell mass (epiblast) during embryogenesis and become deposited in the bone marrow. These cells are able to last through adulthood and are recruited to injury sites to assist in tissue repair.

Mature Mesenchymal Stem Cells (mMSCs) and Recycling Stem cells (RS-1 and RS-2)

Prockop's group reported the identification and characterisation of a group of cells (termed Recycling Stem (RS) cells) which are distinct from MSCs by virtue of their very small round shapes and their ability to rapidly self-renew (Prockop *et al.*, 2001). These cells were isolated from adult bone marrow and cultured at very low densities (as low as 0.5 cell/cm^2) (Colter *et al.*, 2000). The RS cells were further divided based on their prevalence at different growth stages of the cultures and their granularity as assessed by flow cytometry scatter plots. The cultures were defined as a heterogeneous mix of cells categorised as follows: mature MSCs (mMSCs) which were large and moderately granular, resting RS-1 cells which were small and agranular and finally cycling RS-2 cells which were small and granular. Their antigenic profiles and differentiation potential was also assayed. Of particular interest, STRO-1 expression was low on the mMSCs while the RS cells were negative for STRO-1, although RS cells displayed a better tri-lineage differentiation potential (adipogenic, osteogenic and chondrogenic lineages) than mMSCs (Colter *et al.*, 2001).

Type of bone marrow derived non-haematopoietic stem cells	Antigenic Phenotype
Mesenchymal stem cells (MSCs)	*International Society for Cellular Therapy Criteria*: $CD105^+$, $CD73^+$, $CD90^+$, $CD45^-$, $CD34^-$, $CD14^-$, $CD11b^-$, $CD79a^-$, $CD19^-$, HLA-DR^-
Endothelial progenitor cells (EPCs)	$CD133^+$, $CD34^+$, c-kit $(CD117)^+$, VE-$cadherin^+$, $VEGFR2^+$, $CD146^+$, vWF^+, $CD31^+$
Multipotent adult progenitor cells (MAPCs)	SSEA-1^+, $CD13^+$, Flk-1^{low}, Thy-1^{low}, $CD34^-$, $CD44^-$, $CD45^-$, CD117 (c-kit)$^-$, MHC I^-, MHC II^-
Marrow-isolated adult-multilineage inducible (MIAMI) cells	$CD29^+$, $CD63^+$, $CD81^+$, $CD122^+$, $CD164^+$, c-met^+, $BMPR1B^+$, $NTRK3^+$, $CD34^-$, $CD36^-$, $CD45^-$, CD117 (c-kit)$^-$, HLA-DR^-
Very small embryonic-like stem cells (VSELs)	$CXCR4^+$, $AC133^+$, $CD34^+$, SSEA-1^+ *(mouse)* or SSEA-4^+ *(human)*, AP^+, c-met^+, LIF-R^+, $CD45^-$, Lin^-, $CD90^-$, $CD29^-$, $CD105^-$, MC I^-, HLA-DR^-
Mature Mesenchymal Stem Cells (mMSCs)	$CD34^-$, CD113 (Mac-1)$^-$, $CD43^-$, $CD45^-$, $CD31^{low}$, $CD38^{low}$, CD117 (c-kit)^{low}, STRO-1^{low}, CD90 (Thy-$1)^+$, Flk-1^-
Recycling Stem Cells 1 (RS-1 cells)	$CD34^-$, CD113 (Mac-1)$^-$, $CD43^-$, $CD45^-$, $CD31^{low}$, $CD38^{low}$, CD117 (c-kit)$^-$, STRO-1-, CD90 (Thy-1)^{low}, Flk-1^+
Recycling Stem Cells 2 (RS-2 cells)	$CD34^-$, CD113 (Mac-1)$^-$, $CD43^-$, $CD45^-$, $CD31^{low}$, $CD38^{low}$, CD117 (c-kit)$^-$, STRO-1-, CD90 (Thy-1)$^-$, Flk-1^{low}

Table 1.2: Non-haematopoietic stem cells identified in the bone marrow and their relative antigenic profiles. Minus sign (-) infers no expression while (low) infers low levels of expression. (Adapted from Ratajczak *et al.*, 2007).

1.3 Therapeutic applications of hMSCs

hMSCs stand out as a very promising therapeutic candidate for a variety of emerging unmet medical needs. Apart from being ethically favoured, hMSCs offer a range of advantages which include: *in vitro* expansion, multipotency and possible plasticity, paracrine effects, immunomodulatory properties and migratory behaviour (Miura *et al.*, 2006). Since the pioneering work of Dr Alexander Friedenstein (Friedenstein *et al.*, 1987, Friedenstein *et al.*, 1970), the last decade has witnessed an overwhelming number of reports documenting the prospects of hMSC application in pre-clinical and clinical settings (reviewed in (Caplan and Bruder, 2001, Salem and Thiemermann, 2009).

1.3.1 Orthopaedic applications

MSCs have been exploited primarily for their multipotential ability and the prospect of differentiating them to bone and cartilage *in vitro* and *in vivo* poses them as a valuable tool in skeletal tissue regeneration. Remodelling of bone is continuous throughout life in order to maintain skeletal integrity and mechanical strength. Bone homeostasis is dependent on the fine balance between bone producing cells (osteoblasts, derived from MSC) and bone resorbing cells (osteoclasts, derived from HSC) (Section 1.4) (Bielby *et al.*, 2007). MSCs play a key role in this process as they directly influence the rate at which osteoblasts are formed and mature into osteocytes. However, under certain conditions, such as fractures and diseases including osteoporosis, osteoarthritis and cancer, this balance is lost leading to poor bone healing and reduced bone strength (Masi and Brandi, 2001). Furthermore, the associated connective tissues including cartilage, tendon and ligament exhibit a limited regeneration capacity in response to damage caused by trauma or disease. To address these issues, a variety of MSC preparations have been assayed as novel cell-based therapies for the repair of damaged skeletal tissues, including cranial bones and articular cartilage (Chang *et al.*, 2004, Chang *et al.*, 2008). These MSC preparations are based on optimal numbers of MSC which are either directly injected into the targeted site or cultured as explants in 2D and 3D cultures.

A wide range of scaffolds have been used as a vehicle for MSC grafts, ranging from biodegradable natural materials such as silk (Kim *et al.*, 2008), extracellular matrix materials such as collagen (Howard *et al.*, 2008) and synthetic polymers like poly glycolic acid (PGA) and poly lactic acid (PLA) (Jiang *et al.*, 2006). While the optimal biocompatibility properties are still being studied, the advent of TheriForm 3D-printing process has made it possible to design 'made-to-measure' scaffolds. This process has already been implemented in clinical trials of cartilaginous defects whereby scaffolds are prepared based on the shape and size required (Sherwood *et al.*, 2002). Furthermore, alternatives to the above-mentioned traditional scaffolds coupled with optimal culture conditions are currently being developed (Frith *et al.*, 2009). In the laboratory setting, MSCs have been successfully grown as sheets and then attached onto bone grafts which facilitate their differentiation into osteochondral derivatives (Ouyang *et al.*, 2006). However, the efficacy of this new generation of tissue engineering awaits validation in large animal pre-clinical and human clinical studies.

1.3.2 Immunomodulation

Solid organ and tissue transplantations often result in alloreactivity whereby the host rejects the grafted foreign material, a condition known as graft-versus-host disease (GVHD). Treatment of GVHD following transplantation requires life-long administration of aggressive immunosuppressive drugs including corticosteroids, anti-metabolites and T cell depletion cocktails. These therapies are often accompanied by opportunistic infections in the immunodeficient individual thereby increasing the risk of graft rejection and relapse. Further complications arise in steroid-refractory GVHD whereby the traditional steroid therapy is rendered ineffective due to resistance. MSCs display two major immunological properties which could potentially be exploited for diseases requiring allografts; MSCs do not express co-stimulatory antigens such as B7 (immunoprivileged) and inhibit T cell proliferation (immunosuppressive) (reviewed in (Brooke *et al.*, 2007).

Canine studies have demonstrated the successful engraftment of major histocompatibility complex (MHC)-mismatched MSCs in large bone defects. The implanted MSCs were able to regenerate new bone tissues at the site of injury with no evidence of immunologic rejection (Kraus and Kirker-Head, 2006). It is possible that the implanted MSCs only act as an initiator of the tissue regeneration cascade, whereby the new or re-modelled tissue is formed from the subsequent mobilisation of autologous migratory MSCs to the repair site. Although, the underlying mechanism related to this procedure is still under investigation, the promising results observed in this pre-clinical study suggest that allogeneic MSCs could be made available as an 'off-the-shelf' therapy for such tissue engineering applications.

The immunosuppressive mechanism of MSCs has not been fully identified but is known to involve several factors such as cytokines which lead to T cell suppression (Aggarwal and Pittenger, 2005, Le Blanc and Ringden, 2007). A number of case reports demonstrate the use of MSC to successfully prevent transplantation rejection and resolve drug refractory GVHD (Le Blanc *et al.*, 2004, Lazarus *et al.*, 2005). On a larger scale, the European Bone Marrow Transplant Group reported a 68 % overall positive response following MSC treatment of 40 patients with grades III-IV GVHD (Brooke *et al.*, 2007). A Phase II trial conducted by Osiris Therapeutics (Osiris Therapeutics Inc. website: www.osiristx.com) reported a higher complete response rate in GVHD patients treated with corticosteroids and MSC compared to those treated with corticosteroids alone. Despite the lack of understanding in the immunosuppressive mechanism of action of MSCs, the promising results from case studies have prompted increased interest in the use of MSCs as GVHD therapy in the clinic.

1.3.3 Cardiovascular applications

Research in the use of MSCs in the instance of cardiovascular disease has increased over the past decade. Whether it be in the case of cardiac dysfunction or myocardial ischaemia, cellular therapy using MSCs represents a promising tool for tissue repair as they may have the potential to generate functional cardiomyocytes and contribute to the generation of new blood vessels to support and nourish the regenerating tissues (Psaltis

et al., 2008). Clinical transplantation of MSCs for cardiovascular applications is also facilitated by the local immuno-suppressive properties and mobilisation of the cells to the site of repair (Wang and Li, 2007, Zannettino *et al.*, 2008). The proposed mechanisms of the reparative action of MSCs are illustrated in Figure 1.2. Of particular interest, an *in vitro* investigation of STRO-1 enriched MSCs from bone marrow mononuclear cells displayed enhanced cardio-therapeutic properties compared to plastic adherent MSCs. The STRO-1 enriched cells displayed paracrine influence on cardiomyocytes with respect to cardiac cell proliferation and migration. Moreover conditioned media from the STRO-1 positive cells was shown to enhance endothelial cell migration and tube formation (Psaltis *et al.*, 2010). Taken together, the successful identification of MSCs with enhanced reparative properties and the prospective successful *in vivo* application to repair cardiac tissues may improve the outcome of clinical trials and speed the use of MSCs in clinical settings.

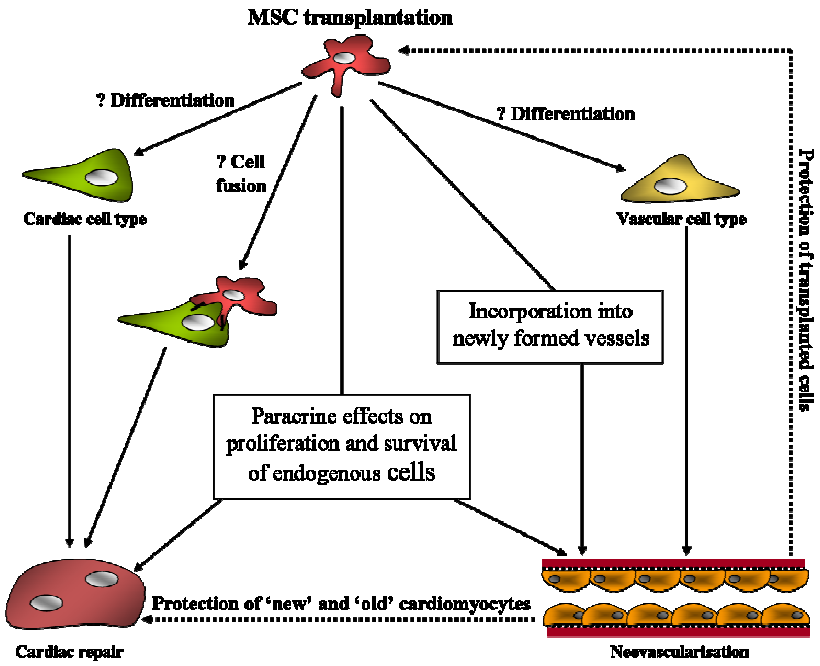

Figure 1.2: Proposed mechanisms of action of MSCs mediating cardiovascular repair. Paracrine mechanisms contributing to the reparative effects of MSC transplantation may be mediated by the release of soluble cytokines or growth factors as well as direct contact between transplanted cells and resident cardiac cells. *In vivo* transdifferentiation of MSCs into functional cardiomyocytes or vascular cells is limited by current transplantation strategies (Adapted from Psaltis *et al.*, 2008).

1.4 Bone development

Bone is a highly specialised form of connective living tissue and functions as an internal support system in all higher vertebrates. With a mineralised extracellular matrix, bone confers strength and rigidity to the skeleton, while maintaining some degree of elasticity. There are two forms of bone distinguished by their structural and functional differences: cortical (compact) bone providing mechanical and protective functions and cancellous (spongy) bone providing metabolic functions. Bone is composed of four different cell types, namely osteoblasts, osteoclasts, bone lining cells present on the bone surface and osteocytes integrated into the mineralised interior (Aubin and Liu, 1996). Osteoblasts, osteocytes and bone lining cells originate from MSCs involved in bone formation while osteoclasts arise from mononuclear precursors (monocyte-macrophage fusion) of haematopoietic origin involved in bone resorption. Osteoblasts are responsible for the formation of the bone matrix by secreting type I collagen and mature to osteocytes which in turn take up the role of maintaining the matrix. Besides synthesising matrix, osteocytes are capable of resorption but to a lesser extent than osteoclasts (Sims and Gooi, 2008). Osteocytes have well-developed filopodial processes which allow communication with adjacent cells, internal and external surfaces of the bone and with blood vessels running through the matrix (Matsuo and Irie, 2008). Bone lining cells are flat and elongated cells which appear dormant on the bone surfaces and possessing no functional characteristics. These cells do not participate in bone formation or resorption but it is speculated that they may be precursors for osteoblasts under specific stimuli (Dobnig and Turner, 1995).

1.4.1 Bone formation (ossification) and the osteoblast lineage

There are two types of bone formation processes occurring during foetal development: endochondral and intra-membranous. Endochondral ossification occurs by the condensation of MSCs to form a primary cartilage model which acts as a template that is later replaced by bone. Long bones of the arms, legs and ribs are formed in this way. Intra-membranous ossification is responsible for the development of flat bones of the skull and remodelling the outer surfaces of long bones (periosteal). It occurs by the condensation of MSCs and direct differentiation to osteoblasts, without the formation of cartilage (Olsen *et al.*, 2000). In this thesis, emphasis will be laid on intra-membranous ossification which occurs during remodelling of long bones of adults.

Irrespective of the route of bone formation, the end result of osteo-induction signals is the formation of mature functional osteoblasts capable of structuring tissues recognizable as bone. The osteoblast lineage consists of four maturational stages and these have been identified *in situ* as: pre-osteoblast, osteoblast, osteocyte and bone lining cell (Figure 1.3). Pre-osteoblasts arise from MSCs and are considered the immediate precursors of osteoblasts. They are positioned adjacent to the osteoblast layers which line the bone forming surfaces. Despite their morphological resemblance to osteoblasts (including positive alkaline phosphatase activity), pre-osteoblasts lack the differentiated characteristics associated with mature osteoblasts. Unlike osteoblasts, pre-osteoblasts are believed to have the ability to proliferate to a limited extent. Osteoblasts are post-proliferative cells with a cuboidal morphology situated along the sites of active bone matrix production (Franceschi, 1999). The mature osteoblasts are characterised by the ability of the cells to synthesise membrane-associated alkaline phosphatase, hormone and specific growth factor receptors (parathyroid hormone receptor PTH-R), bone matrix macro-molecules such as α1 collagen type I (Col1A1) and a variety of non-collagenous proteins including osteocalcin (OCN), osteopontin (OP), bone sialoprotein (BSP) and proteoglycans (Franz-Odendaal *et al.*, 2006).

The osteoblast repertoire is a spectrum of cells at different stages of maturation and therefore, different osteoblasts may express only a subset of these molecules at a given time. Osteoblasts are metabolically active and have well-developed organelles; large

eccentric nucleus with one to three nucleoli, prominent rough endoplasmic reticulum (RER) and Golgi bodies. A small proportion of osteoblasts, estimated at 10-20 %, incorporate themselves within the newly formed extracellular matrix (osteoid). These cells are considered to be at the most mature differentiation stage of the osteoblast lineage and are termed osteocytes. The sequential transition of osteoblasts to osteocytes is characterised by a reduction in intracellular organelles corresponding to a decrease in protein synthesis and secretion (Dudley and Spiro, 1961). Many of the previously expressed bone markers become down-regulated or switched off. The mature osteocytes may adopt different shapes depending on the bone type: woven bone consisting of random organisation of collagen fibres and mechanically weak have isodiametric osteocytes while lamellar bone consisting of regular parallel alignment of collagen sheets (lamellae) and mechanically strong has flattened osteocytes. Within the bone matrix, mature osteocytes are stellate-shaped with long cell processes (Currey, 2003).

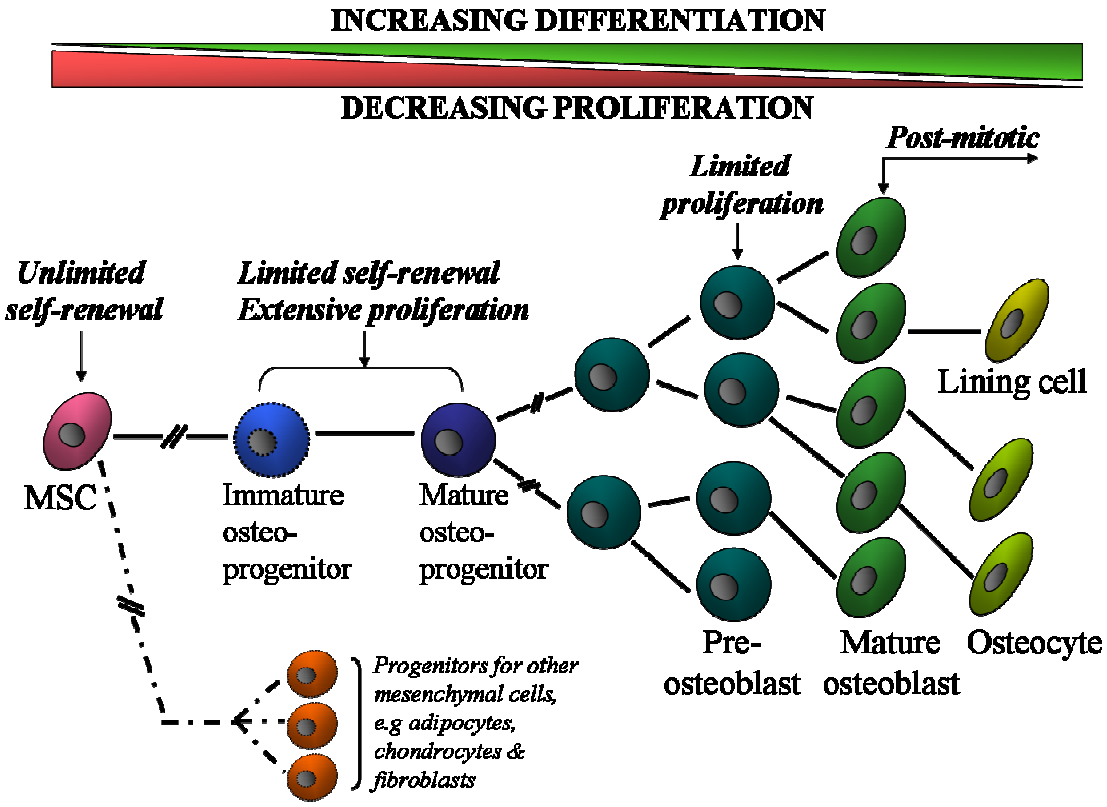

Figure 1.3: The different stages in osteoblast differentiation. Multipotent mesenchymal stem cells (MSC) commit to the osteoblast lineage by giving rise to the osteo-progenitor cells which possess limited self-renewal but extensive proliferation potential. As the progenitor cell differentiates, they lose their proliferative potential and in response to specific stimuli become specialised cells which maintain the bone structure (Adapted from Aubin and Liu, 1996).

1.4.2 Regulation of the osteoblast lineage

Bone formation during both development and remodelling requires stringent control of osteoblast proliferation and differentiation. The regulation of these processes involves the temporal expression of cell growth and bone-specific genes in response to physiological mediators, such as growth factors and hormones. Once MSCs are committed to the osteoblast lineage, they undergo a series of morphological and functional changes which are triggered by specific changes in gene expression. The sequential progression of the uncommitted stem cell to the mature osteocyte is tightly regulated and any failure in the control mechanism may result in diseased conditions (Aubin and Liu, 1996).

The key molecular players in osteogenesis can be divided into intracellular messengers including the transcription gene *Cbfa-1* (core binding factor 1) and the Wnt-β-catenin canonical pathway and extracellular messengers such as bone morphogenic proteins (BMPs). Other equally important factors influencing osteogenesis has been reviewed in (Deschaseaux *et al.*, 2009).

Cbfa-1 as the master gene of bone formation

Cbfa-1 is a runt-related gene also referred to as *Runt-related 2* (*Runx2*). It is the master transcription factor involved in commitment to the osteogenic lineage and functions by binding DNA via its runt domain (Figure 1.4). Cbfa-1 is a nuclear factor binding to OSE2 (osteoblast-specific *cis*-acting element 2) found at the promoter sites of bone-specific genes such as osteocalcin (OCN), bone sialoprotein (BSP), osteopontin (OP) and the α1 type I collagen gene (Col1A1) (Ducy, 2000). The involvement of *Cbfa-1* in the regulation of these vital osteoblastic genes was revealed by functional experiments in the first instance *in vitro* and later confirmed by *in vivo* work. Forced expression of Cbfa-1 in primary fibroblasts resulted in the expression of OCN and BSP (Ducy *et al.*, 1997) while silencing the gene inhibited the expression of these proteins (Banerjee *et al.*, 1997, Ducy *et al.*, 1997). Hinoi *et al.* (2006) demonstrated that *Cbfa-1* deficient (*Cbfa-1*$^{-/-}$) mice were unable to survive and exhibited no bone formation further indicating that *Cbfa-1* is a major factor in osteoblastic differentiation.

The binding of Cbfa-1 to DNA has been shown to be affected by various factors (Figure 1.4). During early development before commitment to the osteoblastic lineage, the nuclear protein Twist-1 and Cbfa-1 are transiently expressed, whereby Twist-1 delays osteogenesis by inhibiting Cbfa-1 activity. Upon initiation to the osteogenic lineage, Twist-1 is degraded causing activation of Cbfa-1 which induces the cell to differentiate (Bialek *et al.*, 2004). During osteoblast differentiation, other nuclear proteins are able to inhibit Cbfa-1 by physically interacting with its DNA binding domain. One such protein is the transcription factor signal transducer and activator of transcription 1 (Stat1), which is modulated by extracellular signals such as interferons (Kim *et al.*, 2003). Schnurri 3 (Shn3) is a zinc finger adapter protein which also acts as an inhibitor

of Cbfa-1 (Jones *et al.*, 2006a). Both Stat1 and Shn3 negatively regulate Cbfa-1 activity by preventing its translocation to the nucleus.

Positive regulators of Cbfa-1 have also been identified; homeobox-containing protein muscle segment homeobox homolog (MSX2), an upstream promoter of *Cbfa-1* (Satokata *et al.*, 2000) and special AT-rich sequence-binding protein 2 (Satb2), a nuclear matrix protein (FitzPatrick *et al.*, 2003). Satb2 positively influence osteoblast differentiation either by directly binding to the promoter element of BSP or in the case of OCN, by physical interaction with Cbfa-1 (Dobreva *et al.*, 2006). Satb2 is also able to exert its influence on bone formation via inhibition of the homeo box A2 (Hoxa2), a negative regulator of bone formation, by binding to the enhancer element present in the *Hoxa2* promoter region (Kanzler *et al.*, 1998). Mouse models have shown the involvement of another transcription factor termed Osterix (Osx), found to be crucial to bone development. Osx is an osteoblast-specific zinc finger-containing transcription factor. Osx specifically affects intra-membranous bone formation whereby *Osx*-deficient mice were deprived of mineralised matrix (Nakashima *et al.*, 2002). Osx is thought to exert its effect downstream of Cbfa-1 in the transcriptional cascade of osteoblast differentiation and that its expression is directly controlled by the binding of Cbfa-1 to the promoter region of *Osx* (Nishio *et al.*, 2006). Recent studies have identified other Osx-interacting molecules which may enhance bone formation. The transcription factor Nfatc1 (nuclear factor activated T cell 1) coupled with Osx form a DNA binding complex which activates the promoter fragment of Col1A1, a vital component in bone formation (Koga *et al.*, 2005). The transcriptional control of osteoblast differentiation is a complex mechanism which requires tight regulation to maintain the balance between cell proliferation and cell differentiation at each stage of the developmental programme.

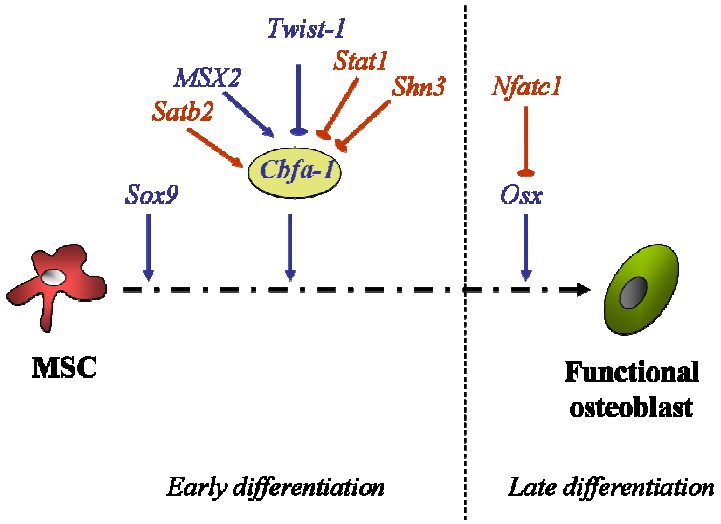

Figure 1.4: Schematic representation of the regulation of cellular differentiation along the osteoblast lineage. Lines with arrowheads indicate activation and lines with bars indicate inhibition. In blue is transcriptional control and in red is post-transcriptional control.

Wnt-β-catenin canonical pathway in bone formation

Wnt molecules are a family of secreted proteins which are crucial to osteogenesis (particularly Wnt 1, 3a, 4, 5, 10b and 13), among many other cellular functions (Liu *et al.*, 2008). Activation of the Wnt-β-catenin pathway positively influences proliferation and differentiation of MSCs to the osteogenic lineage while inhibiting the formation of adipocytes and chondrocytes (Takada *et al.*, 2007). Wnts act by binding to their membrane receptors, Frizzled 1 (Fzd1), 2, 4 and 5, and their co-receptor low-density lipoprotein receptor-related protein 5 (Lpr5) and 6. Following receptor binding, the canonical signalling pathway is activated and β-catenin is translocated to the nucleus (Etheridge *et al.*, 2004). This involves dishevelled (Dsh) and axin cytoplasmic proteins moving to the membrane to inhibit β-catenin degradation, consequently causing accumulation of β-catenin in the cytoplasm and nucleus. In the nucleus, β-catenin interacts with a transcription repressor lymphoid enhancer-binding factor/T-cell-specific transcription factor (LEF/TCF). This allows activation of gene transcription via the recruitment of the histone acetylase CBP/p300 (CREB binding protein). In the absence of Wnt, β-catenin is phosphorylated by GSK3β leading to its degradation by ubiquitination. Wnts are able to act endogenously and their effects appear to be concentration dependent. High levels of endogenous Wnt appear to favour proliferation to differentiation (Deschaseaux *et al.*, 2009). On addition of specific inhibitors such as

Dickkopfs 1 (DKK1), Wnt signals are decreased and osteogenesis is induced. DKK1 binds to Lpr5 co-receptor to modulate Wnt signalling and its effect has been demonstrated in DKK1-deficient mice which showed increased bone mass (Morvan *et al.*, 2006).

Bone Morphogenetic Proteins (BMPs)

BMPs are members of the transforming growth factor β (TGFβ) family of paracrine factors (Grimaud *et al.*, 2002). There are two major forms of BMP receptors; type I receptors also known as Activin receptor-like kinase (Alk) 1-7 and type II receptors which are constitutively active and phosphorylate type I receptors upon ligand binding. Alk2, 3 and 6 are targets for BMPs while Alk4 and 5 are targets for activin (TGFβ-like protein) and TGFβ1, respectively. On activation by the type II BMP receptors, Alks transduce signals to Smad proteins within the cytoplasm. The different Smad molecules are then able to form complexes which are translocated to the nucleus to activate specific target genes (Chen *et al.*, 2004). The BMPs (notably BMP2 and BMP4) play a crucial role in terminal differentiation of osteoblasts and do so by activating the transcription factor *Osx* downstream of *Cbfa-1* via the Smad pathway (Nakashima *et al.*, 2002). However in a recent study by Seib and colleagues (Seib *et al.*, 2009), endogenously expressed BMPs (particularly 2, 4 and 6) were found to be active through a mitogen-activated protein kinase pathway (MAPK) rather than the Smad pathway.

The MAPK pathway acts at different stages of the differentiation process and is involved in activating molecules by phosphorylation. MAPK responds to the extracellular molecular environment and exerts its effect on either proliferation of MSC or commitment to differentiation depending on the stimuli, which includes growth factors and pro-inflammatory molecules (Xiao *et al.*, 2000). The pivotal roles of MAPK include phosphorylation of master transcription factor Cbfa-1 in pre-osteoblasts, activation of GSK3β in the Wnt pathway leading to β-catenin accumulation and pro-osteogenic signal transduction triggered by endogenous BMPs (Thornton *et al.*, 2008).

1.5 Osteosarcoma (OS)

The mechanism of bone formation is a complex process involving intricate pathways which necessitate numerous regulatory checkpoints. Despite advances in the field of bone biology, the molecular mechanisms and transcriptional regulators mediating the decisions of cell differentiation and osteoblast-specific gene expression are not well understood. Impaired regulatory elements at any stage of the osteoblast lineage results in bone pathologies, among which is osteosarcoma (OS).

OS is a tumour of the bone and mainly affects adolescents when skeletal growth is at its peak. OS is the most common non-haematopoietic cancer and has a poor prognosis in patients with relapse or recurrence (Bruland and Pihl, 1997, Meyers and Gorlick, 1997, Toledo *et al.*, 2010). Several proto-oncogenes such as *c-myc*, *c-ras*, *c-sis*, *c-bos* and *c-abl* have been implicated in OS induced conditions, but none of them could be attributed to a particular osteoblast phenotype (Schon *et al.*, 1986, Bogenmann *et al.*, 1987, Nardeux *et al.*, 1987). As in other cancer pathologies, inactivating mutations in the tumour suppressor genes pRb and p53 have been found to contribute to uncontrolled cellular proliferation in OS (Diller *et al.*, 1990, Miller *et al.*, 1996). While there is no one specific gene mutation identified in osteosarcoma specimens, one key player, the nuclear oncogene and transcription factor c-Fos, has been identified as an important regulator of the fate of specific bone cell populations, both in normal development and in bone disease (Grigoriadis *et al.*, 1995). The expression of *c-fos* is known to be elevated in OS derived from both mice and human (Wu *et al.*, 1990, Honoki *et al.*, 1992). The c-fos onco-protein is a major component of AP-1 transcription factor complex, which also includes several other Fos-related and Jun-related proteins (Ransone and Verma, 1990). Fos-Jun complexes activate gene transcription by directly binding to the regulatory region of the target gene (Angel and Karin, 1991) and suppress gene transcription by physical protein-protein interaction (Beato *et al.*, 1995). In response to extracellular signals, c-fos is able to mediate short and long-term changes in gene expression to modulate cellular proliferation and differentiation suggesting its involvement in the osteoblastic lineage.

1.5.1 Stem Cells and Cancer

Under normal circumstances, stem cells generate tissue-specific differentiated cells in response to damage or to tissue renewal. However, genetic mutations in the precursor cells may result in uncontrolled tissue regeneration and tumour formation. The two major properties of stem cells are that of extensive self-renewal ability and differentiation potential. Based on these criteria, cancers are believed to be a disease of stem cells (McDonald *et al.*, 2009). Firstly, according to the mutation and selection theory of cancer, stem cells represent a rare population of cells which are able to survive long enough to accumulate the requisite number of genetic changes leading to aberrant self-renewal and tumour formation (Tomlinson and Bodmer, 1999). Secondly, the presence of multiple cell types within a tumour mass points towards a multipotent cell origin (Pierce, 1977).

Many reports suggest similarities between normal stem cells and tumourigenic cells. To better illustrate this comparison, it is fair to view a tumour as an aberrant organ (Reya *et al.*, 2001). According to the principles of normal stem cell biology and organogenesis, the aberrant organ is believed to originate from a tumorigenic cancer cell which has acquired the ability for unlimited proliferation via accumulated mutations (Morrison *et al.*, 1997). As such, both normal stem cells and tumorigenic cancer cells have an extensive proliferative potential and the ability to form new tissues (normal and abnormal) (Weissman, 2000). Normal tissues as well as tumours are composed of a heterogeneous population of cells with varied phenotypic characteristics and proliferative potentials (Fidler and Hart, 1982, Heppner, 1984).

Although some of the heterogeneity observed in tumours is due to continuing mutagenesis, it is likely that the heterogeneity also arises from aberrant differentiation of cancer cells. The presence of cancer cells with heterogeneous phenotypes within a tumour has been reported in different cancers and appears to depict the normal aspects of differentiation in the tissues from which the tumours arise (Fialkow, 1976). This is further supported by the variable expression of normal differentiation tissue-specific markers on cancerous cells within a tumour indicating anomalous differentiation of the

tumour cells (Sell and Pierce, 1994). Analogous to normal stem cells, tumorigenic cells are able to give rise to phenotypically heterogeneous cells which exhibit different levels of differentiation. The anomaly resides in the fact that the aberrant organ (tumour) formed from the cancer cells has no functional characteristics and is detrimental to the individual.

1.5.2 Evidence of Cancer Stem Cells (CSCs)

In 1977, Hamburger and Salmon proposed the cancer stem cell theory which was based on the observation that only a sub-population of cancer cells was able to form colonies in a soft agar *in vitro* assay (Hamburger and Salmon, 1977). The first set of in culture and *in vivo* experiments were carried out on haematopoietic cancers such as leukaemia and multiple myeloma (Park *et al.*, 1971, Bruce and Van Der Gaag, 1963). These observations were later extended to solid cancers whereby it was shown that the tumours were phenotypically heterogeneous and only a small proportion of cells (1 in 1000 to 1 in 5000 for lung, ovarian and neuroblastoma cells) was able to proliferate *in vitro* and *in vivo* (Fidler and Kripke, 1977, Nowell, 1986). Although the rarity of these tumourigenic cells is still being debated, the cancer stem cell theory is gaining popularity and putative markers for the identification of this cell subset are being investigated (Yoo and Hatfield, 2008). Existing cancer therapies which are aimed at tumour shrinkage are based on the stochastic model (Figure 1.4 A) but the failure of these approaches suggests that the cancer stem cell model (Figure 1.4 B) may be more appropriate.

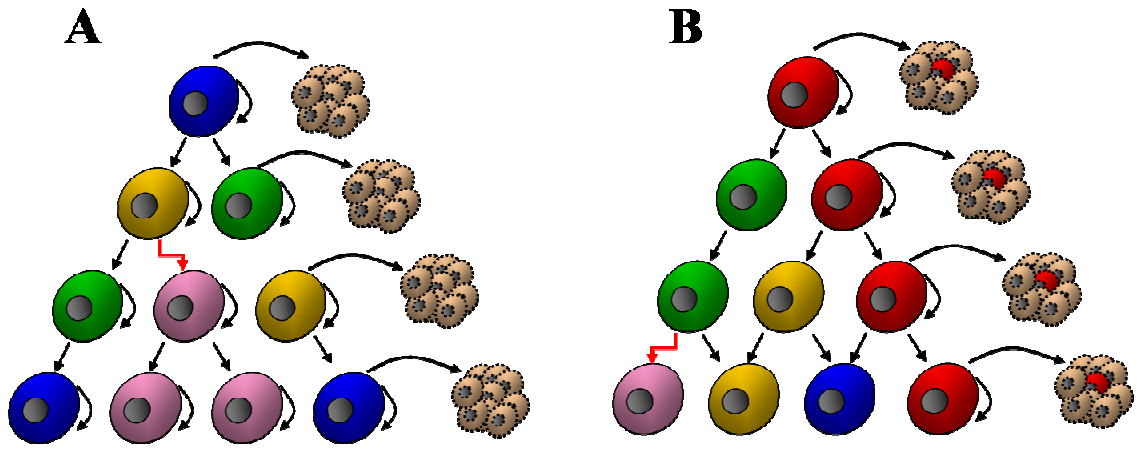

Figure 1.5: Two models of heterogeneity in solid cancer cells. (A) Stochastic model; cancer cells of different phenotype have extensive proliferation potential and any one cell is able to generate new tumours when transplanted. (B) Cancer Stem Cell model; cancer cells are heterogeneous and only the cancer stem cells (CSCs; in red) have extensive proliferation potential and are able to generate tumours when transplanted. (Adapted from (Reya *et al.*, 2001).

1.5.3 Markers of CSCs

CSCs feature as a promising target in cancer therapy as these cells are thought to be responsible for cancer relapses, due to their resistance to chemotherapy and ability to extensively proliferate (Mimeault *et al.*, 2007). Considerable effort is being invested in the quest for markers of CSCs and there is mounting evidence to suggest that these malignant cells would have retained certain molecules expressed by their normal counterparts (McDonald *et al.*, 2009). Most of the markers studied appear to be restricted to the tissue the tumours are derived from and may not represent a general marker for all CSCs. Among them are molecules involved in maintaining stemness, niche adhesion and cytoprotection (Alison and Islam, 2009).

CD44 is a multi-structural and multi-functional transmembrane glycoprotein often over-expressed on tumour cells. Originally described as a lymphocyte homing receptor (Gallatin *et al.*, 1983), the different splice variants of CD44 were later shown to be implicated in cancer metastasis (Gunthert *et al.*, 1991). Cancer progression is greatly dependent on the tumour cell's ability to attach to and detach from the various cellular components during migration. CD44 has been shown to play a crucial role as an

adhesion molecule mediating cell to cell and cell to extra-cellular matrix interaction, promoting dissemination of malignant cells (Jothy, 2003, Marhaba and Zoller, 2004). As such the enhanced expression of CD44 in combination with other markers has been used to identify CSCs in a number of solid cancers (Section 1.5.3). More recently, CD44 is being investigated as a therapeutic target for metastasising tumours by induction of apoptosis in the cancer cells (Orian-Rousseau, 2010).

Putative CSCs are able to withstand cytotoxic insults by efficient enzyme-based detoxifying mechanisms or rapid efflux of potentially harmful xenobiotics. Indeed, these cells have been shown to have elevated expression of aldehyde dehydrogenase (ALDH) gene superfamily encoding detoxifying enzymes and ATP-binding cassette (ABC) superfamily of membrane transporters (Vasiliou and Nebert, 2005). Treatment of human colorectal tumours with cyclophosphamide resulted in an enrichment of $CD44^{+}ALDH^{+}$ cells, subsequently found to be more tumourigenic than cells enriched on the basis of CD44 alone (Dylla *et al.*, 2008), indicating that the double positive cells may represent the CSC population. The ABC proteins are able to hydrolyse ATP and efflux substrates against concentration gradients. These transporters are found on a subpopulation of cells, referred to as the 'side population' (SP) by virtue of their ability to efflux the Hoechst dye (Goodell *et al.*, 1996). The SP phenotype has often been associated with the stem cell population in cancers, for instance ABCG2 transporter, also known as the breast cancer resistance protein (Hirschmann-Jax *et al.*, 2005). However, this observation does not stand for all tissues as SP cells have been found to correspond to a non stem cell population in the human and mouse epidermis (Triel *et al.*, 2004). In a study by Alison and co-workers (Alison *et al.*, 2006b), it was found that the SP cells from colorectal cancers were not enriched in CSCs and that both SP-enriched and SP-negative cells were equally able to induce tumours in immunodeficient mice.

In the recent years, the molecule CD133 (Prominin-1) has gained widespread popularity in the CSC field. CD133 is a pentaspan membrane protein originally identified on plasma membrane protrusions such as epithelial microvilli and epididymal ductal epithelial sterocilia. AC133 antigen, a glycosylation-dependent epitope of CD133, was

later found to be expressed on $CD34^+$ progenitor populations from adult blood and bone marrow, featuring CD133 as a marker of haematopoietic progenitors (Yin *et al.*, 1997). Since then, CD133 has been explored as a cell surface marker of adult stem cells. A number of studies have reported the use of CD133 positive cells as stem cells capable of self-renewal and multi-lineage differentiation (Mizrak *et al.*, 2008). For instance, $CD133^+$ cells isolated from the adult human kidney were shown to regenerate renal tissues by differentiating to both the epithelial and endothelial lineages (Bussolati *et al.*, 2005) and more recently $CD133^+$ cells isolated from the human embryonic forebrain were used to enrich for neural progenitors (Barraud *et al.*, 2007). While CD133 has been used as a marker of stem cells in many adult tissues, it has also been studied as a marker of CSCs in various human tumours (Table 1.3). $CD133^+$ cells are generally assessed as being CSCs by their ability to form colonies and proliferate *in vitro* and their potential to recapitulate the original tumour phenotype when transplanted either subcutaneously or into the renal capsule of immunodeficient mice (O'Brien *et al.*, 2007, Yin *et al.*, 2007).

Recent work by Tirino and co-workers (Tirino *et al.*, 2008) reported to have identified the CSC population in osteosarcoma using CD133 as a positive marker. Using three osteosarcoma cell lines (MG-63, Saos-2 and U-2-OS), they found that about 3 to 5 % of the whole population were $CD133^+$ by flow cytometry while immuno-fluorescence data revealed that all the three cell lines exhibited positive intracellular staining. Of the cell subset displaying surface CD133 expression, only a small proportion (0.97 %) exhibited characteristics attributed to CSCs, namely the SP profile and presence of the ABCG2 transporter (member of the ABC superfamily of membrane transporters). However, the tumorigenicity of the $CD133^+$ population remains to be confirmed *in vivo* given that to date there is no robust mouse model able to successfully engraft osteosarcoma cells. Due to inconsistency in screening methodology, there are contradictory data suggesting that CD133 may not be a marker of CSCs but a marker of normal progenitor cells restricted to certain specific cell type, for instance in human brain tissues and haematopoietic cells (Uchida *et al.*, 2000, Corbeil *et al.*, 2000, Patru *et al.*, 2010). Furthermore, it is important to distinguish between CD133 and the glycosylated epitope

AC133 as being a reliable CSC marker given that these two terms have been used interchangeably in the literature.

Tumour origin	Antigenic phenotype	Reference
Osteosarcoma	CD133, ABCG2, SP	(Tirino *et al.*, 2008)
Prostate tumours	CD133, CD44, $\alpha_1\beta_2$	(Collins *et al.*, 2005)
Pancreatic adenocarcinoma	CD133, ABCG2	(Olempska *et al.*, 2007)
Colon carcinoma	CD133	(Ricci-Vitiani *et al.*, 2007)
Hepatocellular carcinoma	CD133	(Suetsugu *et al.*, 2006)
Neural tumours	CD133, nestin	(Singh *et al.*, 2003)
Renal tumours	CD133	(Bruno *et al.*, 2006)

Table 1.3: CD133, often in combination with other markers, used to identify cancer stem cells (CSCs) in a variety of human solid cancers.

1.5.4 Epithelial-Mesenchymal Transition (EMT)

The epithelial-mesenchymal transition (EMT) is a major developmental process occurring during cancer metastasis and invasion. It involves a phenotypic shift whereby epithelial cells from the primary tumour breaks down cell-cell and cell-extracellular matrix connections and then migrate as mesenchymal cells to distant locations in the body. Upon EMT, the mesenchymal cells acquire a stem cell phenotype allowing them to spawn secondary tumours in the body. Once the migrating cells become lodged in their destination, they undergo reverse EMT, mesenchymal-epithelial transition (MET) and form a tumour recapitulating the phenotype of the tumour of origin (Figure 1.6) (Radisky and LaBarge, 2008).

EMT is a natural process which takes place during ontogeny. It is vital during gastrulation (early embryonic developmental phase to produce the three germ layers) and post-natal organ morphogenesis (tissue reconstruction and regeneration) (Shook and Keller, 2003). Recently, with the growing acceptance of the involvement of CSCs in oncology, EMT or EMT-like processes have been implicated in the metastatic and invasive mechanisms of tumour growth and the migrating cells are thought to be the putative CSCs (Thiery and Sleeman, 2006, Hugo *et al.*, 2007). A number of experiments in epithelial tumours have attempted to prove this theory and CD44 has

been a marker commonly used to achieve this. Al-Hajj and co-workers (Al-Hajj *et al.*, 2003) demonstrated that in metastatic human breast cancer, a small subset of the carcinoma cells exhibiting the stem cell antigenic phenotype $CD44^{high}/CD24^{low}$ were able to initiate new tumours in mice unlike the majority of the tumour cells of $CD44^{low}/CD24^{high}$ phenotype. The metastatic process parallels the processes of tissue regeneration, whereby stem cells exit their niche (for instance MSC exiting the bone marrow) and enter the circulation to home into injury sites where they proliferate and differentiate to contribute to tissue repair. *In vivo* the ability of the cancer cells to colonise a distant location would require them to survive dissemination via the lymphatic or vascular system and to possess self-renewal capacity characteristic of stem cells.

A compelling study by Mani and co-workers (2008) has established a link between putative CSCs and the migrating cells in an induced EMT model of immortalised human mammary epithelial cells. By inducing EMT in the mammary epithelial cells (via ectopic expression of transcription factors Snail and Twist or exposure to TGFβ1), the cells adopted a mesenchymal phenotype characterised by down-regulation of E-cadherin, and up-regulation of fibronectin and vimentin. Further to this the induced mesenchymal cells expressed the stem cell antigenic profile $CD44^{high}/CD24^{low}$, previously ascribed to neoplastic mammary stem cells (Al-Hajj *et al.*, 2003, Sleeman *et al.*, 2006, Liao *et al.*, 2007). In a tumour forming assay, the $CD44^{high}/CD24^{low}$ mesenchymal induced population were found to readily form mammospheres (between 30-40 % more) compared to their $CD44^{low}/CD24^{high}$ epithelial counterparts (Mani *et al.*, 2008). These results clearly illustrate the vital role played by the EMT process in the metastasis of carcinomas and that the CSCs may be the migrating mesenchymal-like cells.

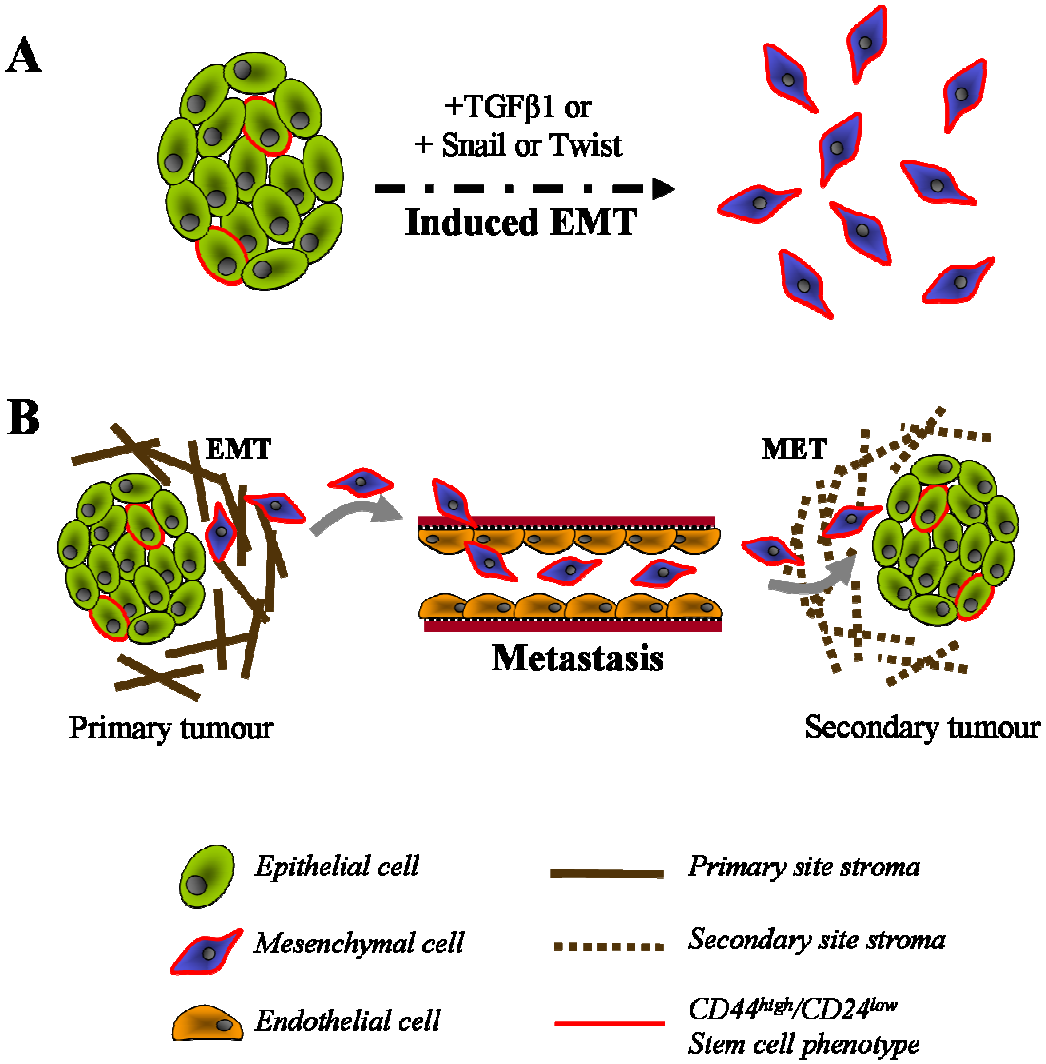

Figure 1.6: Proposed model of EMT induction in epithelial cells mediating cancer metastasis. (A) Induced EMT, via ectopic expression of Snail/Twist or exposure to TGFβ1, gives rise to migratory cells possessing the cancer stem cell phenotype $CD44^{high}/CD24^{low}$. (B) EMT facilitates intravasation of tumour cells into blood or lymph vessels, allowing them to migrate to different anatomical locations, where MET results in the formation of secondary tumours (Adapted from Mani *et al.*, 2008).

1.5.5 Cellular hierarchy in cancers

It has long been established that the basic key properties defining stem cells are high self-renewal capacity and the ability to generate cells that can differentiate to maintain tissue structure and function (Lajtha, 1979). In continuously renewing tissues, such as blood and epithelia, an additional proliferative phase has been described whereby the cells produced by stem cell divisions (symmetric and asymmetric as illustrated in Figure 1.7) enter the differentiation pathway by undergoing a series of divisions to amplify the maturing population prior to terminal differentiation (Potten, 1981, Morrison *et al.*, 1997). While emerging evidence shows that tumour development follows the CSC model (Figure 1.5 B), a similar stem cell pattern to that seen in normal tissues has been proposed in cancers (Mackenzie, 2005). Mackenzie's group characterised the cellular hierarchy which exists within epithelial tissues by identifying three categories of cells as: (i) stem cells with infrequent cell divisions but retaining extensive self-renewal potential, (ii) amplifying cells with limited capacity to proliferate and (iii) post-mitotic differentiating or terminally differentiated cells (Tudor *et al.*, 2004). Thereafter, a cellular hierarchy analogous to that observed in normal epithelial tissues was identified in carcinoma cell lines and the three cell types were indentified as holoclones, meroclones and paraclones (Locke *et al.*, 2005).

Studying the cellular hierarchy exhibited by stem cells *in vivo* is very difficult and *in vitro* systems that retain similar stem cell patterns have been found appropriate for such investigations (Sherley, 2002). However, malignant cell lines naturally exhibit marked morphological heterogeneity due to the cellular diversity caused by genetic instability and possibly *in vitro* conditions (Burdall *et al.*, 2003), thus leading to criticisms of such *in vitro* studies (Pardal *et al.*, 2003). Nevertheless, the morphological heterogeneity described in carcinoma cells lines (Locke *et al.*, 2005) parallels the cellular hierarchy previously described in normal keratinocytes *in vitro* (Barrandon and Green, 1987) therefore supporting the *in vitro* system as a reliable method to study stem cell patterns in malignant cell lines. As such, the characterised colonies identified in carcinoma cell lines reflect those characterised in normal keratinocyte populations whereby holoclones appear as compact round colonies, paraclones forming irregular loosely attached colonies and meroclones exhibiting intermediate features (Mackenzie, 2005).

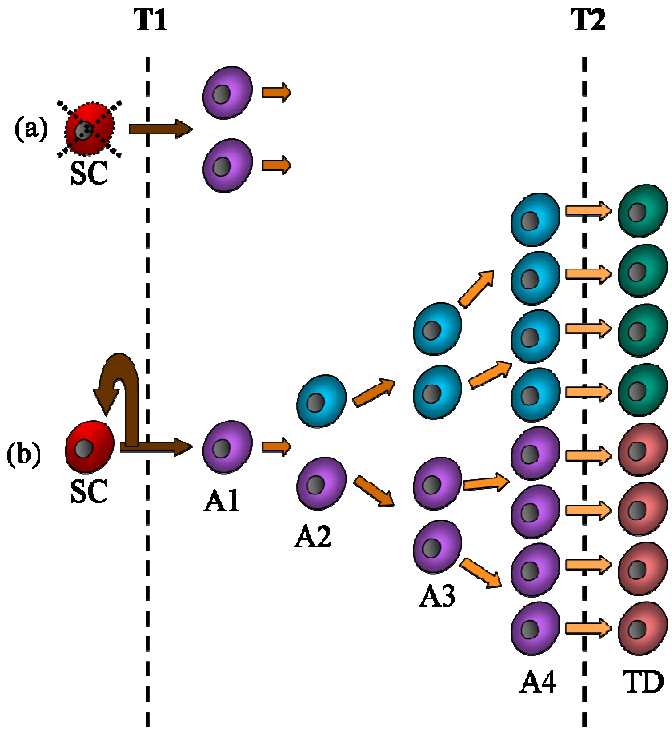

Figure 1.7: Stem cell pattern of division in epithelial tissues (a) Symmetric pattern of division produces two identical daughter cells and leads to the depletion of the stem cell reservoir (SC). (b) Assymetric pattern of division produces two dissimilar cells, one which remains identical to the parental cell and replenishes the stem cell reservoir (SC) and the other which enters the differentiation pathway and loses stem cell properties. The pathway is represented by three tiers separated by dashed lines T1 and T2. The tiers are categorised as stem cells (SC), transient amplifying cells (A1 to A4) and terminally differentiated cells (TD). The amplification pathway follows a series of cell divisions resulting in expansion of the differentiating cell population (A1 to A4) which ultimately become terminally differentiated (TD). The ratio of cells present in each tier is influenced by numerous factors, including the rate of stem cell division and the time taken for cells to differentiate (Adapted from Mackenzie 2006).

An in-depth combined investigation of fifteen cell lines derived from oral carcinomas, the prostate cell line DU145, breast cancer cell line MCF7 and a range of established and freshly derived head and neck squamous cell carcinoma cell lines by Mackzenzie's group described the presence of cells of holoclonal, meroclonal and paraclonal morphologies, although the meroclonal cells were arbitrarily classified because of the continuous gradient of change from one colony form to the other (Locke *et al.*, 2005, Harper *et al.*, 2007). The malignant holoclonal cells were found to be small, rapidly adhesive and highly clonogenic exhibiting high levels of β1-integrin, β-catenin, E-cadherin and cytokeratin 15, markers normally over-expressed in epithelial stem cells (Cotsarelis *et al.*, 1999, Tudor *et al.*, 2004). In addition to the epithelial markers, the holoclones displayed stronger CD44 expression than paraclones, a selective molecule in identifying CSCs in breast cancers (Al-Hajj *et al.*, 2003) and exhibited high levels of CD133 staining at the centre of the holoclonal colonies in line with previous reports of CD133 as a marker of CSC in solid tumours (Table 1.3). Moreover, contrary to the paraclonal cells, cells isolated and expanded from the holoclonal colonies were able to generate colonies of heterogeneous morphology as observed in the parental cell line. The lack of expansion potential of paraclones indicated that these cells may represent the late amplifying or differentiated cells in the stem cell pattern of division described above, while the holoclones by virtue of their stem cell expansion and marker properties may represent the malignant stem cell population in the carcinoma cell lines (Mackenzie, 2005, Mackenzie, 2006).

1.6 Thesis hypothesis and aims

The primary hypothesis of this thesis is that STRO-1 is an antigen expressed by multipotent hMSCs and therefore a potential biomarker in the isolation of homogeneous populations of *in vitro* expanded multipotent hMSCs. The STRO-1 antigen is as yet unidentified. Characterising and elucidating the identity of STRO-1 antigen will further our knowledge on factors maintaining hMSC primitive properties and enable isolation of pure hMSC populations for clinical applications. Furthermore, knowing the antigenic determinant of STRO-1 will open up avenues to generate novel antibodies against the multipotent hMSCs and subsequently developing new tools promoting successful MSC isolation. Secondly, STRO-1 is hypothesised as a putative marker for CSCs in osteosarcoma. There is mounting evidence in the literature to suggest that osteosarcomas are mesenchymal tumours which arise from CSCs originating from mutated MSCs. Following this principle, CSCs in osteosarcoma may have retained certain stem cell markers such as STRO-1. By employing STRO-1 as a CSC marker in osteosarcoma, and possibly applying it to other mesenchymal tumours, these rare tumourigenic cells can be identified leading to development of targeted chemotherapy.

In order to investigate the hypotheses, the main aims of the thesis are to achieve the following:

- **Characterise STRO-1 expression on *in vitro* expanded hMSCs.** Freshly derived bone marrow hMSC populations have been shown to heterogeneously express STRO-1. Culture expanded hMSCs will be monitored for their STRO-1 expression and differentiation potential and a relationship between the level of STRO-1 expression and multilineage ability will be established.

- **Elucidate the identity of the STRO-1 antigen.** Two methods will be used in an attempt to identify the STRO-1 antigen. In the first instance, phage display technology will be undertaken as an epitope mapping approach. Secondly, a comparison of gene expression microarray profiles of osteosarcoma cell lines will be employed to identify potential candidate genes encoding the STRO-1 antigen.

- **Identify putative CSCs in osteosarcoma cell lines.** A panel of osteosarcoma cell lines will be characterised in terms of their antigenic and cellular phenotypes as well as stem cell properties. The relationship between STRO-1 expression and retention of MSC characteristics will also be studied. A cellular hierarchy in osteosarcoma will be proposed and investigated.

Chapter 2
Materials and Methods

2.1 Materials

All reagents, histochemical stains and general chemicals were obtained from Sigma-Aldrich (Dorset, UK) unless otherwise stated. All tissue culture media and reagents were obtained from Invitrogen (GIBCO®; Paisley, UK), unless otherwise stated. Antibodies used in cell profiling are listed in Table 2.2 and those used for other applications are specified within relevant sections. Primers used in gene expression analysis (Table 2.3) were commercially synthesised by Invitrogen (Paisley, UK). The source of all other materials is specified in the relevant sections.

Human Mesenchymal Stem Cells (hMSCs: M24♂, N24♂, 31♂, 38♀) were isolated previously in this laboratory (Westwood 2006 and Vujovic 2006). The seven osteosarcoma cell lines (143B, CAL72, G-292, HOS, MG-63, Saos-2 and U-2-OS) were generous gifts from Professor Adrienne Flanagan and Dr Nadege Presneau (The Cancer Institute, University College London).

2.2 Cells

hMSC isolation (Westwood 2006 and Vujovic 2006)

Human bone marrow derived mesenchymal stem cells (hMSCs) were obtained from four healthy donors and labelled as M24♂ (24 year old male), N24♂ (24 year old male), 31♂ (31 year old male) and 38♀ (38 year old female). Bone marrow aspirates (about 10 mL) were taken from the iliac crest of transplantation donors after informed consent and with prior approval from University College London Hospital ethics of human research committee, in association with the Molecular Haematology Department, UCL. Briefly, mononuclear cells were isolated by Ficoll-Plaque gradient and seeded at $2x10^5$ bone marrow mononuclear cells/cm^2 in 6-well plates. Non-adherent cells were removed two days after plating, adherent cells fed with fresh media and colonies formed were designated as passage 0 (p0).

Osteosarcoma cell lines

The panel of osteosarcoma cell lines used in this study are 143B, CAL72, G-292, HOS, MG-63, Saos-2 and U-2-OS. The cell lines were derived from bone tumours in teenagers and are banked by ATCC® (American Type Culture Collection) except for CAL 72 which was derived by Rochet *et al.* (1999) (Table 2.1). 143B and HOS were derived from the parent TE85 by Ki-ras transformation (McAllister *et al.*, 1971) and *N*-methyl-*N*'-nitro-*N*-nitrosoguanidine (MNNG) treatment (Rhim *et al.*, 1977) respectively.

Cell line	Source	ATCC® number
143B*[1]	13 year old, female	CRL_8303
CAL72	10 year old, male	#
G-292	9 year old, female	CRL_1423
HOS*[2]	13 year old, female	CRL_1543
MG-63	14 year old, male	CRL_1427
Saos-2	11 year old, female	HTB_85
U-2-OS	15 year old female	HTB_96

Table 2.1: Osteosarcoma cell lines screened. * indicates cell lines derived from TE85 by *Ki-ras* transformation (*[1]) and by *N*-methyl-*N*'-nitro-*N*-nitrosoguanidine MNNG treatment (*[2]). # indicates ATCC® bank number not available; cell line derived by (Rochet *et al.*, 1999).

2.2.1 Cell culture

hMSCs were cultured in Alpha-Minimal Essential Medium (α-MEM) supplemented with 10 % FCS (HyClone, Fisher Scientific) and 1 ng/mL basic Fibroblastic Growth Factor (bFGF) (Peprotech, UK). Osteosarcoma cell lines were cultured in DMEM supplemented with 10 % Fetal Calf Serum (FCS) (GIBCO®) and antibiotic-antimycotic (GIBCO®:100X stock, 10 000 units/mL penicillin G sodium, 10 000 µg/mL streptomycin sulphate and 25 µg/mL amphotericin) where required. To initiate culture, cells from liquid nitrogen storage were quickly thawed in a 37 ºC water bath, washed with warm complete media to remove traces of freezing medium and seeded in tissue culture dishes. After seeding, cells were cultured in a humid 37 ºC incubator (BINDER APT.line™ C150), maintained at 5 % CO_2, and fed every three days with appropriate media.

2.2.2 Passaging cells

During hMSCs expansion, cells were maintained at sub-confluency. When 75-85% confluency was reached, they were passaged and re-seeded or frozen down. Briefly, the adherent monolayer was washed with DPBS (Calcium and Magnesium free), detached with 0.25 % trypsin enzyme treatment (10x stock) for 2-3 min at 37 °C and the trypsin inactivated with 10 % FCS-containing media. The cells were then centrifuged at 1000 rpm for 5 min (IEC CL30 Centrifuge, Thermo Scientific) and the cell pellet suspended in the appropriate volume of media and seeded at $4x10^3$ cells/cm^2 or suspended in FCS containing 10 % v/v dimethyl sulfoxide (BD Biosciences) for storage in liquid nitrogen.

Osteosarcoma cells lines were grown to 80-90% confluency before passaging either 1:4 (one dish subcultured into four dishes) (CAL72, Saos-2) or 1:5 (one dish subcultured into five dishes) (143B, G-292, HOS, MG-63, U-2-OS). Osteosarcoma cells were detached using trypsin enzymatic treatment and passaged or frozen down as described above.

2.2.3 STRO-1 hybridoma culture

STRO-1 hybridoma frozen cell line was purchased from DSHB (Developmental Studies Hybridoma Bank, Iowa, USA). The cells were grown in suspension in RPMI-1640 media supplemented with 10 % FCS (HyClone). Three days after seeding in 20 mL media, the cells were split 1:2, media volume adjusted to 20 mL and a further 20 mL fresh media added at 2 day intervals for 4 days. After 14 days, the cells reached stationary phase and the supernatant was collected via centrifugation (IEC CL30 Centrifuge, Thermo Scientific, 1000 rpm, 5 min), filtered (0.2 µm pore size), dispensed in aliquots and stored at 4 ºC.

2.2.4 STRO-1 antibody concentration from hybridoma culture

The concentration of STRO-1 antibody produced from the hybridoma culture was quantified by ELISA against a standard curve drawn from known concentrations of STRO-1 antibody purchased from R&D Systems (Oxford, UK). Commercially obtained STRO-1 was reconstituted in DPBS to a concentration of 500 µg/mL and stored at -20 ºC as 10 µL aliquots. Wells of a 96-well plate were coated (overnight at 4 ºC in a humid chamber) with 100 µL of different concentrations of commercial STRO-1 antibody, 100 µL neat supernatant and RPMI complete media, in triplicate. The following day, the wells were washed once with DBS (200 µL/well), blocked with 1 % BSA/PBS (200 µL/well) for 2 h, washed twice with DPBS and incubated 1:2000 with goat anti-mouse IgM (µ chain specific) HRP conjugated antibody (Southern Biotech, Birmingham, USA) for 2 h at room temperature. The colour was developed using 100 µL reconstituted ABTS per well for 20 min in the dark and absorbance read at 405 nm (Sunrise, TECAN™).

2.2.5 Soft agarose assay

Osteosarcoma cell lines were assayed for anchorage-independent growth in 6-well plate formats in triplicates. A 2 % stock of agarose solution was prepared by melting 6 % low melting point agarose solution, uniformly mixed with complete DMEM medium (containing antibiotic/antimycotic) and kept at 55 ºC. For the base layer, the 2 % agarose stock solution was diluted to 0.6 % in complete media and 2 mL of the solution was layered in each well. The base layer agarose was left to set for 30 min at 4 ºC and prior to seeding the top layer, the plate was warmed for 5 min at 37 ºC. The cells were trypsinised, counted using a haemocytometer and suspended in 2 % agarose to make a final concentration of 0.35 % agarose of which 2 mL was seeded per well to give a density of $1x10^4$ cells per well. The agarose was set for 30 min at 4 ºC and then placed in the incubator at 37 ºC. The next day, the cells were fed with 2 mL complete DMEM and every 3 days from then on, for up to 12 days. Colony formation was monitored at specific time points under phase contrast microscope (Inverso 3650, Medline Scientific Limited).

2.3 Differentiation

2.3.1 Differentiation assays

The monolayer cultures were grown to confluency in appropriate media and induced to the adipogenic and osteogenic lineages by the addition of specific differentiation cocktails as described in the relevant sections.

2.3.1.1 Adipogenic differentiation

Cells were grown to confluency and induced at one day post-confluency. On the day of adipogenic induction (day 0), the medium was changed to adipogenic differentiation medium comprising of basal media with 10 % FCS (α-MEM for MSC and DMEM for osteosarcoma cells) supplemented with 1 µM Dexamethasone, 500 µM Isobutyl-methylxanthine, 100 µM Indomethacin and 10 µg/ml Insulin (Roche). The cells were fed every 3 days with freshly prepared adipogenic differentiation medium and differentiated for 8 days.

2.3.1.2 Osteogenic differentiation

Cells were grown to confluency and induced at one day post-confluency. On the day of osteogenic differentiation (day 0), the media was changed to osteogenic differentiation medium comprising of basal media with 10 % FCS (α-MEM for MSC and DMEM for osteosarcoma cells) supplemented with 0.1 µM Dexamethasone, 10 mM β-glycerophosphate and 50 µM L-Ascorbic acid 2 phosphate. The cells were fed every 3 days with freshly prepared osteogenic differentiation medium and differentiated for up to 21 days.

2.3.2 Staining protocols for assessment of differentiation

2.3.2.1 Adipogenesis: Oil Red O

After 8 days of adipogenic differentiation, the lipid droplets inside the adipocytes were stained with Oil Red O. Cells were carefully washed with DPBS and fixed with fixative solution (4 % formaldehyde, 75 mM sodium phosphate buffer pH 7, 1.5 % methanol) for 30 min at room temperature. Cells were then washed 3 times with DPBS and stained with Oil Red O solution for 2-3 h in the dark. Oil Red O dye was prepared by making up a 1 mg/mL stock solution in 60 % triethyl phosphate. After allowing the crystals to dissolve for 1 h, a working solution of the dye of 60:40 in distilled water was prepared and filtered through Whatman filter paper. After staining the cells, the dye solution was removed and washed twice with DPBS to remove unbound dye. Stained cells were covered with DPBS and either stored at 4 °C or quantified for adipogenesis.

2.3.2.2 Osteogenesis: Alkaline phosphatase (ALP) activity

After the specified period of differentiation, osteogenesis was assayed by alkaline phosphatase activity. Using Vector® Blue substrate kit III (Vector Laboratories, Peterborough UK) and following the manufacturer's protocol, cells undergoing osteogenesis were stained blue, positively indicating ALP activity. Stained cells were visualised using phase contrast microscope (Inverso 3650).

2.3.2.3 Osteogenesis: Alizarin Red S (AR) staining

Calcium deposition was assessed by using 1 % w/v AR solution (VWR). Using the protocol adapted from (Gregory *et al.*, 2004), the monolayers were fixed in fixative solution (4 % formaldehyde, 75 mM sodium phosphate buffer pH 7, 1.5 % methanol) for 15 min at room temperature, washed twice with distilled water and stained with AR solution (pH 4.2) for 30 min. Unincorporated dye was then aspirated and cells washed 3 times with distilled water. After the staining procedure, cells were covered with distilled water and observed using phase contrast microscope (Inverso 3650).

2.3.3 Quantification of differentiation

2.3.3.1 Adipogenesis: Adipocyte count

Adipogenic differentiation for quantification was carried out in 24-well formats unless otherwise stated. Cells containing Oil Red O stained lipid droplets indicative of adipocyte formation were counted under x10 magnification of phase contrast (Inverso 3650) per three random fields of view per well. The number of adipocytes formed was expressed as an average of the 3 wells.

2.3.3.2 Adipogenesis: Oil Red O dye extraction

Adipogenic differentiation was also quantified using a protocol adapted from (Gregory *et al.*, 2005). Briefly, Oil Red O stained cells were washed with DBPS and 500 µL of extraction buffer (50 % v/v ethanol, 2 % SDS) was added to each well and incubated for 30 min at 37 ºC. The extracted dye was transferred in triplicates of 100 µL to a 96-well plate and the absorbance measured at 405 nm (Sunrise, TECAN™). The amount of extracted dye was normalised to cell number using the Cyquant® NF Cell Proliferation assay kit (Invitrogen, Molecular Probes®).

2.3.3.3 Osteogenesis: Alkaline phosphatase (ALP) activity

ALP activity was assayed in 24-well formats in triplicate. At the end of differentiation, cell monolayer was washed with DPBS and 200 µL of 0.1 % Triton X-100 was added to each well which was then stored at -80 ºC. Subsequently, the plates were thawed on ice and cell monolayer scraped into 1.5 mL tubes and sonicated for 10 min on ice (Branson 200, 40 KHz). An aliquot of 50 µL sample was added to 500 µL of p-nitrophenyl phosphate (p-NPP) reaction buffer (526 mg diethanolamine, 23.2 mg p-NPP dissolved in 4 mL 0.1 M HCl, 50 µL 1 M $MgCl_2$, made up to 100 mL with distilled water). Phosphate standards (0 to 4 mM) were prepared in duplicate and added to 500 µL p-NPP buffer. After incubating the tubes for 20 min at 37 ºC, the reactions were stopped by the addition of 500 µL of 0.2 M Sodium hydroxide solution. The yellow colour developed from the phosphatase reaction was measured at 405 nm as 100 µL triplicates in a 96-well plate. The amount of ALP enzyme was deduced from the standard curve drawn from phosphate standards at each quantification procedure and normalised to cell number using the Cyquant® assay (Appendix Figure I).

2.3.3.4 Osteogenesis: Alizarin Red S (AR) dye extraction

Following AR staining, cell monolayer in 24-well format was washed with distilled water and air-dried. Using the protocol adapted from (Gregory *et al.*, 2004), the dye was recovered by acetic acid extraction. Briefly, 400 µL of 10 % v/v acetic acid (Fisher) was added to each well and incubated for 30 min while shaking at room temperature. Using a wide-mouthed pipette, the loosely attached cells were scraped and transferred to a 1.5 mL tube and vortexed for 30 sec. The slurry obtained was covered with approximately 500 µL mineral oil, and heated for 10 min at 85 ºC. The tubes were then iced for 5 min and centrifuged (accuSpin™ Micro) at 13 000 rpm for 15 min. A volume of 300 µL of the supernatant was transferred to a fresh tube containing 100 µL of 10 % v/v ammonium hydroxide and the pH measured to ensure a range of between 4.1-4.5. Aliquots of 100 µL were read in triplicate in a 96-well plate at an absorbance of 405 nm. The amount of dye extracted was normalised to cell number using the Cyquant® assay.

2.3.3.5 Cell number normalisation: Cyquant® NF Cell Proliferation assay

Quantification of differentiation was normalised to cell number via DNA content measurements, following manufacturer's protocol. The dye binding solution was diluted in cell lysis buffer (Invitrogen) and 600 µL of the solution was aliquoted in each well of DPBS washed differentiated cells in a 24-well plate. After 30 min incubation at 37 ºC, the cells were detached and 100 µL aliquots transferred in triplicates to a black walled 96-well plate. The fluorescence intensity was measured using FLUOstar OPTIMA™ (BMG Labtech) set at 480 nm excitation/520 emission. All quantification measurements were normalised to approximately $3x10^4$ cells.

2.4 Immunofluorescence

Cells were seeded, expanded and/or differentiated on coverslips in 6-well plates after which they were fixed in 4 % formaldehyde for 15 min. The cells were then washed twice with DPBS and stored in DPBS at 4 ºC. For internal cellular staining, cells were permeabilised for 10 min with 0.2 % Triton X-100/DPBS while cells for surface staining were left in DPBS. They were then blocked for 30 min in PBS containing 5 % milk, 5 % FCS and 2 % fish gelatine at room temperature. The coverslips were washed in PBS, incubated in a humid chamber for 1 h in 10 µg/mL STRO-1 solution (5 % FCS/ 2 % fish gelatine/ PBS), washed 3 times in PBS and incubated in goat anti-mouse IgM (µ chain specific) FITC conjugated secondary (Southern Biotech) 1:50 solution (5 % FCS/ 2 % fish gelatine/ PBS), along with DAPI and phalloidin when required, for 45 min in the dark. After the secondary incubation, the coverslips were washed 3 times in PBS with a final wash in distilled water and mounted on pre-warmed Mowiol. The slides were left to dry overnight in the dark and subsequently viewed by fluorescent microscopy (Axioplan, Zeiss) and confocal scanning laser microscopy (Leica SP2 TCS Confocal microscope; image analysis performed by Leica Software Version 2.6.1).

2.5 Flow cytometry

2.5.1 Antibody staining for marker expression profiling

Cells at specified confluency and passage were harvested (Section 2.3.2) and washed in MACS buffer (DPBS containing 1 % FCS and 2 mM EDTA, pH 7.2) via centrifugation at 1000 rpm for 5 min (IEC CL30 Centrifuge) to remove traces of media. Aliquots of $5x10^5$ cells per sample were incubated with the appropriate primary antibody (monoclonal raised in mouse) for the specific time (Table 2.2 for antibody information, dilutions and incubation time) in MACS buffer (final volume 100 µL) on ice and in the dark. Cells incubated with the anti-CD133 antibody were simultaneously incubated with human Fc receptor blocking reagent (Miltenyi Biotech, Surrey, UK) to avoid cross-reaction of the antibody with this receptor. After removal of excess antibody via three MACS buffer washes (2000 rpm, 3 min, accuSpin ™ Micro), the secondary antibody (goat anti-mouse IgM µ chain specific, fluochrome conjugated) incubation was carried out as before if required, followed by a further two MACS buffer washes. Control samples were labelled with FITC-secondary antibody only for FITC conjugated antibodies, RPE-secondary antibody only for RPE-conjugated antibodies and control cells were unlabelled for APC-conjugated antibodies. Surface marker expression was then determined by counting at least 20 000 events per sample and normalised to 10 000 events per sample (unless otherwise stated) on a CyAn™ ADP flow cytometer (DakoCytomation). Isotype control profiles are illustrated in Appendix Figure II.

Using the Summit v4.3 software, protocols were set up using unlabelled samples to accommodate cell size and shape and gates (indicated as R to represent Region on histograms) were set up to exclude debris and cell doublets. Control cells (either unlabelled or labelled with the appropriate control antibody) were analysed on the wavelength corresponding to the fluorescent signal being detected. Positive events in specific antibody-labelled cells were then scored as those above the background level and represented as an overlay or scatter plot.

Antibody	Antibody conjugation		Dilution		Incubation time (min)		Source	
	1°	2°	1°	2°			1°	2°
CD13	PE	-	1:100	-	15	-	S Biotech	-
CD45	FITC	-	1:100	-	15	-	Miltenyi	-
CD105	FITC	-	1:100	-	30	-	BioLegend	-
CD133*	PE	-	1:10	-	15	-	Miltenyi	-
CD146	FITC	-	1:10	-	15	-	Miltenyi	-
CD271	FITC	-	1:10	-	15	-	Miltenyi	-
HLA-ABC	FITC	-	1:50	-	30	-	BD Bios	-
STRO-1	-	FITC	1:100	1:50	40	30	R&D Sys	S Biotech
STRO-1	-	RPE	1:100	1:100	40	15	R&D Sys	S Biotech

Table 2.2: Antibodies used to define cell surface marker profile of hMSCs and osteosarcoma cell lines by flow cytometry. The dilution, incubation time and source of each antibody are indicated. * indicates co-incubation with Fc Receptor block whilst staining. All primary antibodies were monoclonal and raised in mouse; all secondary antibodies were polyclonal goat anti-mouse immunoglobulins. Southern Biotech (Birmingham, USA); Miltenyi Biotec (Gladbach, Germany); BioLegend (San Diego, USA); BD Biosciences (Oxford, UK); R&D Systems (Oxford, UK).

2.5.2 MACS enrichment

The STRO-1 highly positive fraction of passage 6 hMSCs (N24♂) was enriched on a miniMACS® columns (Miltenyi Biotech) according to manufacturer's protocol. Briefly, $4x10^6$ cells were labelled with 100 µg/mL primary STRO-1 antibody (2.6.1) and conjugated to rat anti-mouse IgM Microbeads (20 µL per $1x10^7$ cells, Miltenyi Biotech). The cells were washed twice with MACS buffer and enriched by allowing the cells to flow freely through the magnetic column. The column was then washed 3 times with MACS buffer to collect the negative fraction. The STRO-1 positive hMSCs bound to the column were recovered by flushing out the cells with a plunger via 3 buffer applications. The cells recovered were counted and seeded at $4x10^3$ cells/cm^2 for expansion and differentiation (Section 2.2.1). An aliquot of each fraction was labelled with the fluochrome conjugated secondary antibody (Table 2.2) and analysed on the flow cytometer (Cyan) to ensure enrichment of STRO-1 positive hMSCs.

2.5.3 Live/Dead Discrimination

In order to exclude dead cells in the flow analysis, propidium iodide (PI) and Live/Dead fixable dead cell stain kit (Invitrogen, Molecular Probes®) were used. PI was used to discriminate dead cells while setting up the analysis protocol. Unlabelled cells were incubated for 15 min on ice in 1 µg/mL PI and analysed on the flow cytometer (CyAn™). Late apoptotic cells incorporate PI into their DNA and can be detected in the PE red channel. These PI positive cells were therefore gated out during the flow analysis.

The Live/Dead kit contains a dye which when reacts with free amines inside the cell fluoresces in the near-IR channel (APC-Cy7). The dye was reconstituted following the manufacturer's protocol and the cells were washed with DPBS and stained (1:1000, 30 min on ice) after fluorescent labelling with appropriate secondary antibodies where required (Table 2.2). After the Live/Dead staining, the cells were washed once with DPBS and suspended in MACS buffer to be analysed by flow cytometry. The Live/Dead discrimination stain was used in conjunction with antibodies conjugated to FITC, PE and RPE and gates were set up to exclude apoptotic cells having compromised cell membrane.

2.5.4 Cell proliferation assay

The seven osteosarcoma cell lines were assayed for their proliferative potential using the CellTrace™ CFSE cell proliferation kit (Invitrogen, Molecular Probes®). Cells were harvested (Section 2.3.2), suspended in DPBS and counted using a haemocytometer. The CFSE dye was reconstituted following manufacturer's protocol and was optimised to be used at a final concentration of 2.5 µM per 2-3x10^6 cells. Briefly, 1 mL cell suspension was incubated with CFSE dye for 15 min at 37 ºC, centrifuged (IEC CL30 Centrifuge, 1000 rpm, 5 min), then incubated in 1 mL warm complete media for 30 min at 37 ºC. Unincorporated dye was washed in excess media, suspended in fresh media at the required dilution and seeded at 1x10^5 cells per well in a 6-well plate. Cells were harvested (Section 2.3.2) after 24 h, suspended in MACS buffer and analysed by flow cytometry (CyAn™) set on the fluorescein filter.

2.6 Phage display

The two phage libraries used in this study were the Ph.D-12^{TM} library (New England Biolabs, Ipswich, USA) and the Dean's library (prepared for R.W Johnson Pharmaceutical Research Institute, gifted by Dr Angray S. Kang). The Ph.D-12^{TM} peptide library expresses 12-mer peptides on the pIII surface coat protein of M13 phage while the Dean's library expresses 16-mer peptides on the pVIII surface coat protein of the M13 phage.

2.6.1 Solid-phase panning

Solid-phase panning was carried out according to the NEB protocol. Wells from a 96-well plate were coated with 100 µL (100 µg/mL) STRO-1 antibody solution (R&D Systems, Oxford, UK) in PBS or with 0.5 % BSA (negative control) overnight at 4 °C. The wells were then blocked for 2 h at room temperature and washed 6 times with TBS containing 0.1 % Tween (TBST). A 100 µL phage suspension of approximately 1x10^{11} pfu/mL in TBST was added to each well in duplicate. After 1 h incubation at room temperature, the wells were washed 10 times with TBST and bound phage was eluted with 100 µL elution buffer (0.2 M Glycine-HCl, 1 mg/mL BSA, pH 2.2) for 10 min at room temperature. The 200 µL eluate was then neutralised with 30 µL 1 M Tris-HCl (pH 9). The eluted phage was titred and propagated for the next round of panning (Figure 2.1).

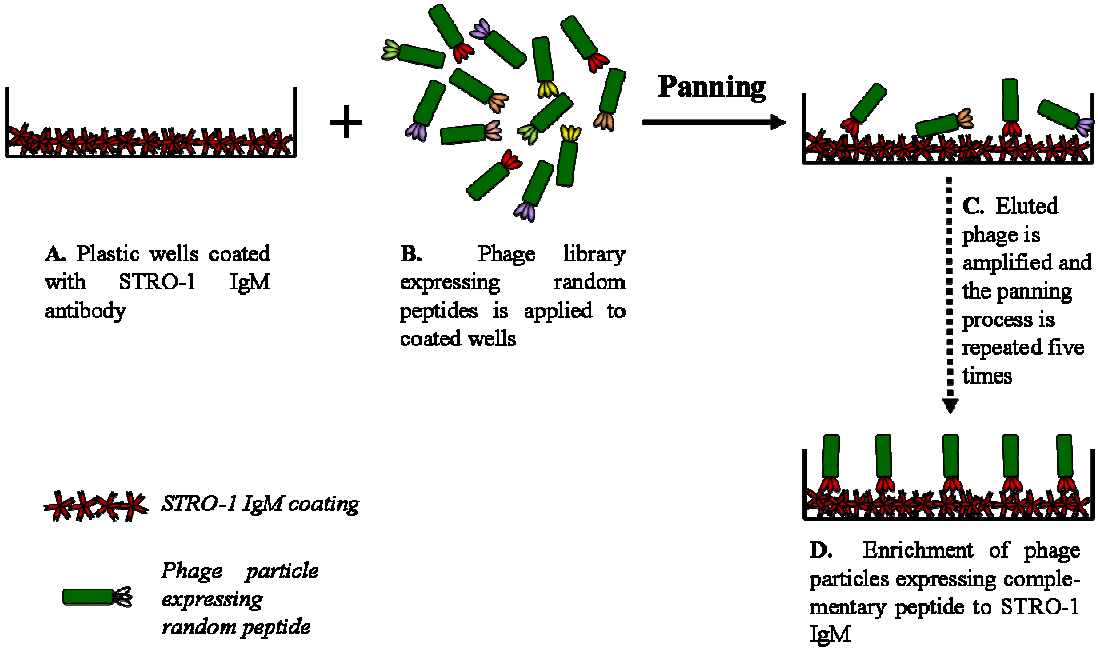

Figure 2.1: Schematic illustration of solid phase panning. (A) Plastic microtitre wells were coated overnight with 100 µg/mL STRO-1 IgM or 0.5 % BSA control. (B) Phage library of input titre $1x10^{11}$ pfu/mL was selected against coated wells, (C) eluted, quantified and propagated for subsequent panning rounds. (D) The specific phage enrichment process was repeated five times.

2.6.2 Liquid-phase panning

Liquid-phase panning was carried out according to the NEB protocol. Protein A agarose beads (Calbiochem, Nottingham, UK) were used. A 50 µL aliquot of the beads (50 % suspension in PBS) was first coated with 1 mL (100 µg/mL) goat anti-mouse IgM antibody (µ-chain specific, Sigma) for 30 min at 4 °C then blocked with 0.5 % BSA/PBS for 30 min at 4 °C. In a separate tube, $1.5x10^{11}$ pfu/mL phage suspension was incubated with 10 nM STRO-1 or 0.5 % BSA/PBS (negative control) at room temperature for 20 min. The phage-STRO-1 complex suspension was transferred to the coated bead suspension and incubated for 10 min at room temperature. The phage-STRO-1 complex was pulled down by the coated beads at 3000 rpm for 1 min (accuSpin™ Micro, Fisher Scientific). A volume of 200 µl of freshly prepared elution buffer was added to the resin to elute the bound phage. The eluate was then neutralised with 30 µL 1 M Tris-HCl. The eluted phage was titred and propagated for the next round of panning (Figure 2.2).

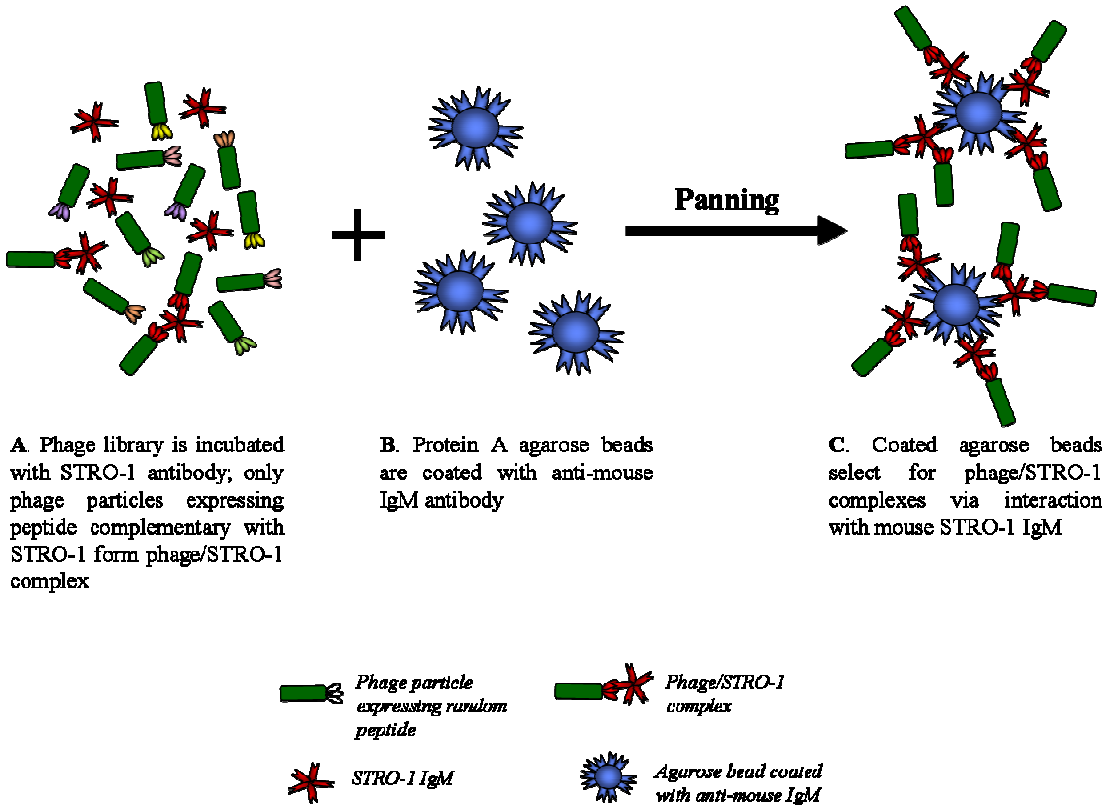

Figure 2.2: Schematic illustration of liquid phase panning. (A) A Phage library titre of $1.5x10^{11}$ pfu/mL was incubated with 10 nM STRO-1 or 0.5% BSA control. (B) In a separate reaction, protein A agarose beads were coated with 100 µg/mL goat anti-mouse IgM . (C) Phage/STRO-1 complex was then pulled down by coated agarose beads and STRO-1 specific peptide phage was eluted, quantified and propagated for subsequent panning rounds. The process was repeated five teams.

2.6.3 Phage propagation

An aliquot of 10 µL of the eluted phage was retained to determine the phage output titre while the remaining eluate was used for propagation in *E.coli* XL1 Blue cells (Stratagene, California, USA). Propagation consisted of infecting 200 µL of XL1 Blue ($O.D_{600}$ 0.4/0.5) with the eluted phage in 20 mL LB medium (Fisher, Loughborough, UK) for 4.5 h at 37 °C with vigorous shaking (250 rpm, Innova®43, New Brunswick Scientific). The bacteria and phage suspension was then separated via centrifugation at 4000 rpm for 10 min at 4 °C (accuSpin™). The bacterial pellet was discarded and 4 mL of PEG/NaCl was added to the supernatant to precipitate the phage overnight at 4 °C. The following day, the precipitated phage was recovered by centrifugation at 10 000 rpm for 15 min at 4 °C (Universal 320R, Hettich Zentrifugen) and suspended in 200 µL TBST/0.02 % sodium azide to be stored at -20 ºC. The titre of the amplified phage was determined by plaque assay.

2.6.4 Plaque assay

The phage titre after each round of panning was determined by serial dilution of the phage suspension in LB medium. A volume of 10 µL of the appropriate phage dilution or LB medium (negative control) was plated with 200 µL XL1 Blue ($O.D_{600}$ 0.4/0.5) in 3.5 mL overlay agar (1.5 % w/v) on 20 mL of set nutrient agar (3 % w/v). The plates were incubated overnight at 37 °C. Each dilution was plated in duplicate and the titre determined from the readings of three dilutions. The titre was assayed as the number of plaque forming units per millilitre of phage suspension (pfu/mL).

2.6.5 Plaque lifts

Plaques formed from the plated phage were transferred to a nitrocellulose membrane for probing with the STRO-1 antibody. The membrane was blocked using 1 % BSA/PBS for 1 h at room temperature. It was then washed three times with PBST (0.05 % Tween) and incubated with 1 µg/mL STRO-1 in 10 mL PBST for 2 h. STRO-1 binding was detected with polyclonal rabbit anti-mouse HRP conjugated immunoglobulins (DakoCytomation, Glostrup, Denmark) or goat anti-mouse IgM HRP conjugated

immunoglobulins (Southern Biotech, Cambridge, UK) in 10 ml PBST (1:1000) for 2 h and peroxidase activity was detected by colour development using 2 mg/mL DAB (3,3'-Diaminobenzidine, Bio-Rad Laboratories, Hertfordshire, UK) for 15 min in the dark.

2.6.6 Dot Blots

A 1 µL volume of antibody solution (mouse STRO-1 IgM or mouse TUJ1 IgG) of appropriate concentrations in PBS were spotted on nitrocellulose membrane and allowed to air dry for 15 min. The membrane was then blocked with 1 % BSA/PBS or 1 % semi-skimmed milk for 1 h before probing with polyclonal rabbit anti-mouse HRP conjugated immunoglobulins (1:1000) or goat anti-mouse IgM HRP (Southern Biotech, Cambridge, UK) for 2 h. The colour was developed using 2 mg/mL DAB for 15 min in the dark.

2.6.7 STRO-1 antibody binding to microtitre plate

Wells from a 96-well plate were coated with 100 µL of 100 µg/mL STRO-1 antibody or 1 % BSA/PBS (negative control) overnight in a humid environment at 4 °C. The following day, the wells were washed 3 times with PBST (0.1 % Tween) and blocked with 1 % BSA for 2 h at room temperature. The wells were then washed 5 times in excess PBST before adding 100 µL of 20 µg/mL goat anti-mouse IgM into each well for 1 h at room temperature. After washing 3 times with PBST and a final wash with PBS, 100 µL of anti-goat HRP (1:2000) (DAKO, Cambridge, UK) was added to each well for 1 h. ABTS (2,2'-Azino-bis(3-Ethylbenzthiazoline-6-sulfonic acid; Roche, Sussex, UK) was used as substrate (100 µL per well for 30 min in the dark) and absorbance readings were taken at 405 nm (Sunrise TECAN™).

2.7 Comparison of gene expression microarray analysis *(performed by Stephen Henderson, The Cancer Institute, University College London)*.

A comparison of gene expression microarray data of the seven osteosarcoma cell lines and MSC cultures was undertaken (Affymetrix HGU133a). The data had been pre-processed, normalised and summarised using the R statistical environment and the 'rma' algorithm (part of the affy package). Probesets which most highly correlated (Pearson's R^2) to the STRO-1 flow cytometry expression values were then retrieved. By inspecting the correlation rankings a cut off of the top 20 probesets were selected.

A heatmap of twenty candidate genes encoding STRO-1 antigen was generated using gplots package for the R statistical environments. Sub-cellular location information, where available, was extracted from the Gene Ontology (GO) database (Appendix Table I).

The procedure is outlined as a flow diagram in Appendix III (Figure III).

2.8 Gene expression analysis

2.8.1 RNA extraction

Total RNA was isolated from differentiating cells at time points indicated. Primarily, the cells cultured in a 10 cm dish were harvested (2.2.1), suspended in 1 mL of TRIzol® reagent (Invitrogen) and stored as 2 aliquots of 500 µL at -80 ºC. To extract the RNA, one aliquot was thawed on ice, and incubated for 3 min at room temperature. A volume of 100 µL of BCP (1-bromo-3-chloro propane) was added and the tube was shaken vigorously for 2 min and left for 3 min at room temperature. Cellular debris was removed by centrifugation at 4000 rpm for 15 min at 4 ºC (Universal 320R). Carefully, 300 µL of the aqueous phase was transferred to a fresh tube to which 75 µL of isopropanol (molecular grade) was added. The tube was gently inverted 3 times and RNA allowed to precipitate overnight at -20 ºC. The following day, the RNA was pelleted by centrifugation at 15 000 rpm for 30 min at 4 ºC. The pellet was then washed with 500 µL of 70 % ethanol, centrifuged at 10 000 rpm for 10 min at 4 ºC, ethanol removed and pellet allowed to air dry for 2 min. The RNA pellet was then suspended in 30 µL DEPC treated water, quantified by Nanodrop 1000 Spectrophotometer (Thermo Scientific) and stored at -80 ºC.

2.8.2 cDNA synthesis

cDNA was synthesised from 0.3 µg total RNA using Protoscript® First Strand cDNA Synthesis Kit (New England Biolabs), following the manufacturer's protocol. RNA was diluted to a volume of 5 µL in DEPC treated water, and 2 µl of dNTP mix and 1 µL of oligo ($dT_{23}VN$) primer were added (stock concentrations 2.5 mM and 50 µM, respectively). The mixture was incubated for 5 min at 70 ºC, spun and iced for 3 min, then 1 µL reverse transcriptase buffer (10x stock), 0.5 µL RNase inhibitor (5 units) and 0.5 µL M-MuLV reverse transcriptase enzyme (12.5 units) were added. First strand cDNA synthesis was carried out for 1 h at 42 ºC, and the reaction was inactivated for 5 min at 95 ºC. Subsequently, the reaction was diluted to 30 µL in DEPC treated water and stored at -20 ºC.

2.8.3 Polymerase Chain Reaction (PCR)

PCR screens were executed using Bio-Rad MJ Mini™ thermal cycler. A typical 25 µL reaction was set up with final concentration of reagents as follows: 1x Qiagen PCR buffer containing 1.5 mM $MgCl_2$ (Qiagen, Crawley, UK), 200 µM dNTP mix (Eppendorf, UK), 1 µM each primer, 1 unit DyNazyme EXT DNA polymerase (Finnzymes) and 20 ng cDNA template. The PCR conditions used for gene screening were: 95 ºC for 5 min, 30 cycles of (94 ºC for 15 sec, *x* ºC for 1 min, 72 ºC for 1 min), then 72 ºC for 10 min, where *x* refers to the annealing temperature used for specific primer pair. Information on the annealing temperatures and primer pairs used for each gene is listed in Table 2.3.

Gene	GenBankID	Sequence		Annealing temp (°C)	Product size (bp)
ALP	NM_000478	F	GGGGTGAAGGCCAATGAGGG	61	417
		R	GCTCTTCCAGGTGTCAACGAG		
β-actin	NM_001101	F	TACCTCATGAAGATCCTCA	52	267
		R	TTCGTGGATGCCACAGGAC		
BMP8	NM_001720	F	CAGTCCAACAGGGAGTCTGACTTGT	60	162
		R	CCCGTCCTCAGTCTCCACATAGA		
CBFA1	NM_004348	F	ATGGCGGGTAACGATGAAAAT	56	421
		R	ACGGCGGGGAAGACTGTGC		
COL1A1	NM_000088	F	TGTTCAGCTTTGTGGACCTCC	59	506
		R	CTCATCATAGCCATAAGACAGC		
MSX2	NM_002449	F	CTACCCGTTCCATAGACCTGTGCTT	60	150
		R	GAGAGGGAGAGGAAACCCTTTGAA		
OCN	NM_199173	F	GAGAGCCCTCACACTCCTCG	58	299
		R	AGACCGGGCCGTAGAAGC		
OPN	NM_000582	F	TTGCTTTTGCCTCCTAGGCA	55	417
		R	GTGAAAACTTCGGTTGCTGG		

Table 2.3: Details of primers used in RT-PCR for gene expression analysis in hMSCs and osteosarcoma cells.

2.8.4 Agarose gel electrophoresis

PCR products were separated on 1.5-2 % w/v agarose gels with 0.5 µg/mL ethidium bromide for DNA visualisation. PCR samples were mixed with DNA loading buffer (6x stock concentration: Bromophenol Blue/Glycerol), electrophoresed for typically 1 h and visualised on Uvitec™ transilluminator imaging system.

Chapter 3

Characterisation of STRO-1 expression on cultured hMSCs

3.1 Introduction and aims

Human Mesenchymal Stem Cells (hMSCs) have the capacity to differentiate *in vitro* and *in vivo* along a number of lineages including the adipogenic, chondrogenic and osteogenic pathways (Pittenger *et al.*, 1999). This population of cells is maintained throughout adulthood and can be isolated from numerous locations in the body (Figure 1.1). The most well characterised hMSC population is derived from the bone marrow and a variety of methods have been employed by different laboratories in an attempt to obtain homogeneous populations of hMSCs (Jones *et al.*, 2002). The classic method of hMSC isolation is via plastic adherence but other methods including antibody-aided selection are also being developed (Table 1.1). Cell surface marker profiles and lineage differentiation assays are frequently used to define the cell populations as hMSCs. A panel of antibodies has been developed which positively identify hMSCs and the most specific one to date is STRO-1, reacting to an as yet unidentified antigen (Simmons and Torok-Storb, 1991). However, little is known about the expression of STRO-1 antigen on hMSCs and its modulation during different culture conditions.

STRO-1 identifies 10 % of bone marrow mononuclear cells of which 95 % are nucleated erythroid progenitors. Following exclusion of erythroid progenitors by glycophorin A depletion, all the cells recovered were found to be plastic adherent with a fibroblastic morphology (reminiscent of the CFU-F description) and able to differentiate to myelosupportive stroma (Simmons and Torok-Storb, 1991). Further investigation demonstrated that clonally derived CFU-F were STRO-1 positive and gave rise to the tri-lineage characteristic of hMSCs (Pittenger *et al.*, 1999). Analysis of fresh bone marrow mononuclear cells demonstrated varying levels of STRO-1 expression which Gronthos and co-workers (2003) characterised as three sub-populations (Dull, Intermediate and Bright). Interestingly, the STRO-1^{BRIGHT} positive fraction bears important phenotypic and functional characteristics attributed to stem cells found in other renewing tissues (Conget and Minguell, 1999). Freshly isolated STRO-1^{BRIGHT} population lack Ki-67 cell cycle surface antigen indicating quiescence *in vivo*; increased telomerase activity indicating extensive proliferation potential; and exhibit an undifferentiated state lacking detectable key differentiation marker expressions

(PPARγ2 in adipogenesis, Cbfa-1 in osteogenesis and Collagen Type II in chondrogenesis) (Minguell *et al.*, 2001).

The STRO-1 heterogeneity within the hMSC population also reflects the heterogeneity in the cells' proliferative and differentiation potential. As initially proposed by Owen and Friedenstein (1988), CFU-F from the bone marrow represent a mixed population of multi-, bi- and uni-potential progenitors at different stages of differentiation (Owen and Friedenstein, 1988). Following this stromal stem cell hierarchy of cellular differentiation, it appears that STRO-1 is identifying a population of undifferentiated cells with the multipotent cells residing in the STRO-1^{BRIGHT} fraction. The notion of stemness of the mesenchymal progenitors therefore follows that this characteristic is not restricted to one cell type but is a spectrum of capabilities within that population. The proliferative hierarchy depicts a structured cell population consisting of stem, committed and mature cells with the highest STRO-1 expressive cells possibly representing the stem cell subset (Gronthos *et al.*, 2003).

Culture expanded hMSCs have been used in several studies in an attempt to elucidate the stem cell characteristics of the population. This is mainly due to the low incidence of hMSCs in the bone marrow (10 % of bone marrow mononuclear cells) resulting in insufficient raw material for the various investigative assays. In addition to the absence of a consensus isolation protocol of hMSC, discrepancy in reports also arise from the difference in culture conditions used in the studies. While some studies suggest that bFGF addition to the growth culture media during expansion has no effect on the multilineage potential of hMSCs (Tsutsumi *et al.*, 2001), others report an enhanced adipogenic (Neubauer *et al.*, 2004), osteogenic (Hanada *et al.*, 1997) and chondrogenic (Solchaga *et al.*, 2005) potential. Previous work in this laboratory (Westwood 2006) showed that addition of bFGF to the expansion media increases the growth rate and life-span of hMSCs without diminishing their differentiation potential. Following these observations, hMSC cultures used in this thesis were expanded in media containing bFGF. However, extensive sub-cultivation of hMSCs (beyond passage 25) has been reported to cause a change in viability, morphology and subsequently immunophenotype (Conget and Minguell, 1999). Apoptosis is triggered in the cycling

hMSC subset at later passages and markers of cell adhesion (ICAM-1 and integrin β1) are downregulated corresponding to the apparent morphological changes. Qualitative assessment of differentiation upon extensive culture indicated a loss in adipogenic but not in osteogenic potential. Therefore it was of interest to evaluate the expression of STRO-1 after multiple rounds of sub-culturing and its influence on differentiation potential quantitatively.

The use of cultured hMSCs in regenerative medicine is unavoidable due to the low incidence of the cells *in vivo.* While clinical intervention to obtain tissue samples containing hMSC is not difficult, the isolation of homogeneous populations of hMSCs is proving to be a challenge due to the lack of a standard protocol. Furthermore, the anatomical location of hMSCs is still being debated with analogies to a perivascular niche being made. Nevertheless, regardless of the source of the hMSCs, the demand for a cultured multipotential population is still prevalent. So far, STRO-1 has been shown to be a promising candidate in the identification of cells with multilineage potential with differential expression during adipogenesis (Simmons and Torok-Storb, 1991).

The STRO-1 status of cultured hMSCs has not been evaluated under an optimised protocol to date. From the discovery of the antibody from a hybridoma supernatant to its commercialisation in the lyophilised form, different laboratories have adopted different approaches to screen their cell populations for STRO-1 expression. Although hybridoma supernatant is chosen over the lyophilised form due to cost constraints, it is important to establish that both sources are directly comparable and equally reliable. Based on early indication that STRO-1 antigen may be a differentiation marker, elucidating the characteristics and expression profiles of STRO-1 on cultured hMSCs is of utmost importance and is the primary focus in this section of the thesis.

Aims

The low frequency of freshly derived bone marrow hMSCs demands for culture expanded hMSCs to be used in regenerative medicine. However, although extensive studies have been performed on the isolation and identification of multipotent cells from fresh bone marrow mononuclear cells, few studies have focused on culture expanded cells. The STRO-1 marker has been shown to select for cells with multilineage potential from fresh bone marrow mononuclear cells. Therefore, in the primary step of this study, the use of differently sourced STRO-1 antibody as a tool for the detection and characterisation of hMSCs in culture was investigated. The expression of STRO-1 antigen on culture expanded hMSCs and its impact on differentiation potential was also studied. In order to address these, the following objectives were achieved.

- characterisation of hMSC populations using antibody marker profiling
- optimising the use of the STRO-1 antibody to screen cell populations
- investigation of STRO-1 expression upon expansion and correlation with differentiation potential
- visualisation of STRO-1 expression in hMSC cultures by dual-colour immuno-staining
- investigation of STRO-1 expression at confluency and its impact on differentiation potential
- Assessment of STRO-1 status during adipogenic and osteogenic differentiation

3.2 Properties of hMSCs

hMSCs can be derived from a variety of sources and are characterised by a plastic adherent culture and a range of marker expression (Table 1.1) and their ability to differentiate primarily to adipocytes, osteocytes and chondrocytes. It is important to establish from the onset that the populations intended to be used in this study are in fact hMSCs. Each laboratory has its own established protocol for isolating hMSCs and characterising the populations. In this thesis, hMSCs isolated by plastic adherence were characterised by immunophenotyping and differentiation potential.

3.2.1 hMSC marker profile

The panel of markers used to define the hMSC population varies in different laboratories but generally refers to the absence of haematopoietic lineage markers and presence of mesenchymal, epithelial and endothelial lineage markers (Jones *et al.*, 2006b). In this study, the hMSC populations were tested for the expression of the documented markers and assayed for their ability to differentiate. This was done to ensure that the hMSC populations studied were comparable to those reported in other studies.

hMSCs from the bone marrow of three healthy donors (N24♂, 31♂ and 38♀) were previously isolated by plastic adherence and colonies derived were expanded to passage 2 and stored in 10 % v/v DMSO in liquid nitrogen (Vujovic 2006 and Westwood 2006). For subsequent analysis, cells from each donor were thawed and expanded to passage 6 (Section 2.2). At subconfluency, cells were harvested and stained with antibodies (Table 2.2) to detect the expression of markers defining hMSCs (Figure 3.1). hMSCs from the three donors were positive for STRO-1 antigen, albeit different levels. The cell population 31♂ exhibited a total positive population shift with distinct STRO-1^{BRIGHT} and STRO-1^{DULL} subsets. These two STRO-1 subsets were also apparent in 38♀ although the total positive population shift was not as pronounced as 31♂. The population N24♂ showed a long thin positive tail of STRO-1^{BRIGHT} cells, while the majority of the STRO-1 positive population was within the STRO-1^{INT} subset. The three hMSC populations were strongly positive for CD13 (mesenchymal marker) and

SH4, CD105 and CD146 (markers previously used to positively identify cultured hMSCs) and were negative for CD133 (marker commonly used to positively identify progenitor cells, mainly of haematopoietic origin). CD271 (positive marker for freshly isolated hMSC) was weakly expressed by the passage 6 hMSCs of the three donors. Overall, among the panel of markers used to characterise the cultured hMSCs, STRO-1 was the only marker to display a heterogeneous expression profile within a cell population and to exhibit different degrees of positivity across the three cell populations.

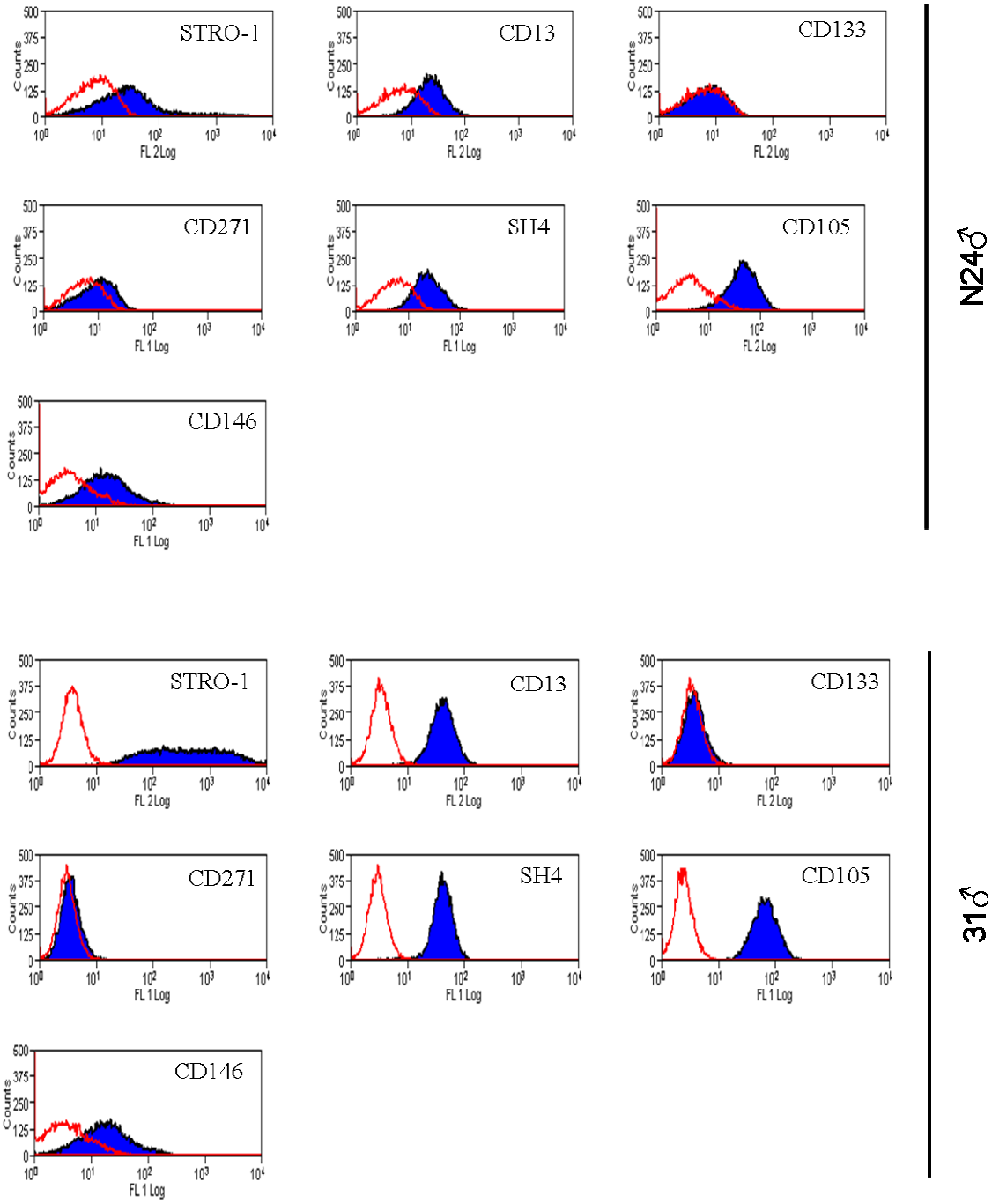

Figure 3.1: Continued overleaf. Flow cytometry analysis of cell surface markers of hMSCs. Subconfluent, passage 6 hMSCs (from three bone marrow donors (N24♂, 31♂ and 38♀)) were harvested, washed and stained with the appropriate primary and secondary antibody if required (Sections 2.2.2 and 2.5.1). Expression was normalised to $1x10^4$ events per sample (* indicates normalisation to $1x10^3$ cells). Shaded histograms (blue) indicate cells stained with the marker-specific antibodies and red lines indicate unstained or secondary antibody controls.

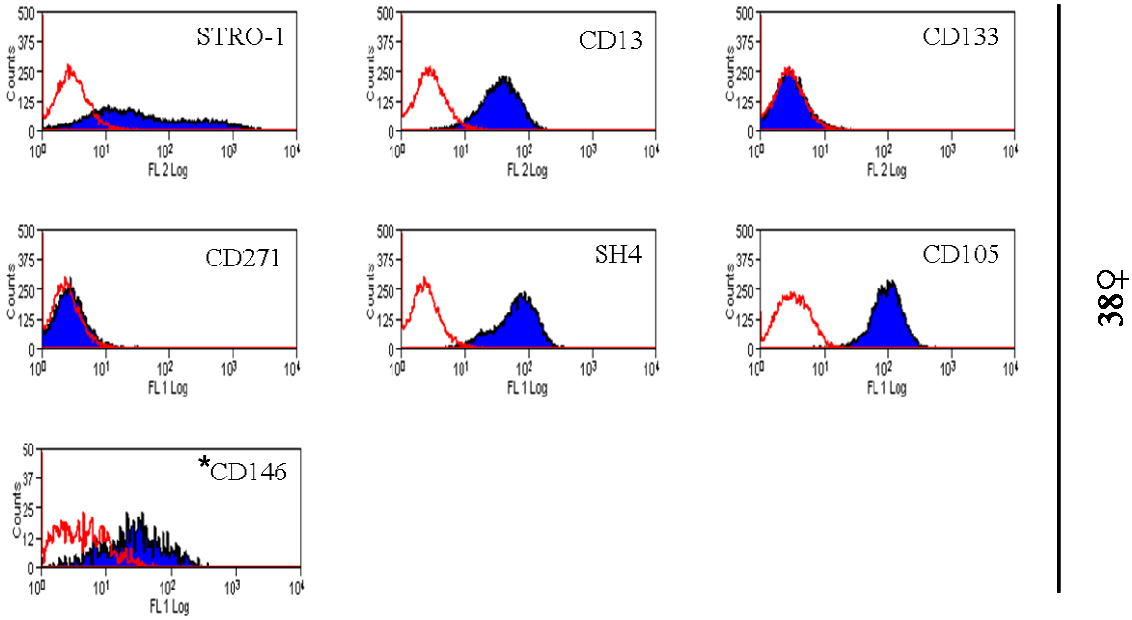

Figure 3.1: Flow cytometry analysis of cell surface markers of hMSCs. Subconfluent, passage 6 hMSCs (from three bone marrow donors (N24♂, 31♂ and 38♀)) were harvested, washed and stained with the appropriate primary and secondary antibody if required (Sections 2.2.2 and 2.5.1). Expression was normalised to $1x10^4$ events per sample (* indicates normalisation to $1x10^3$ cells). Shaded histograms (blue) indicate cells stained with the marker-specific antibodies and red lines indicate unstained or secondary antibody controls.

3.2.2 Differentiation potential of hMSCs

The immunophenotyped hMSC populations were induced to differentiate to the adipogenic and osteogenic lineages, for 8 and 21 days respectively and stained as appropriate (Section 2.3). Chondrogenesis in the cell populations has been successfully achieved previously (Vujovic 2006 and Westwood 2006) and was not repeated in this context. Adipogenic differentiation was apparent as from day 2 of induction, characterised by a change from polygonal to rounded morphology, with peri-nuclear phase bright lipid droplets which coalesced as differentiation proceeded (data not shown). On day 8, the population was stained with Oil Red O for lipid accumulation (Figure 3.2 A1, A2 and A3). Osteogenesis was apparent as from day 7 of induction, with the cells forming a mesh-like structure and becoming alkaline phosphatase positive (data not shown). At day 21, differentiation was terminated and the cells assayed for alkaline phosphatase activity (Figure 3.2 B1, B2 and B3) and mineral deposition using Alizarin Red salt solution (Figure 3.2 C1, C2 and C3).

When stained for differentiation, not all the cells within the population showed positive differentiation. The heterogeneous pattern observed was similar in the three cell populations. At the end of adipogenesis, some cells had extensive lipid accumulation while in other cells, lipid droplets were very small to totally absent. Upon osteogenesis, alkaline phosphatase activity was stronger in some cells characterised by bright blue staining and weaker in others characterised by faint blue staining. Mineral deposition was very patchy with the monolayer indicating nodule formation by a restricted cell subset.

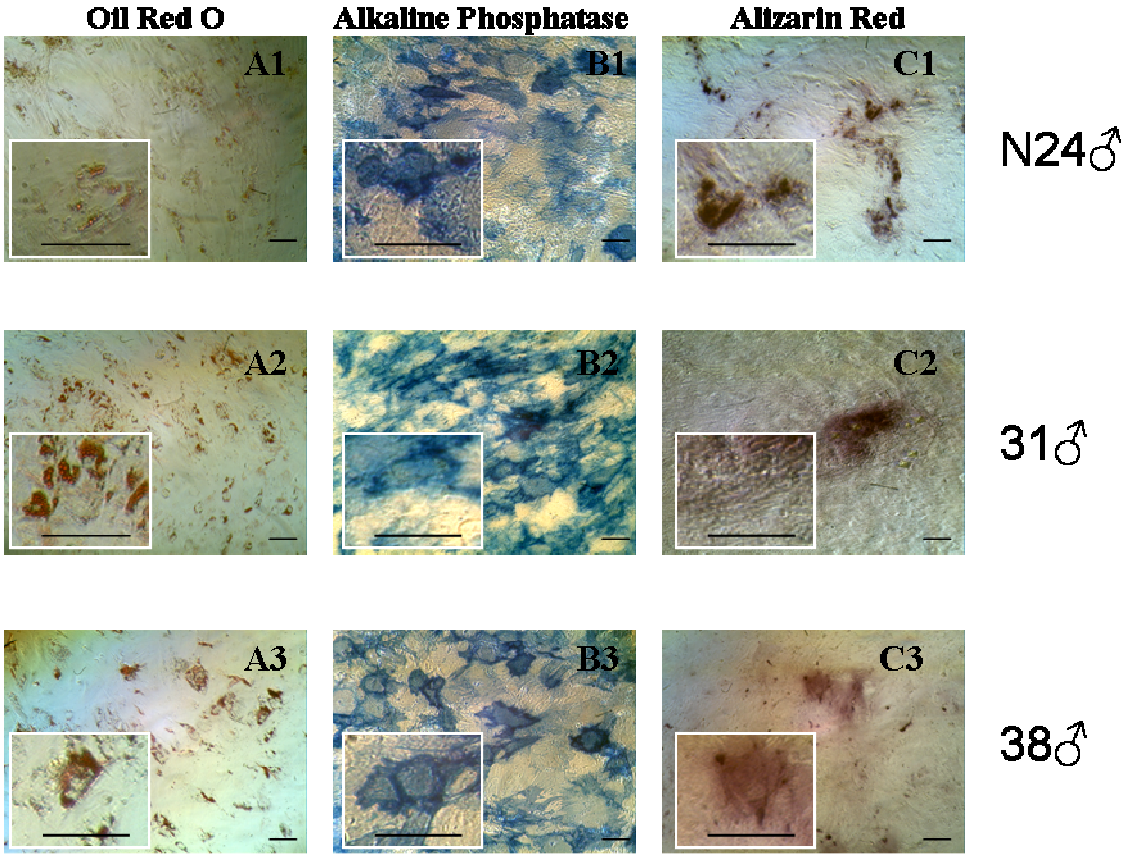

Figure 3.2: Differentiation potential of hMSCs from three bone marrow donors (N24♂, 31♂ and 38♀). Cells at passage 6 were induced to differentiate to adipocytes and osteocytes using different combinations of induction reagents (Section 2.3.1). A1, A2&A3: At day 8, adipogenesis was assayed by Oil Red O to visualise lipid accumulation (Section 2.3.2.1); B1, B2&B3: At day 21, osteogenic cells were assayed for alkaline phosphatase activity (Section 2.3.2.2, blue staining) and C1, C2&C3: mineralisation by Alizarin Red staining (Section 2.3.2.3). Scale bars represent 125 µm.

3.3.3 Heterogeneity of hMSCs cultures

Although the three hMSC cultures were able to terminally differentiate to the adipogenic and osteogenic lineages, the pattern of differentiation observed was not homogeneous (Figure 3.2); only a sub-population of cells within the induced adherent populations had accumulated lipid droplets (adipocytes) or had strong alkaline phosphatase activity and mineralised nodules (osteocytes). While the presence of committed progenitors in the hMSC cultures could not be ruled out, it appeared plausible to suggest that the heterogeneous differentiation observed within one cell population is directly related to the heterogeneous expression of STRO-1 within the

cultured population observed (Figure 3.1). Therefore it was of interest to further investigate the heterogeneity of STRO-1 within cultured monolayers.

In order to visualise the heterogeneous STRO-1 staining, hMSCs from passage 6 N24♂ were grown on coverslips and immunostained; FITC-conjugated secondary was used to detect STRO-1 and DAPI stained the nuclei blue (Section 2.4). An overview of the stained population at x10 magnification (Figure 3.3 A) showed a heterogeneous population, with only a few cells positive for STRO-1 (green staining). Among the positive cells, a gradation in the green fluorescence was observed indicating that some cells expressed STRO-1 to a higher extent that others within the same population. At a higher magnification of x40 (Figure 3.3 B), STRO-1 appeared to be unevenly distributed within the cell membrane and regardless of the cell morphology, STRO-1 staining was stronger on the cell extremities. As such, not only STRO-1 was heterogeneously expressed within the population, but it was also localised at selective positions on the cell membrane. These observations clearly indicate that plastic-adherent hMSC populations are heterogeneous in STRO-1 antigen staining.

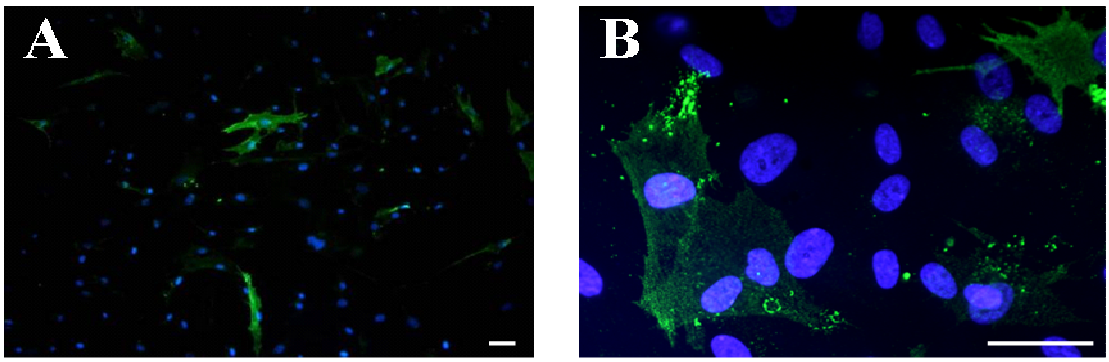

Figure 3.3: Expression of STRO-1 on hMSCs demonstrated by dual-colour immunofluorescence. Passage 6 cells of N24♂ were grown on coverslips were stained with DAPI (blue nuclei) and STRO-1/FITC (Section 2.4). STRO-1 expression was visualised at x10 magnification (A) and x40 magnification (B). Scale bars represent 125 µm.

3.3 STRO-1 antibody optimisation

STRO-1 has been used by various laboratories to isolate and characterise hMSCs (Table 1.1). However, there is no established protocol for the usage of STRO-1, given that some groups use hybridoma supernatant produced in house, while others use commercially obtained antibody. Moreover, the use of hybridoma supernatant is not consistent as some document using the supernatant neat (Mirmalek-Sani *et al.*, 2006), while others document a 1 in 2 dilution (Jones *et al.*, 2002), with no reference to the concentration of antibody present. STRO-1 antibody is of IgM isotype with a low binding affinity (Svehag *et al.*, 1967). The impact on the stability of the antibody with freeze-thaw cycles and storage period has not yet been optimised, hence the purpose of this experiment.

Hybridoma cells purchased from DSHB (Iowa, USA) were expanded, the supernatant harvested (Section 2.2.3), STRO-1 content quantified by ELISA as 4.2 µg/mL (Section 2.2.4) and stored at 4 ºC. Sub-confluent hMSCs (N24♂) at p4 were harvested, stained for STRO-1 and detected with a RPE-conjugated secondary (Table 2.2). The hybridoma supernatant was used as 100 µL neat or 1:2 diluted per $5x10^5$ cells. Commercially obtained STRO-1 was reconstituted, dispensed in aliquots and stored at -20 ºC. When required, the aliquot was thawed, diluted to 100 µL of 5 µg/mL and incubated with $5x10^5$ cells. The commercial antibody was also assayed in this way after two freeze-thaw cycles and after two months of storage at 4 ºC.

Although all the antibody conditions used positively detected STRO-1 on the hMSCs, the number of bright cells detected varied widely (Figure 3.4 and data summarised in Table 3.1). The use of the neat supernatant detected nearly twice as many bright cells as using it at 1:2 dilution (Table 3.1). Repeated freeze-thawing and 4 ºC storage of the commercial antibody had a negative effect on the stability of the antibody and therefore reduced the number of bright positive cells detected which in turn reduced the population geometric mean value by 74 and 103 respectively. The combined data in Table 3.1 shows considerable variation in the geometric mean value when using differently sourced and stored STRO-1. Furthermore, dilution of the antibody supernatant and storage conditions of the commercial antibody directly affected the

percentage of STRO-1^{BRIGHT} cells detected. Therefore, using the commercially sourced STRO-1 at a single freeze-thaw cycle was the method of choice for the work described in this thesis as it gave the strongest straining.

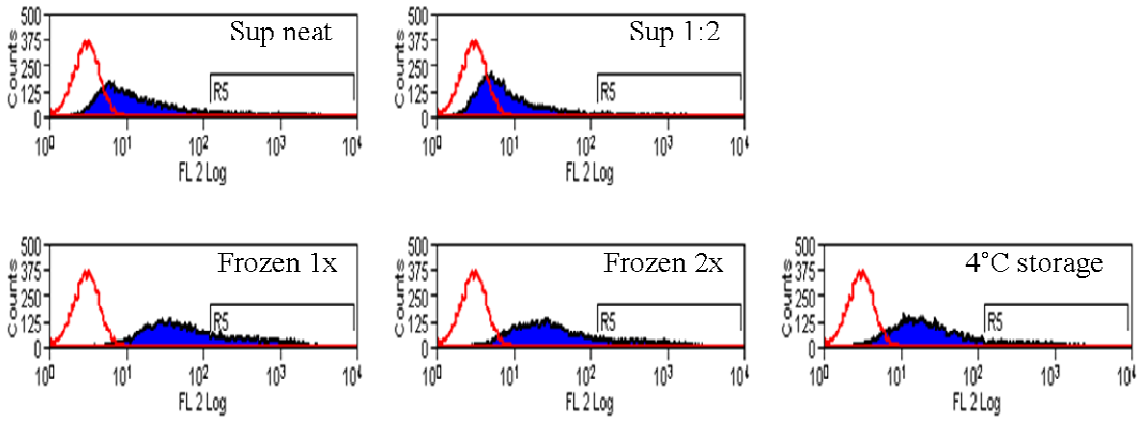

Figure 3.4: Optimisation of STRO-1 usage on passage 4 N24♂ hMSCs. Cells were incubated with STRO-1 as specified and detected with RPE-conjugated secondary antibody (Table 2.2). Flow cytometry analysis was carried out on a sample size of $5x10^5$ cells per 100 µL of supernatant/antibody solution, analysis normalised to $1x10^4$ events and gate (R5) set to include 0.02 % of the total control population (Section 2.5). Secondary antibody control is indicated by the red line and STRO-1 labelled population by the shaded histogram (blue).

STRO-1 antibody condition	Gate percentage	Geometric mean
Supernatant neat	13.24	131
Supernatant 1:2	7.34	66
Commercial frozen once	29.18	234
Commercial frozen twice	20.62	160
Commercial 4 ºC storage	14.20	131
Control	0.02	3

Table 3.1: Detection of STRO-1^{BRIGHT} population on passage 4 N24♂ hMSCs. Stained STRO-1/RPE cells were analysed by flow cytometry (Section 2.5.1) and gated to include 0.02 % of positive cells in the secondary only control population. STRO-1 at different conditions was assayed and the percentage within the gated population of bright cells and geometric mean of the whole population were recorded.

3.4 Effect of passage number on STRO-1 expression and differentiation potential

Culture conditions are known to affect the expression of certain markers, especially CD271 on bone marrow derived hMSCs (Jones *et al.*, 2002). These changes in marker expression are believed to arise from the lack of stimuli from the *in vivo* microenvironment or as a phenomenon resulting from extensive expansion. A possible correlation between marker expression in hMSC cultures and differentiation potential has not been studied before. Work in this laboratory has previously shown that an increase in passage number decreases the adipogenic potential of hMSCs (Westwood 2006), an effect which has also been reported by other groups (Conget and Minguell, 1999, Pal *et al.*, 2009). Therefore, this experiment aimed to investigate the effect of passage number on STRO-1 expression and its correlation with adipogenic and osteogenic differentiation potentials of the cells.

One-day post confluent hMSCs from the three healthy donors (N24♂, 31♂ and 38♀) were harvested at passages 4, 7 and 10 or 11 and stained with STRO-1/RPE or induced to differentiate to the adipogenic and osteogenic lineages. With increasing passage number, hMSCs from the three donors showed a decreased proliferation rate and distinct morphological changes from predominantly small and compact to large and flat, indicative of senescence (Figure 3.5). However, the rate at which hMSCs from each donor reached the stage of senescence varied. hMSCs from 38♀ reached their expansion limit at passage 10, and could not be sub-cultured further. It was possible to expand 31♂ hMSCs until passage 12, but passage 11 cells were used for the purpose of this experiment. Later passage cells (p7 to p11) became very fragile and were susceptible to physical damage during the STRO-1/RPE staining procedure resulting in a lower event count during flow cytometry analysis. RPE secondary controls and STRO-1/RPE stained cells were normalised pairwise to 10 000 or 6000 events per passage, after gating to exclude cell debris. N24♂ and 38♀ hMSCs showed a decrease in STRO-1 expression with increasing passage number (Figure 3.5). Cells from 31♂ had elevated expression of STRO-1 at passage 7 which then decreased at passage 11, showing that modulation of STRO-1 expression upon sub-culture was dependent on donor (Figure 3.5).

When hMSCs from each passage point were induced to differentiate to adipocytes and osteocytes (Section 2.3), the extent of differentiation matched the level of STRO-1 expression (Figure 3.5), whereby an elevated level of STRO-1 antigen resulted in a higher adipogenic and osteogenic potential both qualitatively (Figure 3.6) and quantitatively (Figure 3.7). The differentiation pattern observed at each passage number for the three donors was heterogeneous.

During adipogenesis, cells with the highest adipogenic potential (N24♂p4, 31♂p7 and 38♀p4) accumulated lipids rapidly and contained a larger subset of cells stained positively for Oil Red O (Figure 3.6, A: N24♂, B: 31♂ and C: 38♀). Osteogenesis was more pronounced in p4 of N24♂ and 38♀ compared to their corresponding later passages. In the case of 31♂, p7 showed higher differentiation potential than p4 and p11. For the osteogenic assay, alkaline phosphatase activity was observed in a few cells in the control populations of p4 and p7 of the three donors. Low level Alizarin Red staining was observed in the control populations of the later passages 10 or 11 (Figure 3.6, A: N24♂, B: 31♂ and C: 38♀). Quantitative analysis of differentiation was performed for both lineages (Figure 3.7, A: N24♂, B: 31♂ and C: 38♀).

Quantification of adipogenesis was primarily carried out by counting the number of cells with red stained lipid droplets (irrespective of size) per field of view. The second method used was dye solubilisation with normalisation to DNA content (Section 2.3.3). Both methods indicated a significantly higher adipogenic potential in N24♂p4 ($p<0.03$), 31♂p7 ($p<0.01$) and 38♀p4 ($p<0.04$) compared to their relevant passage numbers. However, the difference in adipogenic potential between the different passage numbers was not as pronounced as what was obtained by the adipocyte count method (Figure 3.7, A1&A2: N24♂, B1&B2: 31♂ and C1&C2: 38♀).

Quantification of osteogenesis was carried out by measuring the level of alkaline phosphatase activity and amount of Alizarin Red recovered, both assays normalised to DNA content (Section 2.3.3). Both assays indicated a significantly higher osteogenic potential in N24♂p4 ($p<0.01$), 31♂p7 ($p<0.01$) and 38♀p4 ($p<0.05$) compared to their relevant passage numbers. While both assays reflected the osteogenic potential observed by the qualitative staining (Figure 3.7, A3&A4: N24♂, B3&B4: 31♂ and C3&C4: 38♀), they did not distinguish between the differentiation heterogeneity within each cell population revealed by the microscopy analysis of the staining assay (Figure 3.6).

Overall, the qualitative staining could be matched to the quantitative assay and differentiation potential observed directly correlated with the STRO-1 profile obtained at the different passage number. Additionally, the three donors regulated their STRO-1 expression differently at different passage number, but all the populations lost STRO-1 expression at later passage numbers (beyond p7). Comparatively, beyond p7, adipogenic and osteogenic potential was significantly reduced ($p<0.04$ and $p<0.01$).

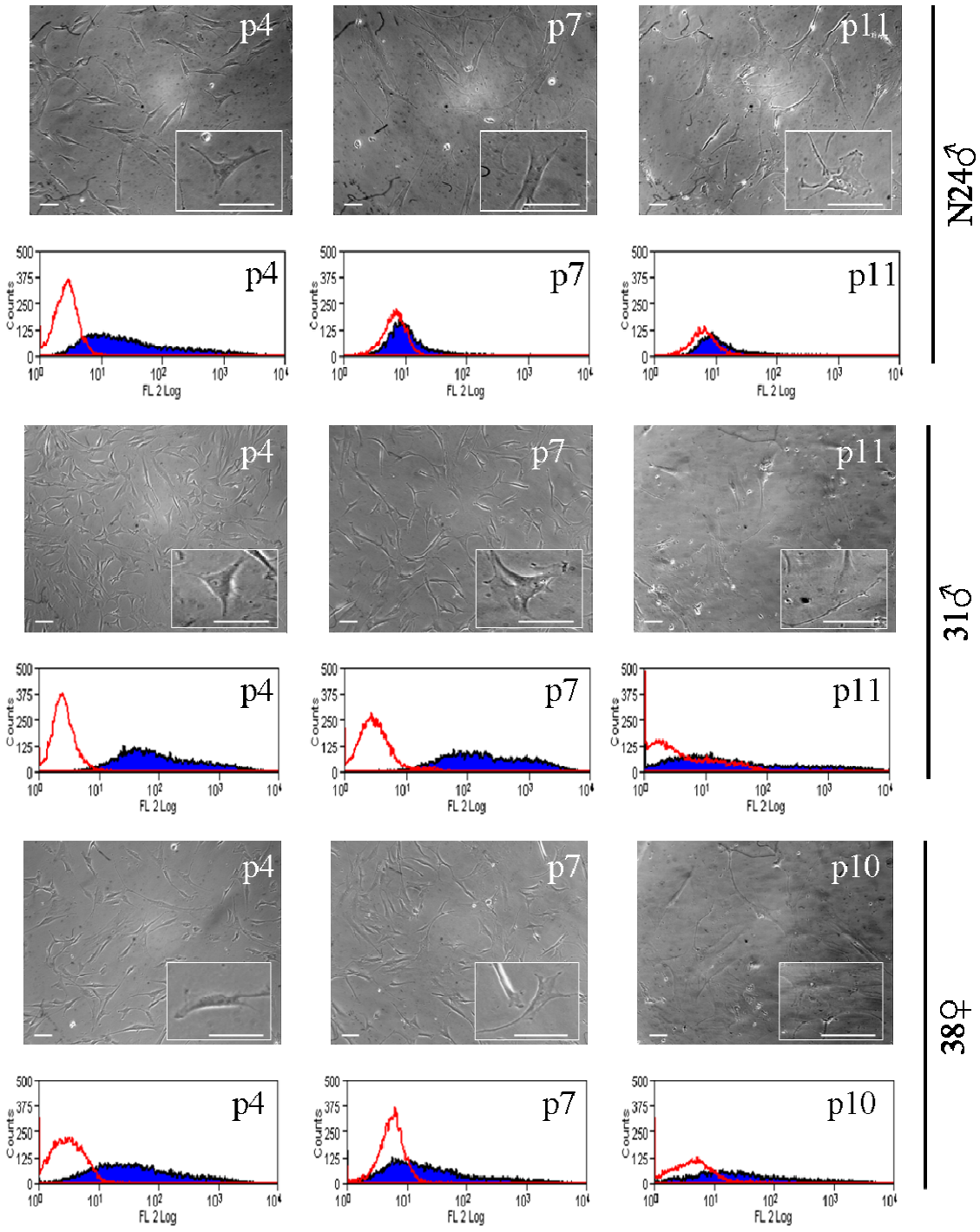

Figure 3.5: Changes in cell morphology and STRO-1 expression with passage number. hMSCs from three donors (N24♂, 31♂ and 38♀) were expanded to specified passage numbers and assayed for STRO-1 expression by flow cytometry (Section 2.5). Prolonged culture progressively initiates cell senescence characterised by large and flat cells (inset). STRO-1 was detected using RPE conjugated secondary and analysed to exclude cell debris. Secondary antibody control is indicated by the red line and STRO-1 labelled population by the shaded histogram (blue). Scale bars represent 125 µm.

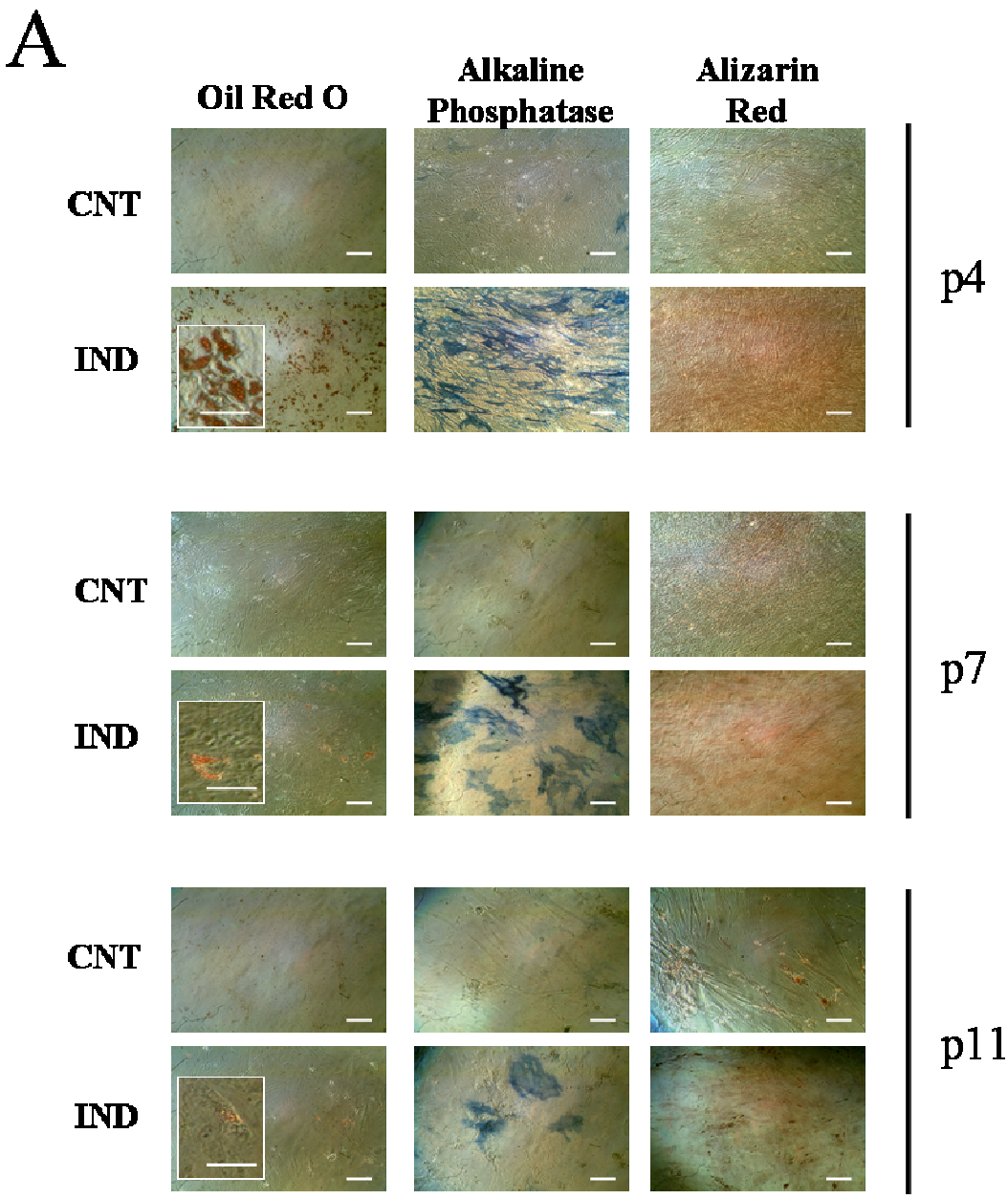

Figure 3.6: Continued overleaf. Qualitative correlation of passage number with adipogenic and osteogenic differentiation potential. One day post-confluent hMSCs from three donors (A.N24♂, B.31♂ and C.38♀) were differentiated to adipocytes and osteocytes via the addition of specific induction cocktails (Section 2.3.1). At day 8, adipogenic differentiation was terminated and cultures stained with Oil Red O; at day 21, osteocytes were assayed for alkaline phosphatase activity (blue) and Alizarin Red mineral deposits (brown-red) (Section 2.3.2). CNT: uninduced control population; IND: lineage-specific induced population. Scale bars represent 125 µm.

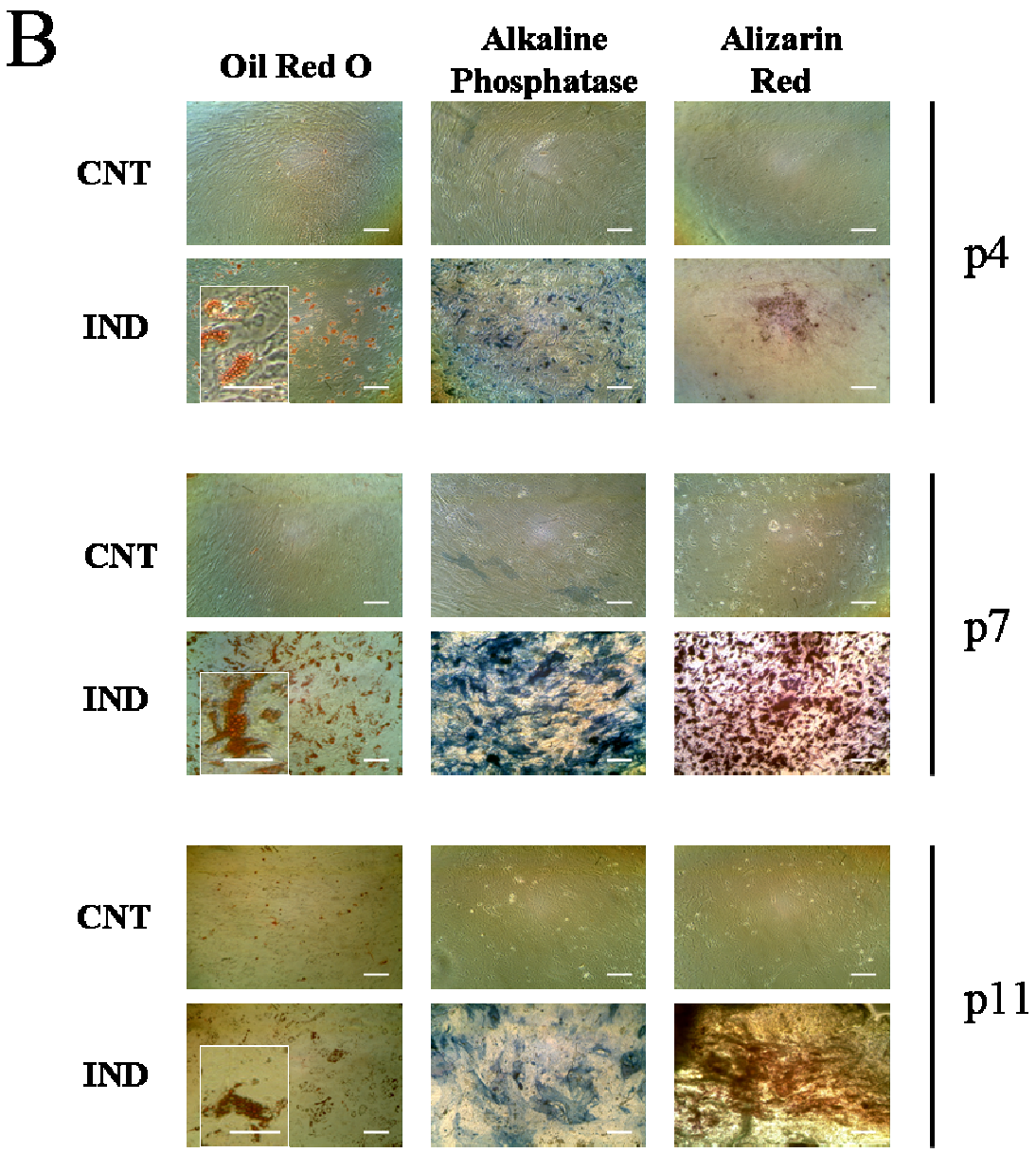

Figure 3.6: Continued overleaf. Qualitative correlation of passage number with adipogenic and osteogenic differentiation potential. One day post-confluent hMSCs from three donors (A.N24♂, B.31♂ and C.38♀) were differentiated to adipocytes and osteocytes via the addition of specific induction cocktails (Section 2.3.1). At day 8, adipogenic differentiation was terminated and cultures stained with Oil Red O; at day 21, osteocytes were assayed for alkaline phosphatase activity (blue) and Alizarin Red mineral deposits (brown-red) (Section 2.3.2). CNT: uninduced control population; IND: lineage-specific induced population. Scale bars represent 125 µm.

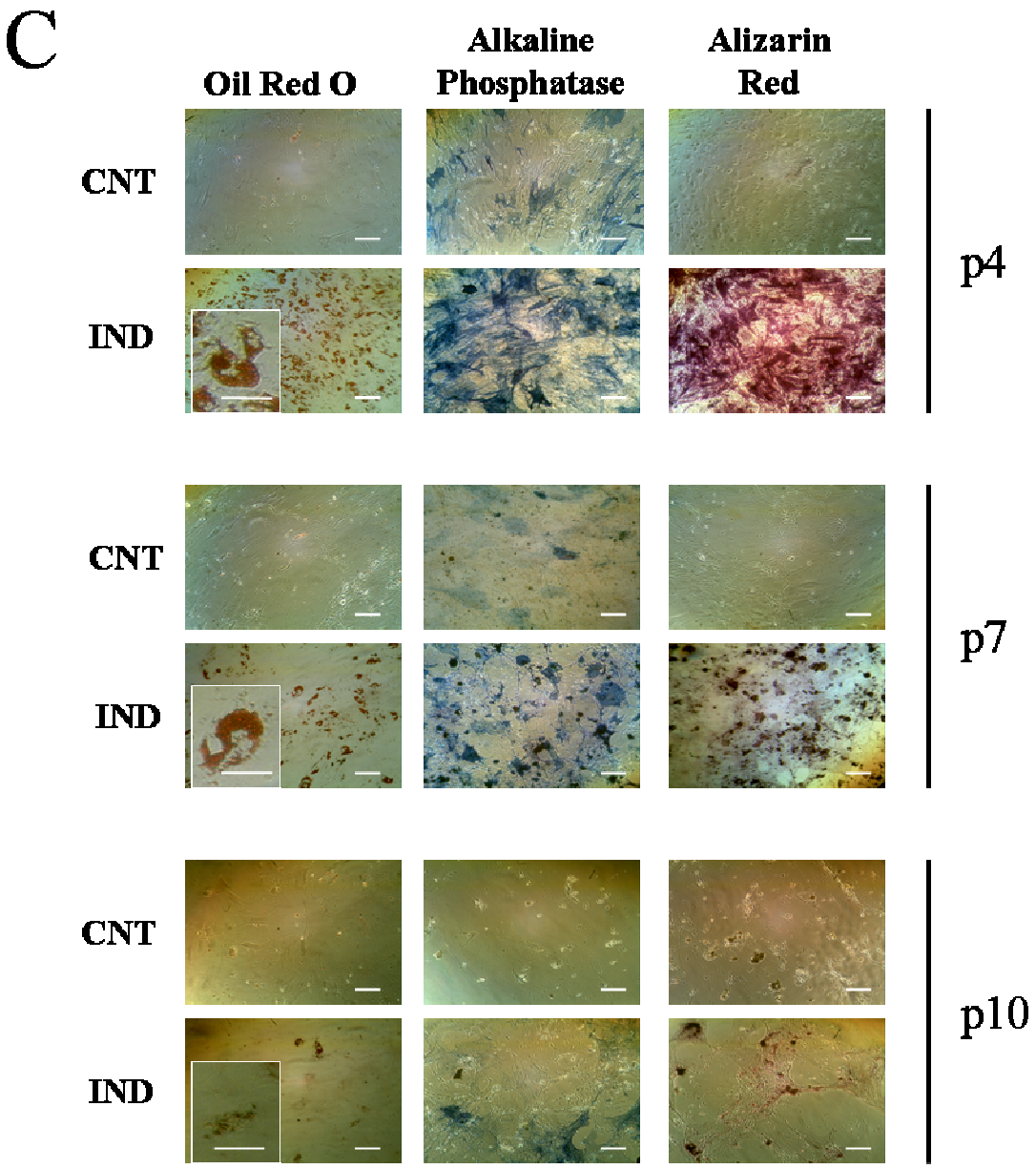

Figure 3.6: Qualitative correlation of passage number with adipogenic and osteogenic differentiation potential. One day post-confluent hMSCs from three donors (A.N24♂, B.31♂ and C.38♀) were differentiated to adipocytes and osteocytes via the addition of specific induction cocktails (Section 2.3.1). At day 8, adipogenic differentiation was terminated and cultures stained with Oil Red O; at day 21, osteocytes were assayed for alkaline phosphatase activity (blue) and Alizarin Red mineral deposits (brown-red) (Section 2.3.2). CNT: uninduced control population; IND: lineage-specific induced population. Scale bars represent 125 µm.

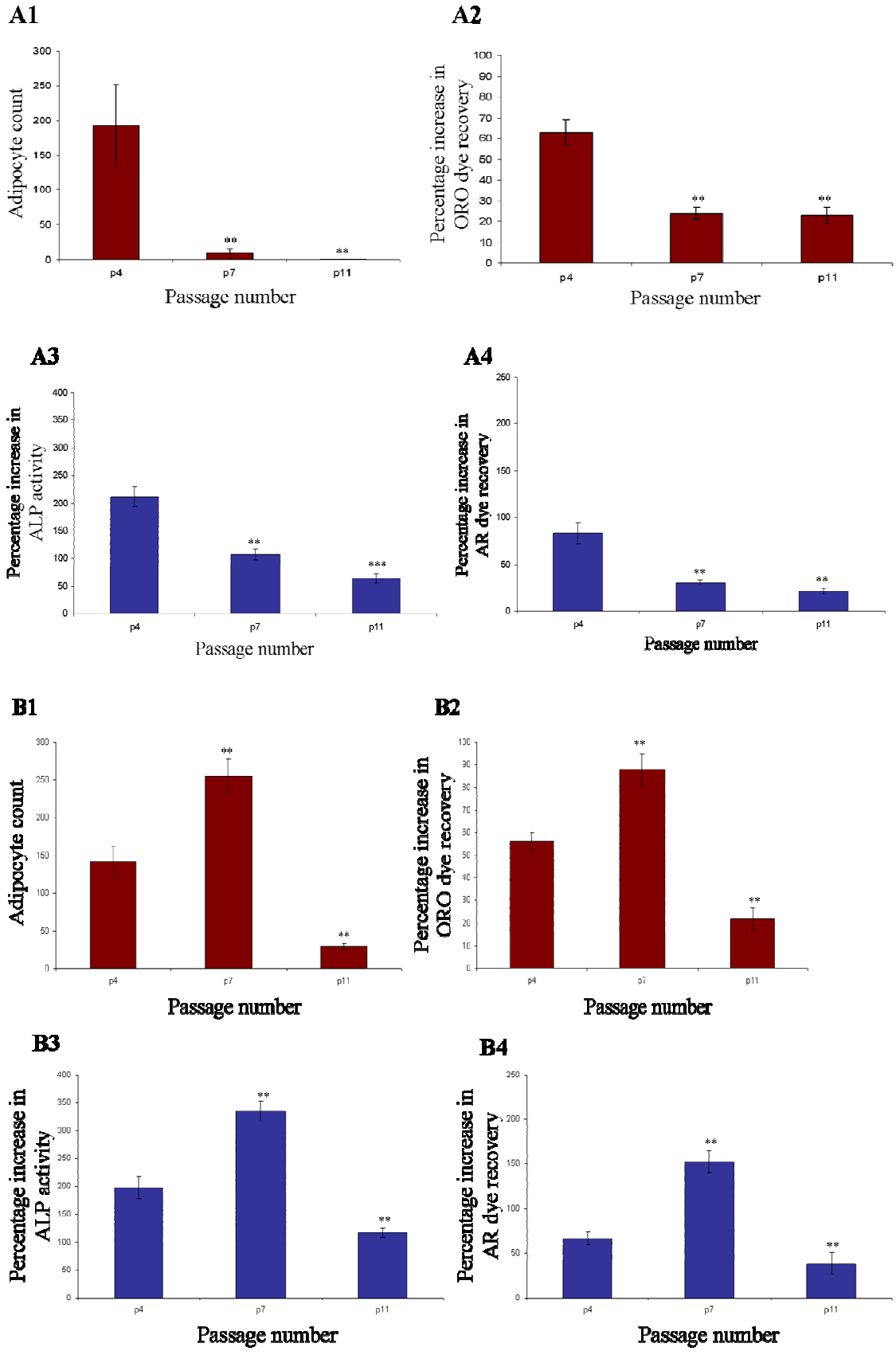

Figure 3.7: Continued overleaf.

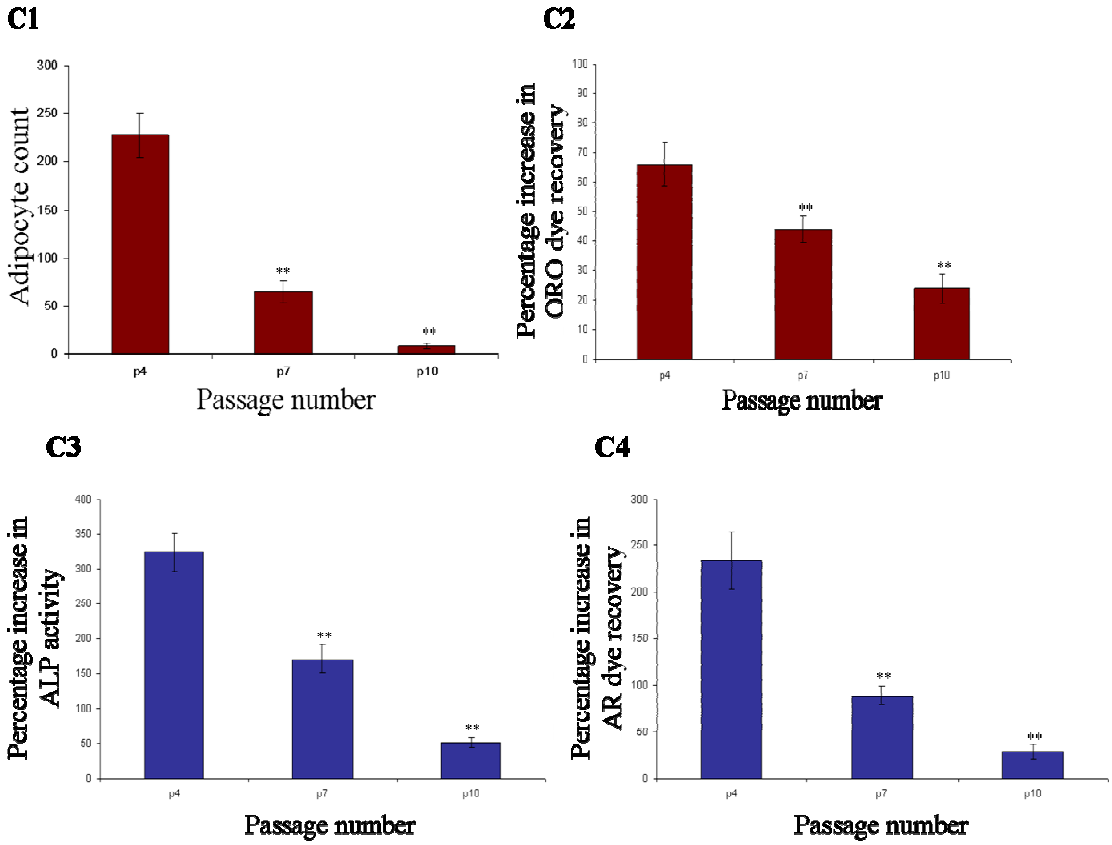

Figure 3.7: Quantitative correlation of passage number with adipogenic and osteogenic differentiation potential. Bar charts represent data from three hMSC donors (A. N24♂, B. 31♂ and C. 38♂). At day 8, the extent of adipogenesis was quantified by adipocyte count per field of view (Section 2.3.3.1) and Oil Red O dye extraction (Section 2.3.3.2) with normalisation to DNA content (Section 2.3.3.5). At day 21, osteogenesis was quantified by alkaline phosphatase activity (Section 2.3.3.3) and Alizarin Red dye extraction (Section 2.3.3.4), both normalised to DNA content (Section 2.3.3.5). Adipocyte count: A1, B1 and C1; Oil Red O dye recovery: A2, B2 and C2; Alkaline phosphatase activity: A3, B3 and C3 and Alizarin Red dye recovery: A4, B4 and C4. Student's t-test p4 versus p7; p4 versus p10/11, $**p<0.04$, $***p<0.01$.

3.5 Enrichment of STRO-1 positive sub-population

hMSCs exhibit variable expression of STRO-1, as shown by flow cytometry and dual-colour immunofluorescence (Figures 3.1 and 3.3). This heterogeneity was reflected in the pattern of differentiation of the cells, whereby the extent of lipid accumulation and mineral deposition was not uniform throughout the culture monolayer. In order to investigate whether the STRO-1 positive cells was the population subset possessing the potential to extensively differentiate, N24♂ hMSCs at passage 6 were separated on a miniMACS® column to enrich for the STRO-1 positive population (Section 2.5.3). Enrichment of STRO-1 cells was confirmed via flow cytometry by labelling the cells with STRO-1/RPE (Figure 3.8). Passage 6 hMSCs were used as that population displayed a wide population spread (Figure 3.8; green line representing pre-enriched population), thus facilitating the enrichment process. A gate (R9) was drawn to include the STRO-1^{BRIGHT} subset of the pre-enriched fraction (31.1 %). Based on R9, an enrichment of 73.5 % was achieved in the STRO-1 enriched fraction while the STRO-1 depleted fraction contained 4.4 % of STRO-1^{BRIGHT} cells (Table 3.2).

After assaying the three populations obtained (pre-enriched, STRO-1 depleted and STRO-1 enriched) for STRO-1 expression, they were induced to differentiate to the adipogenic and osteogenic lineages. On termination of differentiation, adipocytes were stained with Oil Red O for lipid accumulation and osteocytes were assayed for alkaline phosphatase activity. Qualitative assays showed that the STRO-1 enriched fraction exhibited extensive differentiation characterised by numerous adipocytes and strong alkaline phosphatase activity, as compared to the STRO-1 depleted and pre-enriched fractions (Figure 3.9). In the STRO-1 enriched fraction, although the population contained numerous adipocytes, there were certain areas which were not as fully loaded with lipid droplets as others (Figure 3.9). Similarly, in the alkaline phosphatase staining, although all cells appeared blue (positive), the gradation in the blue staining varied. However, this heterogeneity in staining was not as pronounced as in the pre-enriched fraction. The STRO-1 depleted fraction exhibited limited differentiation, characterised by sparse adipocytes and faint blue patches (Figure 3.9). Due to the limited number of cells recovered after enrichment, it was not possible to quantify the extent of differentiation observed.

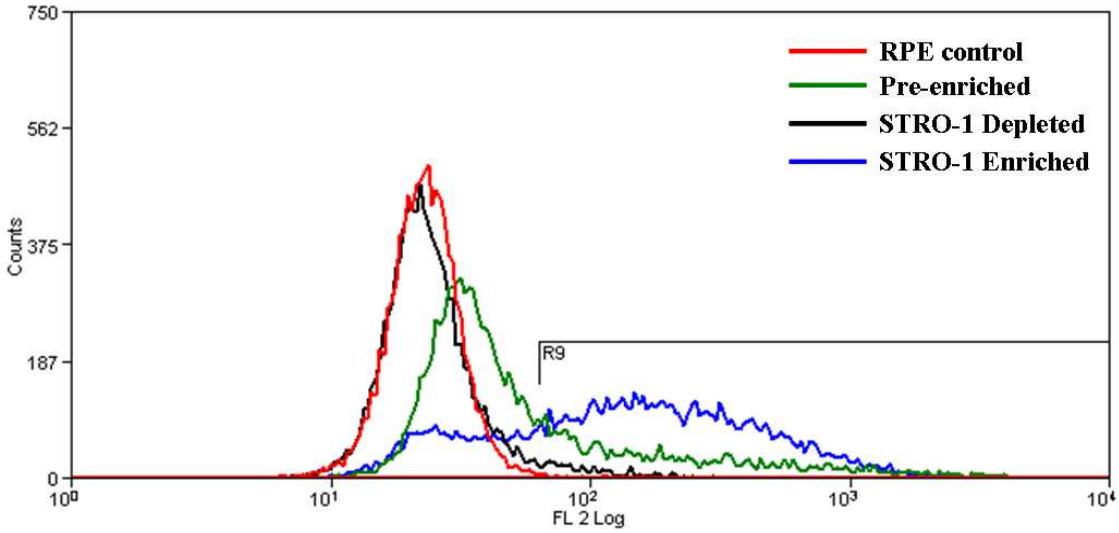

Figure 3.8: Overlay of flow cytometry analysis of MACS separated passage 6 N24♂ hMSCs. Cells were harvested, STRO-1 enriched by passing through magnetic column (Section 2.5.3) and the different fractions stained with STRO-1/RPE as appropriate (Section 2.5.1 but without final wash). Gate R9 represent the STRO-1^{BRIGHT} cell subset based on the pre-enriched fraction.

hMSC fraction	Percentage of STRO-1^{BRIGHT} cells (R9)
RPE control	0.5
Pre-enriched	31.1
STRO-1 depleted	4.4
STRO-1 enriched	73.5

Table 3.2: Percentage of STRO-1^{BRIGHT} cells during MACS separation. Cell fractions analysed by flow cytometry using STRO-1/RPE staining were gated (R9) to select for the STRO-1^{BRIGHT} subset.

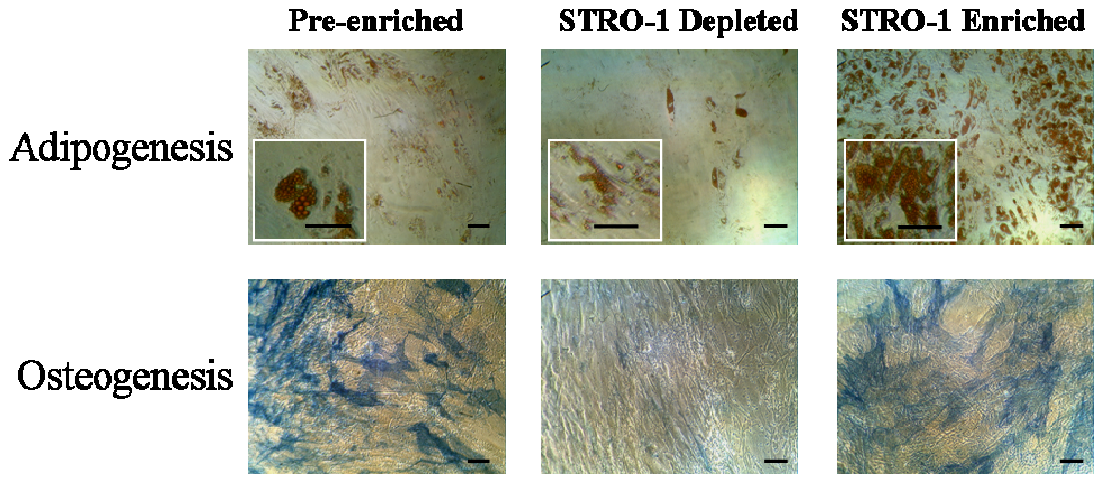

Figure 3.9: Adipogenic and osteogenic differentiation of MACS separated hMSC fractions. Pre-enriched, STRO-1 depleted and STRO-1 enriched fractions of p6 N24♂ were induced to differentiate to adipocytes for eight days (stained lipid droplets with Oil Red O) and osteocytes for twenty-one days (stained blue for alkaline phosphatase activity) (Section 2.3). Scale bars represent 125 µm.

3.6 Modulation of STRO-1 expression at confluency and its impact on differentiation potential

The established and validated protocol for differentiation of hMSCs is the addition of lineage-specific induction medium to the cells at one day post-confluency (Pittenger *et al.,* 1999). During expansion, hMSCs are maintained at sub-confluency to maximise proliferation and prevent possible contact induced differentiation. However, upon adipogenic and osteogenic differentiation, the cells are induced at post-confluency to encourage lineage specific maturation. Cell to cell contact has been shown to be a potent mediator of differentiation in addition to chemical stimuli (Jaiswal *et al.,* 2000). It is unknown if STRO-1 expression is modulated at post-confluency and whether it has any influence on differentiation potential. To test this possibility, STRO-1 expression was investigated at different time points of post-confluency and then induced to the adipogenic and osteogenic lineages. The two time points investigated were set up in parallel using the cell line M24♂.

Passage 4 hMSCs (M24♂) were allowed to expand for one and seven days post-confluency, at which points the cells were harvested and stained for STRO-1/RPE for flow cytometry analysis (Section 2.5.1) or induced to the adipogenic and osteogenic lineages (Section 2.3). The level of STRO-1 expression at seven days post-confluency was lower than the expression at one day post-confluency, indicating that upon cell to cell contact the surface expression of STRO-1 is reduced (Figure 3.10). Upon differentiation, adipogenesis was reduced when induced at seven days post-confluency compared to when induced at one day post-confluency. This was shown qualitatively by sparse adipocyte formation with few lipid droplets (Figure 3.11) and quantitatively by the reduced adipocyte count ($p<0.05$) and Oil Red O recovery ($p<0.04$) (Figure 3.12 A&B). However, osteogenesis was not affected as shown by the similar staining profile of ALP activity and AR staining for both time points (Figure 3.11). This observation was subsequently confirmed by the quantitative measurement assays which showed no difference in the level of ALP activity and AR dye recovery (Figure 3.12 A&B).

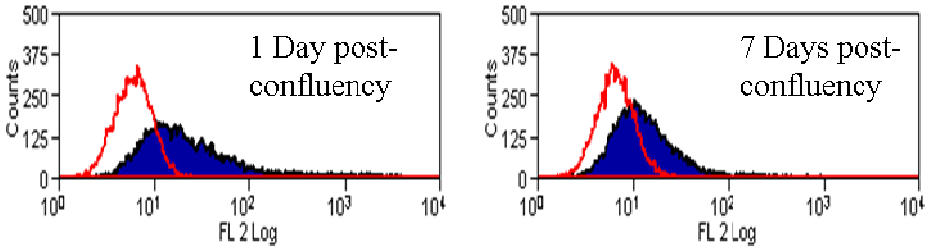

Figure 3.10: STRO-1 expression of passage 4 hMSCs (M24♂) at confluency. Cells were grown until one and seven days post-confluency, then harvested and stained for STRO-1/RPE (Section 2.5.1). Red lines indicate RPE control and blue shaded histograms represent STRO-1/RPE labelled populations.

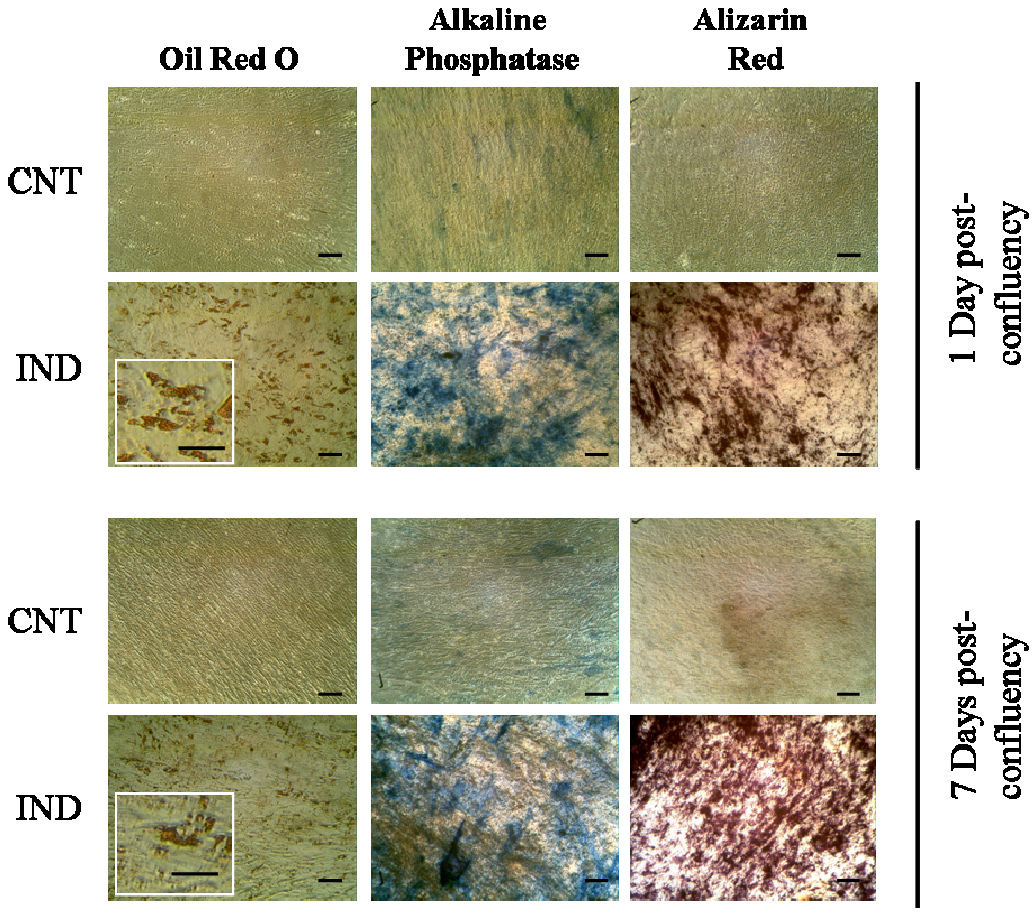

Figure 3.11: Differentiation of passage 4 hMSCs (M24♂) at confluency. Cells were induced in lineage-specific medium (IND) at one and seven days post-confluency. Adipogenesis was assayed after eight days by Oil Red O staining and osteogenesis was assayed after twenty-one days by blue alkaline phosphatase activity staining and Alizarin Red staining (Section 2.3). Control populations (CNT) were grown in the absence of induction cocktail and assayed for differentiation in a similar manner. Scale bars represent 125µm.

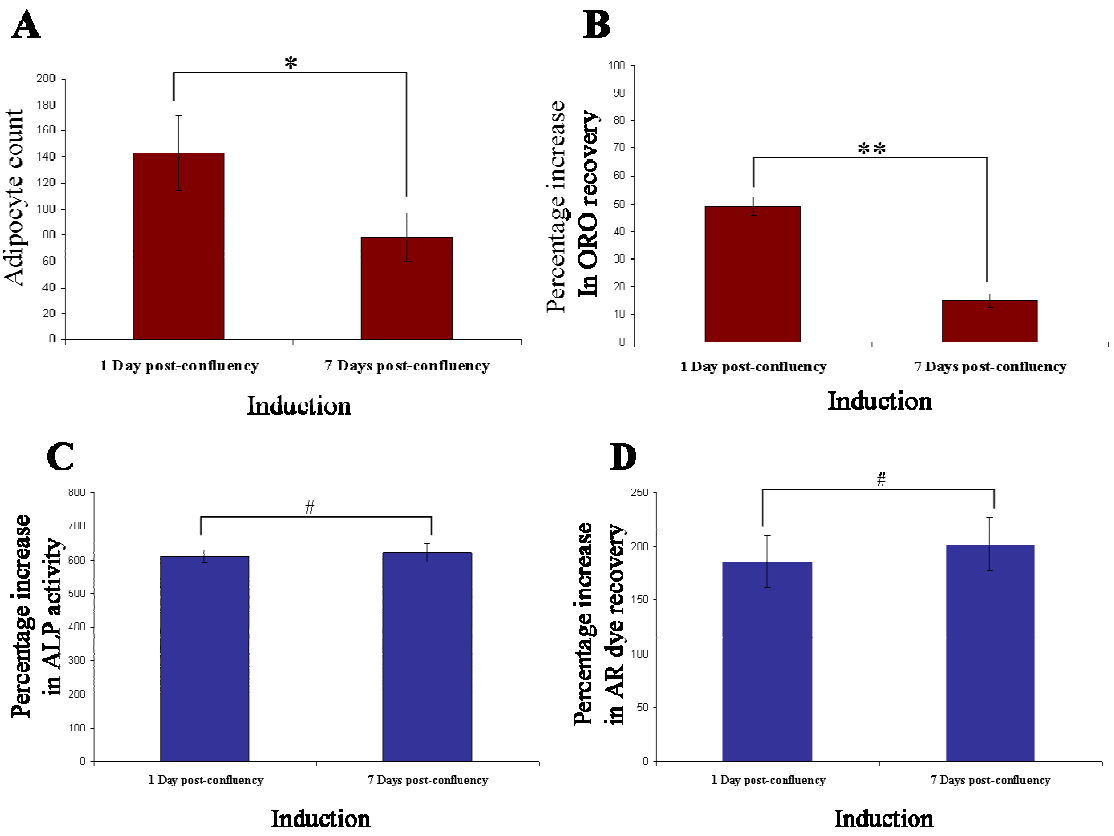

Figure 3.12: Quantification of adipogenic and osteogenic differentiation of passage 4 hMSCs (M24♂) at confluency. Cells were induced in lineage-specific medium at one and seven days post-confluency, after which they were assayed for adipogenic and osteogenic differentiation (Section 2.3). A&B: Adipogenesis was quantified by adipocyte count per field of view and Oil Red O dye extraction normalised to DNA content. C&D: Osteogenesis was quantified by alkaline phosphatase activity and Alizarin Red dye extraction, both normalised to DNA content. Student's t-test 1 Day versus 7 Days; *p<0.05, **p<0.04, # p>0.5.

3.7 STRO-1 expression during differentiation

The process of differentiation is driven by an initial commitment stage and gradually proceeds to a final maturation stage. During each of these stages, the cell undergoes morphological and phenotypical changes based on the induced lineage (Pittenger *et al.*, 1999). Here, the expression of STRO-1 as a marker of stemness and its modulation during differentiation on passage 5 hMSCs from three donors (N24♂, 31♂ and 38♀) was investigated. Adipogenesis takes place over a period of 8-10 days (Nakamura *et al.*, 2003) after which fully matured adipocytes (round cells with peri-nuclear lipid droplets) are formed. Osteogenesis, on the other hand, is a 21-day process, whereby hMSCs initially turn into osteoblasts and then slowly mature and deposit calcium phosphate (Shur *et al.*, 2001). However, in order to assay for STRO-1 expression by flow cytometry, cells beyond day 8 of differentiation could not be analysed. Adipocytes beyond day 8 became very fragile and did not withstand the staining procedure, giving an anomalous scatter profile characteristic of apoptotic cells and cell debris (data not shown). Osteocytes beyond day 8 of differentiation were difficult to dissociate by trypsin enzymatic treatment to a single-cell suspension as they had started depositing extracellular matrix, thus hindering flow cytometry analysis. CD13 is a transmembrane protein previously used as mesenchymal marker and was therefore used as a positive control of marker expression, as it is expected to be consistently expressed. Non-induced cells were also analysed for STRO-1 and CD13 expression at days zero (on the day of induction), two and seven.

CD13 expression was donor dependent but remained constant throughout differentiation, in both the non-induced and induced cells (Figure 3.13). STRO-1 expression decreased with time in the non-induced control population (Figure 3.13 A), consistent with STRO-1 down-regulation upon confluency (Figure 3.10). The process of adipocyte formation was consistent with a loss in STRO-1 expression as the cells matured. However, 31♂ showed a slight increase in STRO-1 expression at day 8 of adipogenesis (* in Figure 3.13 B). It is to be noted that this population of cells had a greater amount of cell debris as compared to the other populations, and therefore the profile obtained may be inclusive of cells with a compromised cell membrane stained intracellularly with STRO-1. Furthermore, the side population of STRO-1^{BRIGHT} cells

was not present, suggesting that those cells have differentiated to adipocytes and therefore exhibited a STRO-1^{DULL} profile. Osteogenesis followed a pattern of initial STRO-1 up-regulation at day 2 and gradual down-regulation as differentiation proceeded. However, the rate and extent of this down-regulation was dependent on the donor population (Figure 3.13 C). Given that later time point analyses were not possible, the level of STRO-1 expression on mature osteocytes was not obtained.

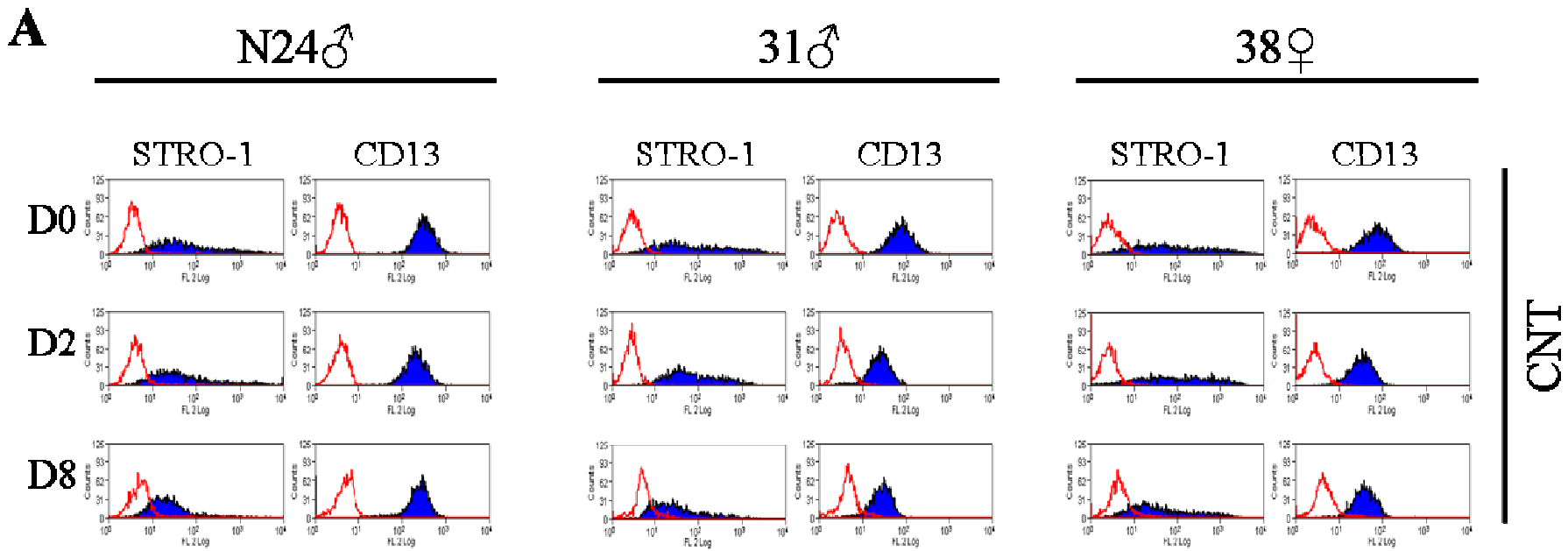

Figure 3.13: Continued overleaf. Flow cytometry analysis of STRO-1 and CD13 expressions during adipogenic and osteogenic differentiation. Passage 5 hMSCs from three donors (N24♂, 31♂ and 38♀) were induced to differentiate to (B) adipocytes and (C) osteocytes, with a (A) control population maintained without induction medium (Section 2.3.1). At days 0, 2 and 8 of differentiation (D0, D2 and D8), cells were harvested, stained for STRO-1/RPE or CD13-PE and analysed by flow cytometry (Section 2.5.1), with normalisation to $2x10^3$ cells. Red lines indicate control population unstained or with RPE only and shaded histograms (blue) marker specific labelled population. The *x*-axis represents FL2 Log scale and the *y*-axis represents counts. * in B indicates population with increased cell debris.

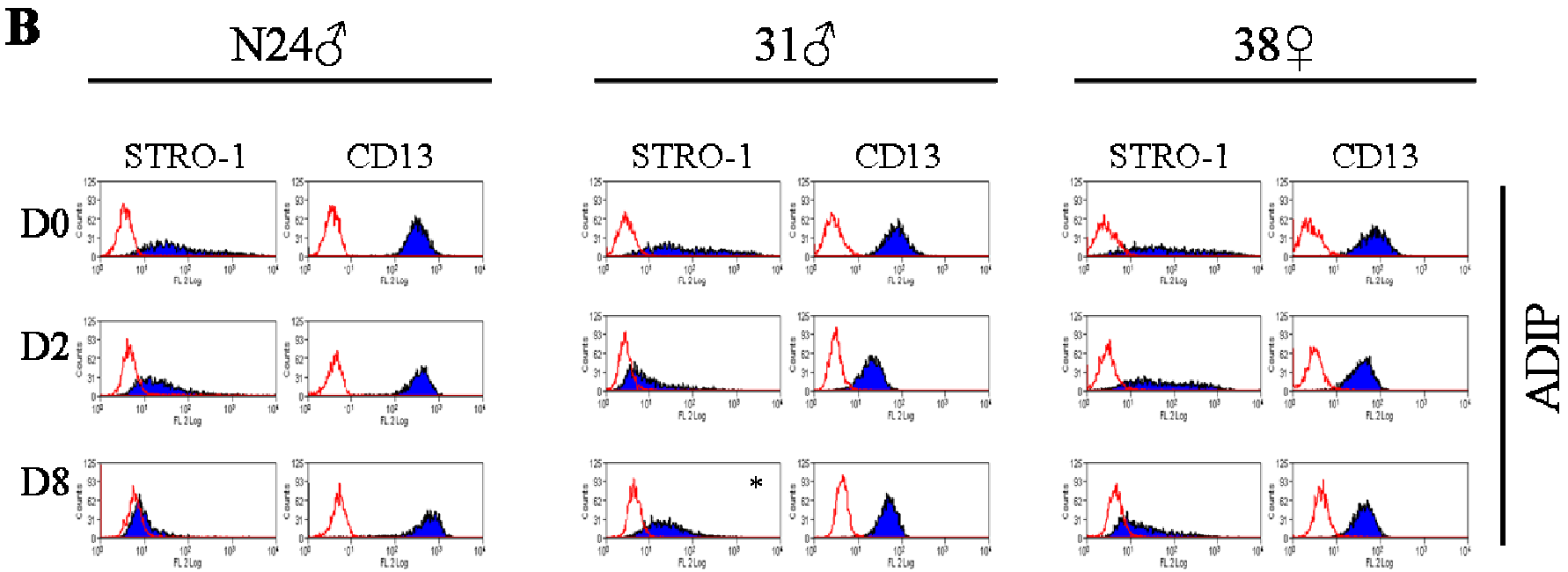

Figure 3.13: Continued overleaf. Flow cytometry analysis of STRO-1 and CD13 expressions during adipogenic and osteogenic differentiation. Passage 5 hMSCs from three donors (N24♂, 31♂ and 38♀) were induced to differentiate to (B) adipocytes and (C) osteocytes, with a (A) control population maintained without induction medium (Section 2.3.1). At days 0, 2 and 8 of differentiation (D0, D2 and D8), cells were harvested, stained for STRO-1/RPE or CD13-PE and analysed by flow cytometry (Section 2.5.1), with normalisation to $2x10^3$ cells. Red lines indicate control population unstained or with RPE only and shaded histograms (blue) marker specific labelled population. The *x*-axis represents FL2 Log scale and the *y*-axis represents counts. * in B indicates population with increased cell debris.

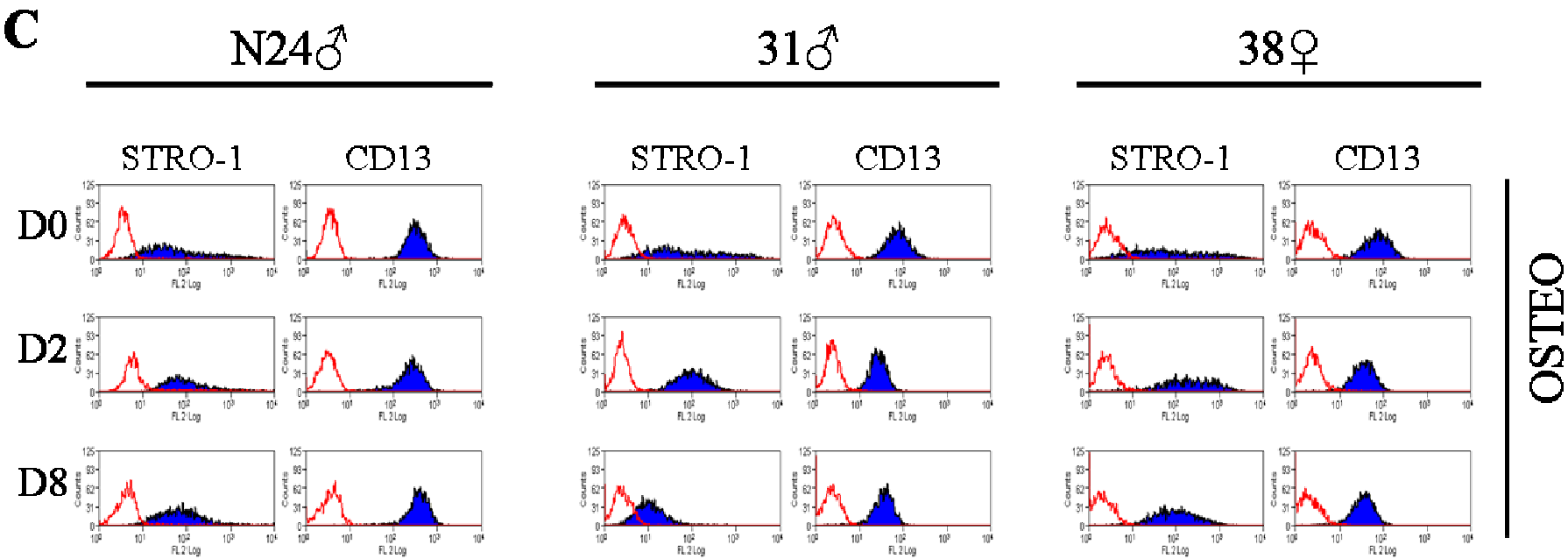

Figure 3.13: Flow cytometry analysis of STRO-1 and CD13 expressions during adipogenic and osteogenic differentiation. Passage 5 hMSCs from three donors (N24♂, 31♂ and 38♀) were induced to differentiate to (B) adipocytes and (C) osteocytes, with a (A) control population maintained without induction medium (Section 2.3.1). At days 0, 2 and 8 of differentiation (D0, D2 and D8), cells were harvested, stained for STRO-1/RPE or CD13-PE and analysed by flow cytometry (Section 2.5.1), with normalisation to $2x10^3$ cells. Red lines indicate control population unstained or with RPE only and shaded histograms (blue) marker specific labelled population. The *x*-axis represents FL2 Log scale and the *y*-axis represents counts. * in B indicates population with increased cell debris.

3.8 Discussion

The aim of the first results chapter of this thesis was to characterise STRO-1 expression on cultured hMSCs and correlate the STRO-1 status of the cells to their multilineage potential. In order to achieve this, hMSCs isolated by plastic adherence from the bone marrow were immuno-phenotyped to ensure that they were in accordance with the profile documented elsewhere (Horwitz *et al.*, 2005). Thereafter, STRO-1 expression was investigated under different culture conditions and its impact on adipogenic and osteogenic differentiations was qualitatively and quantitatively assayed.

Due to different isolation and growth protocols, some variability in the phenotype of hMSC has been reported (Jones *et al.*, 2002, Tsutsumi *et al.*, 2001, Campioni *et al.*, 2003). Under standard growth conditions as proposed by Pittenger and co-workers (1999), both the morphology and the marker profile of the hMSC populations observed in this study (Figures 3.5 and 3.1 respectively) resembled those documented elsewhere (Pittenger *et al.*, 1999, Majumdar *et al.*, 1998). Uniform expression of mesenchymal CD13, endothelial CD105 and hMSC SH4 (epitope of CD73 present on hMSC) markers suggested the absence of contaminating cells of different lineage origin (Barry *et al.*, 2001, Campioni *et al.*, 2003). The hMSC populations investigated here were also positive for the multipotent perivascular cell marker CD146, which has been linked to MSCs by virtue of a proposed common niche (Covas *et al.*, 2008). CD133, a marker most commonly found on protrusions of haematopoietic progenitor cells was not expressed by cultured hMSCs as previously reported (Wagner *et al.*, 2005, Buhring *et al.*, 2009).

However, this study differed from others in that CD271 was weakly detected on the cultured hMSCs (formerly known as Low-affinity Nerve Growth Factor Receptor, LNGFR). It is to be noted that the hMSCs used in the profiling were at passage 6 and the culture conditions used for expansion included bFGF. In contrast, Jones and co-workers showed high levels of CD271 in freshly isolated hMSCs from bone marrow samples (Jones *et al.*, 2002). Here, the difference lies in the state of the cell population used (cultured or fresh) and the conditions under which the cells were expanded.

Indeed it has been shown that CD271 is quickly down-regulated upon culture (as low as passage 3) especially in bFGF supplemented media, therefore explaining the weak expression of CD271 observed in the cultured hMSCs in my study (Jones *et al.*, 2002, Quirici *et al.*, 2002).

The three cell hMSC populations screened in my study were positive for STRO-1 although the profile obtained appeared to be donor-dependent as reported by others (Stewart *et al.*, 2003). Among the panel of markers used, STRO-1 was found to be the only marker variably expressed in the hMSC populations and the antigen appeared to be non-uniformly distributed on the cell surface. The STRO-1 profile has been classified as three subsets indicated by STRO-1^{DULL}, STRO-1^{INTERMEDIATE} and STRO-1^{BRIGHT}, possibly with the primitive cells residing in the STRO-1^{BRIGHT} subset (Gronthos *et al.*, 2003). In my study, this heterogeneity in antigen expression appeared to be correlated with the heterogeneous differentiation observed when induced to the adipogenic and osteogenic lineages. Although the populations terminally differentiated as assayed by histochemical stainings, only islands of adipocytes and osteocyte nodules were observed, therefore leading to the hypothesis that STRO-1 antigen is a marker of multipotency.

Before STRO-1 could be employed in further assays, it was important to optimise its use as a number of reports have documented conflicting protocols for STRO-1 screening. Furthermore, the most common STRO-1 source which is the antibody supernatant has been used at different concentrations, such as neat supernatant (Mirmalek-Sani *et al.*, 2006) or a 1:2 dilution (Jones *et al.*, 2002). Moreover, the concentration of antibody produced in hybridoma supernatant is not consistent in every culture system and such batch variability should be considered when using antibody supernatant (Mohan *et al.*, 1993). The lack of quality control on STRO-1 hybridoma supernatant makes it difficult to determine the molecular integrity and concentration of the IgM produced, thus causing variability in the degree of STRO-1 expression detected when screening cell populations. Comparison between hybridoma supernatant and reconstituted commercially obtained lyophilised antibody showed that the binding ability of STRO-1 antibody was optimal when used at the recommended concentration

of 5 µg/mL of the commercial STRO-1 with the least number of freeze-thaw cycle. Therefore, this protocol was adopted to detect STRO-1 expression throughout this thesis.

Comparative studies of potential hMSC markers indicated that STRO-1 expression is lost during *in vitro* expansion due to the lack of the necessary stimuli normally present in the *in vivo* microenvironment (Jones *et al.,* 2002), but to date, there has been no correlation between the modulation of STRO-1 upon culture and its influence on multilineage differentiation. This study demonstrated that STRO-1 expression is not consistent throughout culture and the level of expression at different passage number is donor-dependent (Figure 3.5). Indeed, when hMSCs from the three donor populations were cultured to passage 4, 7 and 10/11, the cells changed from a compact polygonal shape to a large flat appearance indicative of senescence (Wagner *et al.*, 2008). However, the rate at which the cells reached the senescence stage varied among the populations, showing that the hMSC populations may have an inherent proliferative ability, which may be dependent on the donor's health, lifestyle or age (Murphy *et al.*, 2002, Coipeau *et al.*, 2009). Once the cells reached passage10/11, they stopped dividing and could not be sub-cultured further. Other reports document bone marrow hMSC cultures for up to passage 25, but it is to be noted that altered conditions including lower plating densities and higher serum concentrations accounted for such extensive expansion potential (Samuelsson *et al.*, 2009).

Interestingly, changes in the cell morphology appeared to be correlated with the level of STRO-1 expression detected, whereby a large flat phenotype exhibited weak STRO-1 expression. Furthermore, upon induction to the adipogenic and osteogenic lineages, the extent of differentiation as assayed qualitatively and quantitatively (Figures 3.6 and 3.7) was directly dependent on the level of STRO-1 expression. It has been shown that cell shape directly influences lineage commitment, but the intracellular mechanism resulting from changes in the actin cytoskeleton has not been fully elucidated (McBeath *et al.*, 2004). In this study, it can be inferred that the morphological changes observed upon *in vitro* expansion regulates the expression of STRO-1 which in turn acts as a differentiation antigen dictating the multilineage status of the cell. However, the natural

process of cell senescence causing a decrease in differentiation cannot be ruled out. It has been proposed that long-term expanded cells can be affected in five different ways: 1) the heterogeneous hMSC cultures exhibit different proliferative rates which affect the rate of culture expansion *in vitro*; 2) spontaneous genetic mutations of cells in culture affecting cell fate; 3) spontaneous differentiation due to culture conditions leading to hindering self-renewal capacity of hMSCs; 4) loss of telomeres restricting cell division; 5) age-related cell senescence depending on hMSC donor (Wagner *et al.*, 2010). Therefore, the implication of STRO-1 at any of the different cellular processes described remains to be investigated once the identity of STRO-1 antigen is elucidated.

STRO-1 antigen as a multilineage marker was further investigated by primary enrichment of STRO-1 positive cells via magnetic cell separation and differentiation assays. Enrichment of passage 6 hMSCs yielded a population of 73.5 % STRO-1 positive cells (Table 3.2). Despite the heterogeneous expression of STRO-1 in the pre-enriched population, it was not feasible to achieve a better enrichment as cells from the STRO-1^{DULL} subset were being selected for when enriched at higher stringency. As such, after various optimisation steps, it was possible to achieve a maximum enrichment of 73.5 %, a population which in this study was classified as STRO-1^{BRIGHT}, while the depleted fraction consisted of 4.4 % of STRO-1^{BRIGHT} cells. In a similar study conducted by Gronthos and colleagues (2003), a population of 75.3 % of STRO-1 positive cells was achieved from a heterogeneous population of freshly derived bone marrow mononuclear cells. Although the starting population in the two experiments differed (uncultured against cultured populations), a directly comparable enrichment was achieved therefore suggesting the enrichment obtained in my study was optimal. Upon induction, the STRO-1 enriched fraction showed enhanced differentiation potential characterised by numerous adipocytes and elevated ALP activity as compared to the pre-enriched fraction. The STRO-1 depleted fraction showed limited differentiation, possibly due to the presence of the contaminating 4.4 % STRO-1^{BRIGHT} cells which retained differentiation potential. Due to the limited number of cells, mineralisation assays and quantification of differentiation was not possible, but despite this, the histological staining pattern observed clearly highlighted STRO-1 as a marker of multipotency. This is the first report of a positive marker which enriches for

multipotential hMSCs from adherent cultures. These data have important implications in regenerative medicine as it addresses one major obstacle in hMSC application that is limited cell number obtained from bone marrow mononuclear cells. By expanding hMSCs and isolating the multipotential STRO-1 positive subsets of the heterogeneous population, enhanced *in situ* differentiation could potentially be achieved, for instance in osteo-chondral injuries where STRO-1 enriched cells could be transplanted to the site of repair.

In agreement with Pittenger's protocol of hMSC culture and differentiation (Pittenger *et al.*, 1999), hMSCs are induced at one day post-confluency. Most evaluations of STRO-1 expression are carried out at sub-confluency and thus, it is unknown whether confluency modulates STRO-1 expression. In this study, upon extended culture, STRO-1 expression was found to be reduced. While a down-regulation of STRO-1 negatively influenced adipogenesis, interestingly, osteogenesis was not affected. The extent of ALP activity and AR staining was similar in cells induced at one and seven days post-confluency. This observation indicated that the cells retained their osteogenic potential upon extended culture and upon chemical stimulation (addition of osteogenic differentiation cocktail), readily differentiated to osteoblasts. An analogous phenomenon has been documented by Seib and co-workers (Seib *et al.*, 2009). This group showed that extended *in vitro* culture of hMSCs may 'imprint' osteogeneic traits on hMSCs (especially those derived from the bone marrow) by the activation of endogenous BMPs, key factors in bone morphogenesis. Indeed, a comparative study showed that bone marrow derived MSCs are superior in their ability to differentiate towards the osteogenic lineage while adipose derived MSCs were more inclined towards the adipogenic lineage (Im *et al.*, 2005). In line with these observations, I speculate that adipogenesis of adipose derived MSCs will not be affected while osteogenesis may be hampered if they were to be induced at seven days post-confluency. Therefore, future studies should take into account the source of MSCs being used as the time of induction may be a crucial factor in determining the outcome of the differentiation process.

When the STRO-1 antibody was first identified, it was highlighted as a marker of undifferentiated adherent cells (hMSCs) by its lack of expression on mature adipocytes (Simmons and Torok-Storb, 1991). Upon differentiation, hMSCs lose their stemness and commit to a specific lineage. On doing so, they change from multipotential to unipotential and mature towards a specific cell type. If STRO-1 were to be a marker of multipotency, then it is fair to hypothesise that its expression will be gradually lost as the cell commits and matures. To investigate this hypothesis, the STRO-1 profile of hMSCs was assayed at different time points of adipogenesis and osteogenesis. Relative to osteogenesis, adipogenesis is a rapid process. Adipogenesis is characterised by lipid accumulation and mature lipid-laden adipocytes become visible within eight days of induction (Ntambi and Young-Cheul, 2000). The expression of STRO-1 was constantly down-regulated as adipogenesis progressed, indicating lineage commitment and maturation as initially proposed by Simmons and Torok-Storb (1991). On the other hand osteogenesis is a temporal event characterised by primary osteoblast formation and subsequent mineral deposition taking place over an average period of twenty-one days. However, beyond day eight of osteogenesis, due to extracellular matrix deposition, trypsin enzymatic treatment was not effective, resulting in samples unsuitable for flow cytometry analysis. Therefore, the latest time point for flow cytometry analysis was day eight. Osteogenesis, as opposed to adipogenesis, showed an initial upregulation of STRO-1 followed by a gradual down-regulation. This phenomenon may be explained by the fact that the experimental design to capture STRO-1 expression during osteogenesis is reliant on the early processes of cell commitment to the lineage, and therefore may be a natural property of STRO-1 to display an initial upregulation before being downregulated upon maturation. This phenomenon was not observed in adipogenesis as the process is rapid and I speculate that if samples were taken at earlier stages of adipogenesis (for instance four hours post induction), the initial upregulation might have been observed. Transcriptional changes have been shown to occur within few hours of hormonal stimulation to the adipogenic lineage (Tang and Lane, 1999) and based on this, it can be suggested that STRO-1 expression is altered during the early stages of differentiation. Since CD13 remained constant throughout the differentiation processes, it can be concluded that the modulation observed by STRO-1 was not an

artefact, but a real phenomenon characterised by the nature of the antigen. This report is the first to document STRO-1 expression during the processes of differentiation.

Although hMSCs express a range of other antigens of mesenchymal, epithelial and endothelial characteristics which aid in the identification of the population, STRO-1, as yet unidentified, is the only antigen which shows heterogeneity in the hMSC population and which may potentially discriminate between the primitive and committed progenitors by identifying the multipotent subset in hMSC cultures. Given that the identity of the STRO-1 antigen is unknown, it is a challenge to explain the behavioural changes observed during the different culture conditions the hMSC populations have been subjected to in this study. However, the evidence provided by this series of experiments highlights STRO-1 as a marker of multipotency but also infers caution to other researchers when it comes to using the STRO-1 antibody as a tool for hMSC identification. The source and condition of the STRO-1 antibody is paramount to successfully characterise STRO-1 positive populations. STRO-1 antigen is therefore a marker worthy of further investigation. Elucidating the identity of this antigen will help in understanding the factors which determine stemness and cell fate. Furthermore, identifying the antigen will help in generating antibodies of different isotypes which are not as sensitive to storage conditions as IgM, therefore promoting STRO-1 as the marker of choice for hMSC isolation in clinical settings.

Chapter 4

Identification of potential candidate targets of STRO-1 antibody

4.1 Introduction

The isolation of multipotent hMSCs is most commonly carried out by plastic adherence and upon culture, these cells are defined by the differentiation potential of the whole population of cells. The inconsistency in MSC preparations from different anatomic locations has led to inconsistent reports thereby urging for a consensus protocol to be adopted (Wagner and Ho, 2007). Although a combination of selective markers has been unanimously employed in the identification of freshly derived hMSCs (Table 1.1), to date, the markers approved by the ISCT do not distinguish the multipotent hMSCs from contaminating fibroblastic cells (Haniffa *et al.*, 2009). Early studies in this laboratory indicated that cultured hMSC can be discriminated from fibroblasts (MRC5 cell line) by selective STRO-1 expression (unpublished data). There is mounting evidence in the literature (Section 1.2.2) suggesting that STRO-1 expression may be an indicator of differentiation potential and in Chapter 3, the significance of STRO-1 modulated expression as a marker of multipotency in cultured hMSCs has been established. However, the antigen to which STRO-1 antibody binds remains unresolved.

Systemic cues as well as cell to cell contact are believed to influence MSC fate *in vivo* (Ball *et al.*, 2004). *In vitro* studies have demonstrated that fate determination is accompanied by modulation of antigenic markers and that stem cell state may be identifiable by its immunophenotype (Salipante and Horwitz, 2007). Initial studies by Simmons and Torok-Storb (1991) indicated that STRO-1 may be a differentiation antigen when it was observed that mature adipocytes did not express the antigen. These observations and the modulation in STRO-1 expression reported in Chapter 3 taken together led to the hypothesis that STRO-1 antigen may be a ligand which is involved in either cell-to-cell signalling or may act as a receptor to inductive stimuli. By identifying the nature of STRO-1 antigen, the downstream signalling cascades involved in the initial commitment stages of hMSC differentiation can be elucidated therefore contributing to the understanding of the mechanisms regulating hMSC fate. This may lead to tailored stem cell therapies whereby homogeneous multipotent hMSC can be manipulated and directed to the specific lineage required for tissue regeneration. Until

now, STRO-1 antigen has been acknowledged as a protein which is resistant to trypsin and collagen treatment (Simmons and Torok-Storb, 1991, Jones *et al.*, 2002). However, it cannot be ruled out that the epitope recognised by the STRO-1 IgM antibody is a carbohydrate moiety although glycosidase treatment studies performed showed that STRO-1 binding was not affected (unpublished data). Identifying the STRO-1 antigen will also help generate higher affinity antibodies given that the currently available STRO- 1 antibody is of IgM isotype with a characteristic low binding affinity.

Multiple approaches have been implemented to identify surface antigens including immunoprecipitation, over-expression libraries, phage display technology and peptide microarrays amongst others. This work focused on peptide phage display as an initial approach to attempt to map the epitope recognised by STRO-1 antibody. An alternative approach was also employed using comparison analysis of gene expression microarray of STRO-1 expressing cells as a means to identify potential candidate gene family the antigen belongs to.

4.1.1 Peptide phage display approach

Phage display technology was first introduced in 1985 whereby short peptide fragments were successfully expressed as a fusion to filamentous phage coat protein (Smith, 1985). Although a variety of biological vectors have been used as peptide display vehicles, the filamentous bacteriophage M13 remains the best characterised system and the platform of choice for the generation of peptide libraries (Rodi and Makowski, 1999).

Structure of the M13 phage particle

The phage particle has a filamentous shape of variable length (average of 930 nm) which is dependent on the size of the genome but has a fixed diameter of 6.5 nm. It contains a circular genome of single stranded DNA (ssDNA) of about 6.4 kb packaged within five coat proteins named pIII, pVI, pVII, pVIII and pIX (Figure 4.1). The structural proteins can be divided into the major coat protein pVIII and the minor coat proteins pIII, pVI, pVII and pIX. The major coat protein pVIII wraps the phage ssDNA and is made up of around three thousand copies while the minor coat protein pIII present as five copies is located at the distal end of the virion (Day *et al.*, 1988).

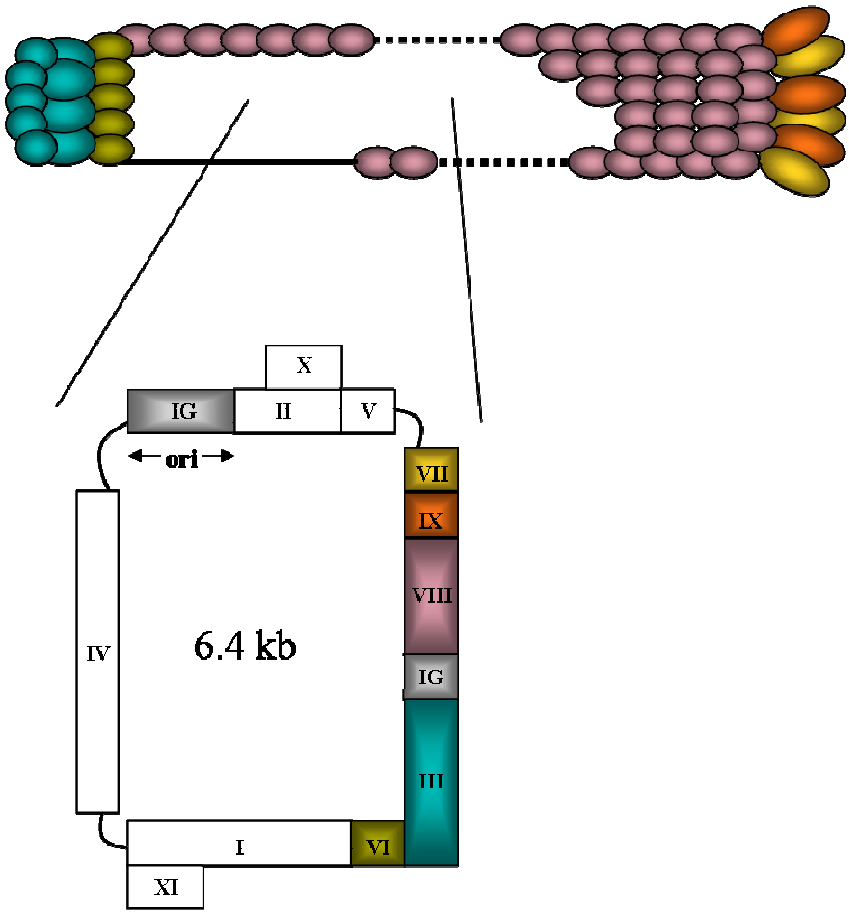

Figure 4.1: Structure of M13 phage particle. The particle is cylindrical with a 6.4 kb ssDNA encapsulated by five coat proteins which can potentially be used to display peptides. The coat proteins are coloured according to their corresponding gene in the genome. The intergenic regions are marked by IG and the non-structural proteins are unshaded (Adapted from (Carmen and Jermutus, 2002).

Although all the five coat proteins are potential peptide display units, pIII and pVIII have been exploited the most. The minor coat protein pIII is the longest coat protein with a sequence consisting of 406 amino acids. The protein consists of two glycine rich flexible segments inter-spaced between two domains downstream from the N-terminus (N1 and N2) (Figure 4.2). The flexible spacers (G1 and G2) facilitate the interaction of N1 and N2 to Tol A protein and F-pilus respectively on the *E.coli* membrane during the process of infection (Riechmann and Holliger, 1997).

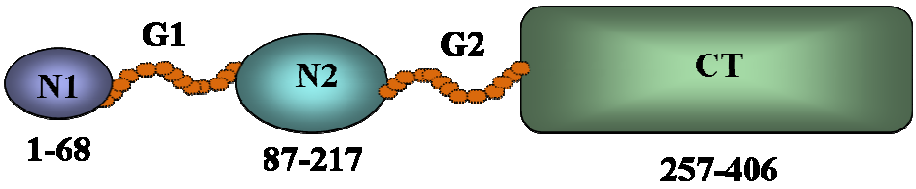

Figure 4.2: The structure of minor coat protein pIII. The N1 domain interacts with the Tol A membrane protein of *E.coli*. The N2 domain binds the F-pilus and the CT domain is necessary for termination of phage assembly. G1 and G2 are the glycine-rich linkers facilitating infection. Fusion of foreign peptides can occur either at the N or CT terminus (Adapted from (Carmen and Jermutus, 2002).

The major coat protein pVIII is a small protein of 50 amino acids. This protein has a helical structure which enables it to compile one on top of the other and over the phage ssDNA to form a 'fish scale' conformation (Cabilly, 1999). The number of displayed peptides on the phage virion is relative to the number of fused coat proteins; five on pIII and about 3000 on pVIII. The insertions vary in length depending on the coat protein fusions as excessively long extensions (longer than 20 amino acids) may be unfavourable to the phage propagation mechanism (Smith and Scott, 1993).

Panning

The fundamental aspect of peptide phage display is the link between genotype and phenotype and as such, the foreign peptide expressed as a fusion protein (phenotype) is dependent on the position at which the peptide DNA (genotype) has been incorporated inside the phage genome. The bacteriophage library therefore consist of viral particles each expressing random fused peptides of defined length on its exterior surface and the DNA encoding this fusion resides inside the phage. The library is screened for a specific target peptide against an immobilised antibody. The selection is carried out *in vitro* and is termed 'panning'. Throughout the subsequent rounds of panning, enrichment of the complementary peptide occurs and thus the peptide target of the immobilised antibody can be recovered. In this study, two panning systems were optimised in order to identify the target epitope of STRO-1 IgM antibody; solid-phase panning (Figure 2.1) and liquid-phase panning (Figure 2.2) and two peptide libraries were screened; Ph.D-12™ (pentavalent display of 12-mer peptides fused to pIII minor coat protein) and Dean's library (multivalent display of 16-mer peptides fused to pVIII major coat protein).

4.1.2 Microarray approach

Comparison of gene expression microarrays

Osteosarcoma is a malignant tumour of the bone often exhibiting clinical and molecular heterogeneity due to a varying degree of mesenchymal differentiation (Olstad *et al.*, 2003). Recent studies have revealed heterogeneity among different osteosarcoma cell lines in terms of their extracellular matrix composition and their antigenic profiles (Pautke *et al.*, 2004, Gibbs *et al.*, 2005). Stewart and colleagues (Stewart *et al.*, 1999) previously reported the high expression of STRO-1 by the human osteosarcoma cell line MG-63 compared to Saos-2 and STRO-1 coupled with ALP was inversely associated with the early progenitors of the osteoblast lineage . This comparative study indicates that STRO-1, among other markers, may be a marker that is differentially expressed at varying levels in osteosarcoma cell lines. Therefore, by comparing the gene expression microarray profiles of different osteosarcoma cell lines and MSC to their respective antigenic phenotype, a list of genes with similar expression pattern to STRO-1 can be

obtained. In this way, a list of potential candidate genes encoding the STRO-1 antigen, hence the epitope, can be obtained.

Flow cytometry characterisation of seven osteosarcoma cell lines was carried out using different antibodies, including STRO-1 (Section 2.5). The pattern of expression observed was scored and calculated as the difference in the mean fluorescence between the control population and the marker-specific labelled population. The pattern obtained by flow cytometry was then compared to the gene expression microarray profile (Microarray analysis was performed by Stephen Henderson, Cancer Institute, University College London, UK). This resulted in a list of candidate genes, of which the first twenty were selected and studied using reviewed protein database softwares (such as Uniprot).

Aims

The main aim of this part of the study was to identify the target protein recognised by STRO-1 antibody. To achieve this, two approaches have been implemented. In the first instance, two phage libraries (Ph.D-12™ and Dean's libraries) were screened by two panning methods in order to map the specific epitope recognised by the STRO-1 antibody. In order to identify potential gene candidates encoding the STRO-1 antigen, seven osteosarcoma cell lines were immuno-phenotyped on the basis of their expression of specific antigens: STRO-1, CD271, CD13, CD133 and HLA-ABC. The profiles obtained were matched to gene expression microarray data, and similar patterns of expression were identified using a bioinformatics approach. To achieve this, the following objectives were employed:

- Confirmation of successful adsorption of STRO-1 to plastic microtitre wells for solid phase panning studies
- Solid and liquid phase panning of Ph.D-12™ and Dean's libraries
- Positive identification of STRO-1 peptide displayed on phage particle using plaque lifts
- Detection level of STRO-1 antibody on a solid membrane
- Optimisation of osteosarcoma cell line screening using a live/dead discrimination
- Marker profiling of seven osteosarcoma cell lines
- Identification of potential gene candidates encoding STRO-1 antigen by comparing gene expression microarray data

4.2 Solid phase panning

The Ph.D-12™ peptide library was primarily screened by solid-phase panning. Ph.D-12™ is a M13 phage library expressing 12-mer peptides in a pentavalent format. The fusion peptides are linked to the pIII coat protein and are exposed at the distal end of the phage particle. The solid phase panning process involved coating of the plastic microtitre plate wells with STRO-1 antibody (100 µg/mL) and selecting for complementary peptides from the library via a series of incubation and washing steps (Figure 2.1). The input phage titre was kept constant at $1x10^{11}$ pfu/mL for each round of panning. Eluted phage was quantified after each round using the plaque assay (Section 2.6.4) and propagated (Section 2.6.3) for the subsequent rounds of panning. In order to confirm the successful binding of the IgM STRO-1 antibody to the plastic wells of the microtitre plate, a colourimetric assay was used. An antibody of a different isotype (IgG TUJ1) was also used as a negative control and the readings were blanked against a BSA control. The immobilised antibodies were bound to a goat anti-mouse IgM which was then detected by an anti-goat conjugated HRP. The colour was developed using ABTS and the absorbance readings measured at 405 nm (Section 2.6.7). A significantly high absorbance reading ($p<0.01$) in the STRO-1 coated well indicated positive adsorbtion of the antibody to the plastic surface. Once the successful immobilisation of STRO-1 antibody was confirmed (Figure 4.3), the panning procedure was undertaken with BSA as a negative control. Each panning round was designated as 'R' and five rounds were carried out altogether (R1 to R5). Due to the increase in the number of washes at R2, the STRO-1 output phage titre declined. A minor enrichment which was more significant from R4 to R5 (20 % increase, $p<0.04$) was observed. The BSA control fluctuated from R1 to R4 but increased significantly ($p<0.04$) at R5, thus suggesting the enrichment observed in the STRO-1 phage output was non-specific.

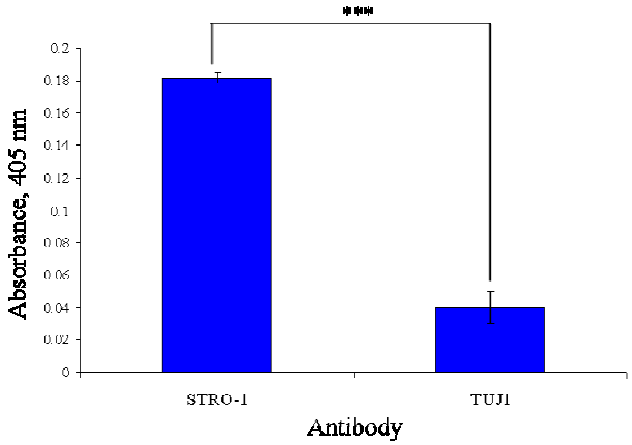

Figure 4.3: Detection of STRO-1 IgM bound to microtitre plate. Overnight STRO-1 IgM/TUJ1 IgG coated wells were incubated with goat anti-mouse IgM and detected with anti-goat HRP. Colour development using ABTS substrate was read at an absorbance of 405 nm (Section 2.6.7). Student's t-test STRO-1 versus TUJ1, ***p<0.01.

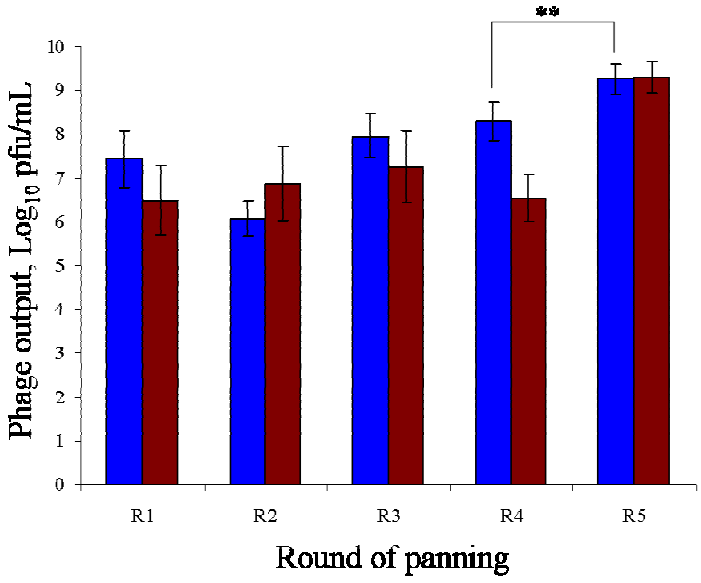

Figure 4.4: Outcome of solid phase panning of Ph.D-12™ peptide library. The Ph.D-12™ library was selected against wells coated with STRO-1 IgM or BSA (control) (Section 2.6.1). Eluted phage was quantified in triplicate after each round of panning as pfu/mL (Section 2.6.4). ■ represents STRO-1 and ■ represents BSA control. Student's t-test R4 STRO-1 versus R5 STRO-1, **p<0.04.

4.3 Liquid phase panning

Following the poor enrichment observed during solid phase panning (Figure 4.4), the liquid phase panning was attempted in the first instance with the Ph.D-12™ library, then with the Dean's library. Dean's library is a multivalent library of 16-mer peptides, expressing the peptide sequences on the pVIII coat protein, compared to the pentavalent expression of the 12-mer peptides of Ph.D-12™ library which are confined to the pIII coat protein. The liquid phase panning is more favourable to antibodies such as low affinity IgM as it provides the right physiological conditions promoting antibody binding. It has been shown that the secondary structure of antibody molecules may be affected when adsorbed to plastic surfaces but by maintaining them in solution at the right pH, the 3D conformation is minimally affected and thus preserved (Brahms and Brahms, 1980). Therefore, in order to allow the 3D structure of the IgM molecules to interact freely with the peptides, the liquid phase panning was implemented. The rounds of panning were carried out on the Ph.D-12™ and the Dean's libraries as described in section 2.6.2 using BSA as a control. For each round, a phage titre of $1.5x10^{11}$ pfu/mL was incubated with 10nM STRO-1 antibody, and the eluted phage was quantified by plaque assay (Section 2.6.4) and propagated (Section 2.6.3).

There was a weak enrichment of output phage in the liquid phase panning of the Ph.D-12™ library. The number of washes before elution was increased from 8 (R1) to 10 (R2 to R5) explaining the decrease in the phage titre at R2. The following round (R3) showed an increase in the STRO-1 eluate titre ($p<0.05$) whilst the BSA remained constant. However, with the subsequent rounds, both the BSA control and the STRO-1 titres coincided with a minimal increase from R3. From R4 to R5, STRO-1 enrichment was weak ($p<0.04$) and concomitant with BSA control increase (Figure 4.5).

The Dean's library was screened by the same liquid phase panning approach. The output phage eluates of the BSA control and STRO-1 remained constant throughout the different rounds of panning indicating no enrichment of a specific peptide (Figure 4.6). The increase in the number of washes from R1 to the subsequent rounds decreased the overall output titres. Although a slight increase in output titres from R2 to R5 was observed, it was not significant ($p>0.5$).

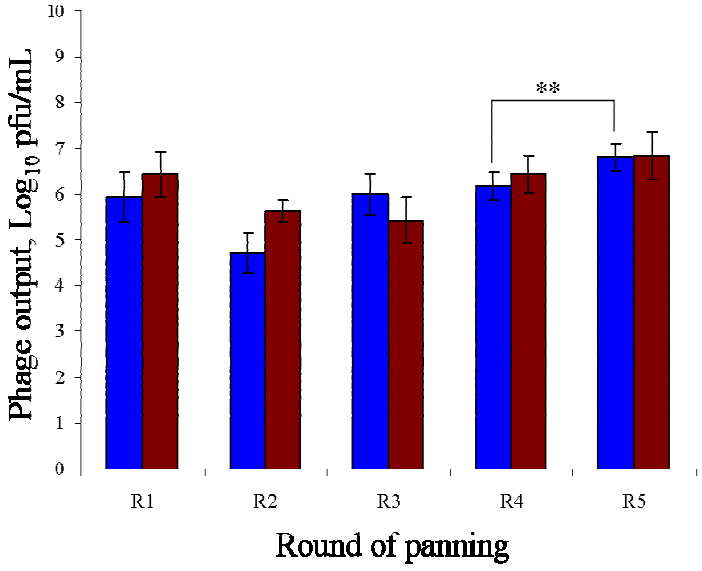

Figure 4.5: Outcome of liquid phase panning of Ph.D-12™ peptide library. The Ph.D-12™ library was selected against STRO-1 IgM or BSA (control). The phage/antibody complex was immuno-precipitated with protein A agarose beads coated with anti-mouse IgM and the bound phage eluted (Section 2.6.2). The eluted phage was quantified in triplicate after each round of panning as pfu/mL (Section 2.6.4). ■ represents STRO-1 and ■ represents BSA control. Student's t-test R4 STRO-1 versus R5 STRO-1, $**p<0.04$.

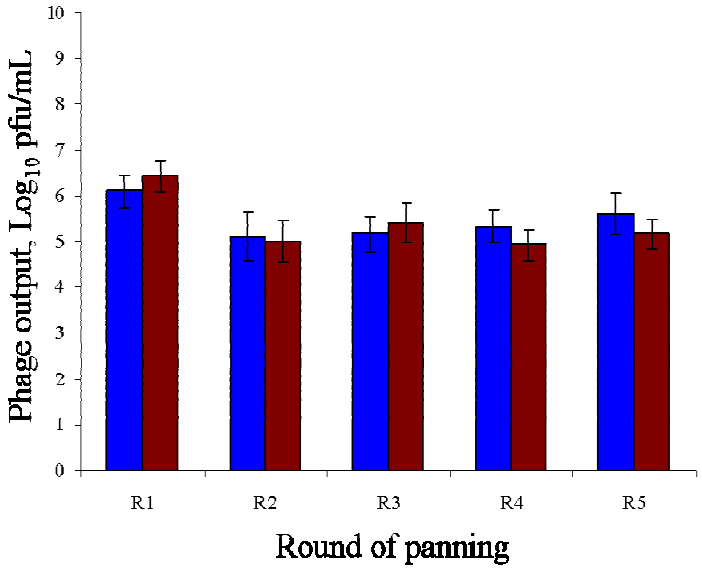

Figure 4.6: Outcome of liquid phase panning of Dean's peptide library. The Dean's library was selected against STRO-1 IgM or BSA (control). The phage/antibody complex was immuno-precipitated with protein A agarose beads coated with anti-mouse IgM and the bound phage eluted (Section 2.6.2). The eluted phage was quantified in triplicate after each round of panning as pfu/mL (Section 2.6.4). ■ represents STRO-1 and ■ represents BSA control.

4.4 Plaque lifts

Plaque lifts were carried out at the end of each panning experiment to confirm if the STRO-1 antibody had enriched phage with the target peptide. The phage plaques were immobilised on nitrocellulose membrane and incubated with 1 µg/mL STRO-1 solution (Section 2.6.6). Bound STRO-1 was then detected using DAB colour development assay by probing with polyclonal rabbit anti-mouse HRP conjugated secondary antibody (1:1000) (Section 2.6.5). When using the standard techniques of plaque lifts, no plaques could be detected indicating no enrichment in STRO-1 target peptide (example blot shown in Figure 4.7 A). The level of detection of the HRP conjugated secondary antibody was examined by spotting the antibody at different dilutions on nitrocellulose membrane. Peroxidase activity was then confirmed using DAB as a substrate for colour development. The outcome of this control experiment showed that the HRP conjugated secondary antibody was efficient down to a 1:3000 dilution (very faint brown spot), beyond which no positive colour development was detectable (Figure 4.7 B).

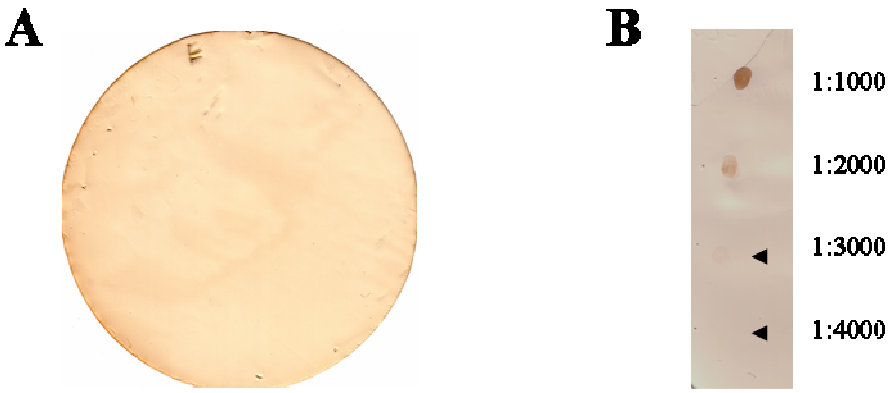

Figure 4.7: Detection of STRO-1 binding on plaque lift. (A) A specimen of negative plaque lift obtained after a panning round. The plaques formed on agar plates were transferred to nitrocellulose membranes and incubated in 1 µg/mL STRO-1 solution and probed with polyclonal rabbit anti-mouse HRP. Binding was detected using 2 mg/mL DAB substrate (Section 2.6.5). (B) Positive detection of polyclonal rabbit anti-mouse HRP spotted at different dilutions (Section 2.6.6). The limit of detection of the HRP conjugate was 1:3000, beyond which no positive colour development was detectable (indicated by arrowheads).

4.5 Sensitivity of STRO-1 detection on nitrocellulose membrane

In order to establish the concentration at which STRO-1 can be successfully detected when bound to a membrane, a dot blot using decreasing concentrations of the STRO-1 antibody was carried out as described in section 2.6.6. The detection level was compared to TUJ1, an antibody of IgG isotype. Two blocking reagents, namely 1 % BSA and 1 % semi-skimmed milk, were also compared. The intensity of the brown colour developed as a result of positive detection decreased with decreasing concentration of the antibodies. STRO-1 IgM could not be detected at or below 10 µg/mL while TUJ1 IgG could still be detected at 1 µg/mL.

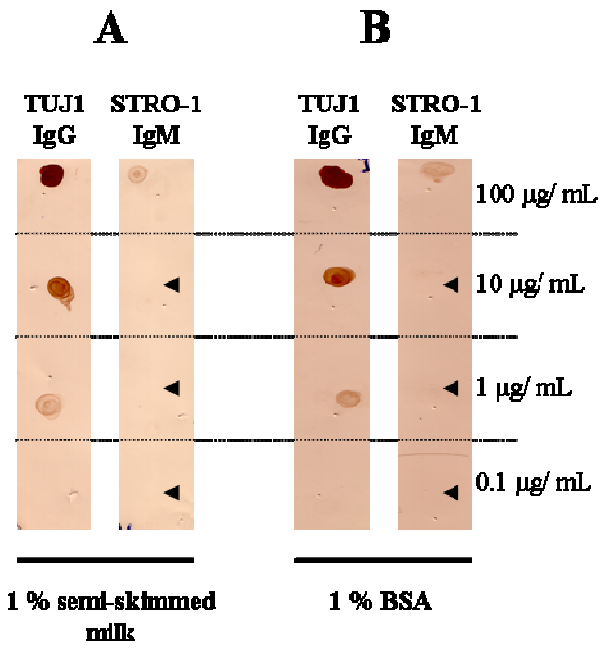

Figure 4.8: Sensitivity of STRO-1 IgM detection compared to TUJ1 IgG detection on nitrocellulose membrane. STRO-1 IgM and TUJ1 IgG were spotted at decreasing concentrations on nitrocellulose membrane and detected using anti-mouse HRP. Two blocking reagents were applied; (A) 1 % semi-skimmed milk and (B) 1 % BSA. DAB substrate was used as colour development and in both cases STRO-1 IgM could not be detected below 100 µg/mL concentration as indicated by arrowheads (Section 2.6.6).

4.6 BSA control enrichment during liquid phase panning

The liquid phase panning was designed as a sandwich reaction between anti-mouse IgM coated protein A agarose beads and phage-STRO-1 complex (Figure 2.2). The concept behind this technique was to combine the coated agarose beads with the phage-STRO-1 complex, and allow the STRO-1 selected phage particles to pull down the target peptide. Enrichment of the BSA controls during the liquid phase panning may have been due to the anti-mouse IgM immobilised on the agarose beads binding to random peptides expressed by the phage particles. To investigate this possibility, plaque lifts at rounds 5 of the liquid phase panning of Ph.D-12™ and Dean's library were incubated with goat anti-mouse IgM and detected with anti-goat HRP. After colour development using DAB, the lifts displayed no positive signal (as shown in figure 4.7A) indicating that the BSA control enrichment observed was not due to the anti-mouse IgM enriching for its complementary peptide.

4.7 Significance of live/dead screening of osteosarcoma cell lines with STRO-1

Some markers, for instance CD133, have been shown to be expressed in cytoplasmic vacuoles inside the cells (Fonseca *et al.*, 2008). Therefore upon flow cytometry analysis, cells with compromised membranes are likely to take up the fluorescent labelled antibodies of the specified marker and show up as positively stained cells on the scatter plots. Upon data analysis, since intracellular staining is not discriminated against surface staining, data interpretation may be misleading as false positives are included in the total cell subset identified as expressing the antigenic marker. I have shown that the STRO-1 antigen is expressed intracellularly (illustrated in Figure 4.14) and thus to identify this rare cell population in osteosarcoma cell lines, it was important to distinguish intracellular staining from cell surface staining. In an attempt to achieve this, a live/dead screening dye compatible with simultaneous RPE staining was employed.

Binding of STRO-1 antibody was detected with anti-mouse IgM RPE conjugated secondary antibody and the population was stained for live/dead discrimination by the APC-Cy7 compatible dye (Section 2.5.3). The live/dead discrimination assay is based on the reaction of the fluorescent dye with cellular amines. This dye is able to permeate cells with compromised membranes and react with the interior and cell surface amines to yield intense staining. In contrast, live cells exhibit dim staining as the dye only reacts with surface amines. The stained cells were analysed by flow cytometry and population counts were normalised to $1x10^4$ cells for each sample. Scatter plots were gated to distinguish between live and dead cells (representative scatter plot shown in Figure 4.9). Upper quadrants R6 and R10 represent live STRO-1 positive cells while lower quadrants R8 and R12 represent STRO-1 negative live cells. When stained with the RPE secondary only, the background staining observed in quadrant R6 (-Live/Dead panel) representing 1.1 % of the total population was also represented by quadrant R11 (1.11 %) in the +Live/Dead panel. Notably, when cells were stained for STRO-1 without live/dead discrimination (R6 in –Live/Dead panel), the STRO-1 positive subset was represented by 6.01 % of the total population. However, when cells were co-stained with STRO-1 with dead cell exclusion dye, the STRO-1 positive subset was represented by only 3.68 % of the whole population (R10 in +Live/Dead panel). This phenomenon was also observed for all the other markers used in this study (scatter plot data not shown). These findings suggest that it is necessary to exclude dead cells in the analysis of cell surface marker expression and was therefore implemented in the marker profiling of the osteosarcoma cell lines.

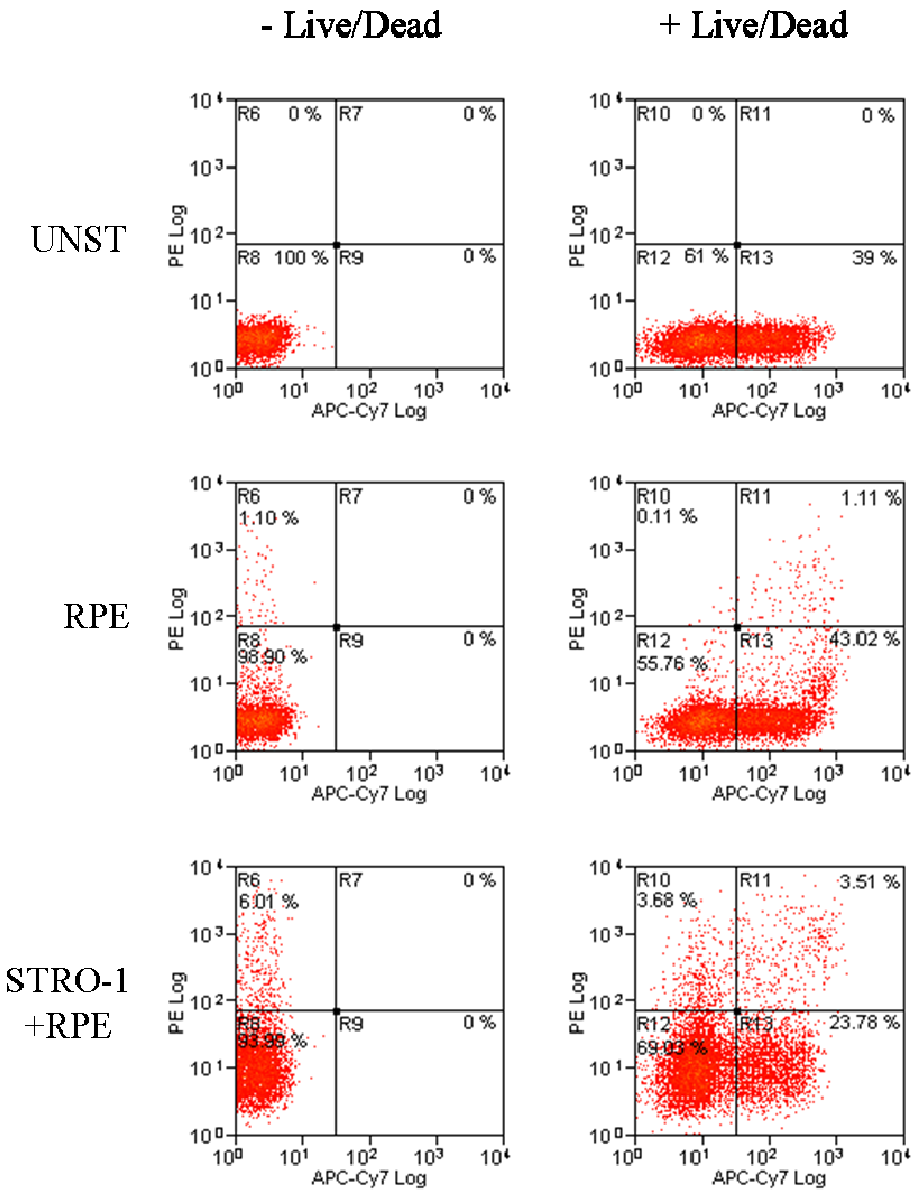

Figure 4.9: Optimisation of STRO-1 screening using Live/Dead discrimination. G-292 cells were harvested and labelled as indicated; (UNST: unstained, RPE: anti-mouse IgM and STRO-1+RPE: STRO-1 IgM detected with anti-mouse IgM), with and without the Live/Dead discrimination stain (Sections 2.5.1 and 2.5.3). The scatter profiles were gated to distinguish between STRO-1 positive live cells (R6&R10), STRO-1 positive dead cells (R7&R11), STRO-1 negative live cells (R8&R12) and STRO-1 negative dead cells (R9&R13). RPE was detected on the PE Log scale and the dye for live/dead discrimination was detected on APC-Cy7 Log scale. The analysis was normalised to $1x10^4$ cells for each sample.

4.8 Marker profile of osteosarcoma cell lines

After optimisation of the live/dead discrimination, the seven osteosarcoma cell lines 143B, CAL72, G-292, HOS, MG-63, Saos-2 and U-2-OS were screened for their expression of the stem cell markers STRO-1, CD271, CD133, CD13 and their HLA-ABC expression. The cells were harvested and incubated with their specific fluorescently labelled primary and secondary antibodies if required (Section 2.5.1) and then stained with the live/dead discriminatory dye (Section 2.5.4). The cells were analysed by flow cytometer and the number of cells for each sample was normalised to $2x10^4$ cells. Each labelled sample was compared to their respective control (either unstained or secondary only stained). An overlay histogram plot was produced (Figure 4.10) and the mean fluorescence between control and labelled cells was recorded (Table 4.1).

All of the cell lines were positive for STRO-1, although MG-63 had the highest STRO-1 expression level (Table 4.1) displaying a heterogeneous population profile. The STRO-1 profile of MG-63 was analogous to the profile observed for hMSCs, whereby three subsets of cells could be distinguished; STRO-1^{DULL}, STRO-1^{INT} and STRO-1^{BRIGHT}. G-292 also appeared to have a side population of STRO-1^{BRIGHT} cells thus giving a difference in mean fluorescence of 9.87. The other cell lines exhibited a minor total population shift to the right hand side of the log scale indicating positive expression although approximately 8-10 fold lower than G292, with 143B having the smallest shift.

All the cell lines were positive for CD271, although Saos-2 was the only population with an extended positive tail giving a mean fluorescence difference of 11.08. HOS had the lowest level of CD271 expression with a difference in mean fluorescence of only 0.25 while the other cell lines exhibited a difference in mean fluorescence ranging from 0.82 to 3.45. CD133 was heterogeneously expressed among the cell lines, with 143B, HOS and Saos-2 expressing it to the highest level while G-292 and MG-63 exhibiting a close to zero shift and CAL72 and U-2-OS not expressing it at all. CD13 was also expressed in a heterogeneous fashion across the different cell lines, with some cell lines expressing it to a high level and others to a lower level. G-292 and MG-63 exhibited a

total population shift to the right hand side of the log scale indicating high binding when stained with CD13, while 143B and HOS exhibited an overlapping shift with their respective controls. CAL72 displayed a near zero population shift while Saos-2 and U-2-OS were negative for CD13. All the cell lines expressed varying levels of HLA-ABC, with HOS being the highest and G-292 the lowest.

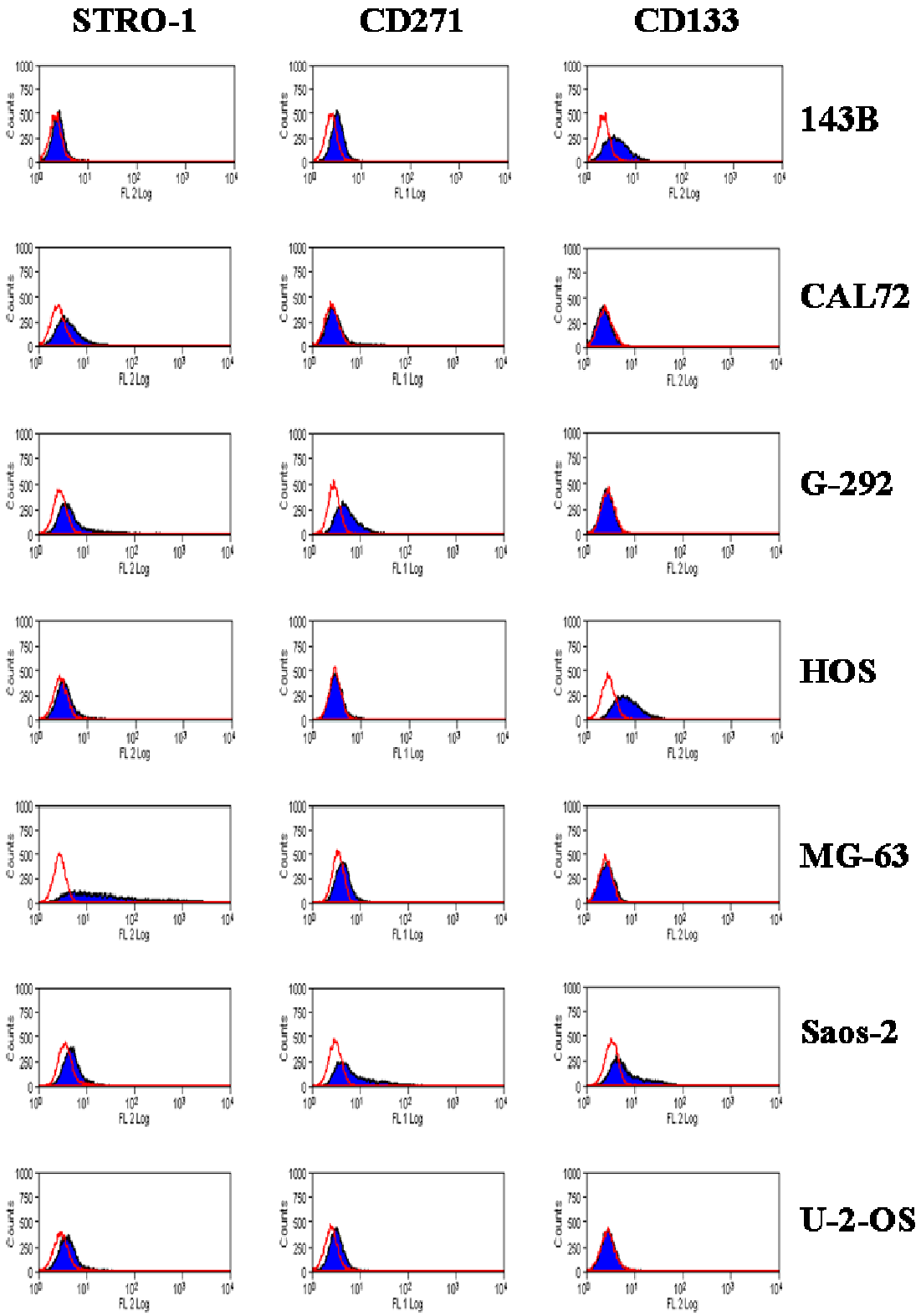

Figure 4.10: Continued overleaf.

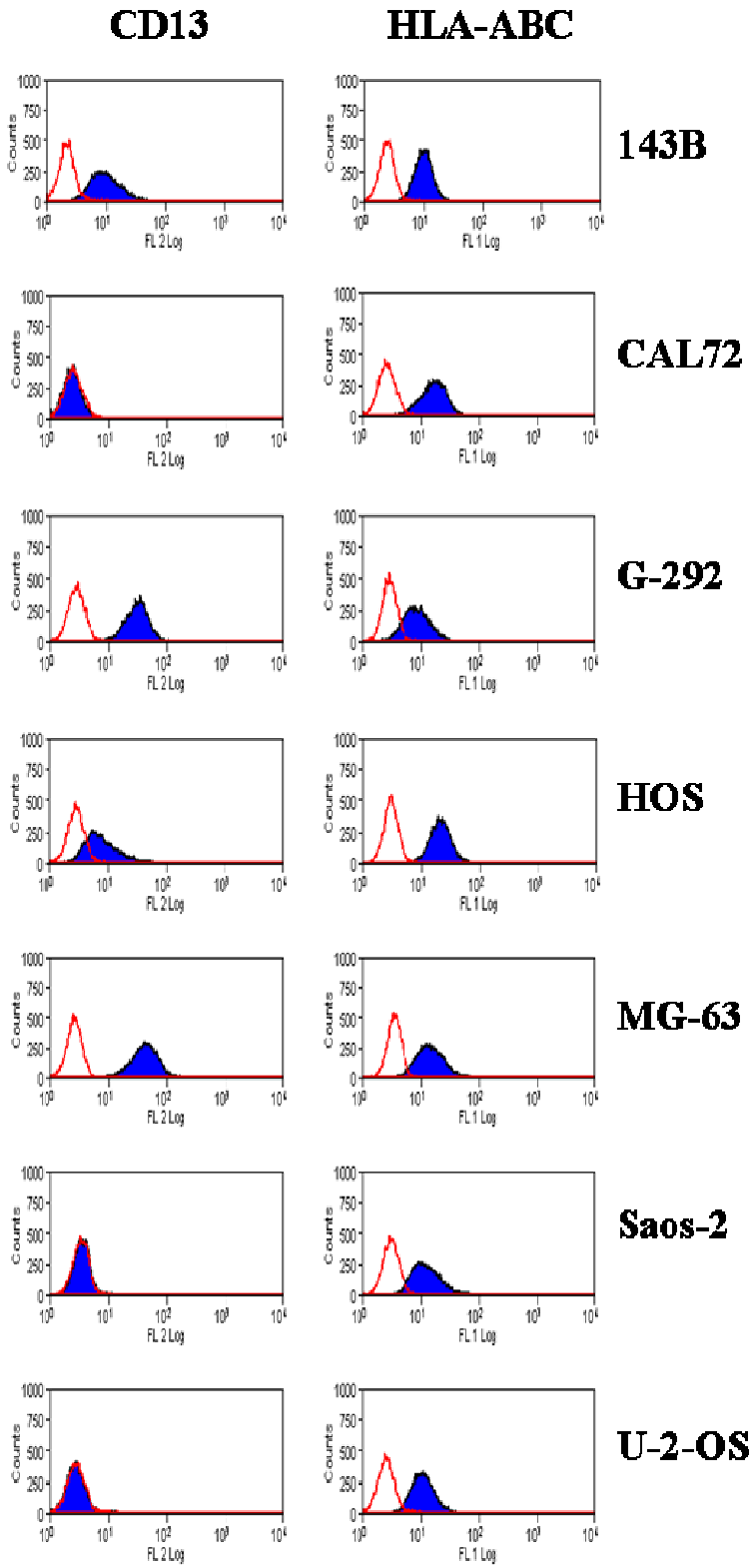

Figure 4.10: Continued overleaf.

Figure 4.10: Flow cytometry overlay analysis of maker profiles of seven osteosarcoma cell lines. Cells were harvested and labelled with primary and secondary antibodies as appropriate (Section 2.5.1) and stained with live/dead discriminatory dye (Section 2.5.4). The stained populations were gated to exclude dead cells and the analysis was normalised to $2x10^4$ cells. The unstained or secondary only control is represented by red lines and the marker-specific labelled cells are represented by the shaded histrograms (blue).

Marker/ Cell line	143B	CAL72	G-292	HOS	MG-63	Saos-2	U-2-OS	hMSC
STRO-1	0.11	2.52	9.87	1.49	166.89	1.87	2.16	230.91
CD271	0.95	1.42	3.45	0.25	1.34	11.08	0.82	12.53
CD133	2.35	0	0.11	5.49	0.19	6.23	0	0.65
CD13	9.52	0	30.48	12.91	43.86	0.2	0	92
HLA-ABC	8.08	13.94	6.5	19.99	13.08	11.56	9.19	6.63

Table 4.1: Marker expression profiles of seven osteosarcoma cell lines and hMSC (M24♂p4). The values indicate the difference in mean fluorescence between control population (unstained or secondary only) and marker-specific labelled population after dead cell exclusion. The degree of positivity of each cell surface marker is based on populations normalised to $2x10^4$ cells. The values indicated in red represent the cell line exhibiting markedly elevated expression of the corresponding marker.

4.9 Identification of candidate genes encoding STRO-1 antigen

The flow cytometry profile obtained was compared to gene expression microarray profiles and a list of the top twenty candidate genes was selected (Appendix Table I) which were subsequently narrowed down to the known antigens which are expressed on the plasma membrane. The gene expression microarray analysis was performed by Stephen Henderson (The Cancer Institute, University College London).

Based on the correlation rankings obtained (Figure 4.11), the top twenty probesets were selected and a heatmap generated using gplots package (Figure 4.12). The gene expression of the twenty candidate genes selected by the software closely matched the cellular expression obtained by flow cytometry analysis (Figure 4.13). Using the Gene Ontology (GO) database, the sub-cellular locations of the candidate genes were extracted and eight potential candidate genes encoding STRO-1 were selected based on plasma membrane expression (Table 4.2). Using the Uniprot database, information on function and size of the proteins were obtained and analysed.

Of the eight potential candidate genes, ARHGEF4 (also known as Asef) bears sub-cellular locations analogous to the expression pattern observed by the STRO-1 antigen when visualised by imunofluorescence staining (Section 4.91). TNFSF11 (clustered as CD254) is an interesting candidate as it is involved in osteoclast differentiation (Lacey *et al.*, 1998). Another interesting candidate is P2RY6 which is a subtype of the family of purinoreceptors which has been shown to be expressed in bone tissues (Maier *et al.*, 1997).

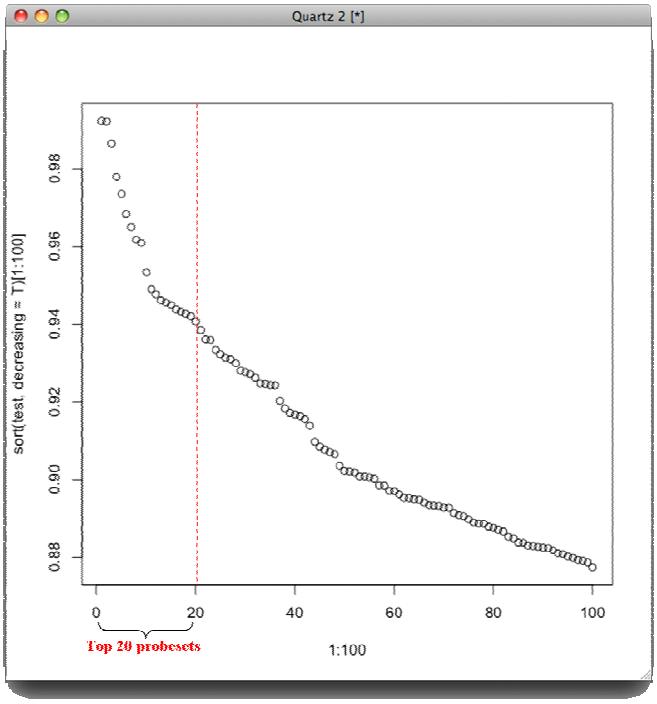

Figure 4.11: Correlation curve to determine candidate genes for STRO-1 antigen. The flow cytometry expression of STRO-1 antigen was compared to gene expression microarray profiles. Using Pearson's R^2 value, the top twenty probesets representing candidate genes for STRO-1 antigen were selected.

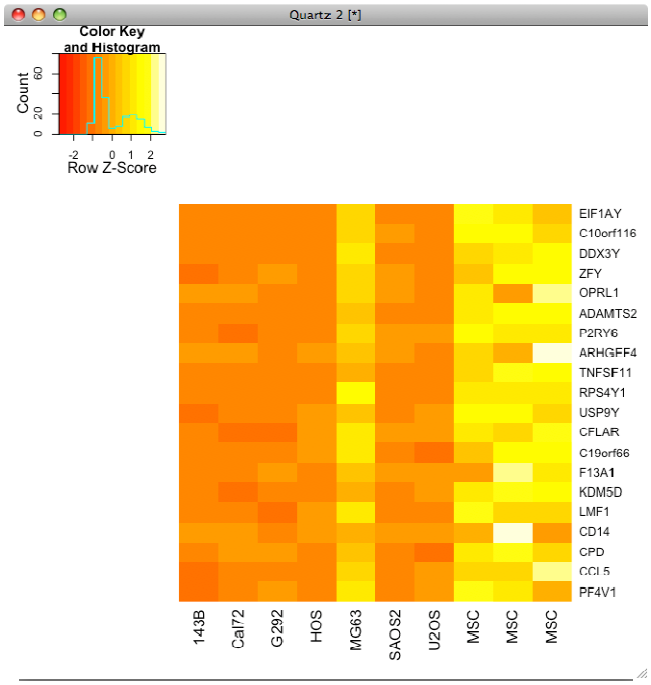

Figure 4.12: Heatmap of potential candidate genes encoding STRO-1 antigen. The heatmap was generated by gene expression comparison of seven osteosarcoma cell lines and three MSC populations.

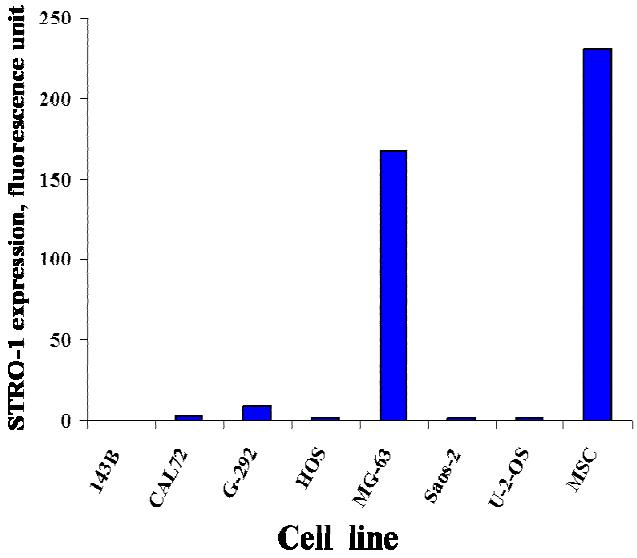

Figure 4.13: Relative expression of STRO-1 antigen in seven osteosarcoma cell lines and one hMSC population. Cells were cultured, harvested, labelled with STRO-1 antibody and analysed by flow cytometry (Section 2.5). The difference between the mean fluorescence units was calculated between the secondary only and STRO-1 labelled populations to obtain the level of STRO-1 expression by each cell line.

HGNC Symbol	Sub-cellular locations	Biological function	Size of protein (AA)
DDX3Y	-Nucleus -Cytoplasm -Plasma membrane	ATP-dependent RNA helicase involved in spermatogenesis	660
OPRL1	-Plasma membrane	G-coupled receptor	336
P2RY6	-Plasma membrane (apical and basolateral)	G-coupled receptor involved in calcium second messenger system	328
ARHGEF4	-Plasma membrane -Cell projection -Intracellular (cytosol, cytoplasm)	Cell migration and E-cadherin mediated cell-cell adhesion	690
TNFSF11	-Plasma membrane -Cytoplasm -Extracellular space	Activation of osteoclast differentiation and involved in immune response	317
LMF1	-Membrane -Endoplasmic reticulum	Maturation and transport of active lipoprotein lipase (LPL)	567
CD14	-Plasma membrane (membrane raft, lipolysaccharide receptor complex) -Extracellular region	Upregulates adhesion molecules and mediates immune response	375
CPD	-Membrane fraction -Nucleus -Microsome (trans-Golgi network)	Proteolysis	1380

Table 4.2: Details of potential candidate antigens representing STRO-1. A summary of their sub-cellular locations and functions is also described. In red is the most promising antigen whose sub-cellular location closely matches that observed for STRO-1.

4.9.1 Sub-cellular characterisation of STRO-1

The sub-cellular localisation of STRO-1 on hMSCs was further characterised by immunofluorescence (Section 2.4). Cells were labelled with STRO-1/FITC (green), nuclei and cytoskeleton were stained with DAPI (blue) and Phalloidin (Texas Red) respectively wherever required. The mounted slides were visualised by fluorescence or confocoal microscopy.

STRO-1 antigen is expressed by a minor subset of cells in hMSC adherent monolayers as illustrated in Chapter 3 (Figure 3.3). To determine the pattern of surface expression of STRO-1 on hMSCs, stained cells were further analysed by confocal microscopy. This procedure revealed 'islands' of STRO-1 antigen over the cell surface, with stronger staining at the cell extremities (Figure 4.14 A). Some cells were also permeabilised using Triton X-100 and stained for STRO-1/FITC to determine whether STRO-1 is expressed in the cytosol. The slides were visualised by confocal microscopy and indicated positive intra-cellular staining of STRO-1 around the nucleus (Figure 4.14 B).

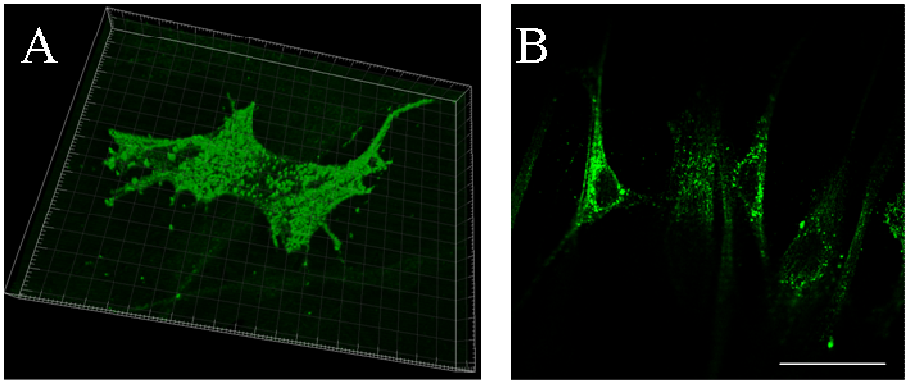

Figure 4.14: Surface and intracellular localisation of STRO-1 antigen. Cells grown on coverslips were stained with STRO-1/FITC as described in section 2.4 and visualised by confocal microscopy. (A) STRO-1 antigen is present on the cell surface as 'islands' and spreads on the cell projections. (B) STRO-1 antigen is expressed intra-cellularly around the nucleus and into the cell extremities. Scale bar represents 100 µm.

Since STRO-1 appeared to be concentrated on the cell extremities, it was interesting to examine whether STRO-1 was co-expressed with the actin filaments of the cytoskeleton. Therefore, the cytoskeleton was stained with Phalloidin (Texas Red), the cells location identified by nuclear staining (DAPI, blue) and STRO-1 labelled by FITC conjugated secondary antibody (green). Interestingly, STRO-1 appeared to localise on one side of the cell as shown by the green staining on part of the cell which was completely stained red for cytoskeleton (Figure 4.15 C). Comparatively to the Phalloidin staining alone (Figure 4.15 B), there was stronger expression of STRO-1 at the cell extremities (Figure 4.15 C, indicated by the white arrowhead). Interestingly, the cell projections were directed towards a neighbouring cell.

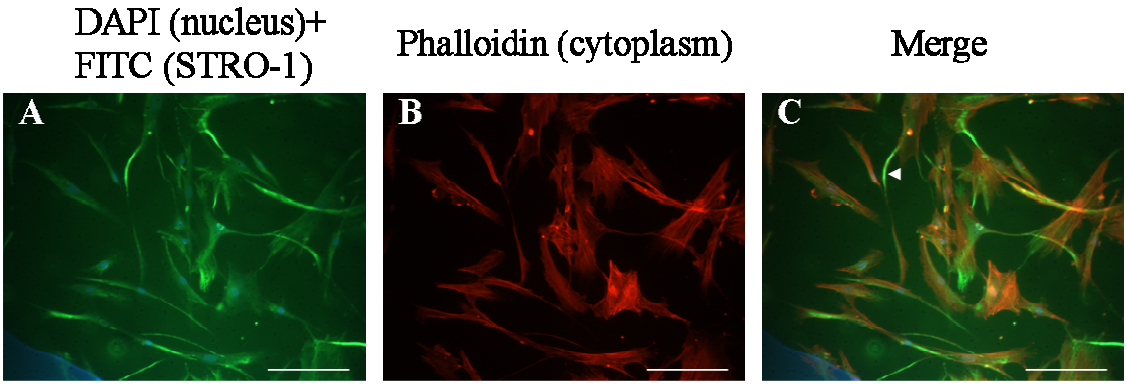

Figure 4.15: Localisation of STRO-1 on cell membrane projections. Cells were cultured on slides and stained as described in section 2.4. (A) Cell nucleus stained blue with DAPI and with STRO-1/FITC, (B) Cytoplasm staining by Phalloidin (Red) and (C) Merged staining showing brighter staining on cell extremities (indicated by white arrowhead). Scale bars represent 200 µm.

Closer analysis of STRO-1 expression in relation to their neighbouring cells was analysed by higher magnification using fluorescence microscopy. Interestingly the cells displayed higher STRO-1 expression on the ruffled part of the membrane (Figure 4.16 A, indicated by white arrowhead). Moreover, at the cell junctions (that is where two cells meet), STRO-1 expression was elevated (Figure 4.16 B, indicated by white arrowheads).

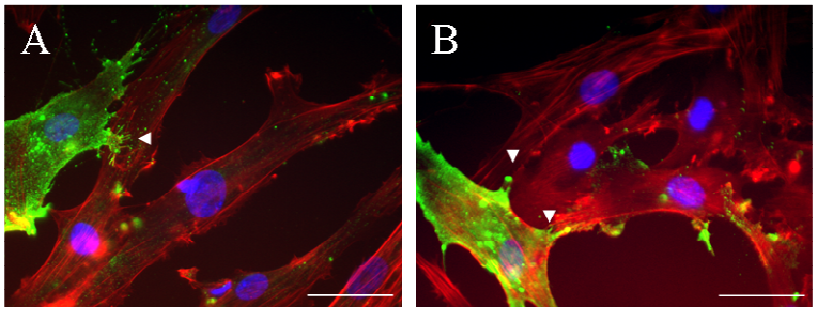

Figure 4.16: Localisation of STRO-1 on ruffle membrane and cell junctions. Cells were permeabilised and stained using DAPI (blue nucleus), Phalloidin (red cytoplasm) and STRO-1/FITC (green) (Section 2.4). (A) STRO-1 antigen is strongly expressed on ruffle membrane as indicated by white arrowhead. (B) STRO-1 localised at point of contact between two cells as indicated by white arrowheads. Scale bars represent 50 µm.

4.10 Discussion

The primary aim of this part of the study was to identify the epitope that STRO-1 antibody binds to, and secondly to identify the potential candidate genes encoding the antigen. In chapter 3, the importance of STRO-1 as a differentiation marker in hMSCs was illustrated. The modulation of STRO-1 expression during differentiation suggests that the protein antigen may be involved in the fate determination process of hMSCs. Moreover, establishing STRO-1 as the marker of multipotency by further defining its characteristics and functions may contribute towards a consensus protocol among researchers to adopt STRO-1 as a key marker in the isolation of hMSCs both *in vivo* and *in vitro*. Given the low binding affinity nature of the current STRO-1 antibody, identification of the STRO-1 antigen will allow for higher affinity antibodies to be engineered.

Among the myriad of techniques available for epitope mapping, phage display technology was chosen as it was a relatively rapid, convenient and proven method for affinity selection of peptides (Rodi and Makowski, 1999). Peptide phage display is primarily employed as a method of raising antibodies against antigens and has recently been adopted to identify novel antibodies against rare cell populations, such as the generation of C15 antibody against MSCs (Letchford *et al.*, 2006). With the success of antibody generation, the display of peptide fragments of different lengths on the surface of the phage particle was improved and the technology has been adapted for epitope mapping against immobilised antibodies, whole cells and even *in vivo* screening (McGuire *et al.*, 2009). The choice of library for epitope mapping depends on many factors and in the absence of structural information regarding STRO-1 to target interaction, it is not possible to predict which specific library will yield the most productive results.

In this study, given that STRO-1 is an IgM with a low binding affinity, two formats of multivalent display were chosen over monovalent displays. Monovalent displays imply the expression of peptides fused to only one copy of the phage coat protein, most commonly pIII, and this format is best suited for high affinity binders (Mullaney and

Pallavicini, 2001). For the IgM STRO-1, the pentavalent pIII fused 12-mer peptide Ph.D-12™ and the multivalent pVIII fused 16-mer peptide libraries were screened. In the first instance, Ph.D-12™ library was screened by solid-phase panning. The direct adsorption of STRO-1 IgM to a plastic surface is mediated by electrostatic and Van-der-Waals interactions. In some cases, where the molecule to be immobilised is very small, conjugation to a carrier protein is recommended. This was not necessary for STRO-1 IgM as being a large pentameric molecule (30 nm in diameter) (Svehag *et al.*, 1967), it could easily expose its epitope binding regions for easy accessibility by the peptide phage particles. Successful binding of STRO-1 to the solid surface was confirmed by ELISA. The level of detection obtained was not as high as what would be expected for an antibody of a different isotype detected with the appropriate secondary. The critical step in this panning procedure was the first round as it had to ensure that all potentially complementary peptides were selected for subsequent amplification and screening. Therefore a low stringency was implemented at the first panning rounds by having a reduced number of washing steps to exclude unbound phage particles.

Although a promising enrichment was observed at round 5 of the panning procedure, the concomitant increase in the BSA control indicated that the enrichment was not specific to STRO-1 antibody. The lack of enrichment of specific peptides could be due to a possible denaturation of the antibody caused by the process of passive adsorption (Brahms and Brahms, 1980). The change in conformation of the STRO-1 IgM might have resulted in non-specific binding of phage particles since the denatured form is bound to expose hydrophobic residues presenting a ‘sticky’ surface to phage particles (Friguet *et al*., 1984). Furthermore, plaque lifts taken at rounds 4 and 5 yielded no positive binding suggesting that the solid-phase panning procedure was not successful.

Given the low affinity of STRO-1 IgM and its weak adsorption and possible denaturation upon attachment to the plastic surface, the liquid-phase panning was implemented. This alternative approach presented an antibody-target binding within the normal physiological condition, which is favoured by the freely available epitope binding sites of the IgM to the target peptides in a 3D interactive format. By selecting for positive peptide phage particles to STRO-1 IgM in solution, the possible drawbacks

posed by solid-phase panning were limited. Both the 12-mer Ph.D-12™ and 16-mer Dean's libraries were screened by the liquid phase panning. Despite using a solution system to promote peptide-antibody interaction, the resulting peptide phage enrichment observed in both selections was not significant. In fact, this system involved the capturing of the phage-antibody complex by protein A agarose beads coated with anti-mouse IgM. Therefore, the number of high molecular weight components involved in the design of this reaction may have reduced its efficiency by increasing the probability of dissociation during the pull-down procedure. The dissociation of the components may have been exacerbated by the low affinity of the STRO-1 IgM, thus resulting in the same level of eluate titre as in the BSA controls, with no positive enrichment specific to STRO-1 as shown by the plaque lifts.

In relation to the BSA control, there was a possibility that the anti-IgM captured on the agarose beads were pulling down their own complementary peptide from the library of unbound phage instead of selecting for STRO-1-phage complexes. In other words, the anti-IgM was enriching for phage particles binding to itself. To explore this probable phenomenon, plaque lifts at the end of each liquid panning experiment was incubated with anti-IgM to detect any positive binding. While it was possible to detect positive anti-IgM binding on nitrocellulose membrane down to a concentration of 1 µg/mL, no plaques were detected on the plaque lifts. This led to the conclusion that anti-IgM was not selecting for its complementary peptide from the phage libraries. The negative plaque lifts for putative STRO-1 epitopes further suggested that either the epitope was not present within the randomly generated libraries or it was simply not possible to detect STRO-1 IgM when it was bound to nitrocellulose membrane. Overall, the level of detection of STRO-1 IgM as compared to a different isotype such as TUJ1 IgG, was very low on nitrocellulose membrane, further emphasising the difficulty of working with an antibody of the IgM isotype. In this case, although the corresponding epitope to STRO-1 antibody might have been present in the phage libraries, the low level of detection on nitrocellulose membranes would have hindered its positive identification.

Optimising the screening strategies (such as method of panning, blocking reagents used and sensitivity of antibody detection) was of utmost importance in this part of the study.

Nevertheless, the main obstacle remains the nature of the STRO-1 IgM antibody. Early studies have revealed the pentameric structure of IgM with a molecular weight of 900 KDa (Svehag *et al.*, 1967). Although the IgM molecule has 10 possible antigen binding sites, the affinity for the antigen is very low and therefore dissociation of the antigen-antibody complex is unavoidable. The interaction between antigen and antibody is either ionic, Van-der-Waals or hydrophobic and these forces help to maintain stability of the antigen-antibody complex. In the case of STRO-1 IgM interaction with its antigen, these forces appear to be overcome by the high molecular weight of the IgM causing the complex to be readily dissociated. Moreover, the probable linear or folded characteristic of the STRO-1 peptide may be limiting the binding affinity of the antibody. Elucidating the nature of the antigen may help to generate antibodies of a different isotype, therefore promoting the use of STRO-1 in hMSC isolation.

Despite the fact the STRO-1 antigen is still unknown, the STRO-1 antibody has been used by many researchers in an attempt to isolate homogeneous populations of hMSCs (Table 1) and also to identify putative cancer stem cells of mesenchymal origin in osteosarcoma (Gibbs *et al.*, 2005). However, from the time that the antibody was discovered in hybridoma supernatant (Simmons and Torok-Storb, 1991) to the commercialisation in its lyophilised form (R&D system), numerous laboratories have employed differently sourced STRO-1 and therefore reported conflicting results, such as enhanced tri-lineage differentiation potential of bone-marrow derived hMSCs in cells lacking STRO-1 expression (Colter *et al.*, 2001). Having established the most reliable source of STRO-1 antibody (Section 3.3), it was important to distinguish between surface expression and intracellular expression of the antigen on osteosarcoma cell lines in order to accurately ascribe an immuno-phenotypic profile to each cell population for subsequent comparison of gene expression microarray data. To date, the use of STRO-1 for the screening of osteosarcoma cell lines has not been optimised and in order to undertake a full comparison of surface expression of markers on these cells, a method to distinguish between live and dead cells was optimised. Many markers, for instance CD133, have been shown to be expressed intracellularly at high levels (Fonseca *et al.*, 2008), and therefore a compromised membrane exhibited by dead cells may lead to false positives in the analysis, especially when attempting to identify rare cell

populations and low expressive cells. Of particular interest in this investigation, approximately half of the cell population which might have been considered as STRO-1 positive were actually a result of intracellular staining. Therefore, the marker expression observed in this study may not be directly comparable to the expression reported by others. For instance, Tirino and colleagues (Tirino *et al.*, 2008) reported a CD133 positive sub-population in three osteosarcoma cell lines, namely MG-63, Saos-2 and U-2-OS. While my study shows CD133 expression in Saos-2 and not in MG-63 and U-2-OS, it is to be noted that the stringency of analysis employed for both studies are dissimilar. Without the live/dead discrimination factor in my study, all the three cell lines were positive for CD133 (data not shown). However, surface expression of CD133 was exhibited by Saos-2 only and not by MG-63 and U-2-OS as reported by Tirino and co-workers (2008). Similarly, the level of STRO-1 expression in MG-63 reported by others (Pautke *et al.*, 2004, Gibbs *et al.*, 2005, Tare *et al.*, 2009) do not necessarily represent surface expression but may also includes intra-cellular staining. This study presents the first report of the characterisation of osteosarcoma cell lines exclusively based on the surface expression of stem cell markers (STRO-1, CD271, CD133), mesenchymal marker (CD13) and marker of nucleated cells (HLA-ABC).

In order to identify the gene encoding STRO-1 antigen, a comparative gene expression microarray analysis was undertaken. This resulted in a list of top twenty matched expression profiles, out of which eight are expressed on the plasma membrane. The sub-cellular localisation of STRO-1 closely matched the reported localisation of ARHGEF4 (Rho guanine nucleotide exchange factor 4 or also referred to as APC-stimulated guanine nucleotide exchange factor, Asef). ARHGEF4 exists as three isoforms and is expressed at low levels in the brain, kidney, lung and muscle (Thiesen *et al.*, 2000). It is involved in colorectal tumour cell migration and mediates cell-to adhesion (Kawasaki *et al.*, 2000, Kawasaki *et al.*, 2003). Apart from the sub-cellular localisation of this protein which resembles that observed for the STRO-1 antigen, the functions described in the literature does not directly relate to the hypothesised function of STRO-1 antigen as being a transmembrane protein involved in differentiation. However, although this protein may not be the STRO-1 antigen, it is plausible to suggest that STRO-1 may be co-expressed with ARHGEF4 as the phenotypic data

observed from the immunofluorescence staining of STRO-1 closely matches the sub-cellular location of ARHGEF4. On the other hand, TNFSF11 (Tumour necrosis ligand of superfamily member 11, clustered as CD254), which is also known as the osteoprotegerin ligand, is a cytokine that binds to RANK (Receptor activator of nuclear factor kappa-B) to activate and induce osteoclast differentiation (Lacey *et al.*, 1998). The expression of an osteoclast activator on hMSCs is an intriguing observation as osteoclasts and osteoblasts follow distinctly different lineages. P2-Purinoreceptors have been shown to be expressed on osteoblast and the Saos-2 cell line (Schofl *et al.*, 1992). They are present as different subtypes and are involved in calcium ion influx when bound to extracellular ATP (Maier *et al.*, 1997). It has been proposed that ATP released by neighbouring damaged cells *in vivo* or by controlled secretion may mediate bone remodelling by acting via the calcium signalling pathway (Schofl *et al.*, 1992). Therefore P2RY6 (purinoreceptor of subtype 6) may be structurally related to the STRO-1 antigen. Interestingly, in chapter 3 (Section 3.7) the level of STRO-1 expression was shown to be elevated two-days after osteogenic induction, a mechanism which may be indirectly related to the expression of the P2RY6 receptor on hMSCs. Overall, the three most likely potential candidate genes of STRO-1 antigen (ARHGEF4, TNFSS11 and P2RY6) may not represent the identity of the antigen itself as this remains to be confirmed by further co-localisation and expression studies, but may represent components of the signalling cascade of hMSC fate determination.

Chapter 5

Identification of putative cancer stem cells in osteosarcoma

5.1 Introduction

Osteosarcoma is the most common bone sarcoma in children and adolescents and can be broadly categorised as central or surface, as approved by the World Health Organisation (Schajowicz *et al.*, 1995) (Section 1.5). In the report of Klein and Siegal (2006) which sub-classified the different types of osteosarcoma based on anatomic and histologic variations, the two most common forms of the disease are central conventional osteosarcoma and surface parosteal osteosarcoma. Conventional osteosarcoma occurs as an intraosseous tumour growth involving the marrow cavity while surface parosteal osteosarcoma appears as a lesion on the surface of the bone. Both types occur as low-grade and high-grade tumours, although central conventional osteosarcoma appears to be more aggressive (Unni, 1998, Klein and Siegal, 2006). The last twenty-five years have witnessed remarkable progress in the management of osteosarcoma. Despite its detrimental side effects, chemotherapy is still the front line treatment and involves the use of immune suppressants including methotrexate and DNA intercalating agents which restrict cell division, such as cisplatin and doxorubicin (Ferrari *et al.*, 2003). In localised disease, a combination of chemotherapy and limb-sparing surgery resulted in an average of five year survival rate in approximately 70 % of patients and more than 90 % of cases of limb preservation (Ferrari *et al.*, 2005). However, despite this improvement in survival rate around 50 % of patients with initially localised disease subsequently develop recurrence. Of newly diagnosed cases, 20 to 30 % present with metastatic disease where neither chemotherapy nor surgical intervention is successful (Ferrari *et al.*, 2003). This data undeniably urges for new therapies to be developed but above all, there is an urgent need for the identification of prognostic factors in osteosarcoma patients in order to predict the outcome of therapy, relapse and survival.

Progress in the understanding of malignant cancers has led to the growing belief that CSCs are implicated in the disease and that this rare cell subset is the cause of recurrence (Section 1.5.2). While current treatments involve tumour shrinkage, there is emerging evidence suggesting that the CSCs remain unaffected by chemotherapy and are responsible for disease relapse (McDonald *et al.*, 2009). The CSC population is now

the prime target of therapy as these cells have been shown to have developed a drug efflux mechanism which renders them resistant to chemotherapy. The CSCs have been identified within distinct SPs by flow cytometry in a number of cancers, a profile indicating their enhanced ability to expel cytotoxic agents such as mitoxantrone, thus conferring cell survival (Hirschmann-Jax *et al.*, 2004). A SP showing drug-resistance features and with cancer-initiating ability *in vitro* and *in vivo* has also been demonstrated in a panel of osteosarcoma cell lines (Murase *et al.*, 2009). The ability of the CSCs to suppress immune response in order to survive has also been proposed but research in this area is still at the early stages (Baguley, 2010). All cancer therapies so far have been based on the classical and now challenged view that tumour cells have equal proliferative potential (Sarraf, 2005). However, with emerging evidence of the existence of CSCs, it has become clear that not all tumour cells divide at the same rate and if the CSCs were to follow the hierarchical patterns of stem cell division (Figure 1.6), then asymmetric cell division may be a model which explains the maintenance of the CSC sub-population within the tumour and recurrence of the tumour after drug-induced atrophy. The presence of CSCs replenishing the tumour mass is analogous to the homeostatic mechanism in normal adult tissues which contain a small sub-population of cells that have the ability to self-renew and give rise to differentiated progeny (Reya *et al.*, 2001). The anomaly resides in the aberrant self-renewal and poorly regulated differentiation of the cells which leads to tumour formation. Based on these characteristics, the cells responsible for this phenomenon, apart from being commonly referred to as CSCs, have also been termed tumour-initiating cells and tumorigenic cells (Clarke *et al.*, 2006). CSCs have been identified in numerous solid tumours based on phenotype by morphological and marker characterisations and the ability of these cells to initiate tumours *in vitro* and in serial transplantation studies (McDonald *et al.*, 2009).

The prime focus of CSC identification has been largely focused on solid tumours of epithelial origin, for instance in breast, colon and prostate (Al-Hajj and Clarke, 2004). In an attempt to identify the CSCs subset in human osteosarcomas, Tirino and co-workers (2008) employed CD133 as a positive marker. By FACS separation, CD133 positive populations of three osteosarcoma cell lines (MG-63, Saos-2, U-2-OS) were

highly proliferative, included in the SP cell subset and able to form sarcospheres in semi-solid serum-free medium, a widely used and accepted *in vitro* tumourigenic assay. Interestingly, the sub-population of cells which did not express CD133 on the cell surface produced detectable amounts of CD133 mRNA transcripts and indeed expressed the CD133 antigen in cytoplasmic vesicles (Tirino *et al.*, 2008). In a canine osteosarcoma model, CSCs were identified by the expression of embryonic stem cell markers (Nanog and Oct4) in sarcospheres. Interestingly, this study also showed that STRO-1 expression was restricted to sarcospheres and the monolayer cultures of the same cell lines lacked STRO-1 expression (Wilson *et al.*, 2008). Many other antigenic markers (including the $CD44^{high}/CD24^{low}$ profile) have been used to identify CSCs in solid tumours, more so in carcinomas, but to date, the presence of CSCs in osteosarcoma are still elusive and require further characterisation.

Following the classic multi-step model of carcinogenesis, there is mounting evidence to suggest that CSCs originate from adult stem cells which are long-lived highly proliferative cells and therefore are potential targets in which multiple genetic hits can occur. It has also been proposed that the multiple genetic hits may occur in the stem cell niche where stem cells have unlimited self-renewal ability, in a progenitor or a differentiated cell with limited or no proliferative potential, thereby acquiring an aberrant ability to extensively undergo cell division (Figure 5.1) (Huntly and Gilliland 2005). Irrespective of the cell of origin, normal adult stem cell or progenitor cell, the CSC is defined by its stem cell-like properties.

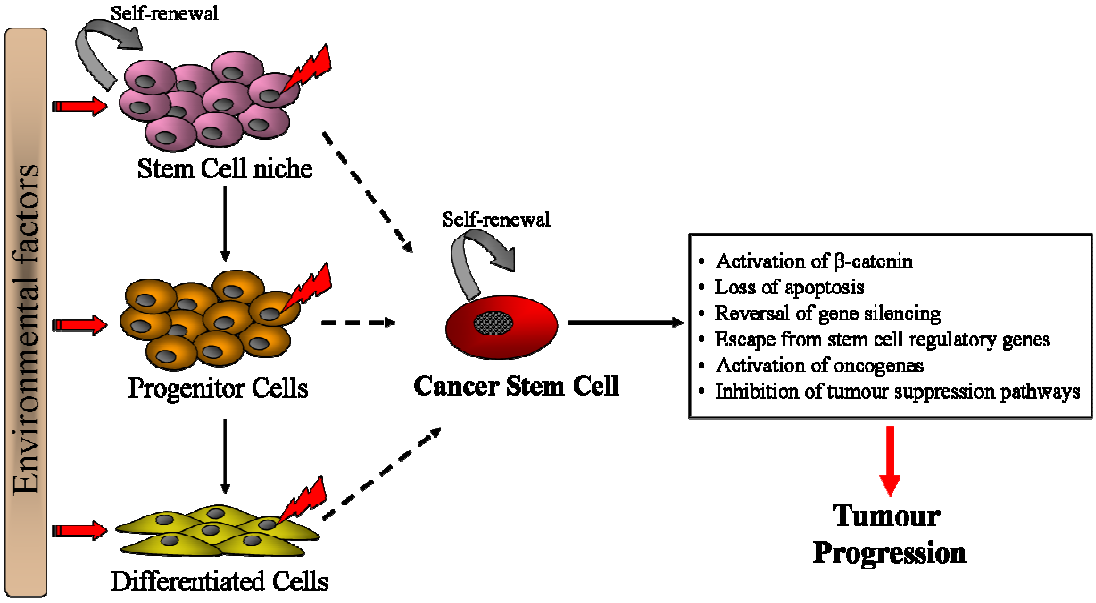

Figure 5.1: Multiple possibilities for the generation of cancer stem cells. Mutations can occur at any stage of the cell lineage which gives rise to causing the cell to acquire self-renewal capacity and become a cancer stem cell. These genetic transformations cause imbalance in the normal regulatory mechanisms of the cell leading to tumour progression (Adapted from (Huntly and Gilliland, 2005).

MSCs, by definition, are able to give rise to mesenchymal tissues and based on the multi-step model of carcinogenesis, it can be hypothesised that mutated MSCs are the origin of sarcomas. As such, Ewing's sarcoma has recently been shown to be a stem cell tumour (Meltzer, 2007). Ewing's sarcoma, a tumour of undefined origin, is characterised by a specific (11:22)(q22:q12) translocation which results in the expression of a chimeric oncoprotein, EWS-FLI1 (Delattre *et al.*, 1992). Mutated MSCs have been implicated as the cell of origin and the work of Torchia and co-workers provided the initial evidence for this. Ectopic expression of EWS-FLI1 in MSCs caused dramatic changes in their cellular morphology and impaired their differentiation potential (Torchia *et al.*, 2003). The involvement of MSC was further supported via silencing studies by Tirode and colleagues (2007). Following long-tem inhibition of the oncoprotein EWS-FLI1 in Ewing's cells, they were successful in showing that the cells acquired an MSC phenotype whereby when induced to the adipogenic and osteogenic lineages, the cells successfully differentiated (Tirode *et al.*, 2007). These studies provide compelling evidence of the involvement of MSC as the precursor cells in Ewing's tumours. However, unlike Ewing's sarcoma, there is no

single mutation characterising osteosarcoma, thus hindering investigations of possible MSC involvement as the precursor cell in osteosarcoma.

Osteosarcoma has a poor prognosis, especially due to the chemoresistant nature of the secondary tumours (Yen, 2009). The lung is the primary site of metastasis and a recent study of ninety-one osteosarcoma patients showed that the rate of metastasis is increased by large tumour volume and elevated levels of serum lactodehydrogenase (Wu *et al.*, 2009). The ability of the cells to form secondary tumours relies on their self-renewal ability in an adaptable environment. Biopsies of secondary pulmonary tumours have revealed differentiated cells within the tumour mass (Halldorsson *et al.*, 2009). In order for the cells to successfully engraft in a distant site and form secondary tumours, they have to be able to break down cell-cell and cell-extracellular matrix connections, enter and survive in the circulation (Kondo *et al.*, 2003). This phenomenon is brought about by a physiological phenotypic shift known as epithelial-mesenchymal transition (EMT) and has been studied in a number of carcinomas (Mani *et al.*, 2008). By adopting the mesenchymal phenotype, the cells are able to migrate away from the primary tumour and invade distant tissues where they undergo mesenchymal-epithelial transition (MET) (Figure 1.4). Studies in breast cancer lines have shown that induction of stem-cell like properties is possible by ectopic expression of Snail and Twist resulting in EMT (Mani *et al.*, 2008). The majority of cells undergoing EMT are derived from progenitors with limited self-renewal capacity making up the tumour bulk. Upon EMT, the epithelial cells gain the stem cell antigenic profile and unlimited self-renewal capacity and are therefore able to colonise a distant site (Radisky and LaBarge, 2008, Hollier *et al.*, 2009).

EMT is a stepwise process whereby studies in carcinoma cell lines revealed three clonal morphologies (holoclones, meroclones and paraclones) that can be adopted by the cell population *in vitro* (Locke *et al.*, 2005). Mackenzie's group established a cellular hierarchy, whereby cells of epithelial morphology forming tightly compacted colonies are termed holoclones and are believed to harbour cells with stem cell characteristics by virtue of their extensive proliferative potential and ability to give rise to differentiating progenitors. Cells exiting the holoclonal stage become flattened and less-compacted

and lose their proliferative potential forming meroclones and ultimately become migratory paraclones (Locke *et al.*, 2005, Harper *et al.*, 2007). While a cellular hierarchy has been established based on phenotype, the functional role of each cell type in the tumour remains to be clarified.

Data accumulated from the studies of solid epithelial tumours and sarcomas strongly implicate CSCs in carcinogenesis. CSCs are nowadays the main target for cancer therapy as there is mounting evidence to suggest that these rare cells are the cause of disease recurrence and relapse (Baguley, 2010). CSCs have been proposed to originate from mutated stem, progenitor or differentiated cells which render them highly proliferative (Figure 5.1). Evidence from Ewing's sarcoma studies show that mutated MSCs are the cause of the tumour (Meltzer, 2007). Therefore, it is of value to identify the CSC population in osteosarcoma and present them as potential targets for therapy. In order to achieve this, the biology of osteosarcoma has to be characterised and its cellular hierarchy established, so that the right cell population can be exploited for successful therapy development.

Aims

As illustrated in Chapter 4, STRO-1 is expressed heterogeneously across the seven osteosarcoma cell lines therefore suggesting that cells may retain MSC-like properties. Having established STRO-1 as a marker of multipotency (Chapter 3), the ability of the seven osteosarcoma cell lines to differentiate to the adipogenic and osteogenic lineages was investigated. Furthermore, due to the limited evidence of CSCs in osteosarcoma, this study investigated the cellular heterogeneity in osteosarcoma cell lines with a view to establishing the identity of the CSC population. The specific objectives of the study are as follows:

- Comparison of the proliferation profiles of osteosarcoma cell lines to determine if this varies between different cell lines
- Investigation of MSC-like characteristics of osteosarcoma cell lines by differentiation to the adipogenic and osteogenic lineages, further illustrating heterogeneity between the different cell lines
- Establishment of cellular heterogeneity within osteosarcoma cell lines when grown in monolayer culture and colony formation in soft agar
- Identification of putative CSCs by anchorage-independent growth potential of different osteosarcoma cell lines
- Isolation of pure holoclones and paraclones from osteosarcoma cell lines pointing towards the persistence of a cellular hierarchy *in vitro*
- Characterisation of the relationship between cells of holoclonal and paraclonal morphologies with identification of an EMT-like process

5.2 Osteosarcoma proliferation and differentiation

Osteosarcomas are tumours made up of a heterogeneous group of cells and the disease outcome varies from patient to patient. By using cell lines in this study, it was interesting to investigate from the onset whether the different osteosarcoma cell lines showed similar proliferative potential *in vitro.* Furthermore, since STRO-1 was expressed heterogeneously among the different cell lines (Chapter 3), their MSC-like differentiation potential was also investigated by induction to the adipogenic and osteogenic lineages. The differentiation potential of the cell lines was assayed both qualitatively and quantitatively. The molecular expression of some key osteogenic markers was also investigated in an attempt to establish a gene expression profile for osteo-inducible cell lines.

5.2.1 Proliferative potential of osteosarcoma cell lines

Seven osteosarcoma cell lines (143B, CAL72, G-292, HOS, MG-63, Saos-2 and U-2-OS) were pulse labelled with green CFSE dye and cultured at 1080 cells/cm^2 density in triplicates in a 6-well plate (Section 2.5.4). At day 1, 2 and 3 post-seeding, the cells were harvested and analysed by flow cytometry. The last harvest was at day 3 as beyond that time point, some cell lines, namely 143B, became confluent and the cells' growth would have been contact inhibited. This procedure was repeated two more times and a representative profile is shown in figure 5.2.

CFSE dye permeates the cells and is cleaved by intracellular esterases to yield a fluorescent compound that is retained by the cell. At each cell division, the dye is diluted and loses fluorescence intensity. The amount of fluorescence loss over a period of time indicates the proliferation rate of the cells. The difference in mean fluorescence intensity between day 1 and day 3 for three independent experiments were recorded and analysed (Figure 5.3). The mean fluorescence intensity decreased steadily over every 24 h period for each of the cell line as shown in figure 5.2. However, day 3 of CAL72 and Saos-2 gave a wide profile spread indicating that the rate at which the dye was lost was not constant among all the cells in the population. Among the seven cell lines, CAL72 and Saos-2 lost the least fluorescence (decrease of approximately 30 % less) indicating their low proliferation rate. Cell lines G-292, MG-63, HOS and U-2-OS divided at similar rates while 143B was the fastest growing cell line in the group (Figure 5.3).

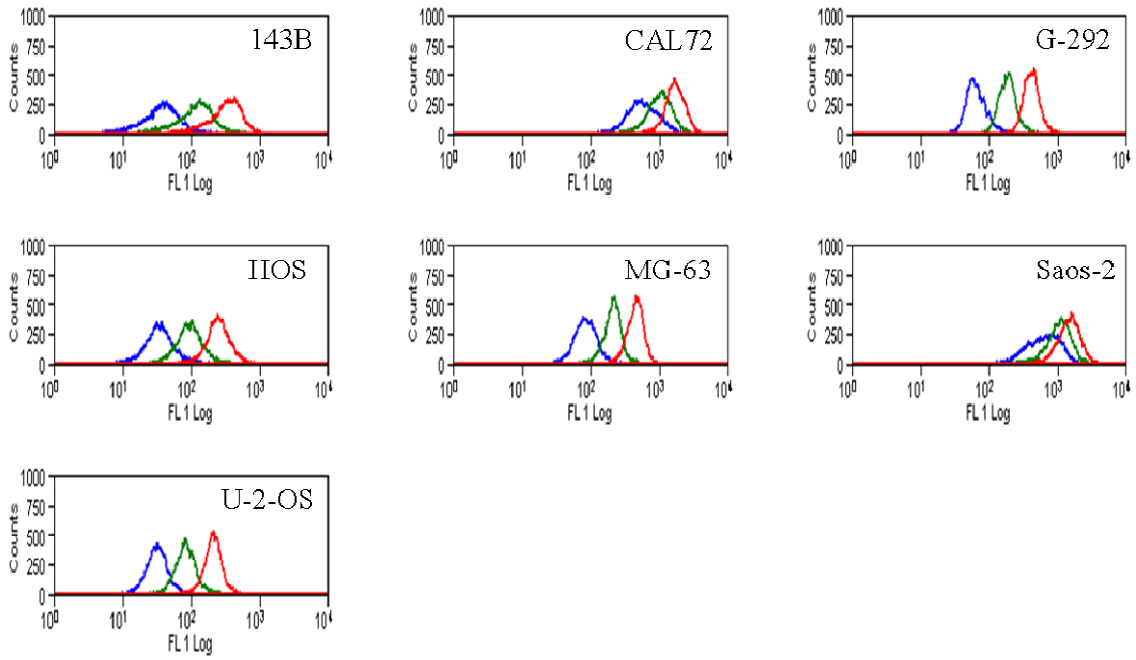

Figure 5.2: Proliferation profile of seven osteosarcoma cell lines analysed by flow cytometry overlay of CFSE stained cells over a period of 3 days. CFSE stained cells were seeded at a density of 10^5 in 6-well plates and harvested at day 1, 2 and 3. Each harvest was analysed on the FITC channel. Red line indicates day 1, green line indicates day 2 and blue line indicates day 3 of the harvest.

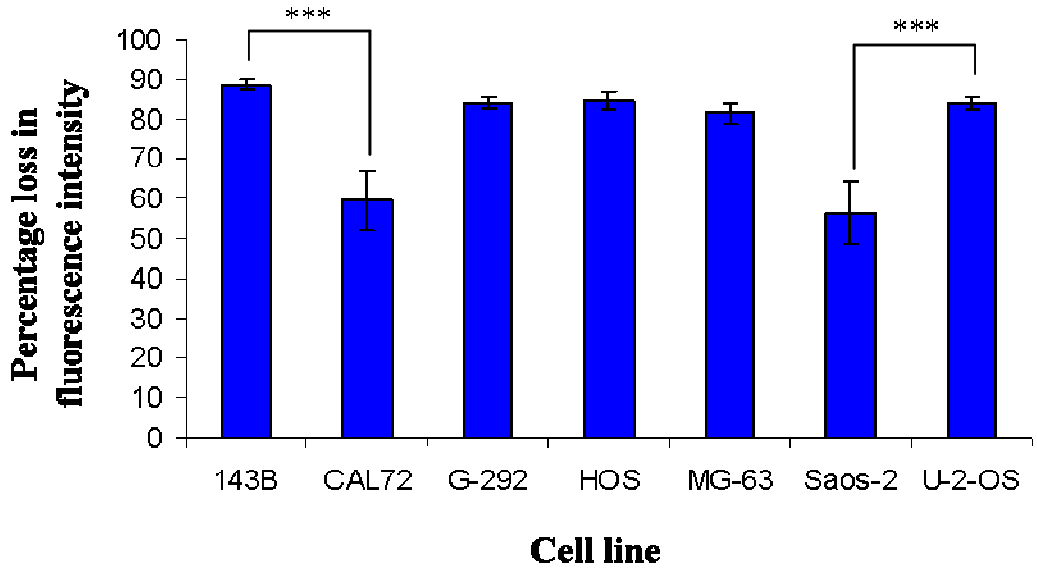

Figure 5.3: Proliferation rate of osteosarcoma cell lines. The chart represents percentage decrease in CFSE fluorescence in seven osteosarcoma cell lines over 48 hours. The difference in mean fluorescence intensity between day 1 and day 3 harvests of three independent experiments were analysed. Student's t-test of 143B versus CAL72 and Saos-2 versus U-2-OS, ***$p<0.01$.

5.2.2 Adipogenic differentiation

The seven osteosarcoma cell lines were grown to confluency (Section 2.2) and induced to the adipogenic lineage at one day post-confluency via the addition of specific induction cocktail (Section 2.3.1.1). The cells were induced for eight days and fourteen days after which they were fixed and stained with ORO dye (Section 2.3.2.1). None of the cell lines showed evidence of lipid accumulation characteristic of adipocyte formation even after extended induction period (14 days). Over-growth of the cells resulted in a high number of apoptotic cells (Figure 5.4) which in turn gave a high ORO background staining (observed as red patches without peri-nuclear lipid vacuoles in Figure 5.5 A and B). The experiment was carried out in triplicate and a representative picture of day 8 analysis is shown (Figure 5.5).

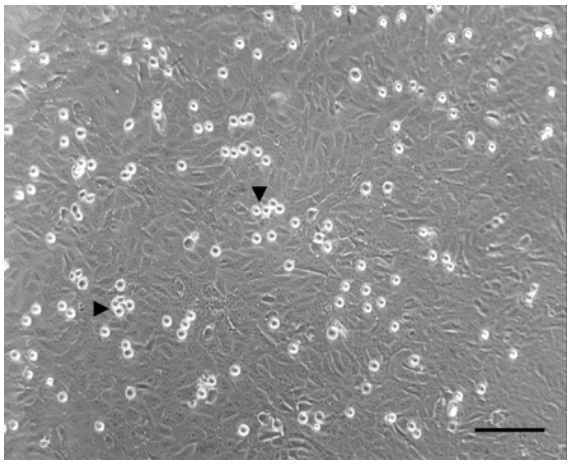

Figure 5.4: Cell death in over-confluent HOS cell line. Non- adherent floating dead cells have a characteristic phase bright appearance, indicated by arrowheads. Scale bar represents 150 µm.

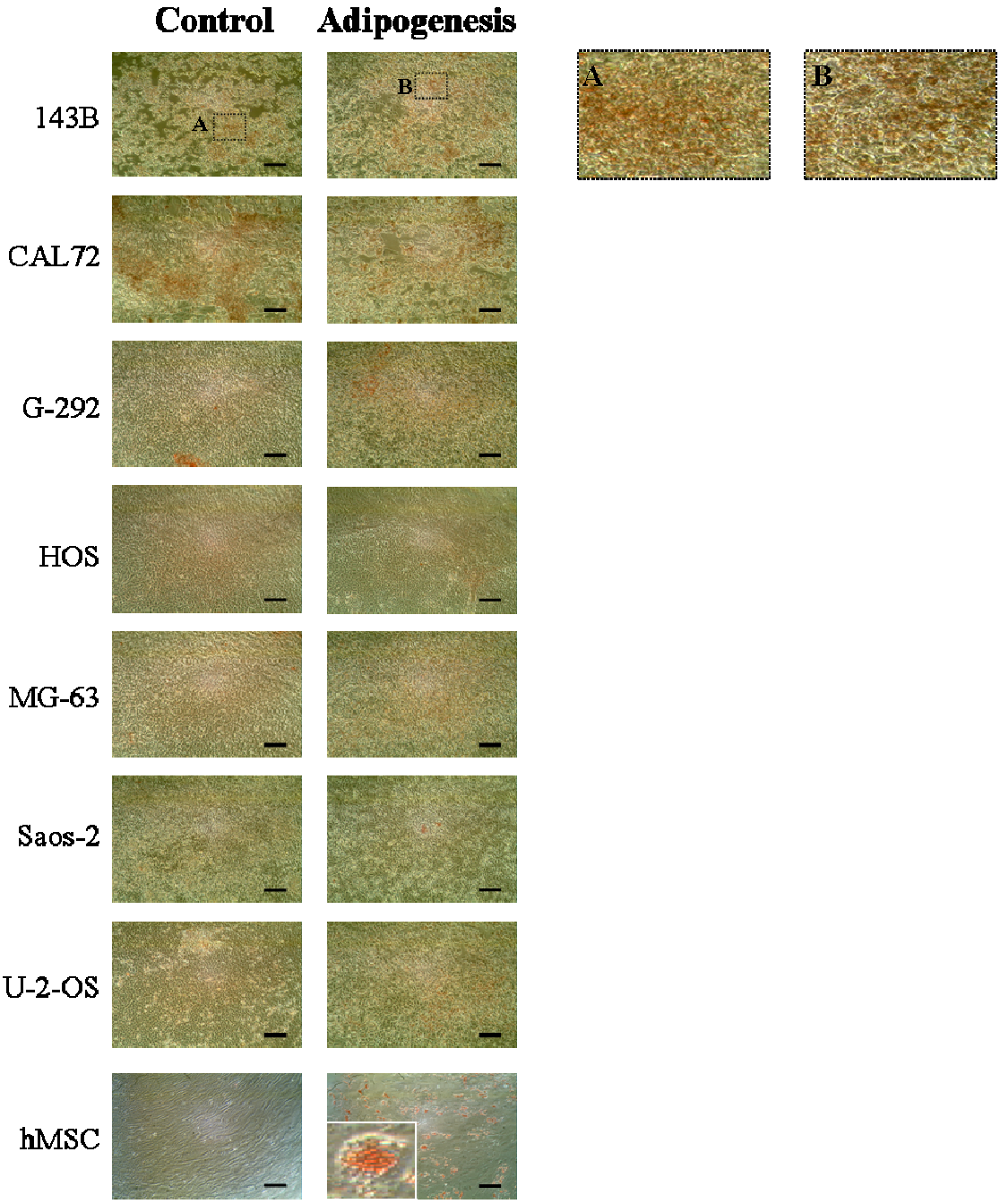

Figure 5.5: Adipogenic potential of osteosarcoma cell lines. Seven osteosarcoma cell lines and hMSC M24♂p5 (positive control) were grown to confluency and induced to the adipogenic lineage at one day post-confluency (Section 2.3.1.1). After 8 days, the cells were stained with Oil Red O (Section 2.3.2.1) and visualised under x10 magnification. (A) represents enlarged section of 143B control and (B) represents enlarged section of 143B induced. Scale bars represent 125 µm.

5.2.3 Osteogenic differentiation

The seven osteosarcoma cell lines were grown to confluency and induced to the osteogenic lineage at one day post-confluency (Day 0 of induction) via the addition of specific induction cocktail (Section 2.3.1.2). The basal level of ALP activity and mineralisation was determined at day 0 before induction and the cells induced for seven and fourteen days. The extent of differentiation was visualised by histochemical staining (Figure 5.6) and also quantified. The inducibility of the cells to the osteogenic fate was determined as the difference in the mean level of ALP concentration or AR dye recovered between the control population and the induced population at days 7 and 14 (ALP: Figure 5.7; AR: Figure 5.8). The assay could not be extended beyond fourteen days as a high number of dead cells were observed in the non-induced population whilst the induced cells became loosely attached and were lost during media changes. The expression of some key osteogenic markers was also investigated by RT-PCR (Section 2.7).

143B

The basal level of ALP activity in 143B was minimal, with only a few specs of blue stained cells (Day 0 control) (Figure 5.6 A). More cells became faintly ALP positive at day 14 both in the control and induced populations indicating a low level of ALP activity in some cells. There was no evidence of mineralisation by day 14 as shown by AR staining.

CAL72

CAL72 showed no ALP activity before induction (Day 0 control) (Figure 5.6 B). At day 7 of induction, a few blue stained cells were observed but at day 14, the few blue stained cells were apparent in both the control and induced population. Both control and induced population had an elevated level of cell death at day 14. The cells retained some AR dye at day 14 of differentiation, but this appeared to be due to the high level of cell death rather than mineralisation.

G-292

The G-292 population showed a few scattered bright blue cells before induction (Day 0 control), indicative of ALP activity (Figure 5.6 C). The number of bright blue cells increased from day 7 to day 14 in the control population, but remained as scattered spots. However, from day 7 of induction, clear patches of blue stained cells were observed and these patches were enlarged at day 14. G-292 was able to mineralise by day 14, appearing only as sparse emerging nodules. However, the non-induced population retained some AR dye at the edge of the monolayer.

HOS

Before induction, the HOS cell line showed clear patches of cells differentially expressing ALP positive cells (Day 0 control) (Figure 5.6 D). With time, both the control and induced population had clear ALP positive patches which grew larger by day 14. Not all the cells in the population were ALP positive, and the degree of positivity in those cells that stained blue was highly variable. The HOS cell line could not be induced to mineralise as shown by AR staining.

MG-63

MG-63 was not able to differentiate although there was some background staining of ALP activity and AR dye accumulation (Figure 5.6 E). The cells were highly proliferative and underwent cell death with time. Cell death was apparent as early as day 7 into induction and loosely attached cells were lost at subsequent feeding rounds.

Saos-2

Saos-2 was the only cell line with a high level of ALP activity before induction (Day 0 control) (Figure 5.6 F). Both the control and the induced population increased their ALP activity with time. It was also the only cell line able to mineralise extensively by day 14. Clear brightly stained nodules were visible by day 7 and by day 14 when staining with AR, with some nodules appearing darker and more concentrated in areas.

U-2-OS

U-2-OS behaved in a similar way to the HOS cell lines (Figure 5.6 G). Before induction, only a few cells stained blue and by days 7 and 14, the ALP positive areas became larger and darker in the induced population. The cells could not be induced to mineralise although some background AR staining was observed.

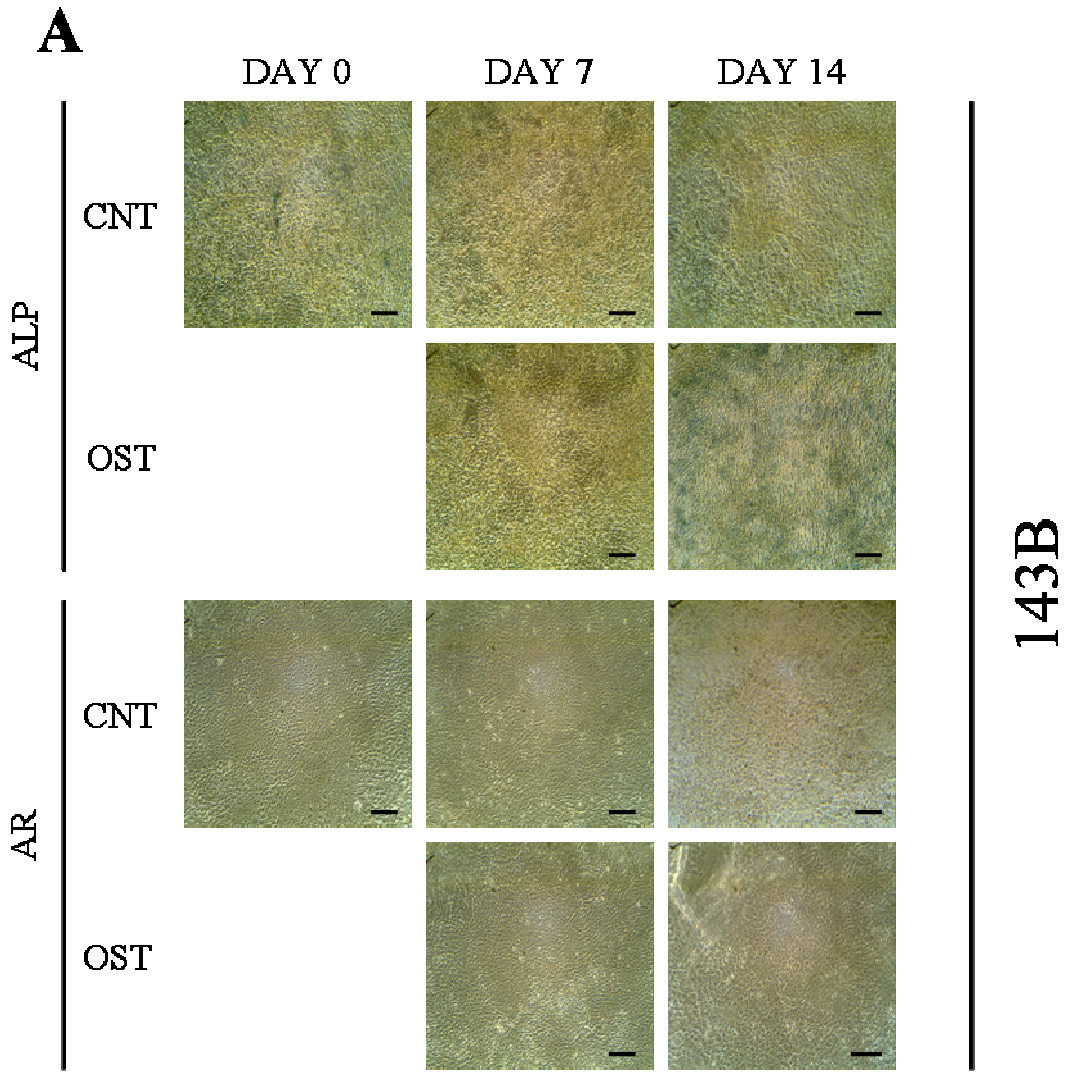

Figure 5.6: Continued overleaf. Osteogenic potential of osteosarcoma cell lines. Seven osteosarcoma cell lines (A. 143B, B. CAL 72, C. G-292, D. HOS, E. MG-63, F. Saos-2 and G. U-2-OS) were gown to confluency and induced to the osteogenic lineage at one-day post confluency via the addition of specific induction cocktail. The populations were assayed for alkaline phosphatase activity (AR, blue staining) and mineralisation was detected by Alizarin Red dye staining (AR, brown-red). Day 0 indicates the population before induction, and day 7 and day 14 indicate 7 and 14 days after induction respectively (Section 2.3). CNT indicates non-induced population and OST indicates osteogenic induced population. Scale bars represent 200 µm.

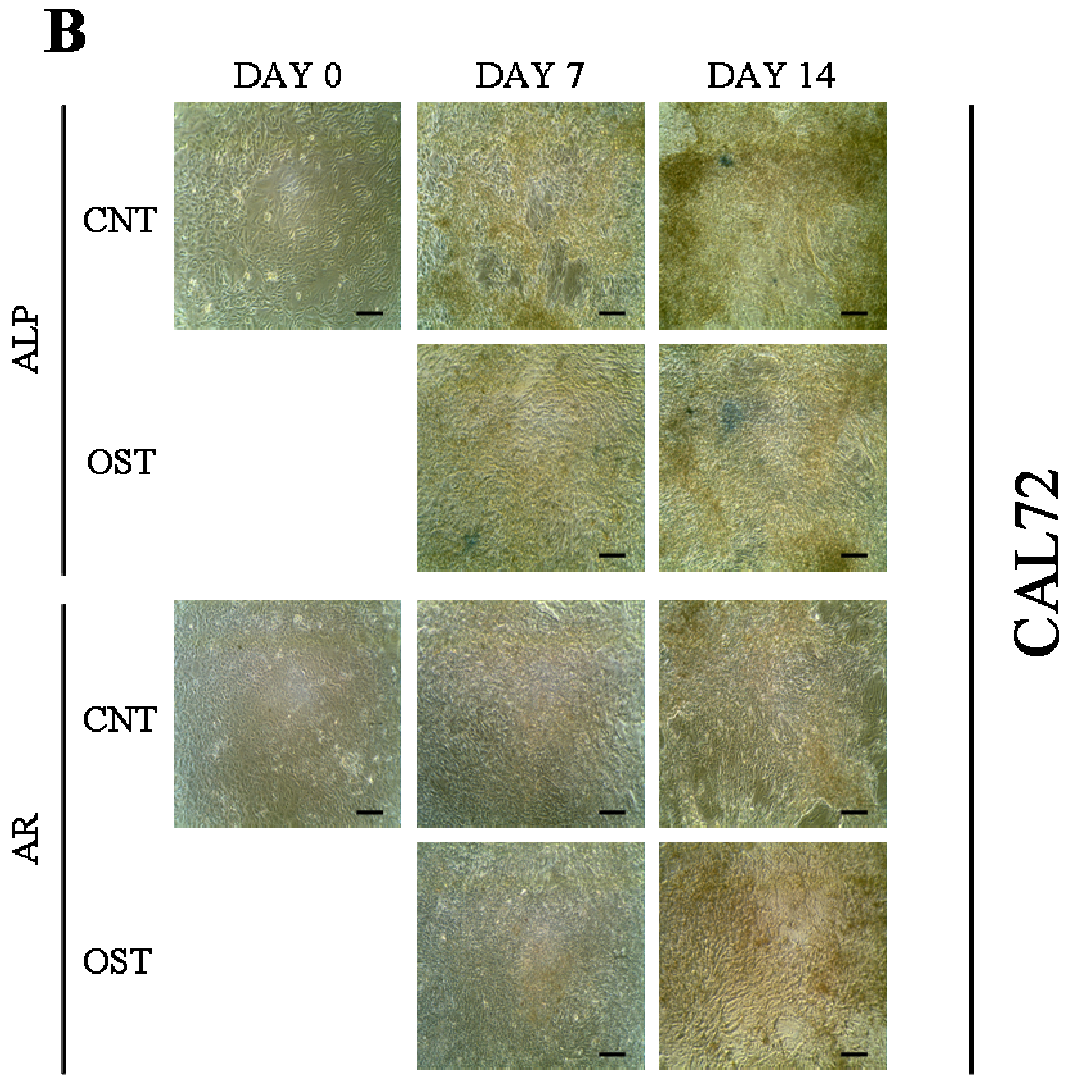

Figure 5.6: Continued overleaf. Osteogenic potential of osteosarcoma cell lines. Seven osteosarcoma cell lines (A. 143B, B. CAL 72, C. G-292, D. HOS, E. MG-63, F. Saos-2 and G. U-2-OS) were gown to confluency and induced to the osteogenic lineage at one-day post confluency via the addition of specific induction cocktail. The populations were assayed for alkaline phosphatase activity (AR, blue staining) and mineralisation was detected by Alizarin Red dye staining (AR, brown-red). Day 0 indicates the population before induction, and day 7 and day 14 indicate 7 and 14 days after induction respectively (Section 2.3). CNT indicates non-induced population and OST indicates osteogenic induced population. Scale bars represent 200 µm.

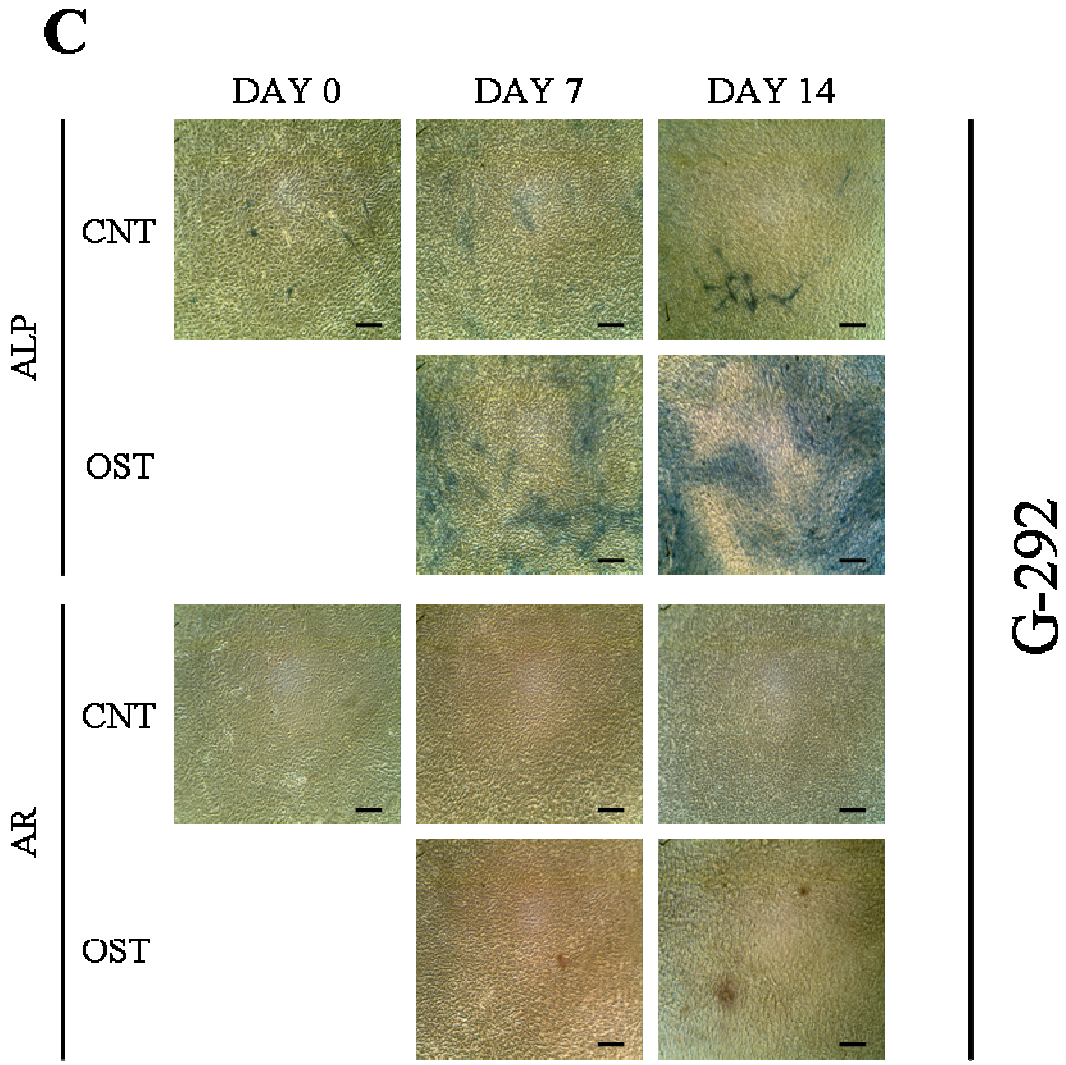

Figure 5.6: Continued overleaf. Osteogenic potential of osteosarcoma cell lines. Seven osteosarcoma cell lines (A. 143B, B. CAL 72, C. G-292, D. HOS, E. MG-63, F. Saos-2 and G. U-2-OS) were gown to confluency and induced to the osteogenic lineage at one-day post confluency via the addition of specific induction cocktail. The populations were assayed for alkaline phosphatase activity (AR, blue staining) and mineralisation was detected by Alizarin Red dye staining (AR, brown-red). Day 0 indicates the population before induction, and day 7 and day 14 indicate 7 and 14 days after induction respectively (Section 2.3). CNT indicates non-induced population and OST indicates osteogenic induced population. Scale bars represent 200 µm.

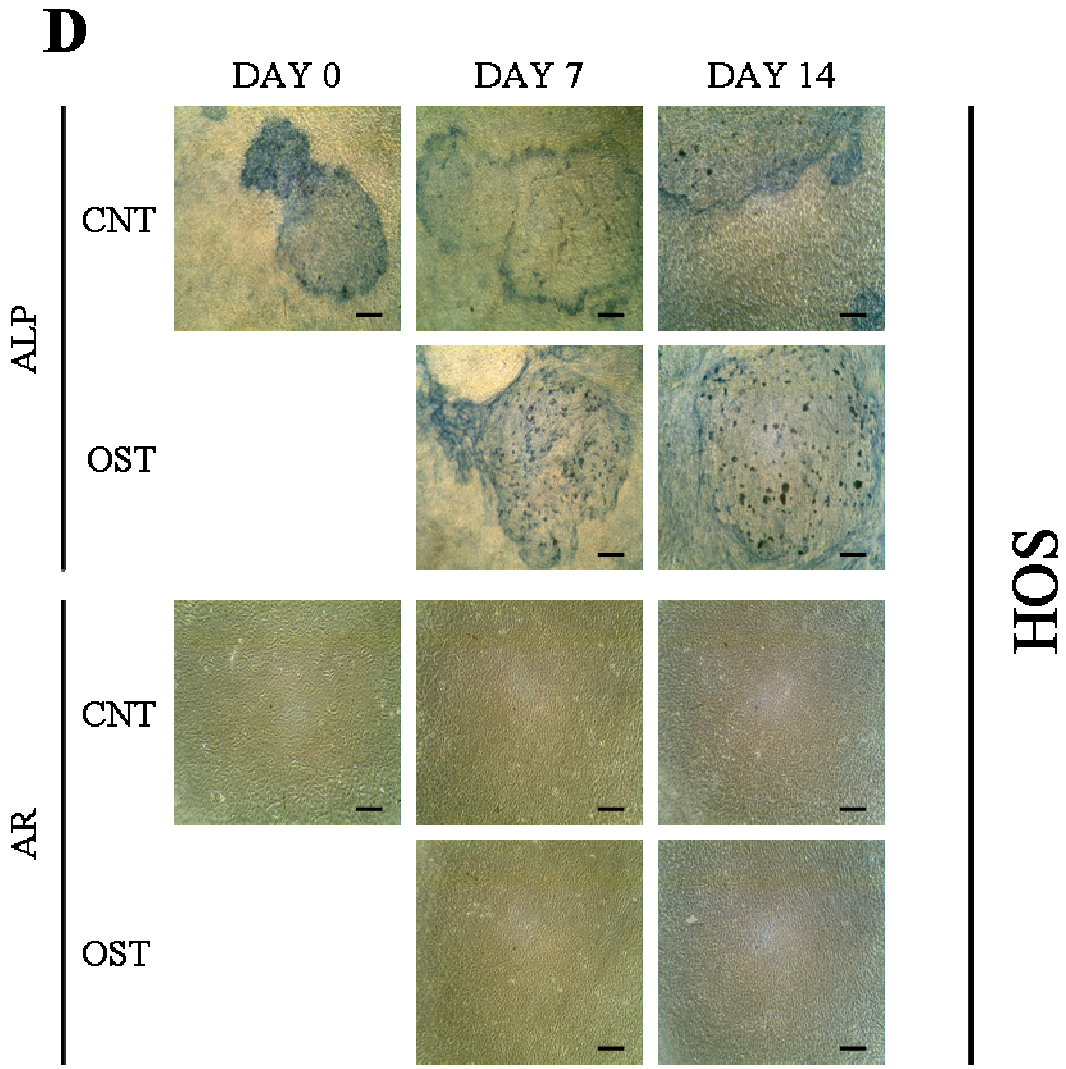

Figure 5.6: Continued overleaf. Osteogenic potential of osteosarcoma cell lines. Seven osteosarcoma cell lines (A. 143B, B. CAL 72, C. G-292, D. HOS, E. MG-63, F. Saos-2 and G. U-2-OS) were gown to confluency and induced to the osteogenic lineage at one-day post confluency via the addition of specific induction cocktail. The populations were assayed for alkaline phosphatase activity (AR, blue staining) and mineralisation was detected by Alizarin Red dye staining (AR, brown-red). Day 0 indicates the population before induction, and day 7 and day 14 indicate 7 and 14 days after induction respectively (Section 2.3). CNT indicates non-induced population and OST indicates osteogenic induced population. Scale bars represent 200 µm.

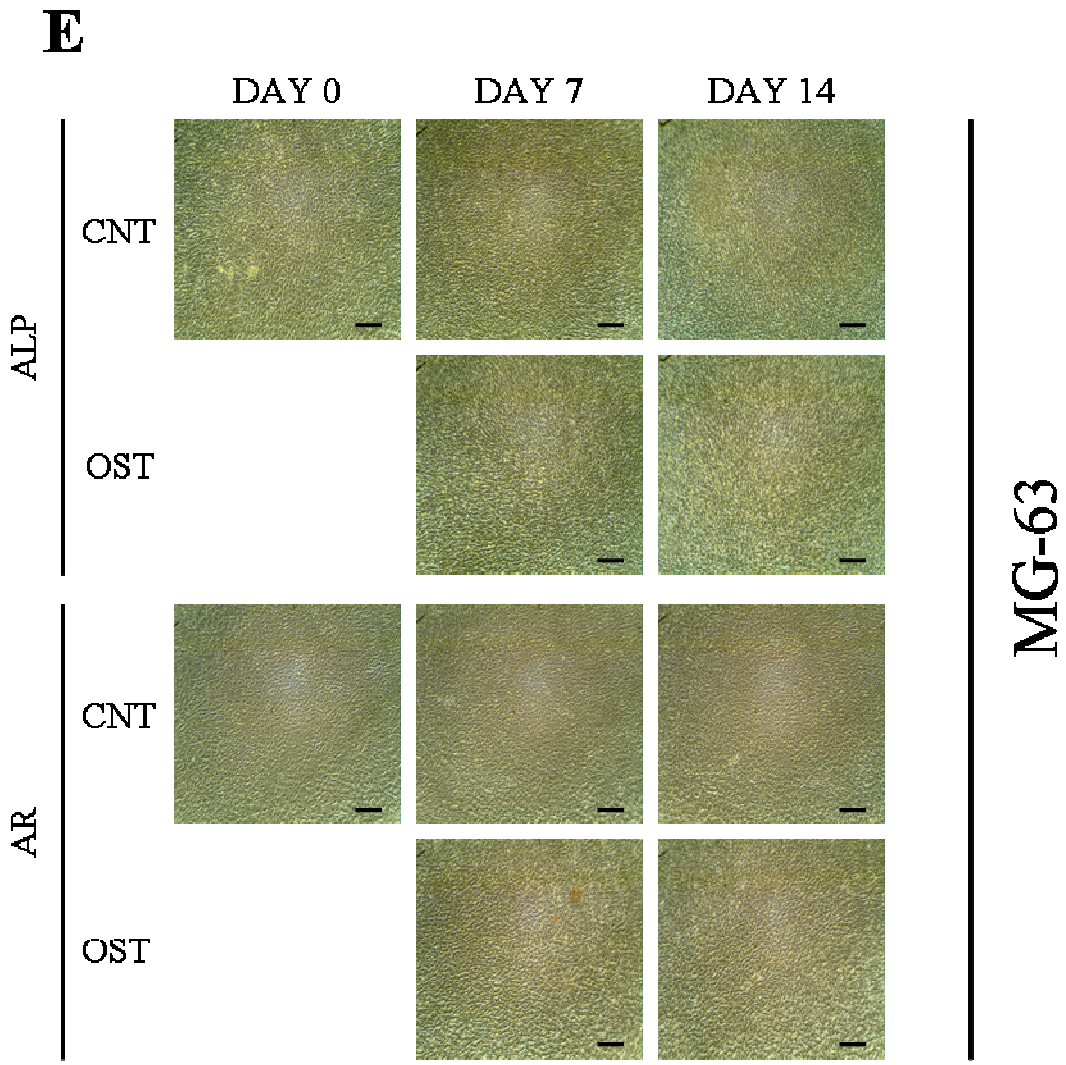

Figure 5.6: Continued overleaf. Osteogenic potential of osteosarcoma cell lines. Seven osteosarcoma cell lines (A. 143B, B. CAL 72, C. G-292, D. HOS, E. MG-63, F. Saos-2 and G. U-2-OS) were gown to confluency and induced to the osteogenic lineage at one-day post confluency via the addition of specific induction cocktail. The populations were assayed for alkaline phosphatase activity (AR, blue staining) and mineralisation was detected by Alizarin Red dye staining (AR, brown-red). Day 0 indicates the population before induction, and day 7 and day 14 indicate 7 and 14 days after induction respectively (Section 2.3). CNT indicates non-induced population and OST indicates osteogenic induced population. Scale bars represent 200 µm.

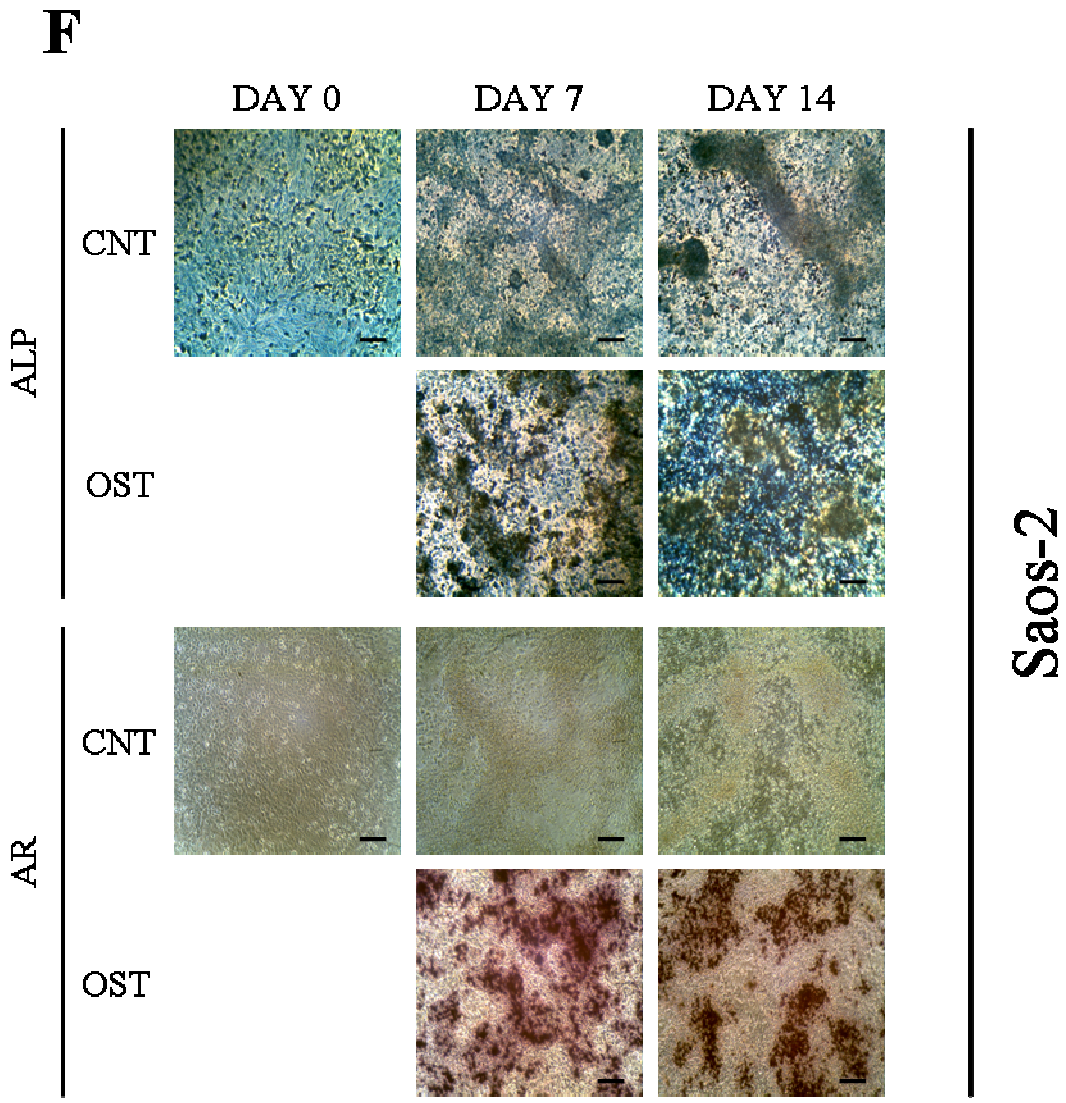

Figure 5.6: Continued overleaf. Osteogenic potential of osteosarcoma cell lines. Seven osteosarcoma cell lines (A. 143B, B. CAL 72, C. G-292, D. HOS, E. MG-63, F. Saos-2 and G. U-2-OS) were gown to confluency and induced to the osteogenic lineage at one-day post confluency via the addition of specific induction cocktail. The populations were assayed for alkaline phosphatase activity (AR, blue staining) and mineralisation was detected by Alizarin Red dye staining (AR, brown-red). Day 0 indicates the population before induction, and day 7 and day 14 indicate 7 and 14 days after induction respectively (Section 2.3). CNT indicates non-induced population and OST indicates osteogenic induced population. Scale bars represent 200 µm.

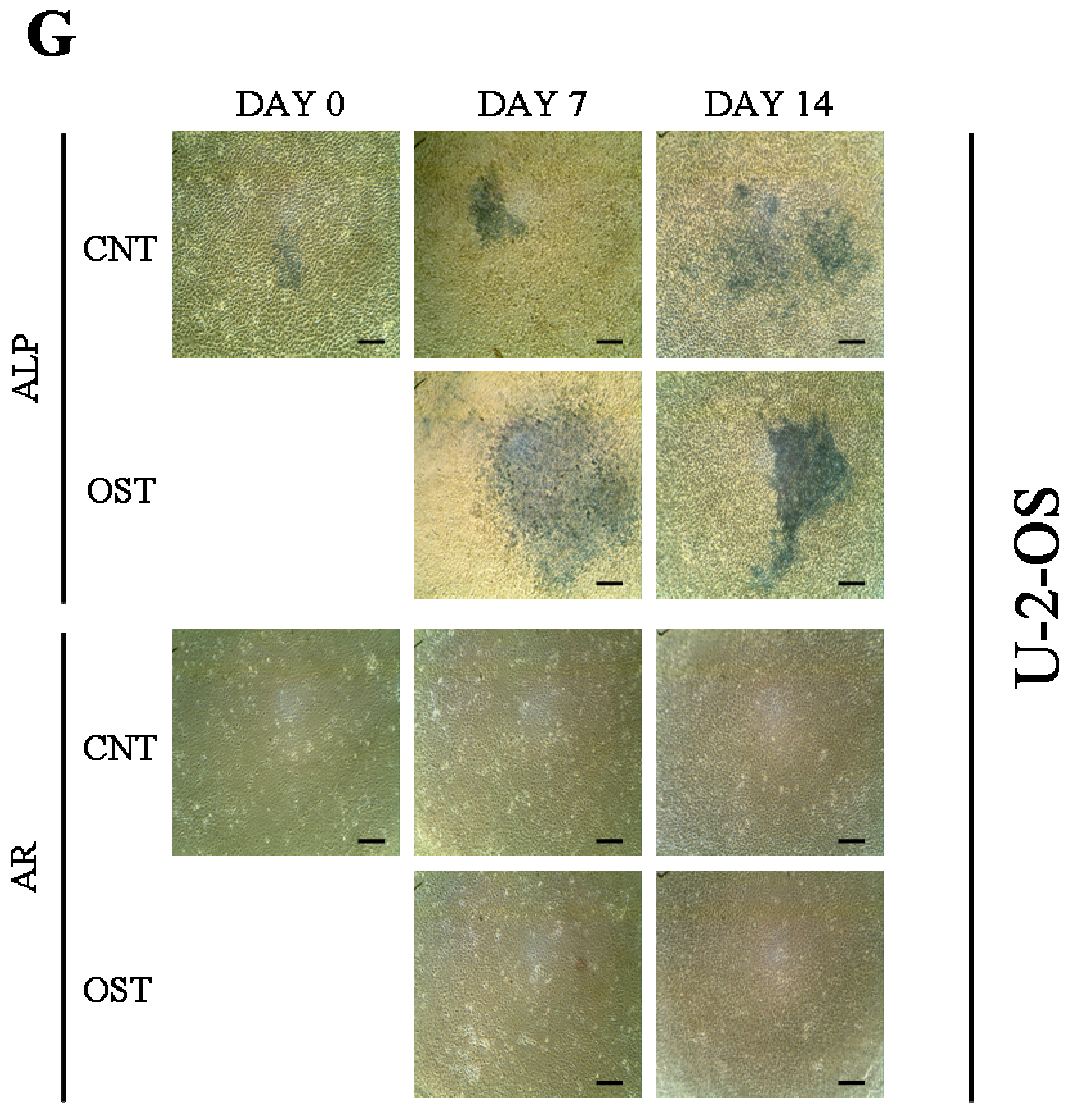

Figure 5.6: Osteogenic potential of osteosarcoma cell lines. Seven osteosarcoma cell lines (A. 143B, B. CAL 72, C. G-292, D. HOS, E. MG-63, F. Saos-2 and G. U-2-OS) were gown to confluency and induced to the osteogenic lineage at one-day post confluency via the addition of specific induction cocktail. The populations were assayed for alkaline phosphatase activity (AR, blue staining) and mineralisation was detected by Alizarin Red dye staining (AR, brown-red). Day 0 indicates the population before induction, and day 7 and day 14 indicate 7 and 14 days after induction respectively (Section 2.3). CNT indicates non-induced population and OST indicates osteogenic induced population. Scale bars represent 200 µm.

Quantification of ALP activity between cell lines

A quantitative assay for ALP activity was performed to allow comparison to be made between cell lines (Figure 5.7). After normalisation to cell number, Saos-2 stood out as the cell line with the highest level of ALP activity at Day 0 (Figure 5.7 A). This enzymatic activity was inherent within the cells as osteogenic induction did not increase its level of activity (both the control and the induced populations showed similar level of ALP activity at day 7 (Figure 5.7 B) and day 14 (Figure 5.7 C). An extended period of confluency appeared to increase ALP activity in the control populations of HOS and U-2-OS, although the levels of ALP activity in the induced populations were higher than the controls.

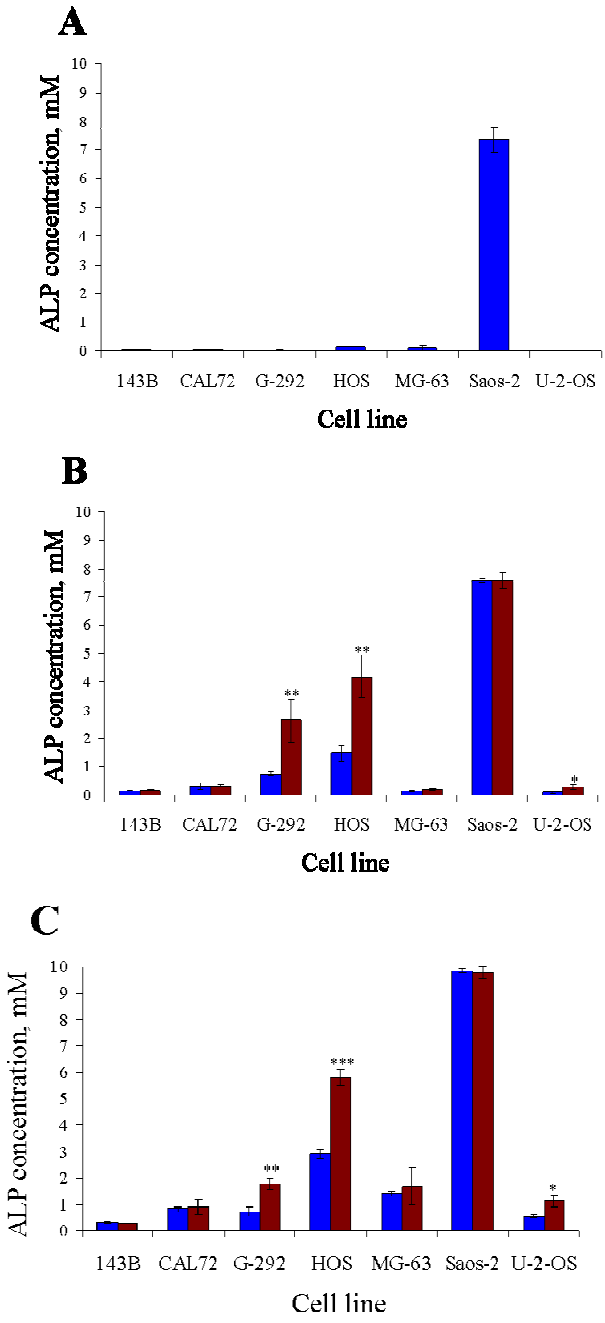

Figure 5.7: Quantification of alkaline phosphatase activity in seven osteosarcoma cell lines. Cells were grown to one-day post-confluency and induced to the osteogenic lineage for seven and fourteen days. After the specific time points, the cells were quantified for alkaline phosphatase activity (ALP) which was then normalised to DNA content (Section 2.3.3). A. Day 0: Basal level of ALP activity before induction; B. Day 7: 7 days after induction and C. Day 14: 14 days after induction. ■ represents control population (uninduced) and ■ represents osteogenic induced population. Student's t-test control against induced; *p<0.05, ** p<0.04, ***p<0.01.

Quantification of AR dye recovered

A quantitative assay for AR staining was performed to allow comparison of mineralisation to be made between cell lines (Figure 5.8). In most of the cell lines, because of the excessive cell growth and limited differentiation, a high level of AR background staining was observed in the uninduced populations. This was evident in the quantification of AR recovery at day 0 (Figure 5.8 A). Although Saos-2 was the only cell line which exhibited extensive mineralisation, CAL72 and MG-63 appeared to show an increase in AR dye recovery at day 7 (Figure 5.8 B) and day 14 (Figure 5.8 C). However, this was not evident in the histochemical staining of the cell lines (Figure 5.6). The increase in G-292 AR dye recovery at day 14 (Figure 5.8 C) was consistent with the very few mineralised nodules observed during the staining procedure in the induced population, but not consistent with lack of staining in the control population (Figure 5.8 C).

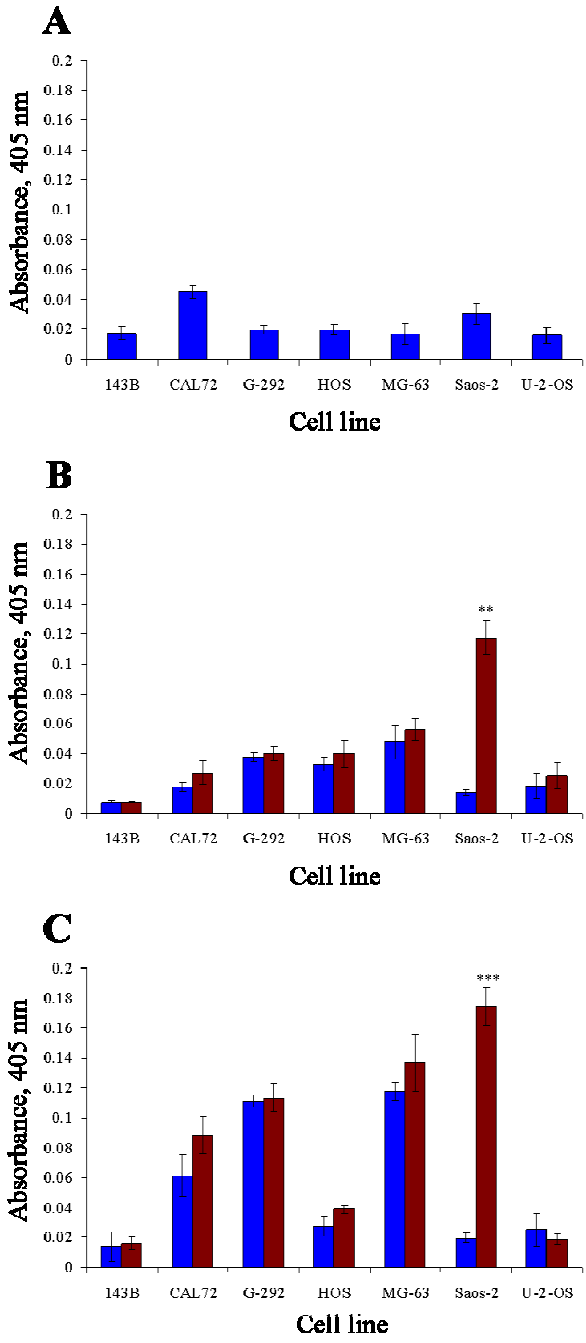

Figure 5.8: Quantification of mineralisation in seven osteosarcoma cell lines. Cells were grown to 1-day post-confluency and induced to the osteogenic lineage for seven and fourteen days. After the specific time points, the cells were quantified for AR staining which was then normalised to DNA content (Section 2.3). A. Day 0: Background level of AR dye before induction; B. Day 7: 7 days after induction and C. Day 14: 14 days after induction. ■ represents uninduced population (control) and ■ represents osteogenic induced population. Student's t-test control against induced;** $p<0.04$, *** $p<0.01$.

Osteogenic inducibility of cell lines

In order to evaluate the inducibility of the cell lines to the osteogenic lineage, the difference in ALP activity and AR dye recovered between the control and induced populations was calculated (Figure 5.9). This was performed for both time points, that is days 7 and 14. G-292 (day 7 and 14: $p<0.04$), HOS (day 7: $p<0.04$, day 14: $p<0.01$) and U-2-OS (day 7 and 14: $p<0.05$) were able to increase their ALP activity upon addition of the inducers indicative of osteogenic differentiation. However, they were unable to undergo terminal differentiation and mineralise. Saos-2 was the only cell line that was AR inducible (day 7: $p<0.04$, day 14: $p<0.01$), indicative of terminal differentiation (Figure 5.8 F).

Cell line	ALP inducibility		AR inducibility	
	DAY 7	DAY 14	DAY 7	DAY 14
143B	0.02	0	0	0
CAL72	0.02	0.10	0.01	0.03
G-292	1.88**	1.06**	0	0
HOS	2.71**	2.89***	0.01	0.01
MG-63	0.06	0.28	0.01	0.02
Saos-2	0.01	0	0.10**	0.15***
U-2-OS	0.20*	0.57*	0.01	0

Table 5.1: Osteogenic inducibility of seven osteosarcoma cell lines. After osteogenic induction and quantification of alkaline phosphatase activity and mineralisation, the mean difference between the control and induced population was analysed at days 7 and 14 of differentiation. The red font indicates osteogenic inducible cells lines calculated as the difference between control and induced population for each line at the specified time point. Student's t-test; *$p<0.05$, **$p<0.04$, ***$p<0.01$.

Gene expression analysis of osteogenic differentiation

Cells were harvested and RNA isolated (Section 2.7.1) at day 0 (before induction), day 7 and day 14. RT-PCR was carried out as per section 2.7.2 and primers flanking specific regions of the genes of interest are listed in Table 2.3. Gene expression analysis was normalised to β-actin level and the absence of contaminating DNA was confirmed by the negative control (-RT) (Figure 5.9). In all of the cell lines except CAL72, the presence of *MSX2* product was concomitant with the expression of the key transcription factor of osteogenesis, *Cbfa-1*. However Cbfa-1 was expressed by all of the cell lines at day 14 of induction (Figure 5.9), despite the lack of positive histochemical staining in some populations (Figure 5.6). Similarly expression of *BMP8*, *Col1A1*, *OCN* and *OP* does not reflect the differentiation status of the cell line. However, the increase in ALP expression from day 0 to day 14 reflected the pattern observed by the histochemical staining of the ALP positive cell lines.

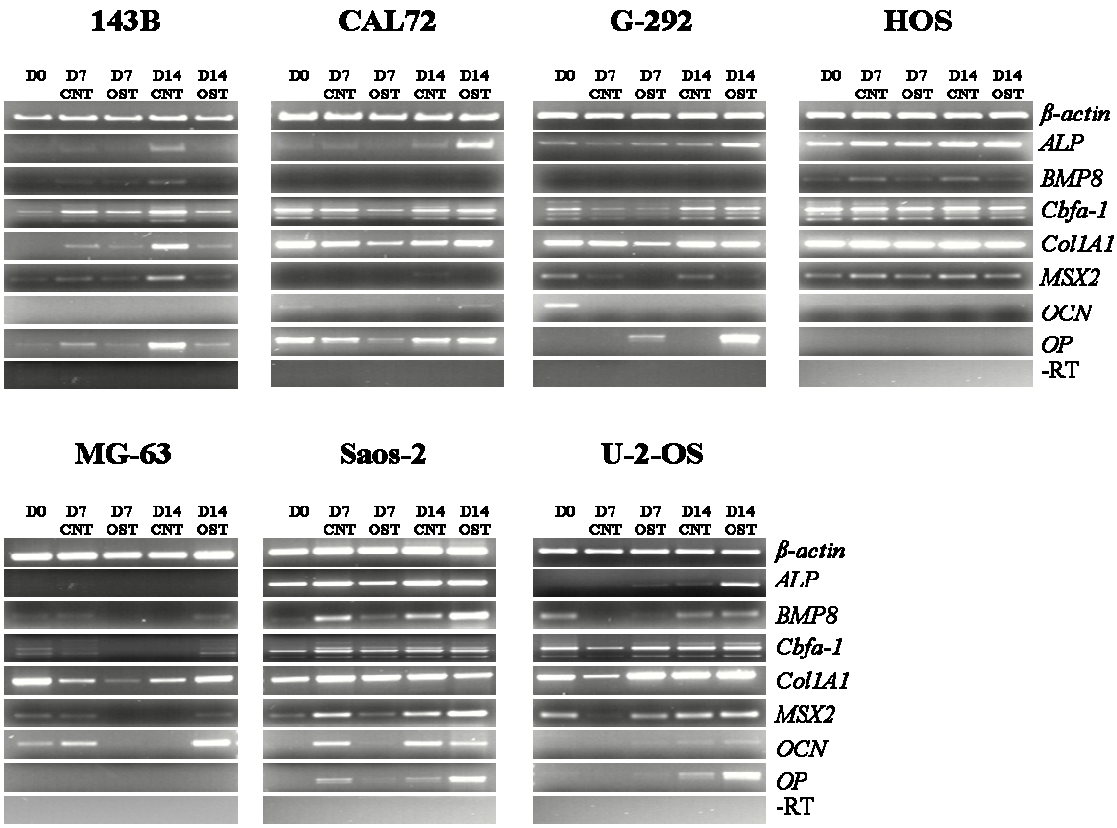

Figure 5.9: Gene expression profile of seven osteosarcoma cell lines during osteogenic differentiation. Total RNA was isolated before induction (D0) and at days 7 (D7) and 14 (D14) of differentiation in control (CNT) and induced (OST) populations. RT-PCR was carried out using gene specific primers. The PCR products were run on agarose gels, stained with Ethidium Bromide and visualised under UV light (Section 2.7).

5.3 Cellular heterogeneity of osteosarcoma cell lines

When osteosarcoma cultures were examined by phase contrast microscopy, some cell lines appeared to have a mixed morphology. Furthermore, when cultured for extended time period, the HOS line exhibited a non-uniform pattern of ALP activity suggestive of a heterogeneous population of cells (Figure 5.6 B). In order to investigate this cellular heterogeneity in the seven osteosarcoma cell lines, cells were seeded at low density and the colonies formed were observed in an adherent monolayer culture and matrix suspension format. The clones identified were further characterised and a cellular hierarchy was investigated.

5.3.1 Cellular heterogeneity within osteosarcoma cell lines

Cells from the seven osteosarcoma cell lines were seeded at 100 cells per 10 cm dish and colonies were allowed to form under standard culture conditions (Section 2.2.1). Colony formation was monitored every 2-3 days and after 7-14 days, distinct epithelial and fibroblastic phenotypes could be observed (Figures 5.10 and 5.11), although one specific phenotype appeared to be predominant in each cell line. CAL72 and Saos-2 took longer to form colonies which appeared smaller compared to the other cell lines. As the colonies grew larger, morphologies typical of holoclones and paraclones were observed (Figure 5.11).

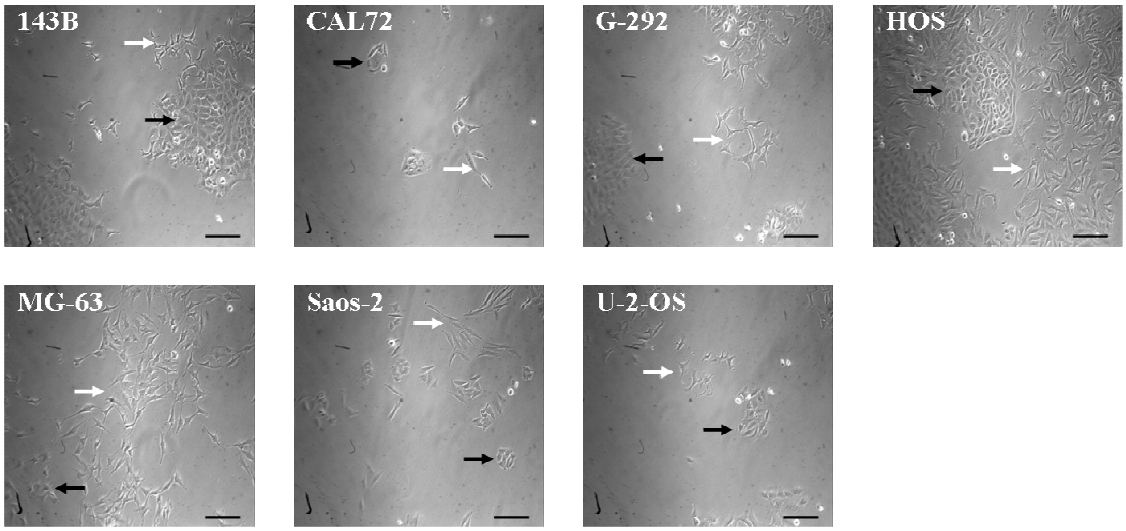

Figure 5.10: Cellular heterogeneity of osteosarcoma cells within monolayer cultures. Cells from the seven osteosarcoma cell lines were seeded at 100 cells per 10 cm dish and allowed to form colonies for 7-10 days under standard culture conditions (Section 2.2.1). Black arrows indicate holoclonal colonies and white arrows indicate paraclonal colonies. Both types of colonies co-exist within the culture monolayer. Scale bars represent 250 µm.

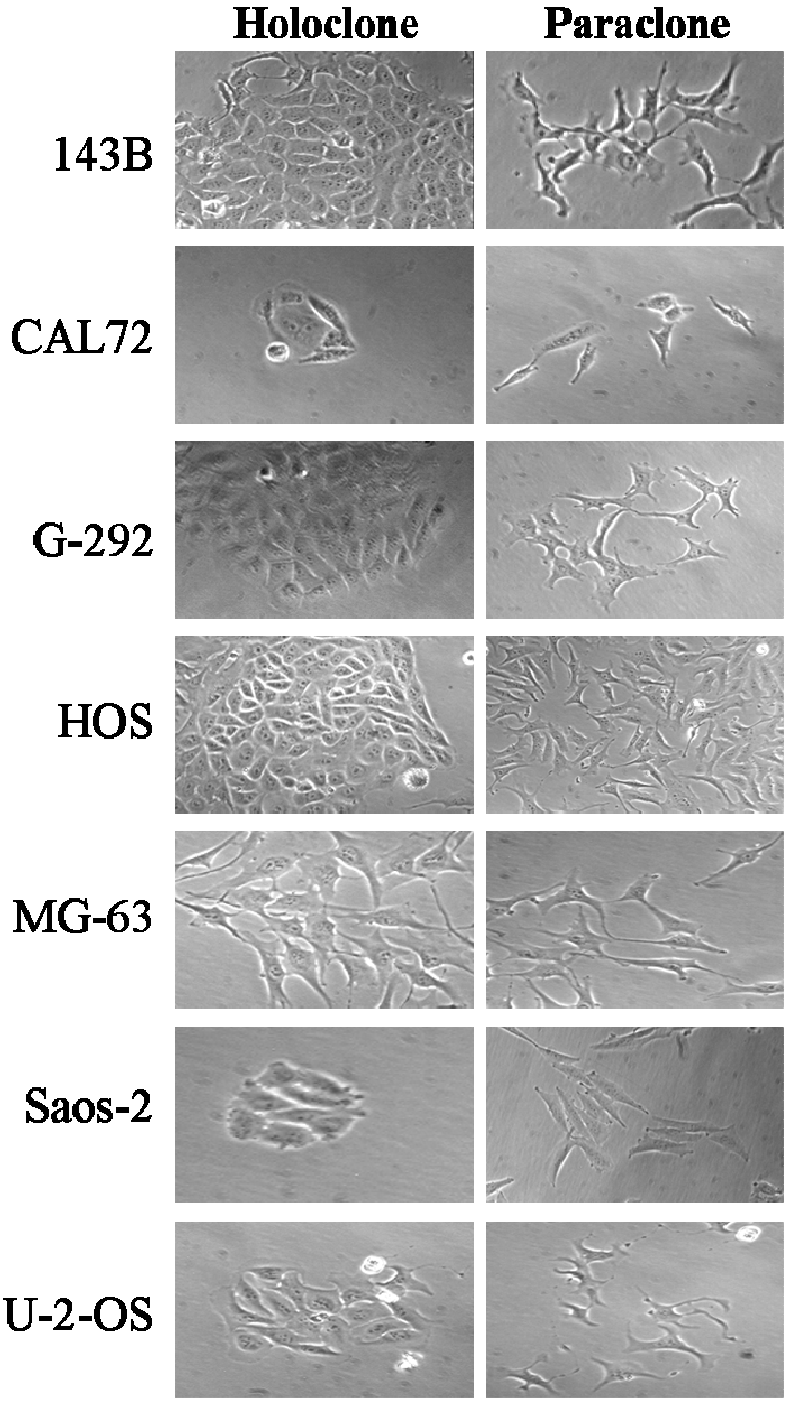

Figure 5.11: Formation of holoclonal and paraclonal colonies. The figure represents enlarged images of examples of holoclones and paraclones observed in low density cultures of the osteosarcoma cell lines. Holoclonal colonies appear circular and cells are in close proximity (epithelial-like) while paraclonal colonies are distant from one another and cells have a polygonal shape (fibroblastic-like). Photo-micrographs adjusted for representation purposes and are not to scale.

5.3.2 Anchorage dependent cell growth

Cells from the seven osteosarcoma cell lines were seeded in soft agar and incubated under standard culture conditions (Section 2.2.5). Spherical colony formation was monitored over twelve days. Beyond this time period, a monolayer of cells started to form on the surface of the agar. Acidification of agar matrix (colour change to yellow) caused apoptosis of cells within the cell clusters. At day 12 post-seeding, the colonies were visualised at x10 magnification (Figure 5.12) and the diameters of the colonies were measured. The rapidly proliferating cells 143B, G-292 and MG-63 formed anchorage independent colonies at a faster rate than the other cell lines. The HOS cell line, which was derived from the same parent as 143B was not able to form colonies in soft agar. U-2-OS despite being a rapidly proliferating cell line in monolayer cultures (Section 5.2.1), did not withstand anchorage independent growth as well as the other cell lines of the same proliferative potential. U-2-OS formed cell clusters of an average diameter of 20 µm while 143B for instance formed colonies of an average diameter of 300 µm. The size and shape of the spherical colonies varied within each cell line illustrating heterogeneity in the ability of individual cells to form colonies within the cell population. The spheres formed had either a smooth or rough edge, reminiscent of the morphology observed during holoclonal and paraclonal colony formation.

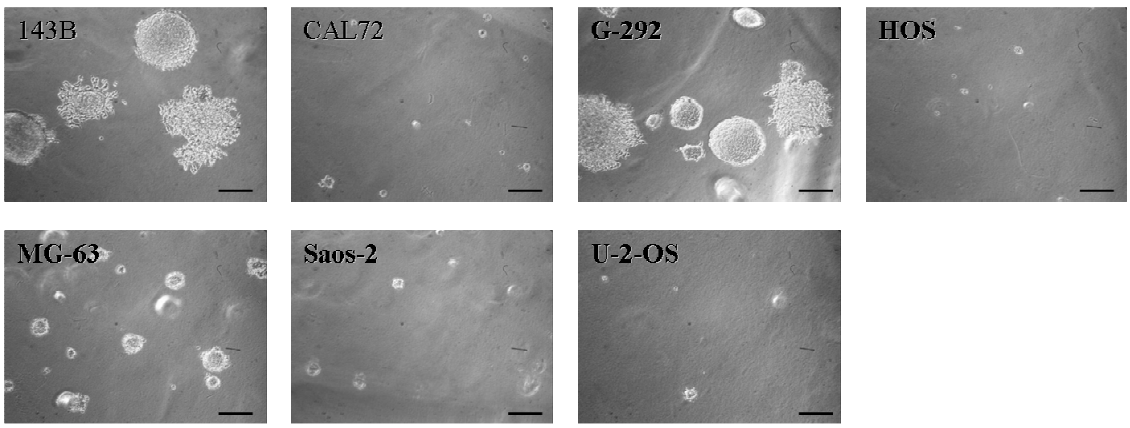

Figure 5.12: Anchorage independent growth potential of osteosarcoma cell lines. Cells at a density of 1080 cells/cm^2 were seeded in soft agar and colonies allowed to form for 9-12 days under standard culture conditions. Spherical colonies were visualised at x10 magnification. Scale bars represent 250 µm.

5.4 Establishment of cellular hierarchy within the HOS osteosarcoma cell line

The identification of holoclonal and paraclonal colonies in the monolayer and soft agar cultures prompted the investigation of a possible cellular hierarchy similar to that observed by Mackenzie's group (Locke *et al.*, 2005, Harper *et al.*, 2007) within the osteosarcoma cell lines. The HOS cell line was chosen as it exhibited a more pronounced difference in cellular morphology, both at low and high density monolayer cultures. The presence of a heterogeneous population within a tumour mass which is subsequently maintained upon cell line derivation implies that different sub-populations of cells possess distinct functional properties. Therefore, clonal populations of epithelial and fibroblastic morphologies were isolated and expanded from the HOS cell line to establish if a cellular hierarchy exists.

5.4.1 Identification and characterisation of clones

HOS cells were clonally selected by low density seeding (Section 2.2.1) and single clones were expanded and labelled as holoclones or paraclones depending of the morphology of colonies they formed (Figure 5.14). Although colonies of meroclonal formation were observed, these were not isolated as they were intermediate colonies and were not expected to stay as meroclones for the duration of the culture period. Holoclonal cells grew well as single clones and were highly proliferative under standard culture conditions. When paraclonal cells were selected as single cell clones under standard culture conditions, they divided very slowly and after only a few divisions they underwent cell death (Figure 5.13). However, when cultured in HOS conditioned media, the paraclonal cells grew readily and healthy colonies were formed (Figure 5.15). The apparent dependency of the paraclones on the holoclones was further investigated by culturing HOS cells at low density (1.3 cell/cm^2) in either fresh medium or HOS conditioned medium and by allowing colonies to grow for one week. The ratio of holoclones to paraclones formed per dish was directly related to the culture medium used (Figure 5.16), whereby out of 50 colonies counted, the ratio was 1:2 and 2:1 in fresh and conditioned media respectively. In monolayer culture, when HOS was seeded

at low density and colonies allowed to form for more than one week, the paraclonal cells appeared to migrate towards the holoclonal population (Figure 5.16 A&B), and when left into culture for an extended time period, the paraclonal cells subsequently formed a tight boundary around the holoclonal colony (Figure 5.16 C). With time, cells at the centre of the holoclonal colony appeared compressed and ultimately became phase bright and underwent cell death.

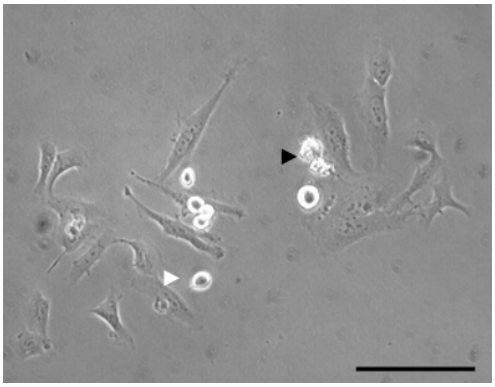

Figure 5.13: Aborted paraclonal colony. Paraclones were clonally selected from a low density culture and expanded under standard culture conditions (Seciton 2.2.1). Paraclones underwent a limited number cell division after which they became large, flat and granular and released their cell contents (indicated by black arrowhead). Ultimately the cells round up and become phase bright (indicated by white arrowhead) indicative of cell death. Scale bar represents 150 µm.

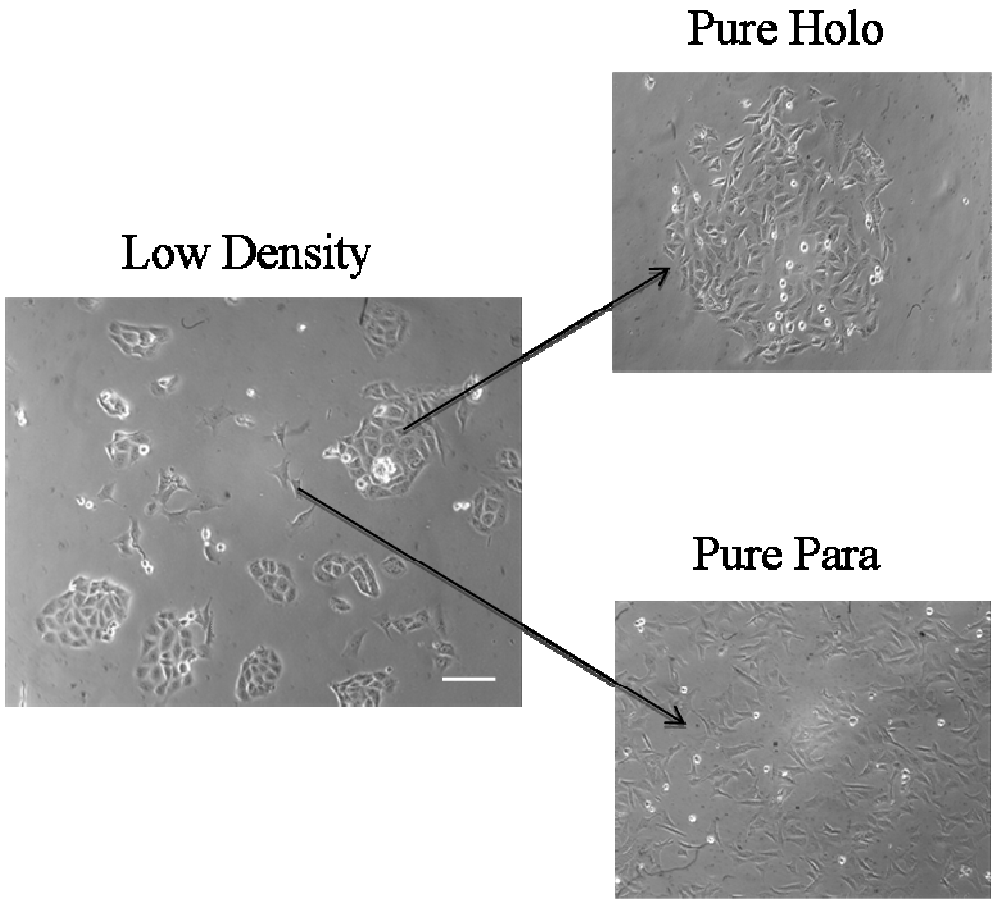

Figure 5.14: Identification of holo- and paraclones in HOS cell line. HOS was seeded at a density of 1.3 cell/cm^2 and colonies allowed to form. By limited dilution, single cell clones were expanded under specified culture conditions and identified as pure holoclones and pure paraclones. Scale bar represents 300 µm.

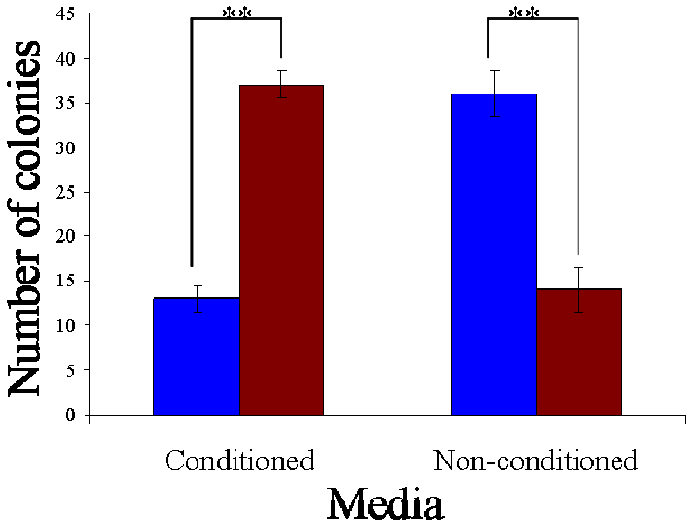

Figure 5.15: Dependency of paraclones on conditioned media. HOS cells were seeded at 50 cells per 10 cm dish and colonies allowed to form, in conditioned and non-conditioned media. After one week, the number of colonies were counted and recorded as either holoclones (■) or paraclones (■), based on cellular morphology. Student's t-test holoclone versus paraclone, $^{**}p<0.04$.

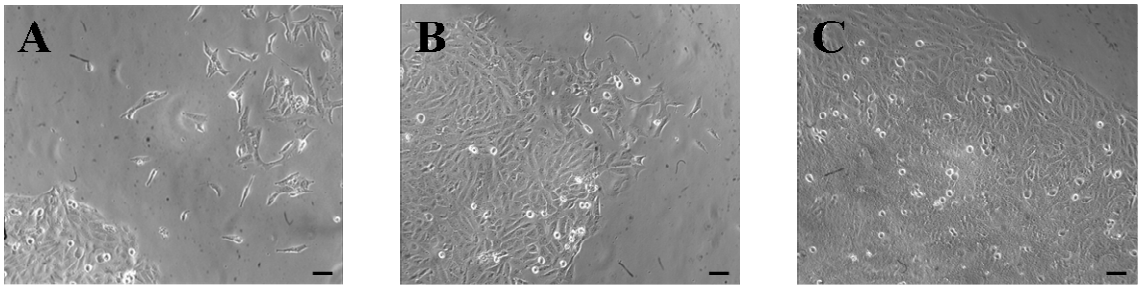

Figure 5.16: Migration of paraclone towards holoclone. HOS cells were seeded at low density and colonies allowed to form. Once a holoclonal and a nearby paraclonal colony were identified, the dish was marked and the migration of the paraclonal cells monitored over 1 week. (A) Initial migration of paraclonal cells was led by cell division in the direction the holoclonal colony, (B) paraclonal cells merging with the holoclonal colony and (C) finally paraclonal cells forming a layer around the holoclonal cells which then became compacted and underwent cell death in the centre. Scale bars represent 125 µm.

5.4.2 Epithelial-mesenchymal transition (EMT) in osteosarcoma

The cellular heterogeneity observed in the HOS cell line appeared to be regulated by a defined cellular hierarchy. When single cells from a holoclonal colony was seeded and allowed to form second generation holoclonal colonies, some cells appeared to exit the tight compact holoclonal morphology and become loose, possibly migrating away from the holoclonal parent colony to form a paraclonal colony. Transition from paraclonal to holoclonal formation was not observed in the pure paraclonal colonies.

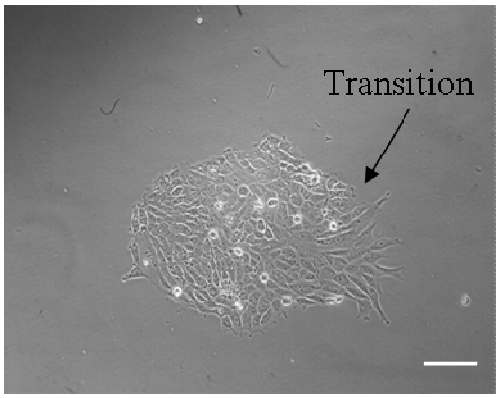

Figure 5.17: Epithelial-mesenchymal transition in HOS cell line. Cells from the parent holoclonal colony detached from the compact organisation and adopted a fibroblastic morphology characteristic of paraclonal cells. Scale bar represents 250 µm.

5.5 Discussion

Osteosarcoma has a poor outcome despite advances in chemotherapy. The obstacle to successful treatment of this disease remains the lack of definite prognostic markers due to the high degree of heterogeneity of the tumour among patients. This heterogeneity arises from the many different possible mutations that are thought to occur in the precursor cells of the tumour, thus determining the prognosis of the disease. Furthermore, the prevalence of putative CSC in the tumour has been identified as the cause of recurrence in patients.

This study investigated the characteristics of seven osteosarcoma cell lines and identified a cellular hierarchy within each cell line which may further our knowledge about the development of sarcomas. Human cell lines have been successfully employed in the study of carcinogenesis from the 1970s onwards and the HOS cell line was among the first successful cell lines to be established (Rhim, 2000). Since then a number of cell lines for the study of osteosarcoma has been generated with the most recent one being UTOS-1. After two years of maintenance in culture, this cell line retained the molecular and phenotypic characteristics of the original tumour cells (Yasuda *et al.*, 2009). These observations support the validity of osteosarcoma cell lines as a reliable *in vitro* system to study the mechanisms of carcinogenesis. Moreover, the maintenance of a culture system allows for an equalised population to develop, which are free from contaminating loosely associated cells which do not actively contribute to the tumour. In cancer drug development, toxic agents have a narrow therapeutic index and cell lines as *in vitro* models are the tool of choice as they represent controlled conditions which can be uniformly monitored (Zhang and Dolan, 2009). Nowadays, drug development companies are advocating for the use of cell lines for targeted cancer therapies before entering the phases of clinical trial, therefore highlighting the importance of understanding and fully characterising oncogenesis in cell lines as a primary step (Tuma, 2006). Characterisation of specific properties in osteosarcoma cell lines has previously involved an average of three cell lines (Tirino *et al.*, 2008). In this study, seven osteosarcoma cell lines were used to account for the high degree of tumour heterogeneity observed among patients.

The immunophenotypic characteristics of the seven osteosarcoma cell lines has been presented and discussed in chapter 4. In this part of the thesis, their proliferative potential and their ability to undergo multilineage differentiation were investigated based on their expression of certain stem cell markers, such as STRO-1 and CD133 (Figure 4.10). The proliferative potential observed in the seven cell lines used could be categorised cell lines as either slow or rapid dividing cells, whereby CAL72 and Saos-2 represented the slow dividing populations and 143B, G-292, HOS, MG-63 and U-2-OS represented the rapid dividing ones. Using a cell density measurement assay, Shapira and Halabi (2009) showed that Saos-2 proliferated at a slower rate than MG-63, which is in line with the observation of this study which employed a fluorimetric dye dilution method to show that indeed, MG-63 had a higher proliferative potential than Saos-2. This difference in *in vitro* proliferative potential was the first indication that not all osteosarcoma behave in a similar manner. Most comparative studies of proliferation rates of osteosarcoma cell lines to date have focussed on population subsets, such as CD133 positive sub-populations, instead of the population as a whole (Tirino *et al.*, 2008). This study is the first evidence of osteosarcoma cell line classification based on their proliferative rates. Taken together, the heterogeneity in *in vitro* proliferative rates of the tumour cells may reflect the heterogeneity of tumour burden observed in patients and hence represent determinant factors in disease outcome.

As illustrated in Chapter 4 (Section 4.8), some osteosarcoma cell lines expressed the MSC marker STRO-1 suggesting that cells within those lines might have retained MSC characteristics. However, unlike MSCs, both the STRO-1 positive and the STRO-1 negative populations failed to undergo adipogenic differentiation. Upon osteogenic differentiation, some cell lines appeared to be more inducible than others, again re-iterating the heterogeneity among osteosarcoma cell lines. Contrary to the other cell lines and in addition to its unique mineralisation potential, the basal level of ALP activity in the Saos-2 cell line was unexpectedly elevated and maintained for fourteen days in the uninduced populations. This observation has been previously reported in a study looking at the osteoblastic properties of Saos-2, where they found that the highest level of ALP activity in the cell culture was at confluency (Rodan *et al.*, 1987). Recent reports have shown that the osteoblastic potential of MG-63 could be enhanced by

different culture conditions, such as alendronate-supplemented media (anti-resorptive agent) (Xiong *et al.*, 2009), 5-azacytidine treatment (DNA methylation inhibitor) (Locklin *et al.*, 1998) or cell growth on titanium coated surfaces (Shapira and Halabi, 2009). Using the standard osteogenic induction medium, in my hands, MG-63 cells were negative for ALP activity and failed to mineralise. This may be due to the different culture conditions used by other groups to assess osteogenic potential of MG-63, whereby the cells are grown on different matrix or expanded in medium supplemented with osteogenic inducers (Shapira and Halabi, 2009, Sun *et al.*, 2009). Apart from the apparent uniform positivity and negativity of ALP activity observed in Saos-2 and MG-63 respectively, the other cell lines displayed heterogeneity in their staining patterns. More precisely, not all the cells within the population were able to commit to the osteoblastic lineage and it appeared that each individual cell within the population possessed inherent differentiation potential. This could be explained by the multi-step model of carcinogenesis which stipulates that various different genetic mutations accumulate in the cells at the different stages throughout the progression of the tumour. Depending on the number of hits and the stage the cell is at when the mutation occurred, the cell's properties are altered by acquiring proliferative potential. Therefore, if the cell had already passed the commitment stage, it would express basal levels of ALP activity but due to the nature of the mutation may not be able to progress to mature osteoblasts. Similarly, certain mutations may impair the cell's commitment mechanism which results in complete inhibition of differentiation. Identifying a positive marker to distinguish between the multipotent cells from the committed ones may help to reveal the mechanisms of carcinogenesis in osteosarcoma.

Differentiation heterogeneity among the seven osteosarcoma lines was further highlighted by molecular characterisation. Expression of key genes traditionally indicative of osteogenic differentiation was detected at the different time points in an induced and non-induced population. Expression of the *ALP* gene correlated with the enzymatic activity recorded in the assays, for instance the continuous ALP activity detected in Saos-2 at the induced and non-induced level was reflected in the strong band products during RT-PCR. However expression of *Cbfa-1* the master regulator of osteogenesis, did not correlate with osteogenic potential of the cell lines. Although

ALP and AR positive Saos-2 expressed *Cbfa-1*, CAL72 which was comparatively negative for ALP and AR expressed *Cbfa-1* to the same level. The expression of *OCN* in Saos-2 is similar to that reported by Benayahu and co-workers (Benayahu *et al.*, 2001) and the molecular heterogeneity among the different cell lines characterised in this study is analogous to the molecular heterogeneity observed in a different set of osteosarcoma cell lines by Olstad and colleagues (Olstad *et al.,* 2003). Although the majority of the cells in a cell line could not differentiate, the small subset of cells which were able to differentiate accounted for the expression of osteogenic specific markers during RT-PCR. As such, molecular characterisation of osteosarcoma cell lines by RT-PCR is not reflective of the differentiation potential of that particular cell line under the standard culture conditions employed in this study. The differentiation and molecular heterogeneity observed across the lines further emphasises on the multi-step model of carcinogenesis.

The uneven pattern of differentiation within the cell lines pointed towards the possible presence of a cellular hierarchy within the population. The phenotype of the seven osteosarcoma cell lines has been described in the literature as either epithelial or fibroblastic or both (Table 5.1). This description of the cell lines is based on the apparent predominant morphology when the cells are seeded at normal/high density and observed at confluency.

Cell line	Phenotype
143B	Mixed
CAL72	Epithelial
G-292	Fibroblastic
HOS	Mixed
MG-63	Fibroblastic
Saos-2	Epithelial
U-2-OS	Epithelial

Table 5.2: Prominent cellular morphology of osteosarcoma cell lines. The phenotypes are as described by the ATCC® bank database. The accession number for each cell line is illustrated in table 2.1.

When the cells were cultured at low density in monolayer and anchorage independent formats, two distinct morphologies became apparent. As a monolayer, the cells adopted an epithelial or a fibroblastic morphology when grown as monolayer, forming holoclonal and paraclonal colonies respectively. A similar observation has been reported by Mackenzie's group working on carcinoma cell lines (Locke *et al.*, 2005, Harper *et al.*, 2007). This cellular heterogeneity was further investigated in soft agar matrix to assay their anchorage independent growth. This is a widely used *in vitro* method to identify cells with tumourigenic potential and has been validated as a method to determine the tumorigenic potential of MSC derived cell lines (Funes *et al.*, 2007). Cells which are able to form spherical colonies in soft agar are anchorage-independent and therefore more tumourigenic than their anchorage-dependent counterparts which are unable to form colonies in the matrix. Here, the osteosarcoma cell lines showed a heterogeneous ability to undergo anchorage-independent growth. In the twelve day period allocated for colony formation, CAL72 and Saos-2 the slow dividing cell lines, formed occasional clusters in soft agar. The cells lines 143B, G-292 and MG-63 readily formed colonies of mixed sizes indicating that within the population not all the cells are able to undergo anchorage-independent growth. Although U-2-OS represented a rapidly dividing population, only occasional colonies were observed.

In sarcosphere formation assays which involved growth of cells in a semi-solid serum-free media, it has been proposed that the rare CD133 positive cells represent the CSC of osteosarcoma (Tirino *et al.*, 2008), although my data contradict the level of CD133 positive cells observed in MG-63 and U-2-OS cell lines reported by that group. Tirino and co-workers (2008) isolated the CD133 positive subset in Saos-2 as CSCs and showed that those specific cells were more tumourigenic than their negative counterparts. This observation leads to the supposition that in my study, the occasional clusters observed in the Saos-2 cell line represent the CD133 positive subset of cells, and by extrapolation, the prominent spheres observed in the other the cell lines also represent the putative CSCs. This hypothesis is further supported by the identification of CD133 positive cells at the centre of the holoclonal colonies in head and neck squamous cell carcinoma cell lines, thus highlighting the holoclonal populations as the CSC population (Harper *et al.*, 2007). However, although CD133 has been shown to identify for the CSC in a number of tumours, recently work on six prostate cancer cell lines showed that CD133 does not identify for the tumour initiating cells. Although colonies of holoclonal, meroclonal and paraclonal morphologies were identified, unlike paraclonal cells which lacked self-renewal ability in standard culture conditions, holoclonal cells were successfully serially passaged. Nevertheless the CD133 positive cells were no more clonogenic and did not form more holoclonal colonies than the CD133 negative subset (Pfeiffer and Schalken, 2009).

Another marker which has been attributed to the holoclonal cells is CD44. CD44 was found to be expressed at higher levels on the holoclonal cells than on the larger paraclonal cells in a breast tumour cell line (MCF7) and squamous cell carcinoma cell line (VB6 subclone of H357 line) (Locke *et al.*, 2005). In carcinoma studies, by serial transplantation in immunocompromised mice, the $CD44^{high}CD24^{low}$ profile has been attributed to the CSC population in breast cancers (Al-Hajj *et al.*, 2003). The question which now remains is whether a similar antigenic profile can be attributed to the subset of cells capable of anchorage-independent growth given that initial surface characterisation of Saos-2 and U-2-OS by Benayahu and colleagues showed positive CD44 expression (Benayahu *et al.*, 2001).

As reported by others, paraclonal colonies in my study showed limited self-renewal ability under standard culture conditions (Locke *et al.*, 2005, Pfeiffer and Schalken, 2009). However, conditioned media of the parent population appeared to support growth of the paraclonal cells. When the HOS cell line was grown as single cell clones by limited dilution, it was possible to derive and expand pure holoclonal (in standard culture media) and paraclonal (in conditioned culture media) populations. This is the first report of colonies of holoclonal and paraclonal morphologies identified in a sarcoma model and successful paraclonal cell expansion in parental cell conditioned media. This dependency of the paraclonal cells on the holoclonal cells was further demonstrated when the HOS cell line was cultured at low density. The migration of paraclonal cells towards holoclonal cells was observed and with time, the paraclonal cells formed a tight boundary around the holoclonal colony. Cancer cell migration has been attributed to response to chemoattractants such as cytokines (Kriebel *et al.*, 2008). The evidence in this study suggests that the holoclonal cells secrete specific cytokines which the paraclonal cells are responsive to and require for proliferation.

The cellular hierarchy established by Mackenzie's group while working on carcinoma cell lines indicate that the holoclonal cells form the CSC population in the tumour as they undergo a series of morphological changes to give rise to intermediate meroclones and terminal paraclones. Based on the pattern of stem cell division and differentiation (Figure 1.6), they concluded that the meroclones are the early amplifying cells while the paraclones are the late amplifying cells (Mackenzie, 2006). The findings in this chapter point towards a transition stage which occurs within the holoclonal colonies, whereby at a specific stage in culture, cells at the periphery of the colony detach, adopt a fibroblastic morphology and appear to migrate away from the main colony. Paraclones have been shown to down-regulate E-cadherin expression (Locke *et al.*, 2005), a profile consistent with aggressive migratory cells of a mesenchymal morphology (Zajchowski *et al.*, 2001). However, the inconsistency lies in the expression of CD44. While the tumour-initiating cells have been associated with a $CD44^{high}$ population consistent with the expression level found in holoclones (Locke *et al.*, 2005), it has been shown that the migratory cells of mesenchymal morphology acquire a $CD44^{high}$ profile upon EMT (Mani *et al.*, 2008). This leads to the hypothesis that the paraclones may actually

represent the migratory cells which lose CD44 expression at the transition stage but are able to re-acquire its expression and other stem cell antigenic profile upon migration to different anatomical locations *in vivo*. Moreover, the CD44 antigen on paraclonal cells is not completely absent but is comparatively lower than on holoclonal cells (Locke *et al.*, 2005), which may lead to the conclusion that CD44 is a modulated antigen on the cell surface and is regulated by systemic cues *in vivo.* While the morphological changes observed point towards a similar identity, further antigenic profiling work is required to conclusively assess the relationship between paraclonal cells and the migratory cells responsible for metastasis.

This study has shown for the first time that osteosarcoma cell lines are comparatively heterogenous. They exhibit varying levels of osteo-inducibility across the different cell lines as well as within an individual cell line. This observation is likely to be due to the variety of genetic mutations accumulated in different osteosarcoma cells therefore giving rise to the cellular heterogeneity within the cell line. Furthermore, the gene expression profile does not correlate with the pattern of mineralisation observed upon osteogenic induction, further highlighting the impact of genetic mutations in osteosarcoma cells. The maintenance of two cellular morphologies within the cell lines *in vitro* suggests that a cellular hierarchy is crucial for the maintenance of the cell population. This study has shown that there is indeed an inter-dependency between the holoclones and the paraclones, although the mediators involved have not yet been identified. Moreover, the EMT-like process observed in the holoclonal-paraclonal transition remains to be confirmed on the basis of antigenic profiles and migration-invasion assays.

Chapter 6

General Discussion, Conclusions and Future Work

6.1 General discussion

This thesis set out to characterise STRO-1 antigen as a marker of multipotency in culture expanded hMSCs. The STRO-1 antigen has previously been established as a marker of multilineage potential in uncultured bone marrow derived hMSCs (Simmons and Torok-Storb, 1991, Pittenger *et al.*, 2000). However, due to the low incidence of hMSC in the bone marrow (0.001 to 0.01 %), there is a need to culture expand those cells before they can be employed as a favoured tool in clinical settings (Gronthos and Simmons, 1996, Habisch *et al.*, 2007). There is a panel of other markers which have been successfully used to identify hMSCs, notably CD271, but to date, they all have been optimised and characterised on freshly isolated bone marrow mononuclear cells (Jones *et al.*, 2002). The aspect that sets STRO-1 apart from the other markers employed until now is the fact that it is expressed heterogeneously on hMSC populations. This has been shown by Gronthos and co-workers (2003) on uncultured bone marrow derived hMSCs and has been re-iterated in my work in section 3.2.1, on culture expanded hMSCs. Furthermore, in my study, this heterogeneous expression of the STRO-1 antigen appeared to be reflected in the uneven differentiation pattern observed in *in vitro* adherent cultures of hMSC upon adipogenic and osteogenic induction (Section 3.2.2). These prime observations formed the basis of the experiments which followed.

In Chapter 3 of this thesis, it was shown that upon expansion of hMSCs in culture, STRO-1 expression was maintained only on a sub-population of cells which retained adipogenic and osteogenic differentiation potential (Figure 3.6). Moreover, the level of STRO-1 expression was found to be modulated at different passage number, a phenomenon which appeared to be donor-dependent and concomitant with a change in cellular morphology (Figure 3.5). As the cells became flatter and larger (a phenotype indicative of senescence), the level of STRO-1 expression decreased. This down-regulation of STRO-1 expression was also concommittant with a reduced adipogenic and osteogenic potential of the total hMSC population, suggesting that STRO-1 antigen can be used as a marker of multipotency (Section 3.4).

Furthermore, a cell population magnetically enriched in STRO-1^{BRIGHT} cells exhibited an enhanced adipogenic and osteogenic potential upon induction compared to the STRO-1 depleted and pre-enriched fractions (Section 3.5). This leads to the assumption that a cellular hierarchy is maintained in bone marrow derived hMSCs whereby cells with a gradient of lineage potential co-exist. This assumption is analogous to the studies carried out in mice bone marrow MSCs, whereby a cellular hierarchy with SSEA-1 (Stage Specific Embryonic Antigen-1) positive cells representing the most primitive cells was established (Anjos-Afonso and Bonnet, 2007). Based on these observations, I speculate that the heterogeneity in differentiation observed in the hMSC populations may be due to a mixed population of cells, some of which are still in the primitive state (multipotential) while others are at different stages of lineage commitment (bipotential or unipotential). Thus, a cellular hierarchy in hMSC population can be proposed based on STRO-1 expression where the highly expressive cells are the multipotent population and the weakly/non-expressive cells are nullipotent (Figure 6.1). This may have important implications in clinical settings, for instance, in orthopaedic applications, whereby a large number of cells with high osteogenic potential are required for transplantation at the site of repair.

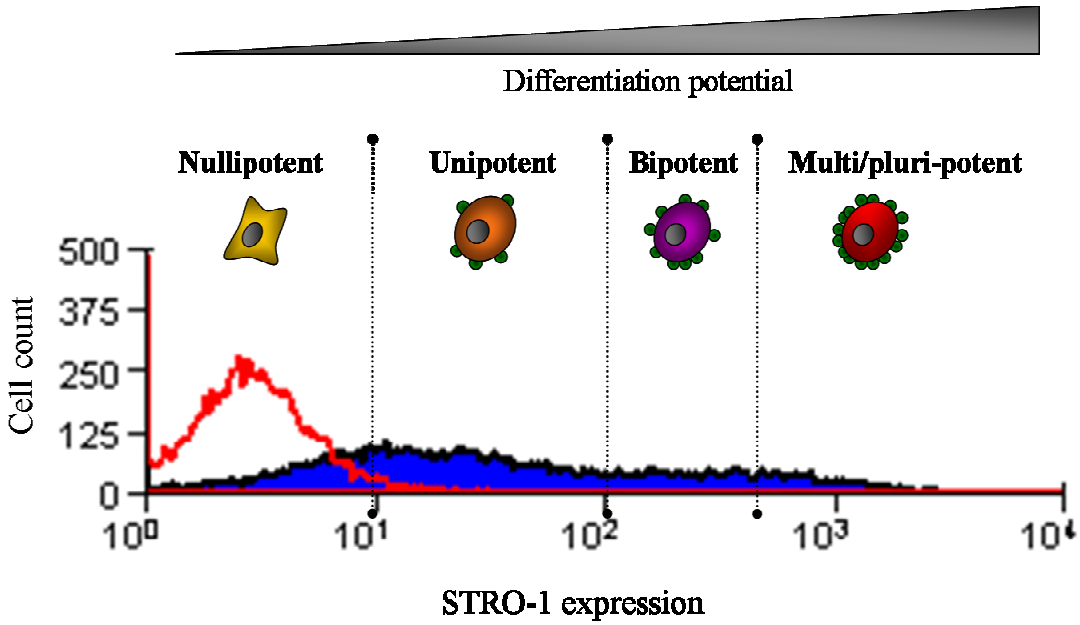

Figure 6.1: Proposed cellular hierarchy of hMSC based on STRO-1 expression. The figure illustrates an overlay analysis of STRO-1/RPE labelled cells (blue shaded histogram) against the secondary control population (red line). Green circles (●) represent STRO-1 antigen molecule on the cell surface. The plastic-adherent hMSCs contain a heterogeneous cell population with a spectrum of potential reflected by the heterogenous STRO-1 expression; the highest STRO-1 expressing cells represent the multi/pluripotent cells while the weakest STRO-1 expressing cells represent the terminally lineage-committed or differentiating cells.

However, if culture expanded hMSCs are to be implemented in the clinic, it is important to consider donor variability in basal STRO-1 level and the extent to which the cells can be expanded so as they retain their hMSC properties. Understanding the ageing effect and fitness of the individual on hMSC is crucial for cell based therapies, especially in autologous transplantation as the elderly people are the primary candidates for hMSC based therapies. It has been recently shown that hMSCs undergo a decline in cell number, expansion and differentiation ability during ageing (Roobrouck *et al.*, 2008, Stolzing *et al.*, 2008). Furthermore, the hMSC pool in disease afflicted individuals may be depleted, for instance in the elderly, inadequate bone marrow hMSC pools is thought to be linked to osteoporosis or metastatic bone diseases (Motaln *et al.*, 2010). The investigation in this thesis showed a relationship between the decrease in expansion potential of hMSCs and loss of STRO-1 expression (Section 3.4). The explanations supporting this observation may be due to out-growth of fast proliferative contaminating fibroblasts. In relation to STRO-1 expression, this observation suggests that the STRO-1

antigen may act as a determinant of self-renewal capacity. While these data are not sufficient to infer STRO-1 as a marker of expansion potential, it will be of interest to thoroughly investigate this hypothesis in future experimental designs. Clonal isolation of STRO-1^{BRIGHT} cells from a wider range of donors of varying age groups could be monitored for their expansion potential and tri-lineage differentiation potential. The outcome of this may further support STRO-1 as a biomarker of multipotent hMSCs.

In Chapter 3, the expression of STRO-1 during the processes of differentiation was investigated and it was found that the level of STRO-1 expression was not constant at induction and during lineage commitment (Section 3.7). Although it can be argued that the overall down-regulation of STRO-1 observed in this setting was due to the extended time in culture (time taken for differentiation to occur), the degree of down-regulation during differentiation was more pronounced than that observed in the control uninduced populations which were in parallel culture for the same period. The down-regulation in the control populations was indeed analogous to that observed in the adherent hMSC populations at seven and fourteen days post-confluency (Section 3.6), suggesting that there may be an auto-inhibitory mechanism of STRO-1 antigen mediated by cell-to-cell contact. Furthermore, the pattern of down-regulation observed during adipogenesis was different to that observed during osteogenesis, further implying STRO-1 as a marker of differentiation (Section 3.7).

The proposed model is based on the hypothesis that the level of STRO-1 antigen expression confers differentiation potential. Therefore depending on the degree of STRO-1 positivity (low or high), the cells have the ability to differentiate to either the adipogenic or osteogenic lineage or both. However, the route the cell takes during commitment is dependent on the lineage to which it is induced as specific transcription factors are involved in each lineage. From the results in Chapter 3, commitment to the adipogenic lineage follows a different STRO-1 expression pattern to that observed upon commitment to the osteogenic lineage. The main difference pertaining to these two *in vitro* assays is the length of time the cells take to undergo differentiation to their specific lineages. Osteogenesis is a process which takes place over twenty-one days while adipogenesis takes place over eight days. Osteogenesis followed a transient up-

regulation of STRO-1 at the early stages of commitment, which is gradually lost as the induced cells progress towards maturation. Given the experimental design of my experiments, relative to osteogenesis, the immediate stages of commitment to adipogenesis were not captured. Therefore, any possible transient up-regulation of STRO-1 expression during the early stages of adipogenic commitment analogous to osteogenic commitment may not have been recorded. To elucidate this possibility, future experiments should focus on the immediate effects of adipogenic induction on STRO-1 expression, for instance analysis of populations on a two-hourly basis post-induction. Based on the behaviour of STRO-1 antigen observed during differentiation, it can be speculated that STRO-1 is a transmembrane protein (for example, a receptor) which translates external stimuli to the cytosol, thus activating the downstream signalling cascades, such as the Notch or Wnt signalling pathways, known to be involved in fate determination of hMSC (Vujovic *et al.*, 2007, Etheridge *et al.*, 2004). On initial stimulation, the cells up-regulate STRO-1 expression to indicate induction which occurs prior to lineage commitment. As commitment progresses, the cells down-regulate STRO-1 expression which is ultimately lost once the cells become fully differentiated.

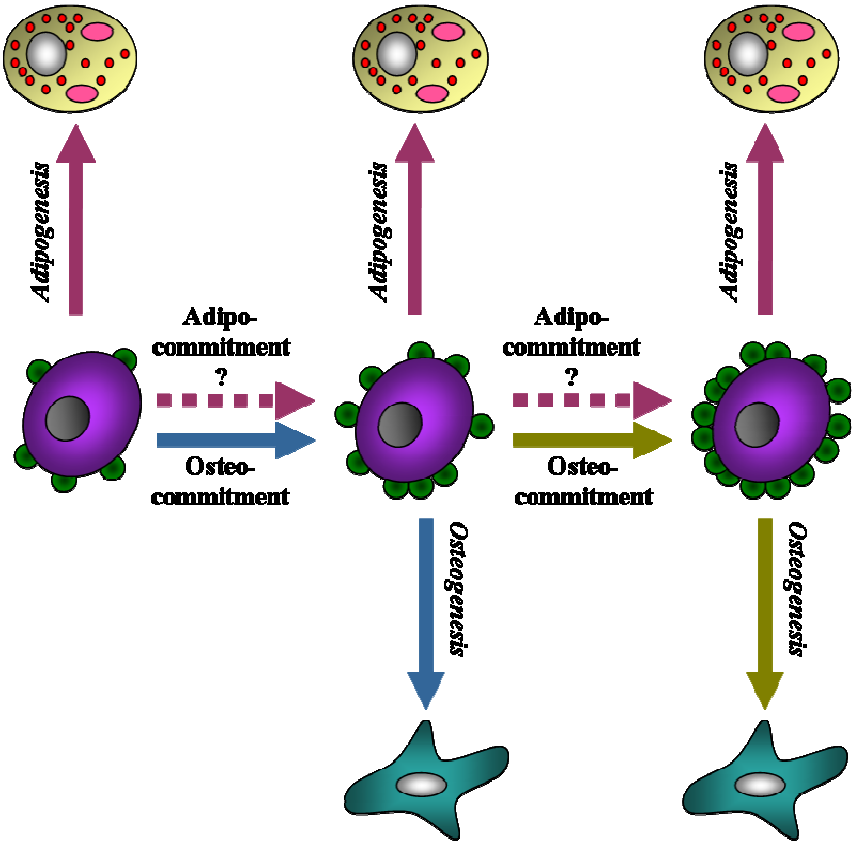

Figure 6.2: Modulation of STRO-1 expression at lineage commitment. Green circles (●) represent STRO-1 antigen molecule on the cell surface. A basal level of STRO-1 expression is required for differentiation to occur. During osteogenesis (blue and green arrows), cells expressing STRO-1 weakly (blue arrow) or strongly (green arrow) are responsive to osteo-inductive stimuli and during the initial commitment stage the cells up-regulate their STRO-1 expression. Upon terminal osteogenic differentiation, STRO-1 expression is lost while the osteo-progenitors mature to fully functional osteoblasts. During adipogenesis (pink arrows), cells expressing STRO-1 are responsive to adipo-inductive stimuli and commit to the adipogenic lineage. The adipogenic commitment pathway is rapid as compared to the osteogenic pathway, and the intermediate up-regulation of STRO-1 as observed during osteogenesis has not been elucidated (pink dashed arrow). Upon adipocyte maturation, STRO-1 expression is quickly lost as the cells accumulate lipid vacuoles.

As illustrated and explained in Chapter 3 and sections above, the STRO-1 antigen appears to have a defined role in hMSC differentiation potential. Identifying the nature of this antigen may reveal its mechanism of action and its potential links with the intracellular pathways of differentiation and the way it affects some key regulators of differentiation such as *PPARγ* in adipogenesis and *Cbfa-1* in osteogenesis (Muruganandan *et al.*, 2009). The first approach to identify the STRO-1 epitope in this

thesis was phage display technology which yielded no promising results, mainly due to the nature of the STRO-1 antibody. This further emphasises the need to elucidate the identity of the antigen, so that novel antibodies of higher affinity can be generated against the putative marker of multipotency, STRO-1. In an attempt to determine the nature of STRO-1 antigen, a gene expression microarray analysis was implemented to compare the STRO-1 expression profiles of seven different osteosarcoma cell lines and hMSC populations. However, before this analysis could be undertaken, it is to be noted that a stringent and thoroughly optimised screening procedure had to be implemented.

First and foremost, the source of STRO-1 antibody and the maintenance of its molecular integrity upon storage had to be validated as, to date, there is no consistent protocol in the literature documenting the use of the antibody as a selective marker, may it be on hMSCs or osteosarcoma cells. In this study, the use of STRO-1 was optimised and the variability in binding efficiency at different storage conditions of resuspended lyophilised and hybridoma culture supernatant of the antibody was demonstrated. In addition to its low binding affinity, the molecular integrity of the STRO-1 IgM antibody was further affected by storage conditions (Section 3.3). The yield of antibody in hybridoma supernatant is batch dependent and thus a lack of quality control at this level may result in weak detection of STRO-1 expression on cell populations. Furthermore, confocal microscopy analysis showed that STRO-1 is also expressed intra-cellularly (Figure 4.11), implying that cells with a compromised membrane may incorporate the antibody inside their cytoplasm and show up as false positives upon flow cytometry analysis. Indeed that was the case when osteosarcoma cell lines, which potentially harboured rare surface expressing STRO-1 positive cells, were profiled without a dead cell exclusion assay (Section 4.7). Therefore, when screening for rare STRO-1 positive cells by flow cytometry, it is important to discriminate between live and dead cells and without a robust dead cell exclusion method, the proportion of positive to negative cells is inaccurate. This is particularly important when identifying rare CSCs in cancer cell lines. When profiling hMSCs, dead cell exclusion is important but need not be carried out simultaneously with STRO-1 staining (dual staining) as the STRO-1 expression levels are high and heterogeneous in hMSCs. Therefore, in my work (Chapter 3), an hMSC population stained solely with PI was included in every experiment and gates

were drawn to exclude PI positive cells (dead cells) to define the flow cytometry protocol. As such, the marker profile of osteosarcoma cell lines illustrated in my study whereby a robust dead cell exclusion procedure was implemented, did not necessarily reflect the profile reported by others; one such example is the expression of CD133 on MG-63, Saos-2 and U-2-OS cell lines which differs from that reported by Tirino and colleagues (2008). Therefore, when screening for surface antigens, especially in comparative studies to identify rare cell populations, it is crucial to undertake a dead cell exclusion assay in order to obtain reliable and reproducible data.

The flow cytometry scores obtained for STRO-1 expression on the different osteosarcoma cell lines was matched to their respective gene expression microarray profiles to identify potential candidate genes encoding STRO-1 antigen. The list obtained was narrowed down to eight potential candidates whose products are expressed on the plasma membrane. Out of those eight candidates, one particular candidate, ARHGEF4, displayed an expression pattern similar to that observed by STRO-1 antigen. More precisely, is it expressed on plasma membrane, cell projections as well as in the cytoplasm. There is no reports of its link to fate determination of stem cells, but has been implicated in cytoskeleton rearrangement and cellular morphology. Co-localisation studies of this antigen with STRO-1 antigen will help to reveal whether the two antigens are one and the same. Further confirmation may be obtained from knock-in and knock-out experiments of candidate genes to determine the identity and function of STRO-1 antigen. The two other promising candidates are P2RY6 (bone formation) and TNFSF11 (bone resorption) which are involved in bone remodelling although the lineage in which they exert their functions is totally different.

The high expression of STRO-1 by the MG-63 cell line in my study led to the investigation of potential stem cell characteristics which may have been maintained by the tumour cells (Section 4.8). This follows from the report by Gibbs and colleagues (2005) which showed that a subset of cells in freshly derived osteosarcoma cell lines exhibited STRO-1 expression and was associated with sarcosphere formation and differentiation potential suggesting the maintenance of MSC-like cells in osteosarcoma. As such, this study is the first to present a full comparative analysis of seven osteosarcoma cell lines (143B, CAL72, G-292, HOS, MG-63, Saos-2 and U-2-OS) in terms of their marker phenotype, molecular profile, cellular morphology and differentiation potential.

STRO-1 expression was retained to different levels in some of the osteosarcoma cell lines, however, unlike hMSCs this did not reflect MSC multilineage potential. Similarly, upon osteogenic induction, the expression of the key osteogenic genes did not reflect the osteogenic differentiation potential of the cell lines. This discrepancy may be due to the variety of mutations accumulated over time in different tumours, resulting in maturation arrest. A mutation in any of the osteogenic transcription factors (illustrated in Figure 1.3) may also lead to maturation arrest, depicting heterogeneity in different tumours. More recently, over-expression of mitotic arrest defective protein 2 (MAD2) was associated with osteosarcoma of lower differentiation and higher clinical stage (Yu *et al.*, 2010). Similarly, depending on the stage of maturation at which the cell was at before it acquired tumorigenic mutations, certain stem cell characteristics were retained, such as STRO-1 expression and osteo-inducibility. This observation suggests that osteosarcoma may be a disease of dis-regulated differentiation caused by MSC transformation, although this theory remains to be proven.

The heterogeneity in osteogenic differentiation potential of osteosarcoma cell lines led to a proposed model characterising the different cell lines with an association to their STRO-1 status. Depending on the nature and extent of the mutations, some cell lines (MG-63, CAL72 and 143B) remained non-inducible as they could not be stimulated to further differentiate. On the other hand, some cell lines (G-292, U-2-OS, HOS and Saos-2) retained the ability to mature, although the extent of differentiation was variable

depending on the stage at which maturation arrest occurred. Interestingly, the stage at which each category of cell lines (inducible and non-inducible) was arrested represents the level of STRO-1 expression observed (Section 5.2.3). The further down the osteoblastic lineage, the lower the level of STRO-1 expression. This proposed model reflects the heterogeneity of the tumours observed among osteosarcoma patients and highlights the difficulty in developing reliable prognostic markers of the disease.

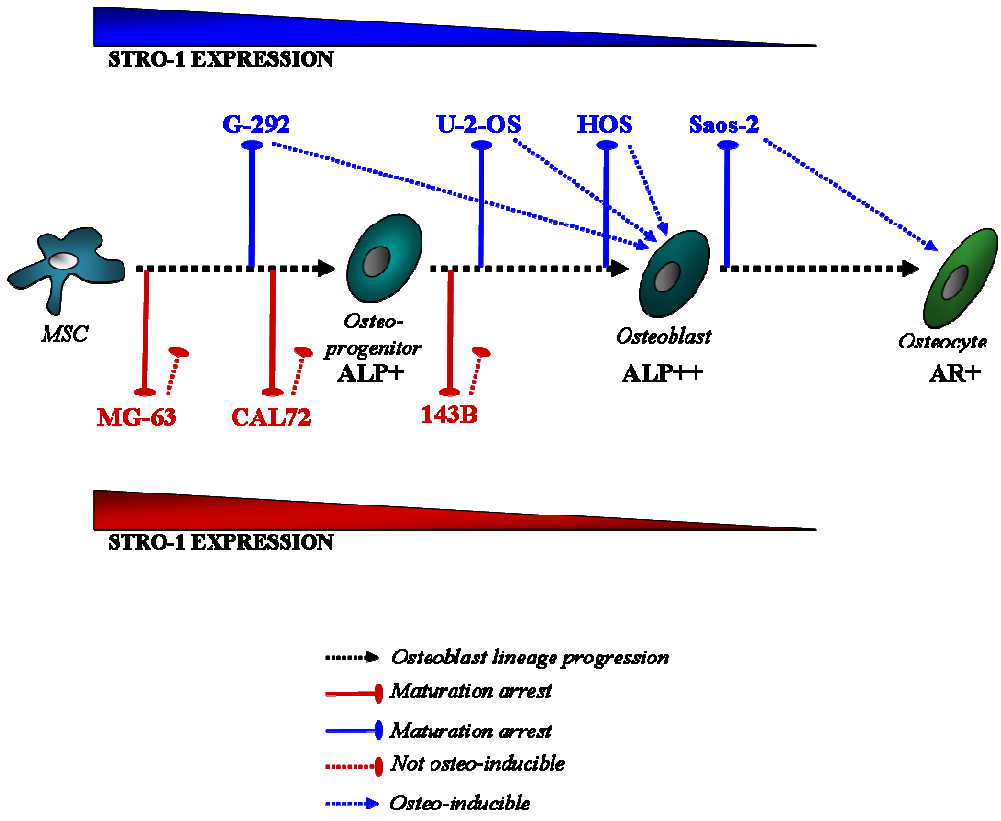

Figure 6.3: Proposed model characterising the osteosarcoma cell lines. The heterogeneity among osteosarcoma cell lines is due to different stages of maturation arrest. The osteoblast lineage follows initial commitment of MSC to osteo-progenitors which are weakly ALP positive. As the progenitor cell differentiates to functional osteoblast, the level of ALP activity increases and further maturation results in mineralising AR positive cell osteocyte. Osteosarcoma arises when the cells accumulate mutations during the differentiation process and are able to exit the lineage at any stage, thus resulting in varying levels of differentiated tumours. In blue are cell lines which are osteo-inducible and in red are cell lines which are not inducible.

The poor prognosis in osteosarcoma patients has been attributed to a lack of reliable early prognostic factors and high metastatic potential of the tumours. In Chapter 4, the level of CD13 expression was higher in the cell lines bearing a dominant fibroblastic morphology (Table 6.1). These cell lines, specifically G-292 and MG-63, exhibited prominent anchorage independent growth potential as illustrated in Section 5.3.2. On the basis of these observations, CD13 appeared to be an interesting molecule which could be further exploited as a prognostic marker for aggressive sarcomas. This speculation is based on a number of studies reporting the pathological significance of CD13 in carcinomas including pancreatic (Ikeda *et al.*, 2003) and gastric (Kawamura *et al.*, 2007). It has also been shown that CD13 positive tumour cells have migratory properties and are able to degrade extracellular matrix, both of which are invasive characteristics of metastatic cells (Saiki *et al.*, 1993). Moreover, CD13 has been shown to be associated with the process of epithelial to mesenchymal transition (EMT) in normal human dermal fibroblasts (Sorrell *et al.*, 2003), a process which has also been associated with the invasive properties of CSCs in breast cancer cell lines (Section 1.5.4).

While immunophenotyping the seven osteosarcoma cell lines, it was interesting to note that the pre-dominating fibroblastic morphology of the cell line was concomitant with an elevated expression of CD13 (G-292 and MG-63). Mixed populations (143B and HOS) exhibited intermediate levels of CD13 and those with a pre-dominating epithelial morphology (CAL72, Saos-2 and U-2-OS) were CD13 negative (Table 6.1). Whether the CD13 expression in those cell lines represents an EMT phenomenon remains to be confirmed, possibly by investigating EMT related genes such as Twist or Snail (Figure 1.5) in future experiments. Regarding mesenchymal tumours, the metastatic potential of CD13 positive cells has not yet been investigated and should therefore be the focus of future studies when trying to identify prognostic markers of osteosarcoma. Recent advances in anti-cancer therapies are focussing on CD13 inhibitors in the hope of preventing metastasis in carcinomas (Zhang and Xu, 2008) and defining CD13 as a prognostic marker of metastatic osteosarcoma may benefit from those inhibitors of EMT.

Cell line	Dominating phenotype	CD13 expression
143B	Mixed	9.52
CAL72	Epithelial	0
G-292	Fibroblastic	30.48
HOS	Mixed	12.91
MG-63	Fibroblastic	43.86
Saos-2	Epithelial	0.2
U-2-OS	Epithelial	0

Table 6.1: CD13 as a potential prognostic marker in osteosarcoma. The values represent the mean difference in fluorescence, determined by flow cytometry (Section 2.5), between CD13 labelled samples and control unstained samples. CD13 expression reflects a dominating fibroblastic morphology (in red) which may be indicative of cancers of a more aggressive nature.

The cellular heterogeneity within osteosarcoma cell lines was first identified by the uneven osteo-inducibility of the G-292, U-2-OS and HOS cell lines but was found to be a common feature of all osteosarcoma cell lines studied by observing distinct morphologically different sub-populations of cells when cultured at low density (Section 5.4). The formation of cells of holoclonal and paraclonal morphology indicates the existence of a cellular hierarchy within osteosarcoma cell lines which is probably present in tumours and subsequently maintained in culture. The generation of paraclonal cells in a sarcoma cell line by EMT has not been proven yet. However, this study is the first to demonstrate the presence of a cellular hierarchy in osteosarcoma cell lines and the transition of paraclonal cells from holoclonal colonies, hypothesising the holoclonal cells as the putative CSCs in osteosarcoma. In order to present the holoclonal cells as the target for chemotherapy, they have to be further characterised and their CSC properties proven both *in vitro* and *in vivo.*

To achieve this, the next step in this study would be to characterise the antigenic profile, especially in terms of CD44 expression of the holoclones and the paraclones in order to establish their CSC identity. CD44 has been shown to be a key molecule that is regulated between the holoclonal and paraclonal cells in carcinoma cell lines, and a $CD44^{high}$ profile has been attributed to the holoclonal cells. In accordance with other studies, it is of interest to investigate the CD44 status of the holoclonal and paraclonal

cells in the seven established osteosarcoma cell lines and possibly in freshly derived osteosarcoma cell lines as well. It is also important to investigate other markers associated with CSCs, such as ALDH and the ability of cells to pump out cytotoxic drugs (Side Population characterised by expression of ABC membrane transporters) (Section 1.5.3). *In vitro* tumour formation assays such as sarcosphere formation in serum starved suspension cultures will need to be implemented once putative CSCs are identified in the osteosarcoma cell lines. *In vivo* assays of tumour formation may also be studied by serial transplantation of the holoclonal cells in animal models, although robust *in vivo* models of osteosarcoma are yet to be achieved (Tirino *et al.*, 2008).

The dependency of the paraclonal cells on the holoclonal cells in the HOS cell line has been demonstrated *in vitro* by the conditioned media culture systems (Section 5.4.1). This phenomenon remains to be confirmed in the other osteosarcoma cell lines and perhaps in other cancer cell lines as well. The most intriguing and interesting aspect of this study would be to identify the cytokines responsible for this dependency. Paraclonal cells exhibit tropism towards the holoclonal colony and this has been illustrated by phase contrast micrographs in this thesis. An interesting approach would be to test the migration of paraclonal cells using a live imaging system. The holoclonal or paraclonal cells can be transfected to express GFP for instance, and the two cell morphologies can be monitored in real time. In addition, the release of known cytokines involved in cancer metastasis (for example, CCL5) can be investigated. Presumably a similar cytokine, if not the same, may be responsible for this paraclonal migration phenomenon. Identifying the nature of this cytokine will help to understand the cause of metastasis and may help tailor therapies to prevent cancer dissemination.

On the basis of these preliminary observations, and combined studies reported in the literature on carcinoma cell lines, I propose a cellular hierarchy in osteosarcoma cell lines whereby the holoclonal cells represent the putative CSCs. This hierarchy is brought about by EMT which mediates metastasis and MET at the site of secondary tumour formation *in vivo* (Figure 6.4). MET has not been observed *in vitro* in this thesis, neither has it been reported in the literature. This may be due to the lack of stimuli inducing MET or perhaps in a culture environment, EMT inducing stimuli are maintained. Furthermore, EMT is part of a process whereby migratory cells home to secondary anatomical sites which are conducive to their growth (by providing the right micro-environment in terms of structural or/and hormonal support). The cells are then able to seed new tumours by undergoing MET and aberrant proliferation, most likely to be driven by the putative holoclonal CSCs. The lack of such a nourishing secondary site in a culture system may potentially explain why MET is not observed *in vitro*. Developing chemotherapeutic agents to target the holoclonal cells may provide a means to better manage osteosarcoma and extend life expectancy of patients.

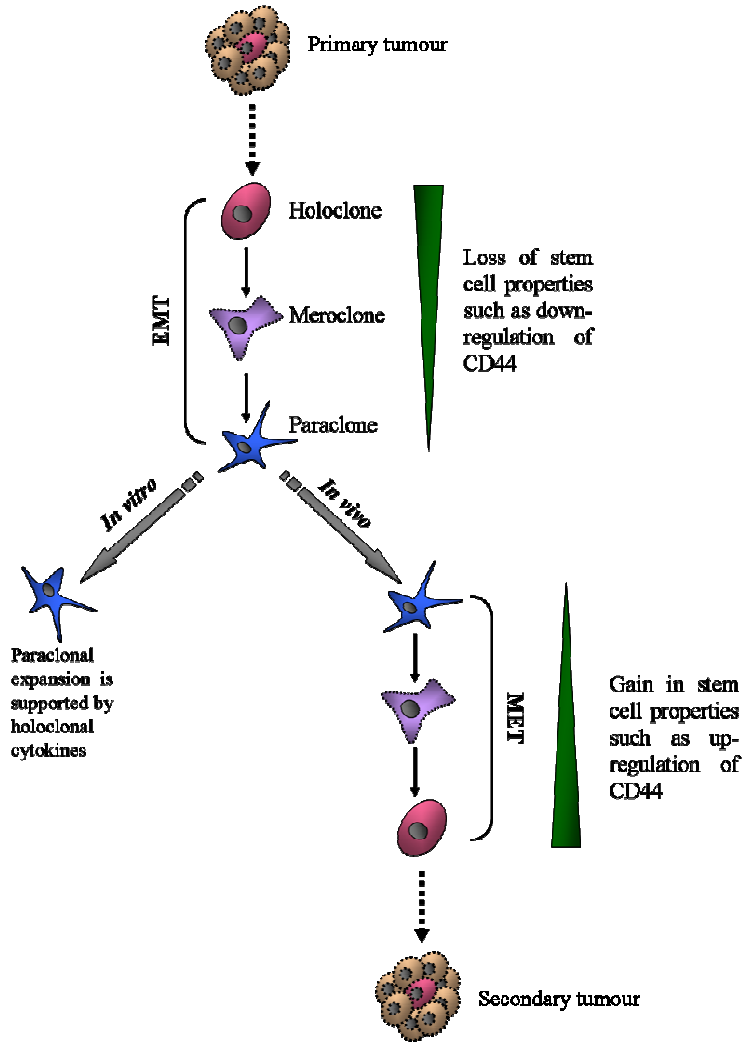

Figure 6.4: Proposed cellular hierarchy in osteosarcoma. The primary tumour is a heterogeneous cell mass in which rare CSCs reside (cell shaded pink). This cellular heterogeneity is maintained in culture and three cell types forming a cellular hierarchy are present; adherent epithelial-like holoclones, intermediate meroclones and migratory paraclones. The holoclones represent the putative CSCs which can give rise to intermediate meroclones and migratory paraclones by EMT, a process accompanied by a loss in stem cell properties, such as down-regulation of CD44 expression. *In vivo* the paraclonal cells are potentially able to enter the blood stream or lymphatic system, survive and home to distant sites (metastasis), where they undergo MET, a process accompanied by a gain in stem cell properties, for instance up-regulation of CD44 expression. MET generates cells with stem cell properties (holoclonal CSCs) which have the potential to spawn secondary tumours. *In vitro,* paraclonal cells are dependent on holoclonal secretory factors to survive and expand.

The proposed metastatic abilities of paraclonal cells have not been established yet. A very interesting experiment that needs to be undertaken is the evaluation of the migratory and invasive properties of the paraclonal cells as compared to the holoclonal cells. *In vitro* assays subsequently remain to be confirmed by *in vivo* studies. In order to confirm that holoclonal cells are the CSCs, pure holoclonal cells have to be xenotransplanted into nude mice, tumour formation evaluated and the cells should be able to be serially transplanted *in vivo* and seed new tumours. Unless this gold standard of CSC assay is achieved, the holoclonal cells can only be hypothesised as being the CSC population in osteosarcoma.

6.2 Conclusions

Hence, to conclude, the study described in this thesis resulted in the following main novel observations:

- STRO-1 antigen is a biomarker of the multipotent subset of adherent cultured hMSCs and is modulated upon different culture conditions.
- STRO-1 antigen is down-regulated in a temporal manner during adipogenic and osteogenic differentiation.
- STRO-1 antigen is localised intra-cellularly and on the cell surface with the identification of surface expressing rare cell populations requiring stringent screening procedure such as optimal antibody staining conditions to retain antibody integrity and dead cell discrimination to exclude false positives.
- The identity of STRO-1 antigen has been narrowed down to eight potential candidate genes, of which ARHGEF4 appears to exhibit similar sub-cellular localisation to the STRO-1 antigen.
- Osteosarcoma cell lines exhibit cellular heterogeneity as demonstrated by varied antigenic profiles, different levels of osteo-inducibility and expression of osteogenic markers.
- Cellular hierarchy is maintained in osteosarcoma cell lines *in vitro*; retention of intrinsic stem cell patterns illustrated by holoclonal colonies may represent the putative CSCs in osteosarcoma.
- Paraclonal cells are migratory and their *in vitro* expansion is dependent on holoclone-derived factors.

To summarise, the study represented in this thesis has firstly contributed towards the potential applications of hMSC in the regenerative field and secondly opened up avenues for anti-cancer therapies by exploring the presence of putative CSCs in osteosarcoma cell lines.

6.3 Future Work

In summary, future directions of this thesis should focus on the following main aspects:

- Co-localisation studies of the expression of potential candidate genes of STRO-1
- On identification of the potential STRO-1 gene, the identity of STRO-1 can be confirmed by ectopic expression of the antigen in fibroblasts (STRO-1 negative cell line)
- Expression of accepted CSC markers such as CD133 and CD44 on holoclones and paraclones to establish the putative CSC population in osteosarcoma
- Migration and invasion assays to confirm proposed migratory properties of paraclones
- Time-lapsed photography to establish the dependency of paraclones on holoclones and identify factors responsible for this dependency

References

AGGARWAL, S. & PITTENGER, M. F. (2005) Human mesenchymal stem cells modulate allogeneic immune cell responses. *Blood,* 105**,** 1815-22.

AL-HAJJ, M. & CLARKE, M. F. (2004) Self-renewal and solid tumor stem cells. *Oncogene,* 23**,** 7274-82.

AL-HAJJ, M., WICHA, M. S., BENITO-HERNANDEZ, A., MORRISON, S. J. & CLARKE, M. F. (2003) Prospective identification of tumorigenic breast cancer cells. *Proc Natl Acad Sci U S A,* 100**,** 3983-8.

ALISON, M. R., BRITTAN, M., LOVELL, M. J. & WRIGHT, N. A. (2006a) Markers of adult tissue-based stem cells. *Handb Exp Pharmacol***,** 185-227.

ALISON, M. R. & ISLAM, S. (2009) Attributes of adult stem cells. *J Pathol,* 217**,** 144-60.

ALISON, M. R., POULSOM, R., BRITTAN, M., SCHIER, S., BURKERT, J. & WRIGHT, N. A. (2006b) Isolation of gut SP cells does not automatically enrich for stem cells. *Gastroenterology,* 130**,** 1012-3; author reply 1013-4.

ANDREEVA, E. R., PUGACH, I. M., GORDON, D. & OREKHOV, A. N. (1998) Continuous subendothelial network formed by pericyte-like cells in human vascular bed. *Tissue Cell,* 30**,** 127-35.

ANGEL, P. & KARIN, M. (1991) The role of Jun, Fos and the AP-1 complex in cell-proliferation and transformation. *Biochim Biophys Acta,* 1072**,** 129-57.

ANJOS-AFONSO, F. & BONNET, D. (2007) Nonhematopoietic/endothelial SSEA-1+ cells define the most primitive progenitors in the adult murine bone marrow mesenchymal compartment. *Blood,* 109**,** 1298-306.

ASAHARA, T., MASUDA, H., TAKAHASHI, T., KALKA, C., PASTORE, C., SILVER, M., KEARNE, M., MAGNER, M. & ISNER, J. M. (1999) Bone marrow origin of endothelial progenitor cells responsible for postnatal vasculogenesis in physiological and pathological neovascularization. *Circ Res,* 85**,** 221-8.

ASAHARA, T., MUROHARA, T., SULLIVAN, A., SILVER, M., VAN DER ZEE, R., LI, T., WITZENBICHLER, B., SCHATTEMAN, G. & ISNER, J. M. (1997) Isolation of putative progenitor endothelial cells for angiogenesis. *Science,* 275**,** 964-7.

BAGULEY, B. C. (2010) Multidrug resistance in cancer. *Methods Mol Biol,* 596**,** 1-14.

BALL, S. G., SHUTTLEWORTH, A. C. & KIELTY, C. M. (2004) Direct cell contact influences bone marrow mesenchymal stem cell fate. *Int J Biochem Cell Biol,* 36**,** 714-27.

BANERJEE, C., MCCABE, L. R., CHOI, J. Y., HIEBERT, S. W., STEIN, J. L., STEIN, G. S. & LIAN, J. B. (1997) Runt homology domain proteins in osteoblast differentiation: AML3/CBFA1 is a major component of a bone-specific complex. *J Cell Biochem,* 66**,** 1-8.

BARRANDON, Y. & GREEN, H. (1987) Three clonal types of keratinocyte with different capacities for multiplication. *Proc Natl Acad Sci U S A,* 84**,** 2302-6.

BARRAUD, P., STOTT, S., MOLLGARD, K., PARMAR, M. & BJORKLUND, A. (2007) In vitro characterization of a human neural progenitor cell coexpressing SSEA4 and CD133. *J Neurosci Res,* 85**,** 250-9.

BARRY, F., BOYNTON, R., MURPHY, M., HAYNESWORTH, S. & ZAIA, J. (2001) The SH-3 and SH-4 antibodies recognize distinct epitopes on CD73 from human mesenchymal stem cells. *Biochem Biophys Res Commun,* 289**,** 519-24.

BEATO, M., HERRLICH, P. & SCHUTZ, G. (1995) Steroid hormone receptors: many actors in search of a plot. *Cell,* 83**,** 851-7.

BELEMA-BEDADA, F., UCHIDA, S., MARTIRE, A., KOSTIN, S. & BRAUN, T. (2008) Efficient homing of multipotent adult mesenchymal stem cells depends on FROUNT-mediated clustering of CCR2. *Cell Stem Cell,* 2**,** 566-75.

BENAYAHU, D., SHUR, I., MAROM, R., MELLER, I. & ISSAKOV, J. (2001) Cellular and molecular properties associated with osteosarcoma cells. *J Cell Biochem,* 84**,** 108-14.

BIALEK, P., KERN, B., YANG, X., SCHROCK, M., SOSIC, D., HONG, N., WU, H., YU, K., ORNITZ, D. M., OLSON, E. N., JUSTICE, M. J. & KARSENTY, G. (2004) A twist code determines the onset of osteoblast differentiation. *Dev Cell,* 6**,** 423-35.

BIELBY, R., JONES, E. & MCGONAGLE, D. (2007) The role of mesenchymal stem cells in maintenance and repair of bone. *Injury,* 38 Suppl 1**,** S26-32.

BOGENMANN, E., MOGHADAM, H., DECLERCK, Y. A. & MOCK, A. (1987) c-myc amplification and expression in newly established human osteosarcoma cell lines. *Cancer Res,* 47**,** 3808-14.

BOIRET, N., RAPATEL, C., VEYRAT-MASSON, R., GUILLOUARD, L., GUERIN, J. J., PIGEON, P., DESCAMPS, S., BOISGARD, S. & BERGER, M. G. (2005) Characterization of nonexpanded mesenchymal progenitor cells from normal adult human bone marrow. *Exp Hematol,* 33**,** 219-25.

BONNET, D. (2003) Biology of human bone marrow stem cells. *Clin Exp Med,* 3**,** 140-9.

BRAHMS, S. & BRAHMS, J. (1980) Determination of protein secondary structure in solution by vacuum ultraviolet circular dichroism. *J Mol Biol,* 138**,** 149-78.

BRAZELTON, T. R., ROSSI, F. M., KESHET, G. I. & BLAU, H. M. (2000) From marrow to brain: expression of neuronal phenotypes in adult mice. *Science,* 290**,** 1775-9.

BROOKE, G., COOK, M., BLAIR, C., HAN, R., HEAZLEWOOD, C., JONES, B., KAMBOURIS, M., KOLLAR, K., MCTAGGART, S., PELEKANOS, R., RICE, A., ROSSETTI, T. & ATKINSON, K. (2007) Therapeutic applications of mesenchymal stromal cells. *Semin Cell Dev Biol,* 18**,** 846-58.

BRUCE, W. R. & VAN DER GAAG, H. (1963) A Quantitative Assay for the Number of Murine Lymphoma Cells Capable of Proliferation in Vivo. *Nature,* 199**,** 79-80.

BRULAND, O. S. & PIHL, A. (1997) On the current management of osteosarcoma. A critical evaluation and a proposal for a modified treatment strategy. *Eur J Cancer,* 33**,** 1725-31.

BRUNO, S., BUSSOLATI, B., GRANGE, C., COLLINO, F., GRAZIANO, M. E., FERRANDO, U. & CAMUSSI, G. (2006) CD133+ renal progenitor cells contribute to tumor angiogenesis. *Am J Pathol,* 169**,** 2223-35.

BUHRING, H. J., TREML, S., CERABONA, F., DE ZWART, P., KANZ, L. & SOBIESIAK, M. (2009) Phenotypic characterization of distinct human bone marrow-derived MSC subsets. *Ann N Y Acad Sci,* 1176**,** 124-34.

BURDALL, S. E., HANBY, A. M., LANSDOWN, M. R. & SPEIRS, V. (2003) Breast cancer cell lines: friend or foe? *Breast Cancer Res,* 5**,** 89-95.

BUSSOLATI, B., BRUNO, S., GRANGE, C., BUTTIGLIERI, S., DEREGIBUS, M. C., CANTINO, D. & CAMUSSI, G. (2005) Isolation of renal progenitor cells from adult human kidney. *Am J Pathol,* 166**,** 545-55.

CABILLY, S. (1999) The basic structure of filamentous phage and its use in the display of combinatorial peptide libraries. *Mol Biotechnol,* 12**,** 143-8.

CAMPIONI, D., LANZA, F., MORETTI, S., DOMINICI, M., PUNTURIERI, M., PAULI, S., HOFMANN, T., HORWITZ, E. & CASTOLDI, G. L. (2003) Functional and immunophenotypic characteristics of isolated CD105(+) and fibroblast(+) stromal cells from AML: implications for their plasticity along endothelial lineage. *Cytotherapy,* 5**,** 66-79.

CAPLAN, A. I. (1991) Mesenchymal stem cells. *J Orthop Res,* 9**,** 641-50.

CAPLAN, A. I. & BRUDER, S. P. (2001) Mesenchymal stem cells: building blocks for molecular medicine in the 21st century. *Trends in Molecular Medicine,* 7**,** 259-264.

CARMEN, S. & JERMUTUS, L. (2002) Concepts in antibody phage display. *Brief Funct Genomic Proteomic,* 1**,** 189-203.

CHANG, F., ISHII, T., YANAI, T., MISHIMA, H., AKAOGI, H., OGAWA, T. & OCHIAI, N. (2008) Repair of large full-thickness articular cartilage defects by transplantation of autologous uncultured bone-marrow-derived mononuclear cells. *J Orthop Res,* 26**,** 18-26.

CHANG, S. C., CHUANG, H., CHEN, Y. R., YANG, L. C., CHEN, J. K., MARDINI, S., CHUNG, H. Y., LU, Y. L., MA, W. C. & LOU, J. (2004) Cranial repair using BMP-2 gene engineered bone marrow stromal cells. *J Surg Res,* 119**,** 85-91.

CHEN, D., ZHAO, M. & MUNDY, G. R. (2004) Bone morphogenetic proteins. *Growth Factors,* 22**,** 233-41.

CHEN, X. D. (2010) Extracellular matrix provides an optimal niche for the maintenance and propagation of mesenchymal stem cells. *Birth Defects Res C Embryo Today,* 90**,** 45-54.

CLARKE, M. F., DICK, J. E., DIRKS, P. B., EAVES, C. J., JAMIESON, C. H., JONES, D. L., VISVADER, J., WEISSMAN, I. L. & WAHL, G. M. (2006) Cancer stem cells--perspectives on current status and future directions: AACR Workshop on cancer stem cells. *Cancer Res,* 66**,** 9339-44.

COIPEAU, P., ROSSET, P., LANGONNE, A., GAILLARD, J., DELORME, B., RICO, A., DOMENECH, J., CHARBORD, P. & SENSEBE, L. (2009) Impaired differentiation potential of human trabecular bone mesenchymal stromal cells from elderly patients. *Cytotherapy,* 11**,** 584-94.

COLLINS, A. T., BERRY, P. A., HYDE, C., STOWER, M. J. & MAITLAND, N. J. (2005) Prospective identification of tumorigenic prostate cancer stem cells. *Cancer Res,* 65**,** 10946-51.

COLTER, D. C., CLASS, R., DIGIROLAMO, C. M. & PROCKOP, D. J. (2000) Rapid expansion of recycling stem cells in cultures of plastic-adherent cells from human bone marrow. *Proc Natl Acad Sci U S A,* 97**,** 3213-8.

COLTER, D. C., SEKIYA, I. & PROCKOP, D. J. (2001) Identification of a subpopulation of rapidly self-renewing and multipotential adult stem cells in colonies of human marrow stromal cells. *Proc Natl Acad Sci U S A,* 98**,** 7841-5.

CONGET, P. A. & MINGUELL, J. J. (1999) Phenotypical and functional properties of human bone marrow mesenchymal progenitor cells. *J Cell Physiol,* 181**,** 67-73.

CORBEIL, D., ROPER, K., HELLWIG, A., TAVIAN, M., MIRAGLIA, S., WATT, S. M., SIMMONS, P. J., PEAULT, B., BUCK, D. W. & HUTTNER, W. B. (2000) The human AC133 hematopoietic stem cell antigen is also expressed in epithelial cells and targeted to plasma membrane protrusions. *J Biol Chem,* 275**,** 5512-20.

COTSARELIS, G., KAUR, P., DHOUAILLY, D., HENGGE, U. & BICKENBACH, J. (1999) Epithelial stem cells in the skin: definition, markers, localization and functions. *Exp Dermatol,* 8**,** 80-8.

COVAS, D. T., PANEPUCCI, R. A., FONTES, A. M., SILVA, W. A., JR., ORELLANA, M. D., FREITAS, M. C., NEDER, L., SANTOS, A. R., PERES, L. C., JAMUR, M. C. & ZAGO, M. A. (2008) Multipotent mesenchymal stromal cells obtained from diverse human tissues share functional properties and gene-expression profile with CD146+ perivascular cells and fibroblasts. *Exp Hematol,* 36**,** 642-54.

CRISAN, M., YAP, S., CASTEILLA, L., CHEN, C. W., CORSELLI, M., PARK, T. S., ANDRIOLO, G., SUN, B., ZHENG, B., ZHANG, L., NOROTTE, C., TENG, P. N., TRAAS, J., SCHUGAR, R., DEASY, B. M., BADYLAK, S., BUHRING, H. J., GIACOBINO, J. P., LAZZARI, L., HUARD, J. & PEAULT, B. (2008) A perivascular origin for mesenchymal stem cells in multiple human organs. *Cell Stem Cell,* 3**,** 301-13.

CURREY, J. D. (2003) The many adaptations of bone. *J Biomech,* 36**,** 1487-95.

D'IPPOLITO, G., DIABIRA, S., HOWARD, G. A., MENEI, P., ROOS, B. A. & SCHILLER, P. C. (2004) Marrow-isolated adult multilineage inducible (MIAMI) cells, a unique population of postnatal young and old human cells with extensive expansion and differentiation potential. *J Cell Sci,* 117**,** 2971-81.

DAY, L. A., MARZEC, C. J., REISBERG, S. A. & CASADEVALL, A. (1988) DNA packing in filamentous bacteriophages. *Annu Rev Biophys Biophys Chem,* 17**,** 509-39.

DELATTRE, O., ZUCMAN, J., PLOUGASTEL, B., DESMAZE, C., MELOT, T., PETER, M., KOVAR, H., JOUBERT, I., DE JONG, P., ROULEAU, G. & ET AL. (1992) Gene fusion with an ETS DNA-binding domain caused by chromosome translocation in human tumours. *Nature,* 359**,** 162-5.

DESCHASEAUX, F. & CHARBORD, P. (2000) Human marrow stromal precursors are alpha 1 integrin subunit-positive. *J Cell Physiol,* 184**,** 319-25.

DESCHASEAUX, F., GINDRAUX, F., SAADI, R., OBERT, L., CHALMERS, D. & HERVE, P. (2003) Direct selection of human bone marrow mesenchymal stem cells using an anti-CD49a antibody reveals their CD45med,low phenotype. *Br J Haematol,* 122**,** 506-17.

DESCHASEAUX, F., SENSEBE, L. & HEYMANN, D. (2009) Mechanisms of bone repair and regeneration. *Trends Mol Med,* 15**,** 417-29.

DILLER, L., KASSEL, J., NELSON, C. E., GRYKA, M. A., LITWAK, G., GEBHARDT, M., BRESSAC, B., OZTURK, M., BAKER, S. J., VOGELSTEIN, B. & ET AL. (1990) p53 functions as a cell cycle control protein in osteosarcomas. *Mol Cell Biol,* 10**,** 5772-81.

DOBNIG, H. & TURNER, R. T. (1995) Evidence that intermittent treatment with parathyroid hormone increases bone formation in adult rats by activation of bone lining cells. *Endocrinology,* 136**,** 3632-8.

DOBREVA, G., CHAHROUR, M., DAUTZENBERG, M., CHIRIVELLA, L., KANZLER, B., FARINAS, I., KARSENTY, G. & GROSSCHEDL, R. (2006) SATB2 is a multifunctional determinant of craniofacial patterning and osteoblast differentiation. *Cell,* 125**,** 971-86.

DOHERTY, M. J., ASHTON, B. A., WALSH, S., BERESFORD, J. N., GRANT, M. E. & CANFIELD, A. E. (1998) Vascular pericytes express osteogenic potential in vitro and in vivo. *J Bone Miner Res,* 13**,** 828-38.

DOMINICI, M., LE BLANC, K., MUELLER, I., SLAPER-CORTENBACH, I., MARINI, F., KRAUSE, D., DEANS, R., KEATING, A., PROCKOP, D. & HORWITZ, E. (2006) Minimal criteria for defining multipotent mesenchymal stromal cells. The International Society for Cellular Therapy position statement. *Cytotherapy,* 8**,** 315-7.

DUCY, P. (2000) Cbfa1: a molecular switch in osteoblast biology. *Dev Dyn,* 219**,** 461-71.

DUCY, P., ZHANG, R., GEOFFROY, V., RIDALL, A. L. & KARSENTY, G. (1997) Osf2/Cbfa1: a transcriptional activator of osteoblast differentiation. *Cell,* 89**,** 747-54.

DUDLEY, H. R. & SPIRO, D. (1961) The Fine Structure of Bone Cells. *J Biophys Biochem Cytol,* 11**,** 627-649.

DYLLA, S. J., BEVIGLIA, L., PARK, I. K., CHARTIER, C., RAVAL, J., NGAN, L., PICKELL, K., AGUILAR, J., LAZETIC, S., SMITH-BERDAN, S., CLARKE, M. F., HOEY, T., LEWICKI, J. & GURNEY, A. L. (2008) Colorectal cancer stem cells are enriched in xenogeneic tumors following chemotherapy. *PLoS One,* 3**,** e2428.

ETHERIDGE, S. L., SPENCER, G. J., HEATH, D. J. & GENEVER, P. G. (2004) Expression profiling and functional analysis of wnt signaling mechanisms in mesenchymal stem cells. *Stem Cells,* 22**,** 849-60.

FARRINGTON-ROCK, C., CROFTS, N. J., DOHERTY, M. J., ASHTON, B. A., GRIFFIN-JONES, C. & CANFIELD, A. E. (2004) Chondrogenic and adipogenic potential of microvascular pericytes. *Circulation,* 110**,** 2226-32.

FERRARI, G., CUSELLA-DE ANGELIS, G., COLETTA, M., PAOLUCCI, E., STORNAIUOLO, A., COSSU, G. & MAVILIO, F. (1998) Muscle regeneration by bone marrow-derived myogenic progenitors. *Science,* 279**,** 1528-30.

FERRARI, S., BRICCOLI, A., MERCURI, M., BERTONI, F., PICCI, P., TIENGHI, A., DEL PREVER, A. B., FAGIOLI, F., COMANDONE, A. & BACCI, G. (2003) Postrelapse survival in osteosarcoma of the extremities: prognostic factors for long-term survival. *J Clin Oncol,* 21**,** 710-5.

FERRARI, S., SMELAND, S., MERCURI, M., BERTONI, F., LONGHI, A., RUGGIERI, P., ALVEGARD, T. A., PICCI, P., CAPANNA, R., BERNINI, G., MULLER, C., TIENGHI, A., WIEBE, T., COMANDONE, A., BOHLING, T., DEL PREVER, A. B., BROSJO, O., BACCI, G. & SAETER, G. (2005) Neoadjuvant chemotherapy with high-dose Ifosfamide, high-dose methotrexate, cisplatin, and doxorubicin for patients with localized osteosarcoma of the extremity: a joint study by the Italian and Scandinavian Sarcoma Groups. *J Clin Oncol,* 23**,** 8845-52.

FIALKOW, P. J. (1976) Clonal origin of human tumors. *Biochim Biophys Acta,* 458**,** 283-321.

FIDLER, I. J. & HART, I. R. (1982) Biological diversity in metastatic neoplasms: origins and implications. *Science,* 217**,** 998-1003.

FIDLER, I. J. & KRIPKE, M. L. (1977) Metastasis results from preexisting variant cells within a malignant tumor. *Science,* 197**,** 893-5.

FITZPATRICK, D. R., CARR, I. M., MCLAREN, L., LEEK, J. P., WIGHTMAN, P., WILLIAMSON, K., GAUTIER, P., MCGILL, N., HAYWARD, C., FIRTH, H., MARKHAM, A. F., FANTES, J. A. & BONTHRON, D. T. (2003) Identification of SATB2 as the cleft palate gene on 2q32-q33. *Hum Mol Genet,* 12**,** 2491-501.

FONSECA, A. V., BAUER, N. & CORBEIL, D. (2008) The stem cell marker CD133 meets the endosomal compartment--new insights into the cell division of hematopoietic stem cells. *Blood Cells Mol Dis,* 41**,** 194-5.

FORBES, S. J., VIG, P., POULSOM, R., WRIGHT, N. A. & ALISON, M. R. (2002) Adult stem cell plasticity: new pathways of tissue regeneration become visible. *Clin Sci (Lond),* 103**,** 355-69.

FRANCESCHI, R. T. (1999) The developmental control of osteoblast-specific gene expression: role of specific transcription factors and the extracellular matrix environment. *Crit Rev Oral Biol Med,* 10**,** 40-57.

FRANZ-ODENDAAL, T. A., HALL, B. K. & WITTEN, P. E. (2006) Buried alive: how osteoblasts become osteocytes. *Dev Dyn,* 235**,** 176-90.

FRIEDENSTEIN, A. J., CHAILAKHJAN, R. K. & LALYKINA, K. S. (1970) The development of fibroblast colonies in monolayer cultures of guinea-pig bone marrow and spleen cells. *Cell Tissue Kinet,* 3**,** 393-403.

FRIEDENSTEIN, A. J., CHAILAKHYAN, R. K. & GERASIMOV, U. V. (1987) Bone marrow osteogenic stem cells: in vitro cultivation and transplantation in diffusion chambers. *Cell Tissue Kinet,* 20**,** 263-72.

FRITH, J. E., THOMSON, B. & GENEVER, P. (2009) Dynamic three-dimensional culture methods enhance mesenchymal stem cell properties and increase therapeutic potential. *Tissue Eng Part C Methods*.

FUNES, J. M., QUINTERO, M., HENDERSON, S., MARTINEZ, D., QURESHI, U., WESTWOOD, C., CLEMENTS, M. O., BOURBOULIA, D., PEDLEY, R. B., MONCADA, S. & BOSHOFF, C. (2007) Transformation of human mesenchymal stem cells increases their dependency on oxidative phosphorylation for energy production. *Proc Natl Acad Sci U S A,* 104**,** 6223-8.

GALLATIN, W. M., WEISSMAN, I. L. & BUTCHER, E. C. (1983) A cell-surface molecule involved in organ-specific homing of lymphocytes. *Nature,* 304**,** 30-4.

GIBBS, C. P., KUKEKOV, V. G., REITH, J. D., TCHIGRINOVA, O., SUSLOV, O. N., SCOTT, E. W., GHIVIZZANI, S. C., IGNATOVA, T. N. & STEINDLER, D. A. (2005) Stem-like cells in bone sarcomas: implications for tumorigenesis. *Neoplasia,* 7**,** 967-76.

GOODELL, M. A., BROSE, K., PARADIS, G., CONNER, A. S. & MULLIGAN, R. C. (1996) Isolation and functional properties of murine hematopoietic stem cells that are replicating in vivo. *J Exp Med,* 183**,** 1797-806.

GREGORY, C. A., GUNN, W. G., PEISTER, A. & PROCKOP, D. J. (2004) An Alizarin red-based assay of mineralization by adherent cells in culture: comparison with cetylpyridinium chloride extraction. *Anal Biochem,* 329**,** 77-84.

GREGORY, C. A., PERRY, A. S., REYES, E., CONLEY, A., GUNN, W. G. & PROCKOP, D. J. (2005) Dkk-1-derived synthetic peptides and lithium chloride for the control and recovery of adult stem cells from bone marrow. *J Biol Chem,* 280**,** 2309-23.

GRIGORIADIS, A. E., WANG, Z. Q. & WAGNER, E. F. (1995) Fos and bone cell development: lessons from a nuclear oncogene. *Trends Genet,* 11**,** 436-41.

GRIMAUD, E., HEYMANN, D. & REDINI, F. (2002) Recent advances in TGF-beta effects on chondrocyte metabolism. Potential therapeutic roles of TGF-beta in cartilage disorders. *Cytokine Growth Factor Rev,* 13**,** 241-57.

GRONTHOS, S. & SIMMONS, P. J. (1996) The biology and application of human bone marrow stromal cell precursors. *J Hematother,* 5**,** 15-23.

GRONTHOS, S., ZANNETTINO, A. C., HAY, S. J., SHI, S., GRAVES, S. E., KORTESIDIS, A. & SIMMONS, P. J. (2003) Molecular and cellular characterisation of highly purified stromal stem cells derived from human bone marrow. *J Cell Sci,* 116**,** 1827-35.

GUNTHERT, U., HOFMANN, M., RUDY, W., REBER, S., ZOLLER, M., HAUSSMANN, I., MATZKU, S., WENZEL, A., PONTA, H. & HERRLICH, P. (1991) A new variant of glycoprotein CD44 confers metastatic potential to rat carcinoma cells. *Cell,* 65**,** 13-24.

GUREVITCH, O., SLAVIN, S. & FELDMAN, A. G. (2007) Conversion of red bone marrow into yellow - Cause and mechanisms. *Med Hypotheses,* 69**,** 531-6.

GUREVITCH, O., SLAVIN, S., RESNICK, I., KHITRIN, S. & FELDMAN, A. (2009) Mesenchymal progenitor cells in red and yellow bone marrow. *Folia Biol (Praha),* 55**,** 27-34.

HABISCH, H. J., JANOWSKI, M., BINDER, D., KUZMA-KOZAKIEWICZ, M., WIDMANN, A., HABICH, A., SCHWALENSTOCKER, B., HERMANN, A., BRENNER, R., LUKOMSKA, B., DOMANSKA-JANIK, K., LUDOLPH, A. C. & STORCH, A. (2007) Intrathecal application of neuroectodermally converted stem cells into a mouse model of ALS: limited intraparenchymal migration and survival narrows therapeutic effects. *J Neural Transm,* 114**,** 1395-406.

HALL, P. A. & WATT, F. M. (1989) Stem cells: the generation and maintenance of cellular diversity. *Development,* 106**,** 619-33.

HALLDORSSON, A., BROOKS, S., MONTGOMERY, S. & GRAHAM, S. (2009) Lung metastasis 21 years after initial diagnosis of osteosarcoma: a case report. *J Med Case Reports,* 3**,** 9298.

HAMBURGER, A. W. & SALMON, S. E. (1977) Primary bioassay of human tumor stem cells. *Science,* 197**,** 461-3.

HANADA, K., DENNIS, J. E. & CAPLAN, A. I. (1997) Stimulatory effects of basic fibroblast growth factor and bone morphogenetic protein-2 on osteogenic differentiation of rat bone marrow-derived mesenchymal stem cells. *J Bone Miner Res,* 12**,** 1606-14.

HANIFFA, M. A., COLLIN, M. P., BUCKLEY, C. D. & DAZZI, F. (2009) Mesenchymal stem cells: the fibroblasts' new clothes? *Haematologica,* 94**,** 258-63.

HARPER, L. J., PIPER, K., COMMON, J., FORTUNE, F. & MACKENZIE, I. C. (2007) Stem cell patterns in cell lines derived from head and neck squamous cell carcinoma. *J Oral Pathol Med,* 36**,** 594-603.

HEPPNER, G. H. (1984) Tumor heterogeneity. *Cancer Res,* 44**,** 2259-65.

HIRSCHMANN-JAX, C., FOSTER, A. E., WULF, G. G., GOODELL, M. A. & BRENNER, M. K. (2005) A distinct "side population" of cells in human tumor cells: implications for tumor biology and therapy. *Cell Cycle,* 4**,** 203-5.

HIRSCHMANN-JAX, C., FOSTER, A. E., WULF, G. G., NUCHTERN, J. G., JAX, T. W., GOBEL, U., GOODELL, M. A. & BRENNER, M. K. (2004) A distinct "side population" of cells with high drug efflux capacity in human tumor cells. *Proc Natl Acad Sci U S A,* 101**,** 14228-33.

HOLLIER, B. G., EVANS, K. & MANI, S. A. (2009) The epithelial-to-mesenchymal transition and cancer stem cells: a coalition against cancer therapies. *J Mammary Gland Biol Neoplasia,* 14**,** 29-43.

HONOKI, K., TSUTSUMI, M., TSUJIUCHI, T., KONDOH, S., SHIRAIWA, K., MIYAUCHI, Y., MII, Y., TAMAI, S., KONISHI, Y. & BOWDEN, G. T. (1992) Expression of the transin, c-fos, and c-jun genes in rat transplantable osteosarcomas and malignant fibrous histiocytomas. *Mol Carcinog,* 6**,** 122-8.

HORWITZ, E. M., LE BLANC, K., DOMINICI, M., MUELLER, I., SLAPER-CORTENBACH, I., MARINI, F. C., DEANS, R. J., KRAUSE, D. S. & KEATING, A. (2005) Clarification of the nomenclature for MSC: The International Society for Cellular Therapy position statement. *Cytotherapy,* 7**,** 393-5.

HOWARD, D., BUTTERY, L. D., SHAKESHEFF, K. M. & ROBERTS, S. J. (2008) Tissue engineering: strategies, stem cells and scaffolds. *J Anat,* 213**,** 66-72.

HUGO, H., ACKLAND, M. L., BLICK, T., LAWRENCE, M. G., CLEMENTS, J. A., WILLIAMS, E. D. & THOMPSON, E. W. (2007) Epithelial--mesenchymal and mesenchymal--epithelial transitions in carcinoma progression. *J Cell Physiol,* 213**,** 374-83.

HUNTLY, B. J. & GILLILAND, D. G. (2005) Leukaemia stem cells and the evolution of cancer-stem-cell research. *Nat Rev Cancer,* 5**,** 311-21.

IKEDA, N., NAKAJIMA, Y., TOKUHARA, T., HATTORI, N., SHO, M., KANEHIRO, H. & MIYAKE, M. (2003) Clinical significance of aminopeptidase N/CD13 expression in human pancreatic carcinoma. *Clin Cancer Res,* 9**,** 1503-8.

IM, G. I., SHIN, Y. W. & LEE, K. B. (2005) Do adipose tissue-derived mesenchymal stem cells have the same osteogenic and chondrogenic potential as bone marrow-derived cells? *Osteoarthritis Cartilage,* 13**,** 845-53.

JAISWAL, R. K., JAISWAL, N., BRUDER, S. P., MBALAVIELE, G., MARSHAK, D. R. & PITTENGER, M. F. (2000) Adult human mesenchymal stem cell differentiation to the osteogenic or adipogenic lineage is regulated by mitogen-activated protein kinase. *J Biol Chem,* 275**,** 9645-52.

JI, K. H., XIONG, J., HU, K. M., FAN, L. X. & LIU, H. Q. (2008) Simultaneous expression of Oct4 and genes of three germ layers in single cell-derived multipotent adult progenitor cells. *Ann Hematol,* 87**,** 431-8.

JIANG, T., ABDEL-FATTAH, W. I. & LAURENCIN, C. T. (2006) In vitro evaluation of chitosan/poly(lactic acid-glycolic acid) sintered microsphere scaffolds for bone tissue engineering. *Biomaterials,* 27**,** 4894-903.

JIANG, Y., JAHAGIRDAR, B. N., REINHARDT, R. L., SCHWARTZ, R. E., KEENE, C. D., ORTIZ-GONZALEZ, X. R., REYES, M., LENVIK, T., LUND, T., BLACKSTAD, M., DU, J., ALDRICH, S., LISBERG, A., LOW, W. C.,

LARGAESPADA, D. A. & VERFAILLIE, C. M. (2002) Pluripotency of mesenchymal stem cells derived from adult marrow. *Nature,* 418**,** 41-9.

JONES, D. C., WEIN, M. N., OUKKA, M., HOFSTAETTER, J. G., GLIMCHER, M. J. & GLIMCHER, L. H. (2006a) Regulation of adult bone mass by the zinc finger adapter protein Schnurri-3. *Science,* 312**,** 1223-7.

JONES, E. & MCGONAGLE, D. (2008) Human bone marrow mesenchymal stem cells in vivo. *Rheumatology (Oxford),* 47**,** 126-31.

JONES, E. A., ENGLISH, A., HENSHAW, K., KINSEY, S. E., MARKHAM, A. F., EMERY, P. & MCGONAGLE, D. (2004) Enumeration and phenotypic characterization of synovial fluid multipotential mesenchymal progenitor cells in inflammatory and degenerative arthritis. *Arthritis Rheum,* 50**,** 817-27.

JONES, E. A., ENGLISH, A., KINSEY, S. E., STRASZYNSKI, L., EMERY, P., PONCHEL, F. & MCGONAGLE, D. (2006b) Optimization of a flow cytometry-based protocol for detection and phenotypic characterization of multipotent mesenchymal stromal cells from human bone marrow. *Cytometry B Clin Cytom,* 70**,** 391-9.

JONES, E. A., KINSEY, S. E., ENGLISH, A., JONES, R. A., STRASZYNSKI, L., MEREDITH, D. M., MARKHAM, A. F., JACK, A., EMERY, P. & MCGONAGLE, D. (2002) Isolation and characterization of bone marrow multipotential mesenchymal progenitor cells. *Arthritis Rheum,* 46**,** 3349-60.

JOSEPH, N. M. & MORRISON, S. J. (2005) Toward an understanding of the physiological function of Mammalian stem cells. *Dev Cell,* 9**,** 173-83.

JOTHY, S. (2003) CD44 and its partners in metastasis. *Clin Exp Metastasis,* 20**,** 195-201.

KANZLER, B., KUSCHERT, S. J., LIU, Y. H. & MALLO, M. (1998) Hoxa-2 restricts the chondrogenic domain and inhibits bone formation during development of the branchial area. *Development,* 125**,** 2587-97.

KAWAMOTO, A., GWON, H. C., IWAGURO, H., YAMAGUCHI, J. I., UCHIDA, S., MASUDA, H., SILVER, M., MA, H., KEARNEY, M., ISNER, J. M. & ASAHARA, T. (2001) Therapeutic potential of ex vivo expanded endothelial progenitor cells for myocardial ischemia. *Circulation,* 103**,** 634-7.

KAWAMURA, J., SHIMADA, Y., KITAICHI, H., KOMOTO, I., HASHIMOTO, Y., KAGANOI, J., MIYAKE, M., YAMASAKI, S., KONDO, K. & IMAMURA, M. (2007) Clinicopathological significance of aminopeptidase N/CD13 expression in human gastric carcinoma. *Hepatogastroenterology,* 54**,** 36-40.

KAWASAKI, Y., SATO, R. & AKIYAMA, T. (2003) Mutated APC and Asef are involved in the migration of colorectal tumour cells. *Nat Cell Biol,* 5**,** 211-5.

KAWASAKI, Y., SENDA, T., ISHIDATE, T., KOYAMA, R., MORISHITA, T., IWAYAMA, Y., HIGUCHI, O. & AKIYAMA, T. (2000) Asef, a link between the tumor suppressor APC and G-protein signaling. *Science,* 289**,** 1194-7.

KIM, H. J., KIM, U. J., KIM, H. S., LI, C., WADA, M., LEISK, G. G. & KAPLAN, D. L. (2008) Bone tissue engineering with premineralized silk scaffolds. *Bone,* 42**,** 1226-34.

KIM, S., KOGA, T., ISOBE, M., KERN, B. E., YOKOCHI, T., CHIN, Y. E., KARSENTY, G., TANIGUCHI, T. & TAKAYANAGI, H. (2003) Stat1 functions as a cytoplasmic attenuator of Runx2 in the transcriptional program of osteoblast differentiation. *Genes Dev,* 17**,** 1979-91.

KLEIN, M. J. & SIEGAL, G. P. (2006) Osteosarcoma: anatomic and histologic variants. *Am J Clin Pathol,* 125**,** 555-81.

KOGA, T., MATSUI, Y., ASAGIRI, M., KODAMA, T., DE CROMBRUGGHE, B., NAKASHIMA, K. & TAKAYANAGI, H. (2005) NFAT and Osterix cooperatively regulate bone formation. *Nat Med,* 11**,** 880-5.

KONDO, M., WAGERS, A. J., MANZ, M. G., PROHASKA, S. S., SCHERER, D. C., BEILHACK, G. F., SHIZURU, J. A. & WEISSMAN, I. L. (2003) Biology of hematopoietic stem cells and progenitors: implications for clinical application. *Annu Rev Immunol,* 21**,** 759-806.

KOPEN, G. C., PROCKOP, D. J. & PHINNEY, D. G. (1999) Marrow stromal cells migrate throughout forebrain and cerebellum, and they differentiate into astrocytes after injection into neonatal mouse brains. *Proc Natl Acad Sci U S A,* 96**,** 10711-6.

KRAUS, K. H. & KIRKER-HEAD, C. (2006) Mesenchymal stem cells and bone regeneration. *Vet Surg,* 35**,** 232-42.

KRIEBEL, P. W., BARR, V. A., RERICHA, E. C., ZHANG, G. & PARENT, C. A. (2008) Collective cell migration requires vesicular trafficking for chemoattractant delivery at the trailing edge. *J Cell Biol,* 183**,** 949-61.

KUCIA, M., HALASA, M., WYSOCZYNSKI, M., BASKIEWICZ-MASIUK, M., MOLDENHAWER, S., ZUBA-SURMA, E., CZAJKA, R., WOJAKOWSKI, W., MACHALINSKI, B. & RATAJCZAK, M. Z. (2007) Morphological and molecular characterization of novel population of CXCR4+ SSEA-4+ Oct-4+ very small embryonic-like cells purified from human cord blood: preliminary report. *Leukemia,* 21**,** 297-303.

KUCIA, M., RECA, R., CAMPBELL, F. R., ZUBA-SURMA, E., MAJKA, M., RATAJCZAK, J. & RATAJCZAK, M. Z. (2006) A population of very small embryonic-like (VSEL) CXCR4(+)SSEA-1(+)Oct-4+ stem cells identified in adult bone marrow. *Leukemia,* 20**,** 857-69.

LACEY, D. L., TIMMS, E., TAN, H. L., KELLEY, M. J., DUNSTAN, C. R., BURGESS, T., ELLIOTT, R., COLOMBERO, A., ELLIOTT, G., SCULLY, S., HSU, H., SULLIVAN, J., HAWKINS, N., DAVY, E., CAPPARELLI, C., ELI, A., QIAN, Y. X., KAUFMAN, S., SAROSI, I., SHALHOUB, V., SENALDI, G., GUO, J., DELANEY, J. & BOYLE, W. J. (1998) Osteoprotegerin ligand is a cytokine that regulates osteoclast differentiation and activation. *Cell,* 93**,** 165-76.

LAJTHA, L. G. (1979) Stem cell concepts. *Nouv Rev Fr Hematol,* 21**,** 59-65.

LAZARUS, H. M., HAYNESWORTH, S. E., GERSON, S. L., ROSENTHAL, N. S. & CAPLAN, A. I. (1995) Ex vivo expansion and subsequent infusion of human bone marrow-derived stromal progenitor cells (mesenchymal progenitor cells): implications for therapeutic use. *Bone Marrow Transplant,* 16**,** 557-64.

LAZARUS, H. M., KOC, O. N., DEVINE, S. M., CURTIN, P., MAZIARZ, R. T., HOLLAND, H. K., SHPALL, E. J., MCCARTHY, P., ATKINSON, K., COOPER, B. W., GERSON, S. L., LAUGHLIN, M. J., LOBERIZA, F. R., JR., MOSELEY, A. B. & BACIGALUPO, A. (2005) Cotransplantation of HLA-identical sibling culture-expanded mesenchymal stem cells and hematopoietic stem cells in hematologic malignancy patients. *Biol Blood Marrow Transplant,* 11**,** 389-98.

LE BLANC, K., RASMUSSON, I., SUNDBERG, B., GOTHERSTROM, C., HASSAN, M., UZUNEL, M. & RINGDEN, O. (2004) Treatment of severe

acute graft-versus-host disease with third party haploidentical mesenchymal stem cells. *Lancet,* 363**,** 1439-41.

LE BLANC, K. & RINGDEN, O. (2007) Immunomodulation by mesenchymal stem cells and clinical experience. *J Intern Med,* 262**,** 509-25.

LE BOURHIS, X., ROMON, R. & HONDERMARCK, H. (2010) Role of endothelial progenitor cells in breast cancer angiogenesis: from fundamental research to clinical ramifications. *Breast Cancer Res Treat,* 120**,** 17-24.

LETCHFORD, J., CARDWELL, A. M., STEWART, K., COOGANS, K. K., COX, J. P., LEE, M., BERESFORD, J. N., PERRY, M. J. & WELHAM, M. J. (2006) Isolation of C15: a novel antibody generated by phage display against mesenchymal stem cell-enriched fractions of adult human marrow. *J Immunol Methods,* 308**,** 124-37.

LIAO, M. J., ZHANG, C. C., ZHOU, B., ZIMONJIC, D. B., MANI, S. A., KABA, M., GIFFORD, A., REINHARDT, F., POPESCU, N. C., GUO, W., EATON, E. N., LODISH, H. F. & WEINBERG, R. A. (2007) Enrichment of a population of mammary gland cells that form mammospheres and have in vivo repopulating activity. *Cancer Res,* 67**,** 8131-8.

LIU, F., KOHLMEIER, S. & WANG, C. Y. (2008) Wnt signaling and skeletal development. *Cell Signal,* 20**,** 999-1009.

LIU, X., LI, Y., LIU, Y., LUO, Y., WANG, D., ANNEX, B. H. & GOLDSCHMIDT-CLERMONT, P. J. (2010) Endothelial progenitor cells (EPCs) mobilized and activated by neurotrophic factors may contribute to pathologic neovascularization in diabetic retinopathy. *Am J Pathol,* 176**,** 504-15.

LOCKE, M., HEYWOOD, M., FAWELL, S. & MACKENZIE, I. C. (2005) Retention of intrinsic stem cell hierarchies in carcinoma-derived cell lines. *Cancer Res,* 65**,** 8944-50.

LOCKLIN, R. M., OREFFO, R. O. & TRIFFITT, J. T. (1998) Modulation of osteogenic differentiation in human skeletal cells in Vitro by 5-azacytidine. *Cell Biol Int,* 22**,** 207-15.

MACKENZIE, I. C. (2005) Retention of stem cell patterns in malignant cell lines. *Cell Prolif,* 38**,** 347-55.

MACKENZIE, I. C. (2006) Stem cell properties and epithelial malignancies. *Eur J Cancer,* 42**,** 1204-12.

MAIER, R., GLATZ, A., MOSBACHER, J. & BILBE, G. (1997) Cloning of P2Y6 cDNAs and identification of a pseudogene: comparison of P2Y receptor subtype expression in bone and brain tissues. *Biochem Biophys Res Commun,* 240**,** 298-302.

MAJUMDAR, M. K., BANKS, V., PELUSO, D. P. & MORRIS, E. A. (2000) Isolation, characterization, and chondrogenic potential of human bone marrow-derived multipotential stromal cells. *J Cell Physiol,* 185**,** 98-106.

MAJUMDAR, M. K., THIEDE, M. A., MOSCA, J. D., MOORMAN, M. & GERSON, S. L. (1998) Phenotypic and functional comparison of cultures of marrow-derived mesenchymal stem cells (MSCs) and stromal cells. *J Cell Physiol,* 176**,** 57-66.

MANI, S. A., GUO, W., LIAO, M. J., EATON, E. N., AYYANAN, A., ZHOU, A. Y., BROOKS, M., REINHARD, F., ZHANG, C. C., SHIPITSIN, M., CAMPBELL, L. L., POLYAK, K., BRISKEN, C., YANG, J. & WEINBERG, R. A. (2008)

The epithelial-mesenchymal transition generates cells with properties of stem cells. *Cell,* 133**,** 704-15.

MARHABA, R. & ZOLLER, M. (2004) CD44 in cancer progression: adhesion, migration and growth regulation. *J Mol Histol,* 35**,** 211-31.

MARTIN, G. R. (1981) Isolation of a pluripotent cell line from early mouse embryos cultured in medium conditioned by teratocarcinoma stem cells. *Proc Natl Acad Sci U S A,* 78**,** 7634-8.

MARTIN, G. R. & EVANS, M. J. (1975) Differentiation of clonal lines of teratocarcinoma cells: formation of embryoid bodies in vitro. *Proc Natl Acad Sci U S A,* 72**,** 1441-5.

MASI, L. & BRANDI, M. L. (2001) Physiopathological basis of bone turnover. *Q J Nucl Med,* 45**,** 2-6.

MATSUO, K. & IRIE, N. (2008) Osteoclast-osteoblast communication. *Arch Biochem Biophys,* 473**,** 201-9.

MCALLISTER, R. M., GARDNER, M. B., GREENE, A. E., BRADT, C., NICHOLS, W. W. & LANDING, B. H. (1971) Cultivation in vitro of cells derived from a human osteosarcoma. *Cancer,* 27**,** 397-402.

MCBEATH, R., PIRONE, D. M., NELSON, C. M., BHADRIRAJU, K. & CHEN, C. S. (2004) Cell shape, cytoskeletal tension, and RhoA regulate stem cell lineage commitment. *Dev Cell,* 6**,** 483-95.

MCDONALD, S. A., GRAHAM, T. A., SCHIER, S., WRIGHT, N. A. & ALISON, M. R. (2009) Stem cells and solid cancers. *Virchows Arch,* 455**,** 1-13.

MCGUIRE, M. J., LI, S. & BROWN, K. C. (2009) Biopanning of phage displayed peptide libraries for the isolation of cell-specific ligands. *Methods Mol Biol,* 504**,** 291-321.

MELTZER, P. S. (2007) Is Ewing's sarcoma a stem cell tumor? *Cell Stem Cell,* 1**,** 13-5.

MEYERS, P. A. & GORLICK, R. (1997) Osteosarcoma. *Pediatr Clin North Am,* 44**,** 973-89.

MILLER, C. W., ASLO, A., WON, A., TAN, M., LAMPKIN, B. & KOEFFLER, H. P. (1996) Alterations of the p53, Rb and MDM2 genes in osteosarcoma. *J Cancer Res Clin Oncol,* 122**,** 559-65.

MIMEAULT, M., HAUKE, R., MEHTA, P. P. & BATRA, S. K. (2007) Recent advances in cancer stem/progenitor cell research: therapeutic implications for overcoming resistance to the most aggressive cancers. *J Cell Mol Med,* 11**,** 981-1011.

MINGUELL, J. J., ERICES, A. & CONGET, P. (2001) Mesenchymal stem cells. *Exp Biol Med (Maywood),* 226**,** 507-20.

MIRMALEK-SANI, S. H., TARE, R. S., MORGAN, S. M., ROACH, H. I., WILSON, D. I., HANLEY, N. A. & OREFFO, R. O. (2006) Characterization and multipotentiality of human fetal femur-derived cells: implications for skeletal tissue regeneration. *Stem Cells,* 24**,** 1042-53.

MIURA, M., MIURA, Y., SONOYAMA, W., YAMAZA, T., GRONTHOS, S. & SHI, S. (2006) Bone marrow-derived mesenchymal stem cells for regenerative medicine in craniofacial region. *Oral Dis,* 12**,** 514-22.

MIZRAK, D., BRITTAN, M. & ALISON, M. R. (2008) CD133: molecule of the moment. *J Pathol,* 214**,** 3-9.

MOHAN, S. B., CHOHAN, S. R., EADE, J. & LYDDIATT, A. (1993) Molecular integrity of monoclonal antibodies produced by hybridoma cells in batch culture

and in continuous-flow culture with integrated product recovery. *Biotechnol Bioeng,* 42**,** 974-86.

MORRISON, S. J., SHAH, N. M. & ANDERSON, D. J. (1997) Regulatory mechanisms in stem cell biology. *Cell,* 88**,** 287-98.

MORRISON, S. J., WHITE, P. M., ZOCK, C. & ANDERSON, D. J. (1999) Prospective identification, isolation by flow cytometry, and in vivo self-renewal of multipotent mammalian neural crest stem cells. *Cell,* 96**,** 737-49.

MORVAN, F., BOULUKOS, K., CLEMENT-LACROIX, P., ROMAN ROMAN, S., SUC-ROYER, I., VAYSSIERE, B., AMMANN, P., MARTIN, P., PINHO, S., POGNONEC, P., MOLLAT, P., NIEHRS, C., BARON, R. & RAWADI, G. (2006) Deletion of a single allele of the Dkk1 gene leads to an increase in bone formation and bone mass. *J Bone Miner Res,* 21**,** 934-45.

MOTALN, H., SCHICHOR, C. & LAH, T. T. (2010) Human mesenchymal stem cells and their use in cell-based therapies. *Cancer*.

MULLANEY, B. P. & PALLAVICINI, M. G. (2001) Protein-protein interactions in hematology and phage display. *Exp Hematol,* 29**,** 1136-46.

MURASE, M., KANO, M., TSUKAHARA, T., TAKAHASHI, A., TORIGOE, T., KAWAGUCHI, S., KIMURA, S., WADA, T., UCHIHASHI, Y., KONDO, T., YAMASHITA, T. & SATO, N. (2009) Side population cells have the characteristics of cancer stem-like cells/cancer-initiating cells in bone sarcomas. *Br J Cancer,* 101**,** 1425-32.

MURPHY, J. M., DIXON, K., BECK, S., FABIAN, D., FELDMAN, A. & BARRY, F. (2002) Reduced chondrogenic and adipogenic activity of mesenchymal stem cells from patients with advanced osteoarthritis. *Arthritis Rheum,* 46**,** 704-13.

MURUGANANDAN, S., ROMAN, A. A. & SINAL, C. J. (2009) Adipocyte differentiation of bone marrow-derived mesenchymal stem cells: cross talk with the osteoblastogenic program. *Cell Mol Life Sci,* 66**,** 236-53.

NAGASAWA, T. (2000) A chemokine, SDF-1/PBSF, and its receptor, CXC chemokine receptor 4, as mediators of hematopoiesis. *Int J Hematol,* 72**,** 408-11.

NAKAMURA, T., SHIOJIMA, S., HIRAI, Y., IWAMA, T., TSURUZOE, N., HIRASAWA, A., KATSUMA, S. & TSUJIMOTO, G. (2003) Temporal gene expression changes during adipogenesis in human mesenchymal stem cells. *Biochem Biophys Res Commun,* 303**,** 306-12.

NAKASHIMA, K., ZHOU, X., KUNKEL, G., ZHANG, Z., DENG, J. M., BEHRINGER, R. R. & DE CROMBRUGGHE, B. (2002) The novel zinc finger-containing transcription factor osterix is required for osteoblast differentiation and bone formation. *Cell,* 108**,** 17-29.

NARDEUX, P. C., DAYA-GROSJEAN, L., LANDIN, R. M., ANDEOL, Y. & SUAREZ, H. G. (1987) A c-ras-Ki oncogene is activated, amplified and overexpressed in a human osteosarcoma cell line. *Biochem Biophys Res Commun,* 146**,** 395-402.

NEUBAUER, M., FISCHBACH, C., BAUER-KREISEL, P., LIEB, E., HACKER, M., TESSMAR, J., SCHULZ, M. B., GOEPFERICH, A. & BLUNK, T. (2004) Basic fibroblast growth factor enhances PPARgamma ligand-induced adipogenesis of mesenchymal stem cells. *FEBS Lett,* 577**,** 277-83.

NISHIO, Y., DONG, Y., PARIS, M., O'KEEFE, R. J., SCHWARZ, E. M. & DRISSI, H. (2006) Runx2-mediated regulation of the zinc finger Osterix/Sp7 gene. *Gene,* 372**,** 62-70.

NOWAK, K., RAFAT, N., BELLE, S., WEISS, C., HANUSCH, C., HOHENBERGER, P. & BECK, G. C. (2010) Circulating endothelial progenitor cells are increased in human lung cancer and correlate with stage of disease. *Eur J Cardiothorac Surg,* 37**,** 758-763.

NOWELL, P. C. (1986) Mechanisms of tumor progression. *Cancer Res,* 46**,** 2203-7.

NTAMBI, J. M. & YOUNG-CHEUL, K. (2000) Adipocyte differentiation and gene expression. *J Nutr,* 130**,** 3122S-3126S.

O'BRIEN, C. A., POLLETT, A., GALLINGER, S. & DICK, J. E. (2007) A human colon cancer cell capable of initiating tumour growth in immunodeficient mice. *Nature,* 445**,** 106-10.

OLEMPSKA, M., EISENACH, P. A., AMMERPOHL, O., UNGEFROREN, H., FANDRICH, F. & KALTHOFF, H. (2007) Detection of tumor stem cell markers in pancreatic carcinoma cell lines. *Hepatobiliary Pancreat Dis Int,* 6**,** 92-7.

OLSEN, B. R., REGINATO, A. M. & WANG, W. (2000) Bone development. *Annu Rev Cell Dev Biol,* 16**,** 191-220.

OLSTAD, O. K., GAUTVIK, V. T., REPPE, S., RIAN, E., JEMTLAND, R., OHLSSON, C., BRULAND, O. S. & GAUTVIK, K. M. (2003) Molecular heterogeneity in human osteosarcoma demonstrated by enriched mRNAs isolated by directional tag PCR subtraction cloning. *Anticancer Res,* 23**,** 2201-16.

ORIAN-ROUSSEAU, V. (2010) CD44, a therapeutic target for metastasising tumours. *Eur J Cancer*.

OUYANG, H. W., CAO, T., ZOU, X. H., HENG, B. C., WANG, L. L., SONG, X. H. & HUANG, H. F. (2006) Mesenchymal stem cell sheets revitalize nonviable dense grafts: implications for repair of large-bone and tendon defects. *Transplantation,* 82**,** 170-4.

OWEN, M. & FRIEDENSTEIN, A. J. (1988) Stromal stem cells: marrow-derived osteogenic precursors. *Ciba Found Symp,* 136**,** 42-60.

PAL, R., HANWATE, M., JAN, M. & TOTEY, S. (2009) Phenotypic and functional comparison of optimum culture conditions for upscaling of bone marrow-derived mesenchymal stem cells. *J Tissue Eng Regen Med,* 3**,** 163-74.

PARDAL, R., CLARKE, M. F. & MORRISON, S. J. (2003) Applying the principles of stem-cell biology to cancer. *Nat Rev Cancer,* 3**,** 895-902.

PARK, C. H., BERGSAGEL, D. E. & MCCULLOCH, E. A. (1971) Mouse myeloma tumor stem cells: a primary cell culture assay. *J Natl Cancer Inst,* 46**,** 411-22.

PATRU, C., ROMAO, L., VARLET, P., COULOMBEL, L., RAPONI, E., CADUSSEAU, J., RENAULT-MIHARA, F., THIRANT, C., LEONARD, N., BERHNEIM, A., MIHALESCU-MAINGOT, M., HAIECH, J., BIECHE, I., MOURA-NETO, V., DAUMAS-DUPORT, C., JUNIER, M. P. & CHNEIWEISS, H. (2010) CD133, CD15/SSEA-1, CD34 or side populations do not resume tumor-initiating properties of long-term cultured cancer stem cells from human malignant glio-neuronal tumors. *BMC Cancer,* 10**,** 66.

PAUTKE, C., SCHIEKER, M., TISCHER, T., KOLK, A., NETH, P., MUTSCHLER, W. & MILZ, S. (2004) Characterization of osteosarcoma cell lines MG-63, Saos-2 and U-2 OS in comparison to human osteoblasts. *Anticancer Res,* 24**,** 3743-8.

PETERSEN, B. E., BOWEN, W. C., PATRENE, K. D., MARS, W. M., SULLIVAN, A. K., MURASE, N., BOGGS, S. S., GREENBERGER, J. S. & GOFF, J. P. (1999) Bone marrow as a potential source of hepatic oval cells. *Science,* 284**,** 1168-70.

PFEIFFER, M. J. & SCHALKEN, J. A. (2009) Stem cell characteristics in prostate cancer cell lines. *Eur Urol,* 57**,** 246-54.

PHINNEY, D. G. & PROCKOP, D. J. (2007) Concise review: mesenchymal stem/multipotent stromal cells: the state of transdifferentiation and modes of tissue repair--current views. *Stem Cells,* 25**,** 2896-902.

PIERCE, G. B. (1977) Relationship between differentiation and carcinogenesis. *J Toxicol Environ Health,* 2**,** 1335-42.

PITTENGER, M. F., MACKAY, A. M., BECK, S. C., JAISWAL, R. K., DOUGLAS, R., MOSCA, J. D., MOORMAN, M. A., SIMONETTI, D. W., CRAIG, S. & MARSHAK, D. R. (1999) Multilineage potential of adult human mesenchymal stem cells. *Science,* 284**,** 143-7.

PITTENGER, M. F., MOSCA, J. D. & MCINTOSH, K. R. (2000) Human mesenchymal stem cells: progenitor cells for cartilage, bone, fat and stroma. *Curr Top Microbiol Immunol,* 251**,** 3-11.

POTTEN, C. S. (1981) Cell replacement in epidermis (keratopoiesis) via discrete units of proliferation. *Int Rev Cytol,* 69**,** 271-318.

POTTEN, C. S. & LOEFFLER, M. (1990) Stem cells: attributes, cycles, spirals, pitfalls and uncertainties. Lessons for and from the crypt. *Development,* 110**,** 1001-20.

POULSOM, R., ALISON, M. R., FORBES, S. J. & WRIGHT, N. A. (2002) Adult stem cell plasticity. *J Pathol,* 197**,** 441-56.

PROCKOP, D. J., SEKIYA, I. & COLTER, D. C. (2001) Isolation and characterization of rapidly self-renewing stem cells from cultures of human marrow stromal cells. *Cytotherapy,* 3**,** 393-6.

PSALTIS, P. J., PATON, S., SEE, F., ARTHUR, A., MARTIN, S., ITESCU, S., WORTHLEY, S. G., GRONTHOS, S. & ZANNETTINO, A. C. (2010) Enrichment for STRO-1 expression enhances the cardiovascular paracrine activity of human bone marrow-derived mesenchymal cell populations. *J Cell Physiol,* 223**,** 530-40.

PSALTIS, P. J., ZANNETTINO, A. C., WORTHLEY, S. G. & GRONTHOS, S. (2008) Concise review: mesenchymal stromal cells: potential for cardiovascular repair. *Stem Cells,* 26**,** 2201-10.

QUIRICI, N., SOLIGO, D., BOSSOLASCO, P., SERVIDA, F., LUMINI, C. & DELILIERS, G. L. (2002) Isolation of bone marrow mesenchymal stem cells by anti-nerve growth factor receptor antibodies. *Exp Hematol,* 30**,** 783-91.

RADISKY, D. C. & LABARGE, M. A. (2008) Epithelial-mesenchymal transition and the stem cell phenotype. *Cell Stem Cell,* 2**,** 511-2.

RAFF, M. (2003) Adult stem cell plasticity: fact or artifact? *Annu Rev Cell Dev Biol,* 19**,** 1-22.

RANSONE, L. J. & VERMA, I. M. (1990) Nuclear proto-oncogenes fos and jun. *Annu Rev Cell Biol,* 6**,** 539-57.

RATAJCZAK, M. Z., ZUBA-SURMA, E. K., MACHALINSKI, B. & KUCIA, M. (2007) Bone-marrow-derived stem cells--our key to longevity? *J Appl Genet,* 48**,** 307-19.

REYA, T., MORRISON, S. J., CLARKE, M. F. & WEISSMAN, I. L. (2001) Stem cells, cancer, and cancer stem cells. *Nature,* 414**,** 105-11.

REYES, M., LUND, T., LENVIK, T., AGUIAR, D., KOODIE, L. & VERFAILLIE, C. M. (2001) Purification and ex vivo expansion of postnatal human marrow mesodermal progenitor cells. *Blood,* 98**,** 2615-25.

RHIM, J. S. (2000) Development of human cell lines from multiple organs. *Ann N Y Acad Sci,* 919**,** 16-25.

RHIM, J. S., PUTMAN, D. L., ARNSTEIN, P., HUEBNER, R. J. & MCALLISTER, R. M. (1977) Characterization of human cells transformed in vitro by N-methyl-N'-nitro-N-nitrosoguanidine. *Int J Cancer,* 19**,** 505-10.

RICCI-VITIANI, L., LOMBARDI, D. G., PILOZZI, E., BIFFONI, M., TODARO, M., PESCHLE, C. & DE MARIA, R. (2007) Identification and expansion of human colon-cancer-initiating cells. *Nature,* 445**,** 111-5.

RIECHMANN, L. & HOLLIGER, P. (1997) The C-terminal domain of TolA is the coreceptor for filamentous phage infection of E. coli. *Cell,* 90**,** 351-60.

ROCHET, N., DUBOUSSET, J., MAZEAU, C., ZANGHELLINI, E., FARGES, M. F., DE NOVION, H. S., CHOMPRET, A., DELPECH, B., CATTAN, N., FRENAY, M. & GIOANNI, J. (1999) Establishment, characterisation and partial cytokine expression profile of a new human osteosarcoma cell line (CAL 72). *Int J Cancer,* 82**,** 282-5.

RODAN, S. B., IMAI, Y., THIEDE, M. A., WESOLOWSKI, G., THOMPSON, D., BAR-SHAVIT, Z., SHULL, S., MANN, K. & RODAN, G. A. (1987) Characterization of a human osteosarcoma cell line (Saos-2) with osteoblastic properties. *Cancer Res,* 47**,** 4961-6.

RODI, D. J. & MAKOWSKI, L. (1999) Phage-display technology--finding a needle in a vast molecular haystack. *Curr Opin Biotechnol,* 10**,** 87-93.

ROMERO-RAMOS, M., VOURC'H, P., YOUNG, H. E., LUCAS, P. A., WU, Y., CHIVATAKARN, O., ZAMAN, R., DUNKELMAN, N., EL-KALAY, M. A. & CHESSELET, M. F. (2002) Neuronal differentiation of stem cells isolated from adult muscle. *J Neurosci Res,* 69**,** 894-907.

ROOBROUCK, V. D., ULLOA-MONTOYA, F. & VERFAILLIE, C. M. (2008) Self-renewal and differentiation capacity of young and aged stem cells. *Exp Cell Res,* 314**,** 1937-44.

SACCHETTI, B., FUNARI, A., MICHIENZI, S., DI CESARE, S., PIERSANTI, S., SAGGIO, I., TAGLIAFICO, E., FERRARI, S., ROBEY, P. G., RIMINUCCI, M. & BIANCO, P. (2007) Self-renewing osteoprogenitors in bone marrow sinusoids can organize a hematopoietic microenvironment. *Cell,* 131**,** 324-36.

SAIKI, I., FUJII, H., YONEDA, J., ABE, F., NAKAJIMA, M., TSURUO, T. & AZUMA, I. (1993) Role of aminopeptidase N (CD13) in tumor-cell invasion and extracellular matrix degradation. *Int J Cancer,* 54**,** 137-43.

SALEM, H. K. & THIEMERMANN, C. (2009) Mesenchymal Stromal Cells: Current Understanding and Clinical Status. *Stem Cells,* 28**,** 585-596.

SALIPANTE, S. J. & HORWITZ, M. S. (2007) A phylogenetic approach to mapping cell fate. *Curr Top Dev Biol,* 79**,** 157-84.

SAMUELSSON, H., RINGDEN, O., LONNIES, H. & LE BLANC, K. (2009) Optimizing in vitro conditions for immunomodulation and expansion of mesenchymal stromal cells. *Cytotherapy,* 11**,** 129-36.

SARRAF, C. (2005) Emerging themes of cancer stem cells: editorial--overview. *Cell Prolif,* 38**,** 343-5.

SASAKI, M., ABE, R., FUJITA, Y., ANDO, S., INOKUMA, D. & SHIMIZU, H. (2008) Mesenchymal stem cells are recruited into wounded skin and contribute to wound repair by transdifferentiation into multiple skin cell type. *J Immunol,* 180**,** 2581-7.

SATO, Y., ARAKI, H., KATO, J., NAKAMURA, K., KAWANO, Y., KOBUNE, M., SATO, T., MIYANISHI, K., TAKAYAMA, T., TAKAHASHI, M., TAKIMOTO, R., IYAMA, S., MATSUNAGA, T., OHTANI, S., MATSUURA, A., HAMADA, H. & NIITSU, Y. (2005) Human mesenchymal stem cells xenografted directly to rat liver are differentiated into human hepatocytes without fusion. *Blood,* 106**,** 756-63.

SATOKATA, I., MA, L., OHSHIMA, H., BEI, M., WOO, I., NISHIZAWA, K., MAEDA, T., TAKANO, Y., UCHIYAMA, M., HEANEY, S., PETERS, H., TANG, Z., MAXSON, R. & MAAS, R. (2000) Msx2 deficiency in mice causes pleiotropic defects in bone growth and ectodermal organ formation. *Nat Genet,* 24**,** 391-5.

SCHAJOWICZ, F., SISSONS, H. A. & SOBIN, L. H. (1995) The World Health Organization's histologic classification of bone tumors. A commentary on the second edition. *Cancer,* 75**,** 1208-14.

SCHOFIELD, R. (1978) The relationship between the spleen colony-forming cell and the haemopoietic stem cell. *Blood Cells,* 4**,** 7-25.

SCHOFL, C., CUTHBERTSON, K. S., WALSH, C. A., MAYNE, C., COBBOLD, P., VON ZUR MUHLEN, A., HESCH, R. D. & GALLAGHER, J. A. (1992) Evidence for P2-purinoceptors on human osteoblast-like cells. *J Bone Miner Res,* 7**,** 485-91.

SCHON, A., MICHIELS, L., JANOWSKI, M., MERREGAERT, J. & ERFLE, V. (1986) Expression of protooncogenes in murine osteosarcomas. *Int J Cancer,* 38**,** 67-74.

SEIB, F. P., FRANKE, M., JING, D., WERNER, C. & BORNHAUSER, M. (2009) Endogenous bone morphogenetic proteins in human bone marrow-derived multipotent mesenchymal stromal cells. *Eur J Cell Biol,* 88**,** 257-71.

SELL, S. (2004) Stem cell origin of cancer and differentiation therapy. *Crit Rev Oncol Hematol,* 51**,** 1-28.

SELL, S. & PIERCE, G. B. (1994) Maturation arrest of stem cell differentiation is a common pathway for the cellular origin of teratocarcinomas and epithelial cancers. *Lab Invest,* 70**,** 6-22.

SHAPIRA, L. & HALABI, A. (2009) Behavior of two osteoblast-like cell lines cultured on machined or rough titanium surfaces. *Clin Oral Implants Res,* 20**,** 50-5.

SHERLEY, J. L. (2002) Asymmetric cell kinetics genes: the key to expansion of adult stem cells in culture. *ScientificWorldJournal,* 2**,** 1906-21.

SHERWOOD, J. K., RILEY, S. L., PALAZZOLO, R., BROWN, S. C., MONKHOUSE, D. C., COATES, M., GRIFFITH, L. G., LANDEEN, L. K. & RATCLIFFE, A. (2002) A three-dimensional osteochondral composite scaffold for articular cartilage repair. *Biomaterials,* 23**,** 4739-51.

SHI, S. & GRONTHOS, S. (2003) Perivascular niche of postnatal mesenchymal stem cells in human bone marrow and dental pulp. *J Bone Miner Res,* 18**,** 696-704.

SHINTANI, S., MUROHARA, T., IKEDA, H., UENO, T., HONMA, T., KATOH, A., SASAKI, K., SHIMADA, T., OIKE, Y. & IMAIZUMI, T. (2001) Mobilization of endothelial progenitor cells in patients with acute myocardial infarction. *Circulation,* 103**,** 2776-9.

SHOOK, D. & KELLER, R. (2003) Mechanisms, mechanics and function of epithelial-mesenchymal transitions in early development. *Mech Dev,* 120**,** 1351-83.

SHUR, I., LOKIEC, F., BLEIBERG, I. & BENAYAHU, D. (2001) Differential gene expression of cultured human osteoblasts. *J Cell Biochem,* 83**,** 547-53.

SIMMONS, P. J. & TOROK-STORB, B. (1991) Identification of stromal cell precursors in human bone marrow by a novel monoclonal antibody, STRO-1. *Blood,* 78**,** 55-62.

SIMS, N. A. & GOOI, J. H. (2008) Bone remodeling: Multiple cellular interactions required for coupling of bone formation and resorption. *Semin Cell Dev Biol,* 19**,** 444-51.

SINGH, S. K., CLARKE, I. D., TERASAKI, M., BONN, V. E., HAWKINS, C., SQUIRE, J. & DIRKS, P. B. (2003) Identification of a cancer stem cell in human brain tumors. *Cancer Res,* 63**,** 5821-8.

SLEEMAN, K. E., KENDRICK, H., ASHWORTH, A., ISACKE, C. M. & SMALLEY, M. J. (2006) CD24 staining of mouse mammary gland cells defines luminal epithelial, myoepithelial/basal and non-epithelial cells. *Breast Cancer Res,* 8**,** R7.

SMITH, G. P. (1985) Filamentous fusion phage: novel expression vectors that display cloned antigens on the virion surface. *Science,* 228**,** 1315-7.

SMITH, G. P. & SCOTT, J. K. (1993) Libraries of peptides and proteins displayed on filamentous phage. *Methods Enzymol,* 217**,** 228-57.

SOLCHAGA, L. A., PENICK, K., PORTER, J. D., GOLDBERG, V. M., CAPLAN, A. I. & WELTER, J. F. (2005) FGF-2 enhances the mitotic and chondrogenic potentials of human adult bone marrow-derived mesenchymal stem cells. *J Cell Physiol,* 203**,** 398-409.

SORRELL, J. M., BABER, M. A., BRINON, L., CARRINO, D. A., SEAVOLT, M., ASSELINEAU, D. & CAPLAN, A. I. (2003) Production of a monoclonal antibody, DF-5, that identifies cells at the epithelial-mesenchymal interface in normal human skin. APN/CD13 is an epithelial-mesenchymal marker in skin. *Exp Dermatol,* 12**,** 315-23.

STEWART, K., MONK, P., WALSH, S., JEFFERISS, C. M., LETCHFORD, J. & BERESFORD, J. N. (2003) STRO-1, HOP-26 (CD63), CD49a and SB-10 (CD166) as markers of primitive human marrow stromal cells and their more differentiated progeny: a comparative investigation in vitro. *Cell Tissue Res,* 313**,** 281-90.

STEWART, K., WALSH, S., SCREEN, J., JEFFERISS, C. M., CHAINEY, J., JORDAN, G. R. & BERESFORD, J. N. (1999) Further characterization of cells expressing STRO-1 in cultures of adult human bone marrow stromal cells. *J Bone Miner Res,* 14**,** 1345-56.

STOLZING, A., JONES, E., MCGONAGLE, D. & SCUTT, A. (2008) Age-related changes in human bone marrow-derived mesenchymal stem cells: consequences for cell therapies. *Mech Ageing Dev,* 129**,** 163-73.

SUBRAMANIAN, K., GERAERTS, M., PAUWELYN, K. A., PARK, Y., OWENS, D. J., MUIJTJENS, M., ULLOA-MONTOYA, F., JIANG, Y., VERFAILLIE, C.

M. & HU, W. S. (2010) Isolation procedure and characterization of multipotent adult progenitor cells from rat bone marrow. *Methods Mol Biol,* 636**,** 55-78.

SUETSUGU, A., NAGAKI, M., AOKI, H., MOTOHASHI, T., KUNISADA, T. & MORIWAKI, H. (2006) Characterization of CD133+ hepatocellular carcinoma cells as cancer stem/progenitor cells. *Biochem Biophys Res Commun,* 351**,** 820-4.

SUN, J., LI, J., LIU, X., WEI, L., WANG, G. & MENG, F. (2009) Proliferation and gene expression of osteoblasts cultured in DMEM containing the ionic products of dicalcium silicate coating. *Biomed Pharmacother,* 63**,** 650-7.

SVEHAG, S. E., CHESEBRO, B. & BLOTH, B. (1967) Ultrastructure of gamma-M immunoglobulin and alpha macroglobulin: electron-microscopic study. *Science,* 158**,** 933-6.

TAKADA, I., MIHARA, M., SUZAWA, M., OHTAKE, F., KOBAYASHI, S., IGARASHI, M., YOUN, M. Y., TAKEYAMA, K., NAKAMURA, T., MEZAKI, Y., TAKEZAWA, S., YOGIASHI, Y., KITAGAWA, H., YAMADA, G., TAKADA, S., MINAMI, Y., SHIBUYA, H., MATSUMOTO, K. & KATO, S. (2007) A histone lysine methyltransferase activated by non-canonical Wnt signalling suppresses PPAR-gamma transactivation. *Nat Cell Biol,* 9**,** 1273-85.

TANG, Q. Q. & LANE, M. D. (1999) Activation and centromeric localization of CCAAT/enhancer-binding proteins during the mitotic clonal expansion of adipocyte differentiation. *Genes Dev,* 13**,** 2231-41.

TARE, R. S., KHAN, F., TOURNIAIRE, G., MORGAN, S. M., BRADLEY, M. & OREFFO, R. O. (2009) A microarray approach to the identification of polyurethanes for the isolation of human skeletal progenitor cells and augmentation of skeletal cell growth. *Biomaterials,* 30**,** 1045-55.

TERADA, N., HAMAZAKI, T., OKA, M., HOKI, M., MASTALERZ, D. M., NAKANO, Y., MEYER, E. M., MOREL, L., PETERSEN, B. E. & SCOTT, E. W. (2002) Bone marrow cells adopt the phenotype of other cells by spontaneous cell fusion. *Nature,* 416**,** 542-5.

THIERY, J. P. & SLEEMAN, J. P. (2006) Complex networks orchestrate epithelial-mesenchymal transitions. *Nat Rev Mol Cell Biol,* 7**,** 131-42.

THIESEN, S., KUBART, S., ROPERS, H. H. & NOTHWANG, H. G. (2000) Isolation of two novel human RhoGEFs, ARHGEF3 and ARHGEF4, in 3p13-21 and 2q22. *Biochem Biophys Res Commun,* 273**,** 364-9.

THOMSON, J. A., ITSKOVITZ-ELDOR, J., SHAPIRO, S. S., WAKNITZ, M. A., SWIERGIEL, J. J., MARSHALL, V. S. & JONES, J. M. (1998) Embryonic stem cell lines derived from human blastocysts. *Science,* 282**,** 1145-7.

THORNTON, T. M., PEDRAZA-ALVA, G., DENG, B., WOOD, C. D., ARONSHTAM, A., CLEMENTS, J. L., SABIO, G., DAVIS, R. J., MATTHEWS, D. E., DOBLE, B. & RINCON, M. (2008) Phosphorylation by p38 MAPK as an alternative pathway for GSK3beta inactivation. *Science,* 320**,** 667-70.

TINTUT, Y., ALFONSO, Z., SAINI, T., RADCLIFF, K., WATSON, K., BOSTROM, K. & DEMER, L. L. (2003) Multilineage potential of cells from the artery wall. *Circulation,* 108**,** 2505-10.

TIRINO, V., DESIDERIO, V., D'AQUINO, R., DE FRANCESCO, F., PIROZZI, G., GRAZIANO, A., GALDERISI, U., CAVALIERE, C., DE ROSA, A.,

PAPACCIO, G. & GIORDANO, A. (2008) Detection and characterization of CD133+ cancer stem cells in human solid tumours. *PLoS One,* 3**,** e3469.

TIRODE, F., LAUD-DUVAL, K., PRIEUR, A., DELORME, B., CHARBORD, P. & DELATTRE, O. (2007) Mesenchymal stem cell features of Ewing tumors. *Cancer Cell,* 11**,** 421-9.

TOLEDO, S. R., OLIVEIRA, I. D., OKAMOTO, O. K., ZAGO, M. A., DE SEIXAS ALVES, M. T., FILHO, R. J., MACEDO, C. R. & PETRILLI, A. S. (2010) Bone deposition, bone resorption, and osteosarcoma. *J Orthop Res*.

TOMLINSON, I. & BODMER, W. (1999) Selection, the mutation rate and cancer: ensuring that the tail does not wag the dog. *Nat Med,* 5**,** 11-2.

TONDREAU, T., LAGNEAUX, L., DEJENEFFE, M., DELFORGE, A., MASSY, M., MORTIER, C. & BRON, D. (2004) Isolation of BM mesenchymal stem cells by plastic adhesion or negative selection: phenotype, proliferation kinetics and differentiation potential. *Cytotherapy,* 6**,** 372-9.

TORCHIA, E. C., JAISHANKAR, S. & BAKER, S. J. (2003) Ewing tumor fusion proteins block the differentiation of pluripotent marrow stromal cells. *Cancer Res,* 63**,** 3464-8.

TRIEL, C., VESTERGAARD, M. E., BOLUND, L., JENSEN, T. G. & JENSEN, U. B. (2004) Side population cells in human and mouse epidermis lack stem cell characteristics. *Exp Cell Res,* 295**,** 79-90.

TSUTSUMI, S., SHIMAZU, A., MIYAZAKI, K., PAN, H., KOIKE, C., YOSHIDA, E., TAKAGISHI, K. & KATO, Y. (2001) Retention of multilineage differentiation potential of mesenchymal cells during proliferation in response to FGF. *Biochem Biophys Res Commun,* 288**,** 413-9.

TUDOR, D., LOCKE, M., OWEN-JONES, E. & MACKENZIE, I. C. (2004) Intrinsic patterns of behavior of epithelial stem cells. *J Investig Dermatol Symp Proc,* 9**,** 208-14.

TUMA, R. S. (2006) Researchers may use cancer cell lines to identify target populations prior to clinical trials. *J Natl Cancer Inst,* 98**,** 810-1.

UCHIDA, N., BUCK, D. W., HE, D., REITSMA, M. J., MASEK, M., PHAN, T. V., TSUKAMOTO, A. S., GAGE, F. H. & WEISSMAN, I. L. (2000) Direct isolation of human central nervous system stem cells. *Proc Natl Acad Sci U S A,* 97**,** 14720-5.

UNNI, K. K. (1998) Osteosarcoma of bone. *J Orthop Sci,* 3**,** 287-94.

VASILIOU, V. & NEBERT, D. W. (2005) Analysis and update of the human aldehyde dehydrogenase (ALDH) gene family. *Hum Genomics,* 2**,** 138-43.

VUJOVIC, S., HENDERSON, S. R., FLANAGAN, A. M. & CLEMENTS, M. O. (2007) Inhibition of gamma-secretases alters both proliferation and differentiation of mesenchymal stem cells. *Cell Prolif,* 40**,** 185-95.

WAGNER, W. & HO, A. D. (2007) Mesenchymal stem cell preparations--comparing apples and oranges. *Stem Cell Rev,* 3**,** 239-48.

WAGNER, W., HO, A. D. & ZENKE, M. (2010) Different Facets of Aging in Human Mesenchymal Stem Cells. *Tissue Eng Part B Rev*.

WAGNER, W., HORN, P., CASTOLDI, M., DIEHLMANN, A., BORK, S., SAFFRICH, R., BENES, V., BLAKE, J., PFISTER, S., ECKSTEIN, V. & HO, A. D. (2008) Replicative senescence of mesenchymal stem cells: a continuous and organized process. *PLoS One,* 3**,** e2213.

WAGNER, W., WEIN, F., SECKINGER, A., FRANKHAUSER, M., WIRKNER, U., KRAUSE, U., BLAKE, J., SCHWAGER, C., ECKSTEIN, V., ANSORGE, W. & HO, A. D. (2005) Comparative characteristics of mesenchymal stem cells from human bone marrow, adipose tissue, and umbilical cord blood. *Exp Hematol,* 33**,** 1402-16.

WANG, X. J. & LI, Q. P. (2007) The roles of mesenchymal stem cells (MSCs) therapy in ischemic heart diseases. *Biochem Biophys Res Commun,* 359**,** 189-93.

WATT, F. M., LO CELSO, C. & SILVA-VARGAS, V. (2006) Epidermal stem cells: an update. *Curr Opin Genet Dev,* 16**,** 518-24.

WEISSMAN, I. L. (2000) Translating stem and progenitor cell biology to the clinic: barriers and opportunities. *Science,* 287**,** 1442-6.

WEISSMAN, I. L. & SHIZURU, J. A. (2008) The origins of the identification and isolation of hematopoietic stem cells, and their capability to induce donor-specific transplantation tolerance and treat autoimmune diseases. *Blood,* 112**,** 3543-53.

WILSON, H., HUELSMEYER, M., CHUN, R., YOUNG, K. M., FRIEDRICHS, K. & ARGYLE, D. J. (2008) Isolation and characterisation of cancer stem cells from canine osteosarcoma. *Vet J,* 175**,** 69-75.

WOODBURY, D., SCHWARZ, E. J., PROCKOP, D. J. & BLACK, I. B. (2000) Adult rat and human bone marrow stromal cells differentiate into neurons. *J Neurosci Res,* 61**,** 364-70.

WU, J. X., CARPENTER, P. M., GRESENS, C., KEH, R., NIMAN, H., MORRIS, J. W. & MERCOLA, D. (1990) The proto-oncogene c-fos is over-expressed in the majority of human osteosarcomas. *Oncogene,* 5**,** 989-1000.

WU, P. K., CHEN, W. M., CHEN, C. F., LEE, O. K., HAUNG, C. K. & CHEN, T. H. (2009) Primary osteogenic sarcoma with pulmonary metastasis: clinical results and prognostic factors in 91 patients. *Jpn J Clin Oncol,* 39**,** 514-22.

XIAO, G., JIANG, D., THOMAS, P., BENSON, M. D., GUAN, K., KARSENTY, G. & FRANCESCHI, R. T. (2000) MAPK pathways activate and phosphorylate the osteoblast-specific transcription factor, Cbfa1. *J Biol Chem,* 275**,** 4453-9.

XIONG, Y., YANG, H. J., FENG, J., SHI, Z. L. & WU, L. D. (2009) Effects of alendronate on the proliferation and osteogenic differentiation of MG-63 cells. *J Int Med Res,* 37**,** 407-16.

YASUDA, T., KANAMORI, M., NOGAMI, S., HORI, T., OYA, T., SUZUKI, K. & KIMURA, T. (2009) Establishment of a new human osteosarcoma cell line, UTOS-1: cytogenetic characterization by array comparative genomic hybridization. *J Exp Clin Cancer Res,* 28**,** 26.

YEN, C. C. (2009) Osteosarcoma: is age an issue? *J Chin Med Assoc,* 72**,** 453-4.

YIN, A. H., MIRAGLIA, S., ZANJANI, E. D., ALMEIDA-PORADA, G., OGAWA, M., LEARY, A. G., OLWEUS, J., KEARNEY, J. & BUCK, D. W. (1997) AC133, a novel marker for human hematopoietic stem and progenitor cells. *Blood,* 90**,** 5002-12.

YIN, S., LI, J., HU, C., CHEN, X., YAO, M., YAN, M., JIANG, G., GE, C., XIE, H., WAN, D., YANG, S., ZHENG, S. & GU, J. (2007) CD133 positive hepatocellular carcinoma cells possess high capacity for tumorigenicity. *Int J Cancer,* 120**,** 1444-50.

YING, Q. L., NICHOLS, J., EVANS, E. P. & SMITH, A. G. (2002) Changing potency by spontaneous fusion. *Nature,* 416**,** 545-8.

YOO, M. H. & HATFIELD, D. L. (2008) The cancer stem cell theory: is it correct? *Mol Cells,* 26**,** 514-6.

YOUNG, H. E. & BLACK, A. C., JR. (2004) Adult stem cells. *Anat Rec A Discov Mol Cell Evol Biol,* 276**,** 75-102.

YOUNG, H. E., DUPLAA, C., YOUNG, T. M., FLOYD, J. A., REEVES, M. L., DAVIS, K. H., MANCINI, G. J., EATON, M. E., HILL, J. D., THOMAS, K., AUSTIN, T., EDWARDS, C., CUZZOURT, J., PARIKH, A., GROOM, J., HUDSON, J. & BLACK, A. C., JR. (2001) Clonogenic analysis reveals reserve stem cells in postnatal mammals: I. Pluripotent mesenchymal stem cells. *Anat Rec,* 263**,** 350-60.

YU, L., GUO, W. C., ZHAO, S. H., TANG, J. & CHEN, J. L. (2010) Mitotic arrest defective protein 2 expression abnormality and its clinicopathologic significance in human osteosarcoma. *Apmis,* 118**,** 222-9.

ZAJCHOWSKI, D. A., BARTHOLDI, M. F., GONG, Y., WEBSTER, L., LIU, H. L., MUNISHKIN, A., BEAUHEIM, C., HARVEY, S., ETHIER, S. P. & JOHNSON, P. H. (2001) Identification of gene expression profiles that predict the aggressive behavior of breast cancer cells. *Cancer Res,* 61**,** 5168-78.

ZANNETTINO, A. C., PSALTIS, P. J. & GRONTHOS, S. (2008) Home is where the heart is: via the FROUNT. *Cell Stem Cell,* 2**,** 513-4.

ZHANG, W. & DOLAN, M. E. (2009) Use of cell lines in the investigation of pharmacogenetic loci. *Curr Pharm Des,* 15**,** 3782-95.

ZHANG, X. & XU, W. (2008) Aminopeptidase N (APN/CD13) as a target for anti-cancer agent design. *Curr Med Chem,* 15**,** 2850-65.

Websites used in this thesis

Osiris Therapeutics Inc.: www.osiristx.com
Gene Ontology Database: www.geneontology.org
Uniprot protein database: www.ebi.ac.uk/uniprot

Appendix

I. Calibration curve to determine ALP concentration

To quantify osteogenic potential, the concentration of ALP was determined for individual sample population (Section 2.3.3.3). For each experiment carried out, a calibration curve of ALP concentration was constructed using two sets of phosphate standards (0 to 4 mM), and absorbance readings at 405 nm were taken in triplicates. An example of the calibration curve obtained for each experiment is shown below (Figure I) and the accepted R^2 value lies between 0.95 and 1.

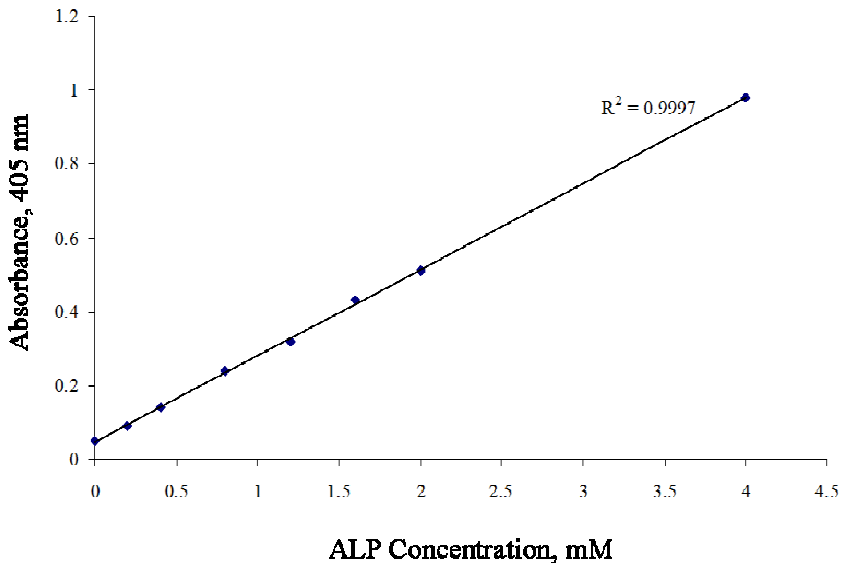

Figure I: Calibration curve of ALP concentration. Phosphate standards were prepared in duplicate (Section 2.3.3.3). Absorbance readings were taken at 405 nm wavelength in triplicates and the average values used to construct the line of best fit.

II. Isotype control for STRO-1 IgM antibody

STRO-1 primary IgM was detected using a FITC or RPE labelled mouse anti-IgM (µ-chain specific) antibody. To determine specific binding of the secondary antibody to the primary STRO-1 IgM, the isotype control used was unlabelled mouse IgM isotype control (Southern Biotech, Birmingham, USA). The binding of the isotype control was compared to the binding of the secondary antibody only (Appendix figure II A). For the IgG binding of the other fluorescent conjugated antibodies used in this thesis, the isotype control used was mouse IgG_1 Isotype Control PE/FITC conjugated (Assay Designs, Michigan, USA). PE detection is illustrated as an example in figure I B.

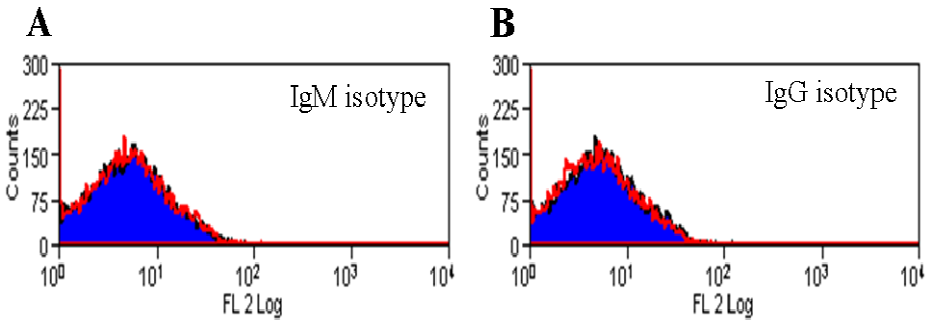

Figure II: Analysis of isotype controls for IgM and IgG antibodies used in flow cytometry. hMSCs were cultured, harvested and labelled using specific isotype controls (Section 2.5). Cells were analysed by flow cytometry and normalised to $1x10^4$ cells. (A) Red line represents secondary RPE labelled population and blue shaded histograms represent IgM isotype labelled population; (B) Red line represents unstained population and blue shaded histogram represents IgG isotype PE labelled population.

III. Gene expression microarray analysis

(Performed by Stephen Henderson, The Cancer Institute, UCL)

The procedure leading to the identification of eight potential candidate genes is outlined below.

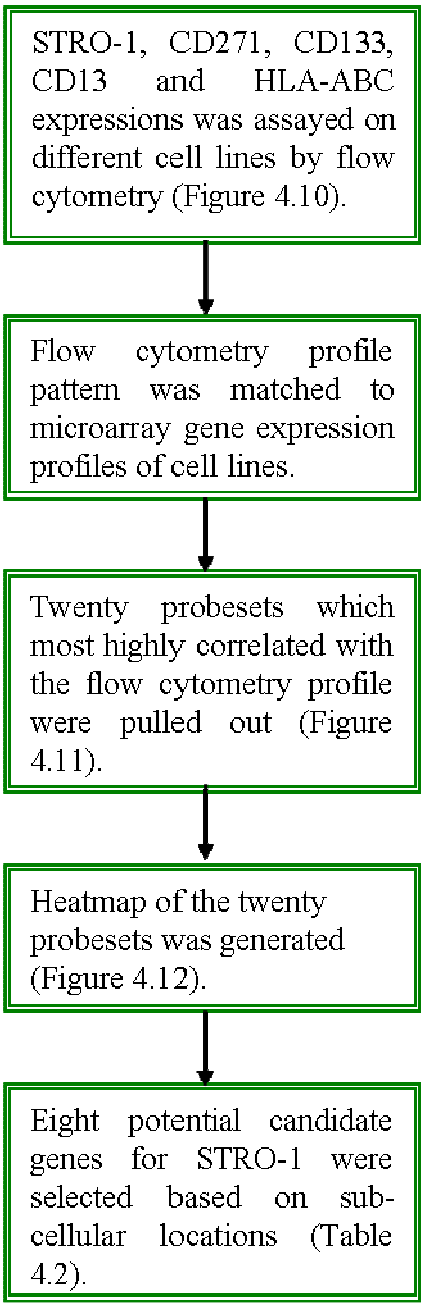

Figure III: Outline of procedure to identify potential candidate genes encoding the STRO-1 antigen (Section 2.7).

From the correlation values obtained (Section 4.9), the twenty probesets with the highest correlation were selected and their sub-cellular locations retrieved from the Gene Ontology (GO) database.

Ensembl Gene ID	GO Term Name (cc)	HGNC symbol	Affy HG U133A
ENSG00000067646	nucleus	ZFY	207246_at
ENSG00000067646	intracellular	ZFY	207246_at
ENSG00000114374	cytoplasm	USP9Y	206624_at
ENSG00000067048	nucleus	DDX3Y	205000_at
ENSG00000067048	cytoplasm	DDX3Y	205000_at
ENSG00000067048	plasma membrane	DDX3Y	205000_at
ENSG00000067048		DDX3Y	205000_at
ENSG00000012817	intracellular	KDM5D	206700_s_at
ENSG00000012817	nucleus	KDM5D	206700_s_at
ENSG00000012817	cellular_component	KDM5D	206700_s_at
ENSG00000198692	cytoplasm	EIF1AY	204409_s_at
ENSG00000198692		EIF1AY	204409_s_at
ENSG00000103227	endoplasmic reticulum	LMF1	219136_s_at
ENSG00000103227	membrane	LMF1	219136_s_at
ENSG00000103227	integral to membrane	LMF1	219136_s_at
ENSG00000103227		LMF1	219136_s_at
ENSG00000120659	extracellular space	TNFSF11	210643_at
ENSG00000120659	plasma membrane	TNFSF11	210643_at
ENSG00000120659	extracellular region	TNFSF11	210643_at
ENSG00000120659	integral to plasma membrane	TNFSF11	210643_at
ENSG00000120659	cytoplasm	TNFSF11	210643_at
ENSG00000120659	membrane	TNFSF11	210643_at
ENSG00000124491	extracellular region	F13A1	203305_at
ENSG00000124491	platelet alpha granule lumen	F13A1	203305_at
ENSG00000124491	cytoplasm	F13A1	203305_at
ENSG00000124491		F13A1	203305_at
ENSG00000130813		C19orf66	218429_s_at

Table I: Continued Overleaf.

ENSG00000108582	nucleus	CPD	201941_at
ENSG00000108582	membrane fraction	CPD	201941_at
ENSG00000108582	membrane	CPD	201941_at
ENSG00000108582	integral to membrane	CPD	201941_at
ENSG00000108582	trans-Golgi network	CPD	201941_at
ENSG00000108582	microsome	CPD	201941_at
ENSG00000170458	membrane raft	CD14	201743_at
ENSG00000170458	lipopolysaccharide receptor complex	CD14	201743_at
ENSG00000170458	extracellular region	CD14	201743_at
ENSG00000170458	plasma membrane	CD14	201743_at
ENSG00000170458	anchored to membrane	CD14	201743_at
ENSG00000170458	extracellular space	CD14	201743_at
ENSG00000161570	extracellular space	CCL5	1405_i_at
ENSG00000161570	extracellular region	CCL5	1405_i_at
ENSG00000161570	soluble fraction	CCL5	1405_i_at
ENSG00000161570	cytoplasm	CCL5	1405_i_at
ENSG00000087116	extracellular region	ADAMTS2	214535_s_at
ENSG00000087116	proteinaceous extracellular matrix	ADAMTS2	214535_s_at
ENSG00000087116	extracellular matrix	ADAMTS2	214535_s_at
ENSG00000087116		ADAMTS2	214535_s_at
ENSG00000125510	integral to plasma membrane	OPRL1	206564_at
ENSG00000125510	plasma membrane	OPRL1	206564_at
ENSG00000125510	integral to membrane	OPRL1	206564_at
ENSG00000148671	cellular_component	C10orf116	203571_s_at
ENSG00000148671		C10orf116	203571_s_at
ENSG00000171631	integral to plasma membrane	P2RY6	208373_s_at
ENSG00000171631	plasma membrane	P2RY6	208373_s_at
ENSG00000171631	basolateral plasma membrane	P2RY6	208373_s_at
ENSG00000171631	apical plasma membrane	P2RY6	208373_s_at
ENSG00000171631	integral to membrane	P2RY6	208373_s_at
ENSG00000136002	intracellular	ARHGEF4	211891_s_at
ENSG00000136002	cytosol	ARHGEF4	211891_s_at
ENSG00000136002	plasma membrane	ARHGEF4	211891_s_at
ENSG00000136002	cell projection	ARHGEF4	211891_s_at
ENSG00000136002	cytoplasm	ARHGEF4	211891_s_at
ENSG00000136002	cellular_component	ARHGEF4	211891_s_at
ENSG00000003402		CFLAR	208485_x_at
ENSG00000129824		RPS4Y1	201909_at
ENSG00000129824	cytosol	RPS4Y1	201909_at
ENSG00000129824	ribosome	RPS4Y1	201909_at
ENSG00000129824	polysome	RPS4Y1	201909_at
ENSG00000129824	cytosolic small ribosomal subunit	RPS4Y1	201909_at
ENSG00000129824	intracellular	RPS4Y1	201909_at

Table I: Sub-cellular locations of top twenty probesets which match STRO-1 antigen expression. The highlighted cells represented potential candidate genes representing STRO-1 antigen based on their location on the plasma membrane.